

Laboratory Medicine

November 2024 Vol 55 No 6 Pgs 677-810

labmedicine.com



BOARD OF EDITORS

Editor in Chief

Roger L. Bertholf, PhD
Houston Methodist Hospital
Weill Cornell Medicine

Reviews

ASSOCIATE EDITOR

Madhu Menon, MD
ARUP Laboratories

ASSISTANT EDITOR

Rahul Matrani, MD, PhD
Rutgers Robert Wood Johnson Medical School

Biostatistics

ASSOCIATE EDITOR

Michal Ordak, PhD
Medical University of Warsaw

Clinical Chemistry

ASSOCIATE EDITOR

Uttam Garg, PhD
University of Missouri Kansas City School of Medicine

ASSISTANT EDITORS

David Alter, MD
Emory University School of Medicine

Hong Kee Lee, PhD
Endeavor Health

Veronica Luzzi, PhD
Providence Regional Core Laboratory

Alejandro R. Molinelli, PhD
St Jude Children's Research Hospital

Cytology

ASSOCIATE EDITOR

Antonio Cajigas, MD
Montefiore Medical Center

Hematology

ASSOCIATE EDITOR

Shiyong Li, MD, PhD
Emory University School of Medicine

ASSISTANT EDITORS

Elizabeth Courville, MD
University of Virginia School of Medicine

A. Zara Herskovits, MD, PhD
Memorial Sloan Kettering Cancer Center

Alexandra E. Kovach, MD
Children's Hospital Los Angeles

Lisa Senzel, MD, PhD
Stony Brook Medicine

Histology

ASSOCIATE EDITOR

Carol A. Gomes, MS
Stony Brook University Hospital

STAFF

DIRECTOR OF SCIENTIFIC
PUBLICATIONS AND EXECUTIVE
EDITOR OF JOURNALS

Kelly Swails, MLS(ASCP)

PRODUCTION EDITOR

Erik N. Tanck, MD

Immunohematology

ASSOCIATE EDITOR

Richard Gammon, MD
OneBlood

ASSISTANT EDITORS

Phillip J. DeChristopher, MD, PhD
Loyola University Health System

Gregory Denomme, PhD
Grifols Laboratory Solutions

Amy E. Schmidt, MD, PhD
CSL Plasma

Immunology

ASSOCIATE EDITOR

Ruifeng Yang, MD, PhD
Nova Scotia Health

Laboratory Management and Administration

ASSOCIATE EDITOR

Lauren Pearson, DO, MPH
University of Utah Health

ASSISTANT EDITORS

Kayode Balogun, MD
Montefiore Medical Center

Vrajesh Pandya, MD
ARUP Laboratories

Microbiology

ASSOCIATE EDITOR

Yvette S. McCarter, PhD
University of Florida College of Medicine

ASSISTANT EDITORS

Alexander J. Fenwick, MD
University of Kentucky College of Medicine

Allison R. McMullen, PhD
Augusta University—Medical College of Georgia

Elitza S. Theel, PhD
Mayo Clinic

Molecular Pathology

ASSOCIATE EDITOR

Jude M. Abadie, PhD
Texas Tech University Health Science Center

ASSISTANT EDITORS

Holli M. Drendel, PhD
Atrium Health Molecular Pathology Laboratory

Rongjun Guo, MD, PhD
ProMedica Health System

Shuko Harada, MD
University of Alabama at Birmingham

Hongda Liu, MD, PhD
The First Affiliated Hospital of Nanjing Medical
University

Pathologists' Assistant

ASSOCIATE EDITOR

Anne Walsh-Feeks, MS, PA(ASCP)
Stony Brook Medicine

Laboratory Medicine (ISSN 0007-5027), is published 6 times per year (bimonthly). Periodicals Postage paid at Chicago, IL and additional mailing offices. POSTMASTER: Send address changes to *Laboratory Medicine*, Journals Customer Service Department, Oxford University Press, 2001 Evans Road, Cary, NC 27513-2009.

SUBSCRIPTION INFORMATION: Annually for North America, \$182 (electronic) or \$241 (electronic and print); single issues for individuals are \$32 and for institutions \$71. Annually for Rest of World, £118/€167 (electronic) or £154/€220 (electronic and print); single issues for individuals are £21/€30 and for institutions £44/€63. All inquiries about subscriptions should be sent to Journals Customer Service Department, Oxford Journals, Great Clarendon Street, Oxford OX2 6DP, UK, Tel: +44 (0) 1865-35-3907, e-mail: jnl.cust.serv@oup.com. In the Americas, please contact Journals Customer Service Department, Oxford Journals, 4000 CentreGreen Way, Suite 310, Cary, NC 27513, USA. Tel: 800-852-7323 (toll-free in USA/Canada) or 919-677-0977, e-mail: jnlorders@oup.com.

MEMBERSHIP INFORMATION: The ASCP membership fees for pathologists are as follows: fellow membership is \$399; fellow membership plus 1-year unlimited online CE is \$529; 2-year fellow membership is \$749; and 2-year fellow membership plus 2-year unlimited online CE is \$1009. The ASCP membership fees for laboratory professionals are as follows: young professional membership is \$59; annual membership is \$119; annual membership plus 1-year unlimited online CE is \$158; 3-year membership is \$389. All inquiries about membership should be sent to American Society for Clinical Pathology, 33 West Monroe Street, Suite 1600, Chicago, IL 60603, Tel: 312-541-4999, e-mail: ascp@ascp.org.

CLAIMS: Publisher must be notified of claims within four months of dispatch/ order date (whichever is later). Subscriptions in the EEC may be subject to European VAT. Claims should be made to *Laboratory Medicine*, Journals Customer Service Department, Oxford University Press, 4000 CentreGreen Way, Suite 310, Cary, NC 27513, USA, Tel: 800-852-7323 (toll-free in USA/Canada) or 919-677-0977, e-mail: jnlorders@oup.com.

Laboratory Medicine is published bimonthly by Oxford University Press (OUP), on behalf of the ASCP a not-for-profit corporation organized exclusively for educational, scientific, and charitable purposes. Devoted to the continuing education of laboratory professionals, *Laboratory Medicine* features articles on the scientific, technical, managerial, and educational aspects of the clinical laboratory. Publication of an article, column, or other item does not constitute an endorsement by the ASCP of the thoughts expressed or the techniques, organizations, or products described therein. *Laboratory Medicine* is indexed in the following: MEDLINE/PubMed, Science Citation Index, Current Contents—Clinical Medicine, and the Cumulative Index to Nursing and Allied Health Literature.

Laboratory Medicine is a registered trademark. Authorization to photocopy items for internal and personal use, or the internal and personal use of specific clients, is granted by ASCP Press for libraries and other users registered with the Copyright Clearance Center (CCC) Transactional Reporting Service, provided that the base fee of USD 15.00 per copy is paid directly to the CCC, 222 Rosewood Drive, Danvers, MA 01923, 978.750.8400. In the United States prior to photocopying items for educational classroom use, please also contact the CCC at the address above.

Printed in the USA

© 2024 American Society for Clinical Pathology (ASCP)

Advertising Sales Office Classified and Display Advertising

CORPORATE ADVERTISING

Jane Liss
732-890-9812
jliss@americanmedicalcomm.com

RECRUITMENT ADVERTISING

Lauren Morgan
267-980-6087
lmorgan@americanmedicalcomm.com

ASCP

Laboratory Medicine
33 West Monroe Street, Suite 1600
Chicago, IL 60603

T: 312-541-4999
F: 312-541-4750

SPECIAL REPORT

- 677 **Laboratory testing consolidation and total laboratory automation improves service efficiency and effectiveness: a study of a medical center in Taiwan**
Chih-Wei Tseng, Ying-Chun Li, Heng-Sheng Lee, Yang-Ming Tseng

OVERVIEW

- 686 **TP53 mutations in myeloid neoplasms: implications for accurate laboratory detection, diagnosis, and treatment**
Linsheng Zhang, Brooj Abro, Andrew Campbell, Yi Ding

SCIENCE

- 700 **Diagnostic value of serum STIP1 in HCC and AFP-negative HCC**
Haiqing Sun, Ning Liu, Jinli Lou
- 708 **Interference of hemoglobin variants with HbA_{1c} measurements by six commonly used HbA_{1c} methods**
Mingyang Li, Song Ge, Xin Shu, Xiongjun Wu, Haiyan Liu, Anping Xu, Ling Ji
- 713 **Impact of an anemia diagnostic management team on follow-up test ordering by primary care providers**
Julie Soder, Christopher Zahner, Jose H. Salazar
- 717 **Patient-derived reference intervals for alkaline phosphatase to support appropriate utility for isoenzymes determinations and hypophosphatasia**
Jonathan Joseph, Ibrahim A. Hashim
- 724 **Lipidomic analysis of serum exosomes identifies a novel diagnostic marker for type 2 diabetes mellitus**
Ling Zhang, Ting Lu, Baocheng Zhou, Yaoxiang Sun, Liyun Wang, Guohong Qiao, Tingting Yang
- 732 **Comparison of quantitative and qualitative anti-dsDNA assays**
Rajeevan Selvaratnam, Pooja Srivastava, Danyel H Tacker, Jennifer Thebo, Sarah E Wheeler
- 739 **A positive correlation of serum SFRP1 levels with the risk of developing type 2 diabetes mellitus: a case-control study**
Ahmed Salim Najm Alhilfi, Reza Afrisham, Alireza Monadi Sefidan, Reza Fadaei, Nariman Moradi, Lotfollah Saed, Nahid Einollahi
- 745 **Medical laboratory scientist motivation to pursue graduate education**
Lorraine N. Blagg

- 754 **Integrated biomarker profiling for enhanced heart failure management: a comprehensive study on the application of chemiluminescence detection of GDF-15 and multi-index models**
Ju Zhang, Jiajia Zhang, Chengyi Huang, Ting Wu, Peipei Jin
- 763 **Absolute CD4 count and percentage values among Libyan patients with HIV by single-platform flow cytometry**
Yosra Lamami, Abdulmunem M. Abulayha, Salah Altabal, Mohamed Elbasir, Abdurhman S. Elbnnani, Laila Aghil, Fawzi Ebrahim, Adam Elzagheid
- 768 **Detection of decreased granules in neutrophils by automated hematology analyzers XR-1000 and UniCel DxH 800**
Yosuke Kato, Daisuke Sakamoto, Hiroaki Ohnishi, Tomohiko Taki
- 776 **The safety and efficacy of transfusing red blood cells stored for different durations: a systematic review and meta-analysis of randomized controlled trials**
Fu Cheng, Dongmei Yang, Jie Chen, Li Qin, Bin Tan
- 785 **The diagnostic value of pleural effusion/serum ratio of carcinoembryonic antigen and pleural effusion/serum ratio of interferon- γ in classification of pleural effusion**
Shu-hui Liang, Cui Li, Si Xie

CASE STUDY

- 791 **Expect the unexpected: endocarditis caused by *Legionella feeleii***
Angelica Moran, Dennise E. Otero Espinal, Megan Parilla, Kathleen G. Beavis, Kathleen M. Mullane, Vera Tesic
- 795 **Acute hemolytic transfusion reaction caused by anti-M antibodies: a case report and literature review**
Yanjing He, Yang Li, Qiushi Wang
- 802 **A simple method to overcome paraproteinemic interferences in chemistry and immunoassays**
Rajarshi Sarkar
- 808 **Early detection of myocardial infarction with reference to baseline levels during health: impact on biological variation of high-sensitivity cardiac troponin**
Alan H.B. Wu, Sally Graglia



ON THE COVER: Clinical laboratory practice has evolved over the past half-century from mostly manual procedures for centrifuging, pipetting, aliquoting, reporting, etc. to an exceptionally high level of automation. Nearly all large hospital and reference laboratories incorporate automated systems to process and deliver specimens to chemistry and hematology analyzers that upload test results directly into the laboratory information system and, ultimately, the patient's electronic medical record. Automation of clinical laboratory processes has dramatically increased productivity and decreased the relative costs per test. In this issue of *Laboratory Medicine*, Tseng and colleagues describe and quantify the effects of total laboratory automation on productivity, staffing, workplace safety, and efficiency in the core laboratory of a large hospital in Taiwan.

Laboratory testing consolidation and total laboratory automation improves service efficiency and effectiveness: a study of a medical center in Taiwan

Chih-Wei Tseng^{1,2}, Ying-Chun Li², Heng-Sheng Lee¹, Yang-Ming Tseng¹

¹Cytogenetic Department, ²Clinical Pathology—Core Hematology, ³College of Allied Health Sciences, ⁴Clinical Laboratory Program, and ⁵Georgia Cancer Center, Augusta University Medical Center, Augusta, GA, US. *To whom correspondence should be addressed: gdeleo@augusta.edu.

Keywords: interprofessional education, attitudes, beliefs, medical laboratory scientists, medical laboratory technicians, educational programs

Abbreviations: IPE, interprofessional education; IPEC, Interprofessional Education Collaborative Expert Panel; NAACLS, National Accreditation Agency for Clinical Laboratory Sciences; MLA, Medical Laboratory Assistant; MLS, Medical Laboratory Science; DCLS, Doctorate of Clinical Laboratory Scientist; MLT, Medical Laboratory Technician; CG, Cytogenetic Technologist; DMS, Diagnostic Molecular Scientist; HT, Histotechnician; HTL, Histotechnologist; Path A, Pathologists' Assistant; Phleb, Phlebotomist; HCP, health care professional; ACOTE, Accreditation Council for Occupational Therapy Education; APPs, advanced practice providers; EMS, emergency medical services; PA, physician assistant; NP, nurse practitioner; CRNA, certified registered nurse anesthetist

Laboratory Medicine 2024;54:555-561; <https://doi.org/10.1093/labmed/lmad006>

ABSTRACT

Background: Interprofessional education is essential for students enrolled in health care professional programs.

Objectives: We assessed the attitudes towards and the beliefs about interprofessional education (IPE) among program directors of medical laboratory science (MLS) and medical laboratory technician (MLT) programs accredited by the National Accrediting Agency for Clinical Laboratory Sciences (NAACLS). We also investigated the inclusion of IPE in the curricula of such programs.

Methods: We emailed the link to an anonymous 22-item cross-sectional survey to 468 program directors and tabulated the responses.

Results: Program directors who support the need to include IPE within the curricula of MLT and MLS programs showed a generally positive attitude towards IPE. The beliefs about IPE among our respondents were not homogeneous. Program directors who have not yet implemented IPE in the curriculum may not have had an opportunity to experience the practical benefits of IPE.

Conclusion: Although barriers to IPE implementation exist, half of the respondents reported having already implemented IPE within their curricula.

Interprofessional education (IPE) is defined as a model in which students from 2 or more disciplines acquire knowledge from each other to generate successful collaboration and improve patient care.¹ In 2011, the Interprofessional Education Collaborative Expert Panel (IPEC) identified 4 core domains of competency: values and ethics, roles and responsibilities, teamwork and team-based care, and interprofessional communication.² In 2016, IPEC decided to broaden its interprofessional competencies to improve the patient experience of care, improve the health of patient populations, and reduce the per capita cost of health care.³

The National Accreditation Agency for Clinical Laboratory Sciences (NAACLS) grants public recognition to education programs that meet established education standards in the following clinical laboratory science disciplines: Medical Laboratory Assistant (MLA), Medical Laboratory Science (MLS), Doctorate of Clinical Laboratory Scientist (DCLS), Medical Laboratory Technician (MLT), Cytogenetic Technologist (CG), Diagnostic Molecular Scientist (DMS), Histotechnician (HT), Histotechnologist (HTL), Pathologists' Assistant (Path A), and Phlebotomist (Phleb).

IPE is essential for students enrolled in health care professional (HCP) educational programs who will transition into clinical settings after graduation.⁴ An explanatory case study published in 2017⁵ reported that students in a clinical laboratory science program at a tertiary-care university hospital desire a curriculum that promotes respect, communication, and equality in their field of study. The study results also reported that clinical laboratory students felt less valued during clinical rotations than students in other HCP programs. IPE activities and earlier interactions with other HCPs may help medical laboratory students feel valued.⁶ Recurrent challenges for IPE integration in laboratory science programs are discipline-specific curricula, content saturation, and difficulties with fully integrating interprofessional experiences.⁵

Medical laboratory scientists and medical laboratory technicians play a crucial role in patient outcomes; they are essential in a team-based health care approach. They may work in various locations: hospitals, clinics, forensic laboratories, public health research laboratories, and

pharmaceutical laboratories. According to the United States Bureau of Labor, the number of jobs in 2020 for medical laboratory scientists and medical laboratory technicians totaled more than 335,500. The job outlook for 2020–2030 is expected to grow 11% faster than the national average for all occupations.⁷ Previous research study reports have highlighted faculty attitudes and beliefs about IPE among faculty members in nursing^{8,9} and in several allied HCP programs, such as respiratory therapy,^{10,11} nutrition,¹² occupational therapy,¹³ physical therapy,¹⁴ and dental hygiene.¹⁵

The goals of our research were to assess the inclusion of interprofessional education and collaboration in the curricula of NAACLS MLS and MLT programs, to determine IPE and collaboration attitudes and beliefs among NAACLS MLT and MLS program directors, and to identify differences among MLS/MLT programs and program directors based on the inclusion of IPE and collaboration in the curricula.

Methods

The target population of this research study was the program directors of NAACLS MLS and MLT programs in the United States. Using a Google Chrome plug-in called webscraper.io,¹⁶ we downloaded a listing of all program directors, their names, and their email addresses from the NAACLS website.¹⁷ The data were filtered to identify only MLS and MLT programs. MLT programs are associate degree–level programs only; MLS programs can be bachelor’s or master’s degree–level programs.

Next, we performed data validation. We removed 13 duplicates because some program directors oversaw MLS and MLT programs. One program director was excluded from the survey because the NAACLS listed their program as being on administrative probation. The IRB office of our institution deemed this study as being exempt (IRB #1833916).

Survey Development

A 22-item survey was developed based on an extensive literature review and on previously used instruments.^{8,10–15} Questions were grouped into the following 6 sections: Section 1 asked questions about the rank of the program directors, their experience teaching, their experience in clinical settings, and the percentage of time they spent on program director activities. Section 2 solicited information about degree level, length of accreditation, current enrollment, institution type, and the current state of IPE in the curriculum. Sections 3 through 5 included questions that focused on the current implementation of IPE, the attitudes of the program directors toward IPE, and the beliefs of those individuals about IPE in the academic setting. Section 6 was created to identify what might prevent the implementation of IPE curricula.

We used Qualtrics XM software to develop the survey and to distribute it anonymously in January 2022. One reminder email was sent out 2 weeks after the initial contact to increase the return rate; the survey remained open for 5 weeks. The survey took less than 15 minutes to complete. Subjects were allowed to skip questions. Partial data were collected.

Data Repository and Data Analysis

The dataset¹⁸ used in this research is available on the secure cloud-based repository Mendeley Data. We used descriptive statistics and crosstabulations to analyze the data. Then, we used the Mann-Whitney *U* test to compare the nonparametric questionnaire responses across

the different subgroups. We collectively reported data from MLS/MLT program directors and used SPSS software (IBM) to perform the data analysis.

Results

The survey was sent by email to 468 program directors. Four emails were returned as undeliverable. A total of 120 program directors completed the survey, for a response rate of 25.6%.

Program Director Demographics and Program Characteristics

All 120 program directors answered the questions in the demographic and program characteristics sections of the survey. **TABLE 1** provides detailed information about the demographics of the program directors and the characteristics of their programs. Of the 62 program directors who identified themselves with a rank of associate or full professor, 36 (58.1%) had already established IPE in their curriculum. Half of the respondents (61 [50.8%]) had more than 15 years of teaching experience, and slightly fewer than half of those people (28 [45.9%]) had implemented IPE in their curricula. Almost half of the respondents (57 [47.5%]) had more than 15 years of clinical experience, and slightly fewer than half of those people (26 [45.6%]) had implemented IPE in their curricula.

One-fifth of the respondents (25 [20.8%]) reported working on program director duties during half of their work time. The remaining respondents reported being equally split between working on program director duties less than half of their time (48 [40.0%]) and more than half of their time (47 [39.2%]).

Half of the program directors whose university awards a bachelor’s level MLS degree (35 [53.8%]) have already implemented IPE in their curriculum. Most of the master’s degree programs (14 [60.9%]) surveyed have also already implemented IPE in their curriculum. Approximately half of program directors of programs with more than 15 years of accreditation (43 [47.3%]) reported that they have already implemented IPE in their curriculum. Programs with more than 25 students (50 [41.7%]) have IPE established in their program more than half of the time (31 [62.0%]). More than three-quarters of respondents (95 [79.2%]) reported being program directors at a public institution, and slightly more than half of them (50 [52.6%]) have IPE currently implemented in their curriculum. Approximately three-fourths of respondents (84 [70.0%]) reported that their institution is not part of a health care center. Among those respondents, fewer than half (35 [41.7%]) already offer IPE in their curriculum. More than half of the program directors who have already implemented IPE (25 [62.5%]) reported having space in the curriculum to teach IPE. In comparison, more than half of the program directors who have not already implemented IPE (36 [65.5%]) reported not having space in the curriculum to teach IPE.

Using a 5-point Likert scale made up of the options never, rarely, most of the time, sometimes, and always, the program directors who had already implemented IPE in their curriculum were asked how often they use 4 instructional methods: case study, clinic, simulation, and a combination of methods to teach IPE. Case study was the method selected most often, followed by a combination of methods and simulation. Clinic was often selected rarely or never. More than three-fourths of program directors (97 [81.0%]) identified the following barriers to

TABLE 1. Program Director Demographics and Program Characteristics^a

Program Director Demographics (n = 120)	Total	IPE in Curriculum	No IPE in Curriculum
Faculty rank			
Lecture/instructor/adjunct	42 (35.0)	16 (38.1)	26 (61.9)
Assistant professor	16 (13.3)	5 (31.2)	11 (68.8)
Associate professor	25 (20.8)	16 (64.0)	9 (36.0)
Professor	37 (30.8)	20 (54.1)	17 (45.9)
Teaching experience, y			
<5	13 (10.8)	9 (69.2)	4 (30.8)
6-10	28 (23.3)	11 (39.3)	17 (60.7)
11-15	18 (15.0)	9 (50.0)	9 (50.0)
>15	61 (50.8)	28 (45.9)	33 (54.1)
Clinical experience, y			
0	2 (1.7)	2 (100)	0
<5	9 (7.5)	7 (77.8)	2 (22.2)
6-10	23 (19.2)	11 (47.8)	12 (52.2)
11-15	29 (24.2)	11 (37.9)	18 (62.1)
>15	57 (47.5)	26 (45.6)	31 (54.4)
Program Characteristics (n = 120)	Total	IPE in Curriculum	No IPE in Curriculum
Degree level ^b			
Associate MLT	45 (37.5)	16 (35.6)	29 (64.4)
Bachelor's MLS	65 (54.2)	35 (53.8)	30 (46.2)
Master's MLS	23 (19.2)	14 (60.9)	9 (39.1)
Accreditation, y			
<5	8 (6.7)	5 (62.5)	3 (37.5)
6-10	10 (8.3)	5 (50.0)	5 (50.0)
11-15	11 (9.2)	4 (36.4)	7 (63.6)
>15	91 (75.8)	43 (47.3)	48 (52.7)
No. of students in program			
<10	27 (22.5)	10 (37.0)	17 (63.0)
11-15	16 (13.3)	7 (43.8)	9 (56.3)
16-20	12 (10.0)	4 (33.3)	8 (66.7)
21-25	14 (11.7)	4 (28.6)	10 (71.4)
>25	50 (41.7)	31 (62.0)	19 (38.0)
Prefer not to answer	1 (0.8)	1 (100)	0
Type of institution			
Public	95 (79.2)	50 (52.6)	45 (47.4)
Private	16 (13.3)	4 (25.0)	12 (75.0)
Other	9 (7.5)	3 (33.3)	6 (66.7)
Is the institution part of a health care center?			
No	84 (70.0)	35 (41.7)	49 (58.3)
Yes	34 (28.3)	21 (61.8)	13 (38.2)
Prefer not to answer	2 (1.7)	1 (50.0)	1 (50.0)

IPE, interprofessional education; MLS, medical laboratory sciences; MLT, medical laboratory technician.

^aData are given as No. (%).

^bSome programs have multiple degree options; total is >120.

implementing IPE in their curricula: logistics (77.3%), faculty resources (75.3%), curricular alignment and integration (64.9%), funding (58.8%), faculty buy-in (46.4%), credit for faculty time (44.3%), administrative support (40.2%), assessment of impact of IPE initiatives (18.6%), and accreditation limitation (19.6%).

TABLE 2 provides details on the current IPE collaborations of MLS and MLT programs surveyed. More than half of the program directors (80/117 [68.4%]) who answered the question about collaboration reported they would like to see a greater emphasis on IPE in their curricula. Among those program directors, approximately half (44 [55.0%]) reported they do not have IPE in their curriculum yet, and the other half (36 [45.0%]) reported they do. Program directors reported having active collaborations with other health care–related programs even when IPE has not been formally introduced in their curricula. Specifically, program directors reported they are currently collaborating with the departments of nursing (31 [25.8%]), pharmacy (18 [15.0%]), and physical therapy (17 [14.2%]), and the medical school (14 [11.7%]). Slightly less than half of program directors (48 [40.0%]) reported they do not collaborate with any other program.

TABLE 2. IPE Emphasis and Collaboration^a

Opinion (n = 117)	Total	IPE in Curriculum	No IPE in Curriculum
Would you like to see a greater emphasis on IPE in your curriculum?			
Yes	80 (68.4)	36 (45.0)	44 (55.0)
No	24 (20.5)	13 (54.2)	11 (45.8)
Prefer not to answer	13 (11.1)	6 (46.1)	7 (53.9)
Current Collaboration ^b	Total	IPE in Curriculum	No IPE in Curriculum
Which programs do you currently collaborate with?			
None	48 (40.0)	6 (12.5)	42 (87.5)
Nursing	31 (25.8)	25 (80.6)	6 (19.4)
Pharmacy	18 (15.0)	13 (72.2)	5 (27.8)
Physical therapy	17 (14.2)	14 (82.4)	3 (17.6)
Medical school	14 (11.7)	13 (92.9)	1 (7.1)
APPs ^c	13 (10.8)	11 (84.6)	2 (15.4)
Respiratory therapy	13 (10.8)	10 (76.9)	3 (23.1)
Occupational therapy	13 (10.8)	11 (84.6)	2 (15.4)
Dentistry	4 (3.3)	3 (75.0)	1 (25.0)
Social work	6 (5.0)	6 (100)	0
Speech and language	9 (7.5)	8 (88.9)	1 (11.1)
Dental hygiene	11 (9.2)	9 (81.8)	2 (18.2)
Prefer not to answer	0	0	0
Other ^d	21 (17.5)	18 (85.7)	3 (14.3)
Radiology	6 (28.6)	6 (100)	0
Public health	4 (19.1)	3 (75.0)	1 (25.0)
Nutrition	3 (14.3)	3 (100)	0
EMS	3 (14.3)	3 (100)	0

APPs, advanced practice providers; CRNA, certified registered nurse anesthetist; EMS, emergency medical services; IPE, interprofessional education; NP, nurse practitioner; PA, physician assistant.

^aData are given as No. (%).

^bn = 120. Some programs collaborate with multiple programs; total is >100%.

^cIncludes PA, NP, CRNA, etc.

^dOnly programs that were selected at least 3 times are shown.

Attitudes Towards IPE

TABLE 3 provides details on the attitudes of the program directors towards IPE. More than half of respondents somewhat disagreed or strongly disagreed (63 [64.3%]) that clinical problem-solving can only be learned effectively when students are taught within their individual departments or schools. Respondents who already have IPE implemented in their programs agreed less with the statement than those who have not implemented IPE ($P < .001$). More than half of the respondents somewhat agreed or strongly agreed (83 [84.7%]) that learning with students in other health care specialties helps MLS/MLT students become more effective members of a health care team. Respondents who are already offering IPE in their programs agreed more with the statement ($P = .02$). Most of the respondents somewhat agreed or strongly agreed (89 [90.8%]) that for small groups learning to work together, students need to trust and respect each other. Respondents already offering IPE in their programs agreed more with the statement ($P = .02$). Most of the respondents somewhat agreed or strongly agreed (90 [91.8%]) that implementing IPE will help students think positively about other professionals within their curriculum. Respondents already offering

TABLE 3. Attitudes of Program Directors Towards IPE^a

Statement	No.	Strongly Disagree	Somewhat Disagree	Neither Agree nor Disagree	Somewhat Agree	Strongly Agree
Clinical problem-solving can only be learned effectively when students are taught within their individual department/school ^b	98	20 (20.4)	43 (43.9)	23 (23.5)	8 (8.2)	4 (4.1)
IPE in curriculum	46	14 (30.4)	22 (47.8)	7 (15.2)	3 (6.5)	0
No IPE in curriculum	52	6 (11.5)	21 (40.4)	16 (30.8)	5 (9.6)	4 (7.7)
Learning with students in other health care professions helps MLS/MLT students become more effective members of a health care team ^c	98	1 (1.0)	3 (3.1)	11 (11.2)	29 (29.6)	54 (55.1)
IPE in curriculum	46	1 (2.2)	0	4 (8.7)	10 (21.7)	31 (67.4)
No IPE in curriculum	52	0	3 (5.8)	7 (13.5)	19 (36.5)	23 (44.2)
For a small group learning to work together, students need to trust and respect each other ^c	98	2 (2.0)	2 (2.0)	5 (5.1)	30 (30.6)	59 (60.2)
IPE in curriculum	46	1 (2.2)	0	1 (2.2)	11 (23.9)	33 (71.7)
No IPE in curriculum	52	1 (1.9)	2 (3.8)	4 (7.7)	19 (36.5)	26 (50.0)
Interprofessional learning will help students think positively about other HCPs ^b	98	0	1 (1.0)	7 (7.1)	35 (35.7)	55 (56.1)
IPE in curriculum	46	0	1 (2.2)	1 (2.2)	13 (28.3)	31 (67.4)
No IPE in curriculum	52	0	0	6 (11.5)	22 (42.3)	24 (46.2)
Patients would ultimately benefit if health care students work together to solve patient problems ^c	97	0	3 (3.1)	6 (6.2)	25 (25.8)	63 (64.9)
IPE in curriculum	46	0	1 (2.2)	0	11 (23.9)	34 (73.9)
No IPE in curriculum	51	0	2 (3.9)	6 (11.8)	14 (27.5)	29 (56.9)
Interprofessional learning integration with health care students will increase their ability to understand clinical problems	97	2 (2.1)	1 (1.0)	13 (13.4)	34 (35.1)	47 (48.5)
MLS students would benefit from working on small group projects with other health care students	98	0	6 (6.1)	11 (11.2)	42 (42.9)	39 (39.8)
Interprofessional learning will help students to understand their own professional limitations	98	2 (2.0)	2 (2.0)	18 (18.4)	42 (42.9)	34 (34.7)
Communication skills should be learned with integrated classes of health care students	98	2 (2.0)	3 (3.1)	14 (14.3)	39 (39.8)	40 (40.8)

HCPs, health care professionals; IPE, interprofessional education; MLS, medical laboratory sciences; MLT, medical laboratory technician.

^aData are given as No. (%).

^bStatistically significant at $P < .001$ between programs that have already IPE in the curriculum and programs that do not.

^cStatistically significant at $P < .05$ between programs that have already IPE in the curriculum and programs that do not.

IPE in their programs agreed more with the statement ($P = .03$). Most of the respondents somewhat agreed or strongly agreed (88 [90.7%]) that patients would ultimately benefit if health care students worked together to solve patient problems by implementing IPE within their curriculum. Respondents who are already offering IPE in their programs agreed more with the statement ($P = .04$).

We found no statistically significant difference between program directors who have already and those who have not yet implemented IPE in their curricula in the answers to the remaining questions related to attitudes towards IPE. In total, 81 respondents (83.6%) selected strongly agreed or somewhat agreed for the question that asked whether IPE integration with health care students will increase their ability to understand clinical problems. For the question asking whether students in MLS programs would benefit from working on small group projects with other health care students, 81 respondents (82.7%) selected strongly agreed or somewhat agreed. For the question of whether IPE will help students to understand their professional limitations, 76 respondents (77.6%) selected strongly agreed or somewhat agreed. For the question asking whether communication skills should be learned within integrated classes of health care students, 79 respondents (80.6%) selected strongly agreed or somewhat agreed.

Beliefs About IPE

TABLE 4 provides details on the beliefs of the program directors about IPE. More than half of the respondents somewhat agreed or strongly agreed (66 [68.8%]) that it is important for the academic health center campuses to provide IPE opportunities. Respondents who are already offering IPE in their programs agreed more with the statement ($P < .001$). Half of the respondents somewhat disagreed or strongly disagreed (49 [51.1%]) that NAACLS should mandate IPE in the CLS curriculum. Respondents who are already offering IPE in their programs agreed more with the statement ($P = .01$). Half of the respondents somewhat agreed or strongly agreed (48 [50.0%]) that their institutions have the resources to implement IPE. Respondents who are already offering IPE in their programs agreed more with the statement ($P = .01$). More than half of the respondents somewhat disagreed or strongly disagreed (55 [57.3%]) with the statement that their program has the resources and personnel to teach IPE courses. Respondents who are already offering IPE in their programs agreed more with the statement ($P = .03$).

No statistically significant difference between program directors who have already and those who have not yet implemented IPE in their curricula was found in the remaining questions related to beliefs about IPE. In total, 70 respondents (72.9%) selected strongly agreed

TABLE 4. Beliefs of Program Directors About IPE^a

Statement	No.	Strongly Disagree	Somewhat Disagree	Neither Agree nor Disagree	Somewhat Agree	Strongly Agree
It is important for academic health care center campuses to provide interprofessional learning opportunities ^b	96	0	5 (5.2)	25 (26.0)	45 (46.9)	21 (21.9)
IPE in curriculum	45	0	3 (6.7)	6 (13.3)	20 (44.4)	16 (35.6)
No IPE in curriculum	51	0	2 (3.9)	19 (37.3)	25 (49.0)	5 (9.8)
NAACLS should mandate IPE in the CLS curriculum ^b	96	30 (31.3)	19 (19.8)	25 (26.0)	15 (15.6)	7 (7.3)
IPE in curriculum	45	10 (22.2)	5 (11.1)	16 (35.6)	9 (20.0)	5 (11.1)
No IPE in curriculum	51	20 (39.2)	14 (27.5)	9 (17.6)	6 (11.8)	2 (3.9)
My institution has the resources to implement IPE ^b	96	10 (10.4)	24 (25.0)	14 (14.6)	26 (27.1)	22 (22.9)
IPE in curriculum	45	2 (4.4)	10 (22.2)	4 (8.9)	15 (33.3)	14 (31.1)
No IPE in curriculum	51	8 (15.7)	14 (27.5)	10 (19.6)	11 (21.6)	8 (15.7)
My program has the resources and personnel to teach IPE courses ^c	96	17 (17.7)	38 (39.6)	17 (17.7)	18 (18.8)	6 (6.3)
IPE in curriculum	45	6 (13.3)	15 (33.3)	8 (17.8)	12 (26.7)	4 (8.9)
No IPE in curriculum	51	11 (21.6)	23 (45.1)	9 (17.7)	6 (11.8)	2 (3.9)
Faculty should be encouraged to participate in IPE courses	96	0	6 (6.3)	20 (20.8)	49 (51.0)	21 (21.9)
IPE courses are logistically difficult	96	3 (3.1)	15 (15.6)	22 (22.9)	37 (38.5)	19 (19.8)
Faculty members like teaching with faculty members from other academic departments	95	0	15 (15.8)	49 (51.6)	28 (29.5)	3 (3.2)
IPE efforts weaken program content	95	33 (34.7)	33 (34.7)	22 (23.2)	6 (6.3)	1 (1.1)
Accreditation requirements limit IPE efforts	95	11 (11.6)	26 (27.4)	30 (31.6)	21 (22.1)	7 (7.4)
IPE efforts require support from campus administration	96	2 (2.1)	1 (1.0)	5 (5.2)	41 (42.7)	47 (49.0)
Certain current curriculum requirements could be removed to make room for additional IPE content	96	19 (19.8)	25 (26.0)	22 (22.9)	25 (26.0)	5 (5.2)
IPE better utilizes resources	96	2 (2.1)	13 (13.5)	40 (41.7)	32 (33.3)	9 (9.4)

CLS, clinical laboratory science; IPE, interprofessional education; NAACLS, National Accreditation Agency for Clinical Laboratory Sciences.

^aData are given as No. (%).

^bStatistically significant at $P < .001$ between programs that have already IPE in the curriculum and programs that do not.

^cStatistically significant at $P < .05$ between programs that have already IPE in the curriculum and programs that do not.

or somewhat agreed for the question that asked whether faculty should be encouraged to participate in IPE courses. For the question asking whether interprofessional courses are logistically difficult, 56 respondents (58.3%) selected strongly agreed or somewhat agreed. For the question asking if IPE efforts require support from campus administration, the number was 88 (91.7%).

In total, 66 respondents (69.4%) selected strongly disagree or somewhat disagree for the question asking whether IPE efforts weaken program content. For the question asking whether accreditation requirements limit IPE efforts, that number was 37 (39.0%). Almost half of the respondents selected the option “neither agree nor disagree” for the question of whether faculty members like teaching with faculty members from other academic departments (49 [51.6%]) and for the question of whether IPE better utilizes resources (40 [41.7%]).

Conclusion

Overall, the program directors of MLS and MLT programs showed a positive attitude towards IPE. However, the beliefs about IPE were not homogeneous. In particular, the program directors were not in agreement on how much the accreditation requirements limit IPE efforts, on the potential effect of a mandate by NAACLS to offer IPE in the curricula, and whether there are current curriculum requirements that could be removed to make room for additional IPE. Program directors who have

not yet implemented IPE in the curriculum may not have had an opportunity to experience the practical benefits of IPE.

Also, program directors of MLS and MLT programs reported challenges in implementing IPE, while recognizing that IPE is important within their curricula. This result is analogous to what respiratory therapy faculty members have reported in a previous study report.¹⁰ As in the report of a previous research study conducted among program directors of nutrition programs,¹² MLS and MLT program directors believe that patients would ultimately benefit if health care students worked together to solve patient problems.

More than half of program directors of occupational therapy programs reported¹³ that they strongly agreed or agreed that the Accreditation Council for Occupational Therapy Education (ACOTE) should mandate IPE in the occupational therapy curriculum. However, only half of the MLS and MLT program directors in our survey disagreed or strongly disagreed that NAACLS should mandate IPE in the CLS curriculum, and one-fourth of the respondents neither agreed nor disagreed with that statement. MLS and MLT program directors believe that some current curriculum requirements could be removed to make room for additional IPE education; more of those respondents believe this, compared with program directors of physical therapy programs.¹⁴ As in the report of a previous research study conducted among dental hygiene faculty members,¹⁵ MLS and MLT program directors strongly support the idea that faculty members should be encouraged to participate in IPE courses.

Among other health care professions, MLS and MLT program directors reported currently collaborating with the nursing department the most. The strong connection with the nursing programs may be explained by the fact that the nursing department handles most of the specimen collections for the medical laboratory. We also note that it appears that programs without IPE have active collaborations with other programs, such as nursing, but such collaborations are not considered by their program directors to be IPE activities.

We investigated whether there were any statistically significant differences in attitudes and beliefs among program directors of programs housed or not housed in health care centers. We only found 1 statistically significant difference ($P = .01$) for the belief “My institution has the resources to implement IPE,” with program directors of programs not housed in health care centers strongly or somewhat disagreeing (29 [44.6%]) more than program directors of programs housed in health care centers (5 [16.9%]). We did not observe any statistically significant differences for attitudes and beliefs between program directors of MLS or MLT programs.

This research project has 2 major limitations: the survey response rate may not represent all NAACLS program directors, and the findings were based on self-reporting. However, we report that a large majority of MLS and MLT programs strongly agree or somewhat agree that implementing IPE will help students think positively about other professionals within their curriculum. Also, more than 50% of the respondents would like to see a greater emphasis on IPE in their curricula.

Conflict of Interest Disclosure

The authors have nothing to disclose.

REFERENCES

1. World Health Organization (WHO). *Framework for Action on Interprofessional Education and Collaborative Practice*. WHO; 2010.
2. Interprofessional Education Collaborative Expert Panel. Core competencies for interprofessional collaborative practice: Report of an expert panel. Interprofessional Education Collaborative Expert Panel, American Association of Colleges of Nursing; 2011.
3. Interprofessional Education Collaborative Expert Panel. Core competencies for interprofessional collaborative practice: Report of an expert panel. Interprofessional Education Collaborative Expert Panel, American Association of Colleges of Nursing; 2016.
4. Buring SM, Bhushan A, Broeseker A, et al. Interprofessional education: definitions, student competencies, and guidelines for implementation. *Am J Pharm Educ*. 2009;73(4):59. doi:10.5688/aj730459
5. Salazar JH. Interprofessional education themes in a clinical laboratory sciences curriculum. *Am Soc Clin Lab Sci*. 2017;30(2):99–104.
6. Weber BW, Mirza K. Leveraging interprofessional education to improve physician/laboratory cooperation and patient outcomes. *Med Sci Educ*. 2022;32(1):239–241. doi:10.1007/s40670-021-01496-4
7. Bureau of Labor Statistics USDoL. *Occupational Outlook Handbook, Medical Scientists*, 2022. <https://www.bls.gov/ooh/life-physical-and-social-science/medical-scientists.htm>. Accessed January 21, 2024.
8. Curran VR, Sharpe D, Forristall J. Attitudes of health sciences faculty members towards interprofessional teamwork and education. *Med Educ*. 2007;41(9):892–896. doi:10.1111/j.1365-2923.2007.02823.x
9. Olenick M, Allen LR. Faculty intent to engage in interprofessional education. *J Multidiscip Healthc*. 2013;6:149–161. doi:10.2147/JMDH.S38499
10. Vernon MM, Moore NM, Cummins L-A, et al. Respiratory therapy faculty knowledge of and attitudes toward interprofessional education. *Respir Care*. 2017;62(7):873–881. doi:10.4187/respcare.05034
11. Vernon MM, Moore N, Mazzoli A, De Leo G. Respiratory therapy faculty perspectives on interprofessional education: findings from a cross-sectional online survey. *J Interprof Care*. 2018;32(2):235–238. doi:10.1080/13561820.2017.1389865
12. Patton Z, Vernon M, Haymond K, Anglin J, Heboyan V, De Leo G. Evaluation of interprofessional education implementation among nutrition program directors in the United States. *Top Clin Nutr*. 2018;33(3):196–204. doi:10.1097/tin.000000000000143
13. Hughes JK, Allen A, McLane T, Stewart JL, Heboyan V, De Leo G. Interprofessional education among occupational therapy programs: faculty perceptions of challenges and opportunities. *Am J Occup Ther*. 2019;73(1):7301345010p1–7301345010p6. doi:10.5014/ajot.2019.030304
14. Ramiscal L, Truelove C Jr, Heboyan V, De Leo G. Attitudes and beliefs of physical therapist and physical therapist assistant program directors in the United States towards interprofessional education. *Internet J Allied Health Sci Pract*. 2022;20(1):13.
15. Tolle SL, Vernon MM, McCombs G, De Leo G. Interprofessional education in dental hygiene: attitudes, barriers and practices of program faculty. *J Dent Hyg*. 2019;93(2):13–22.
16. Web Scraper. <https://webscraper.io/>. Accessed January 21, 2024.
17. *The National Accreditation Agency for Clinical Laboratory Sciences*. <https://www.naacls.org/about.aspx>. Accessed January 21, 2024.
18. De Leo G, Bamfield-Cummin S, Bayhaghi G, Bufkin K, Jones S, Kashyap H. Data from: status of Interprofessional Education among NAACLS MLS and MLT programs directors. 2022. doi:10.17632/345cygfv29.2

TP53 mutations in myeloid neoplasms: implications for accurate laboratory detection, diagnosis, and treatment

Linsheng Zhang, MD, PhD,¹  Brooj Abro, MD,¹ Andrew Campbell, PhD,² Yi Ding, MD, PhD²

¹Department of Pathology and Laboratory Medicine, Emory University School of Medicine, Atlanta, GA, US; ²Department of Laboratory Medicine, Geisinger Medical Center, Danville, PA, US. Corresponding author: Yi Ding; yding1@geisinger.edu

Key words: myelodysplastic syndrome; acute myeloid leukemia; myeloid neoplasm; TP53; genetic techniques; sequence analysis

Abbreviations: AML, acute myeloid leukemia; MDS, myelodysplastic neoplasms/syndrome; MPN, myeloproliferative neoplasm; IPSS-M, Molecular International Prognostic Scoring System; WHO-HEAM5, World Health Organization Classification of Tumors of Haematopoietic and Lymphoid Tissues, 5th Edition; ICC, International Consensus Classification; SNVs, single nucleotide variants; MNVs, multiple nucleotide variants; indels, insertions and deletions; SVs, structural variants; 17p, whole arm; IHC, immunohistochemical; NGS, next-generation sequencing; VAF, variant allele frequency; MRD, measurable residual disease; AEL, acute erythroid leukemia; WHO-4RE, World Health Organization Classification of Tumors of Haematopoietic and Lymphoid Tissues, Revised 4th Edition; LFS, Li-Fraumeni syndrome; WT, wild type; GOF, gain-of-function; tMNs, therapy-related myeloid neoplasms; tMDS, therapy-related MDS; HSCT, hematopoietic stem cell transplantation; PARPi, poly (ADP-ribose) polymerase inhibitor CNV, copy number variation/alteration; HSPCs, hematopoietic stem/progenitor cells; CHIP, clonal hematopoiesis of indeterminate potential; LOH, loss of heterozygosity; UPD, uniparental disomy; OS, overall survival; EAp53, evolutionary action score; RFS, relative fitness score; OGM, optical genome mapping; WES, whole exome sequencing, WGS, whole genome sequencing; PCR, polymerase chain reaction; VUS, variants of unknown significance; FFPE, formalin-fixed paraffin-embedded; NCCN, National Comprehensive Cancer Network; HMAs, hypomethylation agents; alloHSCT allogeneic HSCT; CIBMTR, Center for International Blood and Marrow Transplant Research; FISH fluorescence in situ hybridization; AACR American Association for Cancer Research

Laboratory Medicine 2024;55:686-699; <https://doi.org/10.1093/labmed/lmae048>

ABSTRACT

Genetic alterations that affect the function of p53 tumor suppressor have been extensively investigated in myeloid neoplasms, revealing their significant impact on disease progression, treatment response, and patient outcomes. The identification and characterization of TP53 mutations play pivotal roles in subclassifying myeloid neoplasms and guiding treatment decisions. Starting with the presentation of a typical case, this review highlights the complicated nature of genetic alterations involving TP53 and provides a comprehensive analysis

of TP53 mutations and other alterations in myeloid neoplasms. Currently available methods used in clinical laboratories to identify TP53 mutations are discussed, focusing on the importance of establishing a robust testing protocol within clinical laboratories to ensure the delivery of accurate and reliable results. The treatment implications of TP53 mutations in myeloid neoplasms and clinical trial options are reviewed. Ultimately, we hope that this review provides valuable insights into the patterns of TP53 alterations in myeloid neoplasms and offers guidance to establish practical laboratory testing protocols to support the best practices of precision oncology.

Introduction

Myeloid neoplasms are a group of hematopoietic disorders originating from the abnormal clonal proliferation of stem or myeloid progenitor cells, resulting in blood cell changes with or without solid organ infiltration by neoplastic myeloid cells and associated clinical presentations. Depending on the clinical onset, peripheral blood cell counts and whether dysplastic features are present in blood and bone marrow hematopoietic cells, the major categories of myeloid neoplasms include acute myeloid leukemia (AML), myelodysplastic neoplasm (MDS), myeloproliferative neoplasm (MPN), and MDS/MPNs. TP53 mutations are detected in approximately 10% of myeloid neoplasms.^{1,2} Due to the well-recognized association with unfavorable clinical outcomes, especially poor response to traditional combined chemotherapy, multihit TP53 mutations have the highest hazard ratio and model weight in the Molecular International Prognostic Scoring System (IPSS-M) for MDS.³ The recently updated 5th edition of the World Health Organization Classification of Tumors of Haematopoietic and Lymphoid Tissues (WHO-HEAM5) and the newly established International Consensus Classification (ICC) have changed the classification scheme by integrating more molecular genetic alterations in the diagnosis and classification of myeloid neoplasms.^{4,5} A significant change from the previous phenotype-defined classification is the promotion of TP53 mutations as a defining criterion for MDS and AML. The updates make the detection of multihit TP53 mutations a requirement for the subclassification of myeloid neoplasms. However, due to the complexities of genetic alterations involving TP53, it is practically challenging to detect all alterations in clinical samples using a single test or simple protocol. In addition, for less well-defined TP53 mutations,

© The Author(s) 2024. Published by Oxford University Press on behalf of American Society for Clinical Pathology.

This is an Open Access article distributed under the terms of the Creative Commons Attribution-NonCommercial License (<https://creativecommons.org/licenses/by-nc/4.0/>), which permits non-commercial re-use, distribution, and reproduction in any medium, provided the original work is properly cited. For commercial re-use, please contact reprints@oup.com for reprints and translation rights for reprints. All other permissions can be obtained through our RightsLink service via the Permissions link on the article page on our site—for further information please contact journals.permissions@oup.com.

interpretation of clinical significance is not always straightforward. In this review, we present an index case of myeloid neoplasm with a *TP53* mutation and complex karyotypic abnormalities as an introduction to demonstrate the significance of detecting genetic alterations involving *TP53*. The similarities and differences between WHO-HEAM5 and ICC in applying *TP53* alterations to the classification scheme will be explained, followed by an in-depth discussion of the complexity of *TP53* mutations in myeloid neoplasms and considerations for clinical diagnostic laboratories to develop tests to detect *TP53* alterations to provide timely and accurate information, not only for better classification of MDS and AML but also to improve genetics-based precision cancer care. To simplify the terminology, in this review “mutation” is used as a general term to include single or multiple nucleotide variants (SNVs and MNVs), insertions and deletions (indels), as well as structural variants (SVs) and whole chromosome 17 or whole arm (17p) abnormalities involving *TP53*, unless otherwise specified.

Case Vignette

The data of this case vignette has been modified to remove patient-specific information.

A 51-year-old male presented with symptomatic anemia. A complete blood cell count revealed moderate anemia and marked thrombocytopenia. The bone marrow aspirate smear showed frequent immature cells with morphologic features of erythroblasts (**FIGURE 1A**); however, accurate enumeration of blasts and nucleated red blood cell percentage was difficult due to significant cell degeneration. On the biopsy core (**FIGURE 1B**), the cellularity was 40%-50%. Immature mononuclear cells with prominent nucleoli represented 30%-40% of the marrow cellularity. These cells were positive for E-cadherin by immunohistochemical (IHC) staining (**FIGURE 1C**); combining E-cadherin and glycophorin-positive cells, erythroid lineage cells comprised 50%-60% of marrow cellularity. The p53-positive cells represented 60%-70% of marrow cellularity (**FIGURE 1D**). CD61 staining revealed frequent small megakaryocytes (**FIGURE 1E**). Flow cytometric analysis showed that the immature cell population had phenotypic characteristics most compatible with erythroblasts (**FIGURE 1F**). Amplicon-based next-generation sequencing (NGS) detected *TP53* (NM_000546.5) chr17:7577094:G:A, c.844C>T (p.R282W) with a variant allele frequency (VAF) of 50.73% (**FIGURE 1G**) and *PPM1D* (NM_003620.3) chr17:58740546:T:G, c.1451T>G (L484*) at 2.46%. Chromosome analysis demonstrated complex karyotype in 12 of 20 cells, but chromosome 17 abnormality was not detected.

Because the erythroid components were less than 80% of the marrow nucleated cells, a diagnosis of high-grade myeloid neoplasm, MDS/AML with mutated *TP53*, was rendered. The patient was started on standard 7 + 3 (cytarabine + idarubicin) induction chemotherapy. A bone marrow biopsy on day 30 of treatment showed normocellularity with trilineage hematopoiesis and <5% blasts (**FIGURE 1H**). Immunohistochemical staining for E-cadherin highlighted immature erythroid precursor cells, which were also strongly positive for p53 (**FIGURE 1I**). NGS detected *TP53* c.844C>T (R282W) at 14.83% and *PPM1D* c.1451T>G (L484*) at 19.67%. Chromosome analysis revealed a normal karyotype, and measurable residual disease (MRD) testing by flow cytometry detected no abnormal myeloblast population. Given the low blast percentage but persistent mutations at relatively high allele frequencies, the treatment protocol was switched to azacitidine + venetoclax. A follow-up bone

marrow biopsy 45 days later showed significant erythroid hyperplasia (**FIGURE 1J**) with no increase in blasts; however, p53 staining revealed clusters of positive cells (**FIGURE 1K**). NGS detected *TP53* c.844C>T (R282W) at 6.5% and *PPM1D* c.1451T>G (L484*) at 9.87%, and chromosome analysis demonstrated a complex karyotype, including the loss of chromosome 17 in 8 of 20 cells. A follow-up bone marrow biopsy 36 days later showed increased blasts representing 15%-20% of the marrow nucleated cells in a background of numerous erythroid precursors with many early forms, representing 50%-60% of the nucleated cells on the aspirate smears. Approximately 80% of the cells showed strong reactivity for p53 (data not shown), indicating relapsed MDS/AML. NGS revealed *TP53* c.844C>T (R282W) at 63.59% and *PPM1D* c.1451T>G (L484*) at 3.09%. The patient was on maintenance therapy with azacitidine + venetoclax but died of systemic infection and respiratory failure while awaiting alternate clinical trials.

This case represents a myeloid neoplasm with a *TP53* mutation. The VAF of *TP53* mutation and p53 positive cell percentage in the bone marrow change in the disease course, reflecting the fluctuation of neoplastic cell burden. However, definite classification is challenging due to some unclear criteria in WHO-HEAM5 and ICC. Based on the morphologic and immunophenotypic findings, with a low percentage of myeloblasts, <80% erythroid precursors in the bone marrow, and *TP53* mutation at a VAF >50%, this case can be classified as acute erythroid leukemia (AEL) or MDS with “biallelic *TP53* inactivation” under the umbrella of “MDS with defining genetic abnormalities.” Based on the ICC criteria, it could be classified as AML with mutated *TP53* if the proerythroblasts were counted as “blasts.” However, although ICC states that “pure erythroid leukemia is typically associated with *TP53* mutations, and these cases are now classified within the category of AML with *TP53* mutations,”⁵ when the morphologic findings do not entirely meet the criteria of pure erythroid leukemia defined by the 4th Revised Edition of the WHO Classification of Tumors of Haematopoietic and Lymphoid Tissues (WHO-4RE), for example, erythroid precursors <80%, it is not clearly described whether the proerythroblasts are considered blasts for the distinction between MDS and AML. **TABLE 1** summarizes the similarities and differences between WHO-HEAM5 and ICC for subtyping MDS and AML with *TP53* mutations. WHO-HEAM5 only recognizes *TP53* as one of the diagnostic criteria for MDS with defining genetic abnormalities, and there is no entity in AML defined by *TP53* mutations. AEL, a name changed from “pure erythroid leukemia” in WHO-4RE, remains under the umbrella of “AML defined by differentiation.” WHO-HEAM5 recognized the existence of cases that share the same clinicopathologic features as AEL but the nucleated erythroid cells constitute <80% of the bone marrow cellularity⁴; however, this is not clearly defined in its online version.⁶ Better clarification by further clinical studies, including the utility of *TP53* mutation status to distinguish these cases from MDS, is needed.

TP53 Alterations in Malignancies and Myeloid Neoplasms

TP53 gene, located on chromosome 17p13.1 (accession number: National Center for Biotechnology Information [NCBI] Reference Sequence Database [RefSeq] number: NM_000546 | Ensembl transcript number: ENST00000269305 | Consensus Coding Sequence [CCDS] number: CCDS11118), is the most frequently mutated gene in human cancer. The *TP53* transcript comprises 11 exons spanning approximately

FIGURE 1. Bone marrow findings of a representative case of myeloid neoplasm with *TP53* mutation. A-G, At initial diagnosis. H and I, First follow-up. J and K, Second follow-up. A, H, J: bone marrow aspirate smear, Wright stain, $\times 500$; B: bone marrow biopsy, H&E, $\times 400$; C, D, E, I, K: immunohistochemical stains, $\times 200$; C: E-cadherin; D, I, K: p53; E: CD61; F: flow cytometry selected dot plots (left, nondebris; right, mononuclear cell gate): red is CD45-dim blast gate, positive for CD36 and CD117; blue is lymphoid gate; green is monocyte gate; G: *TP53* mutation, sequencing result displayed in the Integrative Genomics Viewer (IGV version 2.8.13, Broad Institute, part of the screenshot). See text for more details of each image.

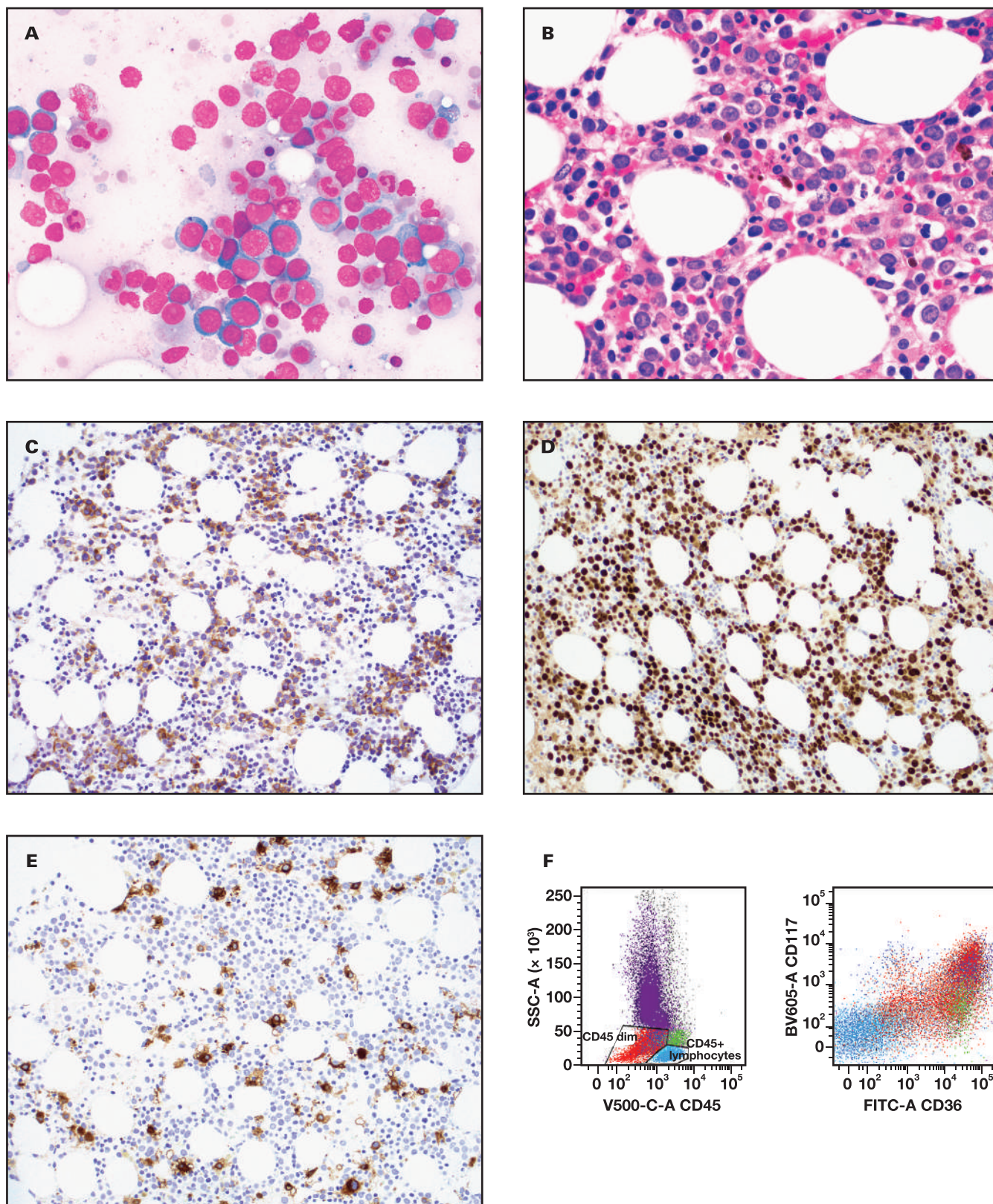
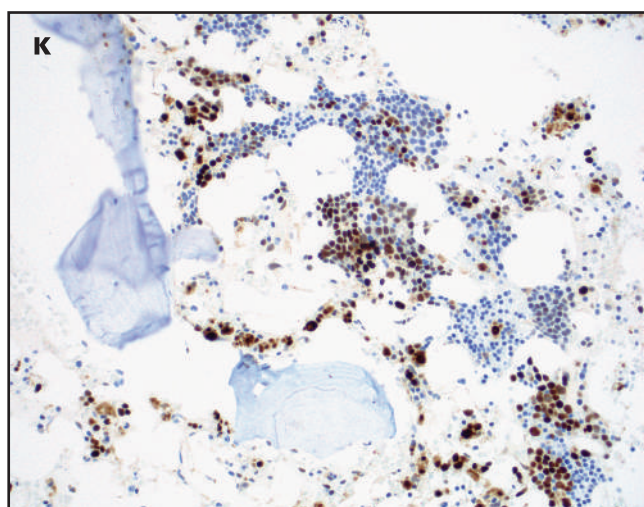
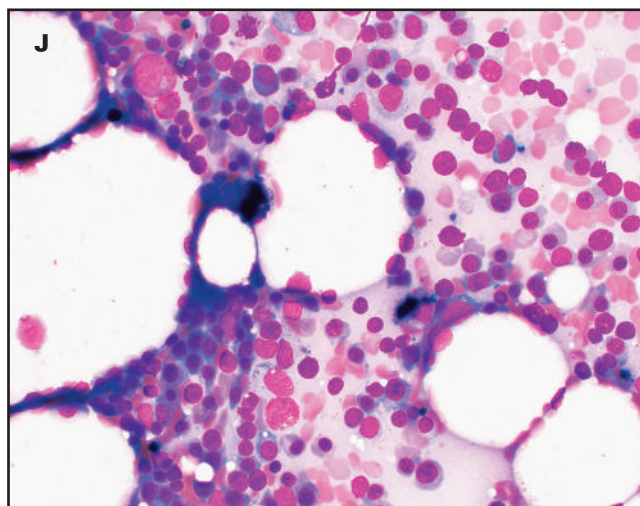
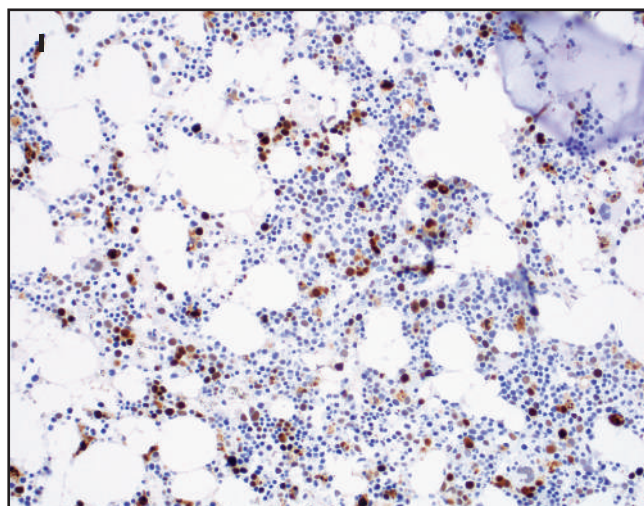
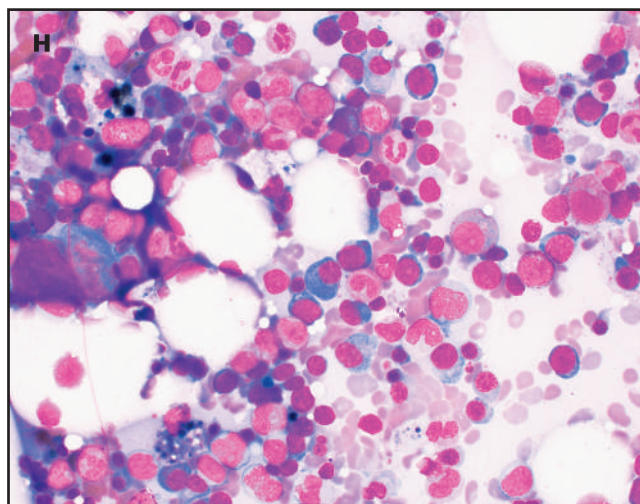
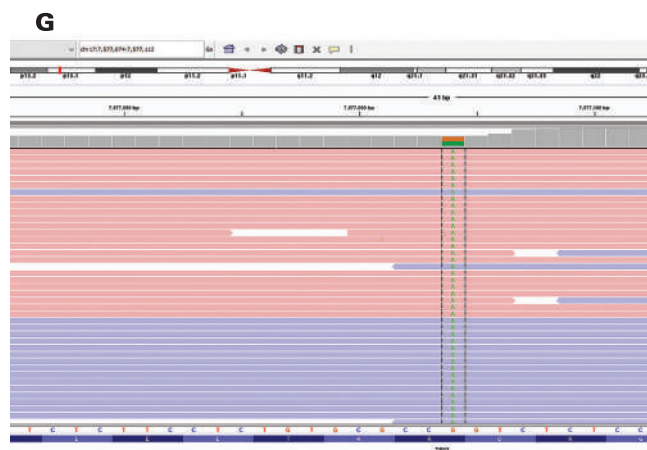


FIGURE 1. (cont)



20 kb, with 1182 nucleotides in the coding sequence, and translates to the p53 protein of 393 amino acids. The protein p53 contains 4 functional domains⁷ (FIGURE 2): a transactivation domain (amino acids

6-29), a DNA-binding domain (amino acids 95-288), an oligomerization domain (amino acids 318-358), and a C-terminal domain that regulates DNA binding (amino acids 357-393). The protein p53 is a key regulator

TABLE 1. Classification of Myelodysplastic Syndrome/Neoplasm (MDS) and Acute Myeloid Leukemia (AML) With *TP53* Mutations: Similarities and Differences Between WHO-HAEM5 and ICC⁴⁻⁶

Entity	Blast percentage	<i>TP53</i> mutation(s)	Note
WHO-HAEM5			
MDS with biallelic <i>TP53</i> inactivation (MDS-bi <i>TP53</i>)	<20% BM and PB	Two or more <i>TP53</i> mutations, or 1 mutation with evidence of <i>TP53</i> copy number loss or cnLOH ^a	Frequently associated with complex karyotype Not defining AML entity
Acute erythroid leukemia (AEL)	Erythroid lineage usually ≥80% of bone marrow elements, of which ≥30% are proerythroblasts.	Evidence of <i>TP53</i> mutation is a desirable diagnostic criterion	Detection of <i>TP53</i> mutation and the presence of a complex karyotype provides supportive data
ICC			
MDS with mutated <i>TP53</i>	0%-9% BM and PB	1. Multihit <i>TP53</i> mutation ^b or 2. <i>TP53</i> mutation (VAF > 10%) and complex karyotype	1. Monoallelic <i>TP53</i> mutations without complex karyotype is not included 2. Complex karyotype, although often present with <i>TP53</i> loss, is not required
MDS/AML with mutated <i>TP53</i>	10%-19% BM or PB	Any somatic <i>TP53</i> mutation (VAF > 10%)	Multihit not required
AML with mutated <i>TP53</i>	≥ 20% BM or PB Or PEL ^c		

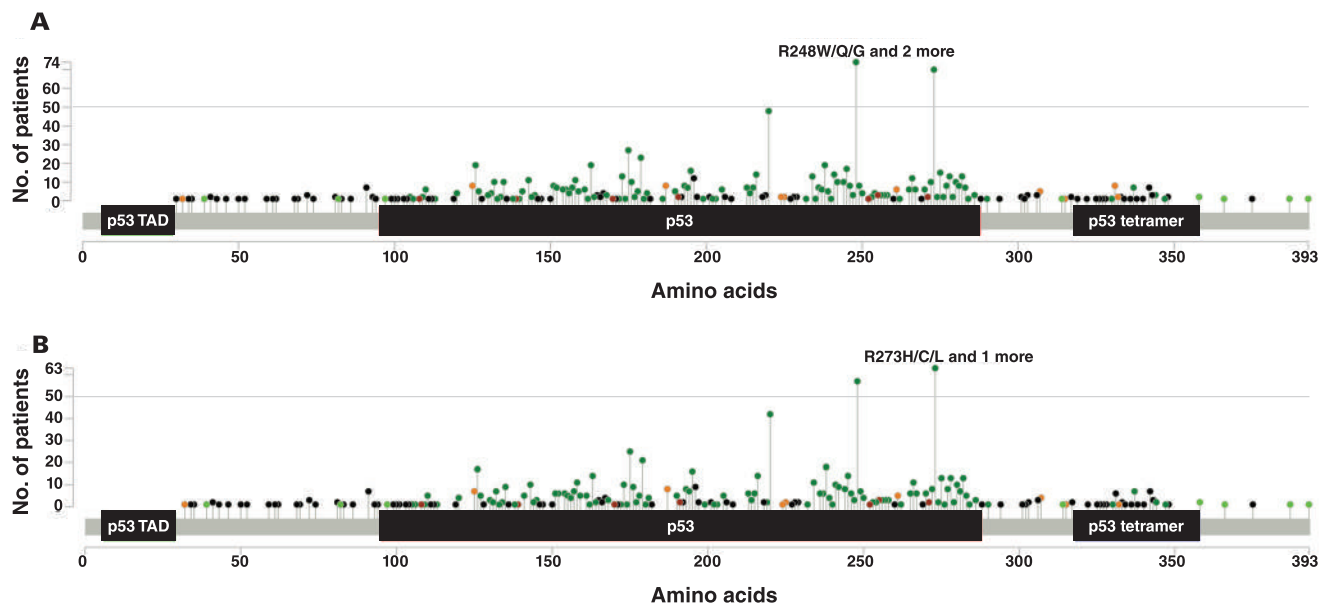
BM, bone marrow; ICC, International Consensus Classification; PB, peripheral blood; PEL, pure erythroid leukemia; VAF, variant allele frequency; WHO-HAEM5, World Health Organization Classification of Tumors of Haematopoietic and Lymphoid Tissues, 5th Edition.

^aA *TP53* VAF ≥ 50% may be regarded as presumptive (not definitive) evidence of copy loss on the trans allele or copy-neutral loss of heterozygosity when a constitutional *TP53* variant can be ruled out.

^bMultihit: 2 distinct *TP53* mutations (each VAF > 10%) or a single *TP53* mutation with (1) 17p deletion on cytogenetics, (2) VAF >50%, or (3) copy-neutral LOH (cn-LOH) at the 17p *TP53* locus.

^cThe blast percentage requirement for PEL is different from that of other types of AML. PEL is classified as “acute erythroid leukemia” under AML in WHO-HAEM5.

FIGURE 2. Distribution of *TP53* mutations in myeloid neoplasms. Figure generated from cBioportal online tool with the American Association for Cancer Research (AACR) GENIE Cohort v15.0-public dataset.⁸⁻¹⁰ A, All myeloid neoplasms. B, Myelodysplastic syndrome/neoplasm and acute myeloid leukemia. Color representations are dark green: pathogenic/likely pathogenic missense variants; light green: missense variants of uncertain significance; black: truncation mutations; brown: inframe insertions or deletions; orange: splice site variants.



of cell proliferation and apoptosis in response to DNA damage. It forms a tetramer via the oligomerization domain, binds to specific DNA sequences (p53 response elements), and activates transcriptional processes through the transactivation domain. In cases where DNA damage is beyond repair, p53 promotes apoptosis and eliminates the terminally damaged cells.

Germline *TP53* mutations contribute to a predisposition to cancer development with a broad phenotypic spectrum. The mutation spectrum of *TP53* has been extensively studied in Li-Fraumeni syndrome (LFS; OMIM 151623),¹¹ and a *TP53* Mutation Database has been curated and maintained at the National Cancer Institute in Bethesda, MD.¹² The majority (approximately 71%) of germline *TP53* mutations are missense

TABLE 2. Mutations in TP53 in Myeloid Neoplasms vs Myelodysplastic Syndrome/Neoplasm (MDS) + Acute Myeloid Leukemia (AML) (Genie Dataset)^{8,a}

Type of genetic alterations	All myeloid neoplasms (13,657/7523)	MDS + AML (9467/5081)	tMN (818/425)	MDS/MPN (741/479)	MPN (2836/1811)
CNV (No. of samples)	30/9153	26/6220	8/651	1/466	0/1938
Mutations (patients/samples) Total (%)	778 (10.34%)/ 1202 (8.80%)	682 (13.42%)/ 1058 (11.18%)	139 (32.71%)/ 224 (27.38%)	17 (3.54%)/ 21 (2.83%)	60 (3.31%)/ 78 (2.75%)
Missense	1209	1072	240	23	70
Truncation	232	213	44	3	7
In-frame	21	20	3	0	0
Splice site	73	59	9	1	9
Fusion	3	2	1	0	1
Most common mutations ^b					
R248W/Q/G/Lfs*20/P	74	57	11	2	10
R273H/C/L/S	70	63	18	0	5

AML, acute myeloid leukemia; CNV, copy number variation/alteration; MDS, myelodysplastic neoplasms/syndrome; MDS/MPN, myelodysplastic/myeloproliferative neoplasm; MPN, myeloproliferative neoplasm; tMN: therapy-related myeloid neoplasm.

^aThe numbers under each disease category are (samples/patient); some patients had more than 1 sample profiled.

Data retrieval links (accessed 15 February 2024):

All myeloid neoplasms: <https://genie.cbioportal.org/study?id=65ac3063b01fff74fbb7643f>.

MDS + AML: <https://genie.cbioportal.org/study?id=65ac3721b01fff74fbb7644a>.

tMN: <https://genie.cbioportal.org/study?id=65ac32241095f74ff799da14>.

MDS/MPN: <https://genie.cbioportal.org/study?id=65ac42f41095f74ff799da25>.

MPN: <https://genie.cbioportal.org/study?id=65ac41831095f74ff799da22>.

^bMutations with first and second highest prevalence in each category of myeloid neoplasms. The nomenclature uses only amino acid changes represented as 1-letter abbreviation, as available in the American Association for Cancer Research (AACR) GENIE dataset (see **FIGURE 2**).

mutations that predominantly affect exons 5 through 8, which encode the DNA-binding domain. These missense mutations most frequently result in altered p53 with dominant-negative effects, interfering with the function of the wild-type (WT) protein. Most individuals with missense mutations retain the WT allele; this “single-hit” dominant negative effect forms the basis of the autosomal dominant inheritance of LFS. In contrast, null mutations, including nonsense mutations, splicing mutations, deletions, and insertions, lead to truncated and non-functional p53 proteins. Most tumors with null mutations exhibit loss of the WT allele, resembling malignancies resulting from other tumor-suppressor gene mutations, with an autosomal recessive inheritance pattern.⁷ A few “hotspot mutations,” including R175H, G245S, R248Q, R248W, R249S, R273H, R273S, and R282W, are well-recognized.

Mutant p53 proteins have been primarily categorized as contact, in which substituted amino acid was directly involved in the interaction with DNA (eg, R273H), or structural, resulting in a global effect on the protein structure (eg, R175H). Based on the functional test of p53 single amino acid substitutions expressed in yeast, TP53 mutations are classified into the following categories¹³: (1) loss of function; (2) partial function and/or temperature sensitive; (3) WT-like or super transactivating; (4) altered specificity (active or partially active on some targets but inactive on others); and (5) dominant-negative, inhibiting the WT protein in a heterozygous condition. Generally, the severity of the deficiency in transactivation capability is associated with cancer proneness syndromes (eg, LFS). Despite the relative complexity of the TP53 mutation pattern, these mutations can be classified as disruptive and nondisruptive; disruptive mutations likely lead to a complete loss of activity and nondisruptive mutations encode proteins that retain some of the original functions. However, the association between TP53 mutation type and prognosis is significantly variable in different malignancies.

Additionally, some mutant p53 proteins may acquire novel oncogenic activities that are not shared with the WT protein, known as gain-of-function (GOF) mutations.

Among the cancer-related somatic mutations, TP53 is the most frequently mutated gene in human cancer.¹⁴ The prevalence of TP53 mutations in tumor samples from 10,000 cancer patients is 42%.¹⁵ The spectrum, functional consequences, and clinical significance of somatic TP53 mutations in malignant tumors are similar to but more complicated than germline mutations. The majority of TP53 mutations found in malignant tumors are hotspot mutations occurring in the DNA binding domain.¹⁴ TP53 loss due to loss of chromosome 17 or whole-arm 17p deletion [del(17p)] with or without other structural abnormalities are more frequently seen as somatic changes and rarely occur as germline abnormalities. The prevalence of TP53 mutation, the types of nucleotide changes (transition vs transversion), and the types of mutations (missense vs truncation) show variable characteristics in different cancer types.¹⁵ Interestingly, mutated p53 is typically stabilized and expressed at high levels in cancer cells; therefore, IHC staining of p53 has been widely used in histopathologic diagnosis, classification, and risk stratification of human cancers.¹⁶ In general, the expression of p53 is negatively correlated with the overall survival of patients with cancer.

Prevalence of TP53 Mutations in Myeloid Neoplasms

Similar to other malignancies, TP53 mutations have been extensively studied in myeloid neoplasms. Myeloid neoplasm cases cataloged in the Genie public database⁸ provide a good representation of somatic mutations associated with myeloid neoplasms (**TABLE 2**). A total of 13,657 samples of myeloid neoplasms were retrieved from the American Association for Cancer Research (AACR) GENIE Cohort v15.0-public, encompassing various types of myeloid neoplasms, with 52.4%

leukemia, 20.8% MPN (including chronic myeloid leukemia, *BCR::ABL1* positive), 18.7% MDS, 5.4% MDS/MPN, 2.6% blood cancer (not otherwise specified), and <0.1% myeloid neoplasms with germline predisposition. When specifically considering cases of MDS and AML, a subset of 9467 samples was retrieved, with 70.3% AML and 29.7% MDS. *TP53* alterations are less frequent in MPN and MDS/MPN cases, even when the patients develop myelofibrosis.¹⁷ Myeloid neoplasms, including MDS, AML, and MDS/MPN, occurring in patients with a history of exposure to cytotoxic chemotherapy and/or radiation therapy have been classified into a separate entity due to their generally poor prognosis. Several studies have reported a high prevalence of *TP53* mutations in therapy-related myeloid neoplasms (tMNs). A study of 108 tMN patients from the MD Anderson Cancer Center revealed *TP53* mutations in 40 (37%) patients, a significantly higher occurrence than in patients with de novo MDS/AML (62/428, 14.5%).¹⁸ In 311 therapy-related MDS (tMDS) patients selected for hematopoietic stem cell transplantation (HSCT), *TP53* mutations were detected in 38% of cases (vs 14% in primary MDS).¹⁹ A similar prevalence of *TP53* mutations (32.71%) is also observed in tMN cases documented in the AACR Genie public dataset (TABLE 2). A recent study observed particularly frequent *TP53* mutations in tMN following poly (ADP-ribose) polymerase inhibitor (PARPi) therapy among patients with breast and/or ovarian cancers. Thirty-two of 45 (71.1%) post-PARPi tMN cases harbored *TP53* mutation(s), of which 24 (75%) were multihit mutations.²⁰ Further studies are required to confirm the conclusion of this study and determine the mechanism resulting in a high prevalence of *TP53* mutations in tMNs post-PARPi.

***TP53* Mutation Patterns in Myeloid Neoplasms**

As displayed in the lollipop graph (FIGURE 2), although a few hotspot mutations are conspicuously more prevalent, mutations are distributed broadly along the whole coding sequence of *TP53* gene, more frequently in DNA binding and oligomerization domains, and characteristically rare in the transactivation domain and C-terminal region. Of note, alterations involving *TP53* include mutations of narrow definition (SNV, MNV, small indel), as well as SVs and copy number variants (CNVs). Complex cytogenetics and allelic imbalances at the *TP53* locus are frequently associated with *TP53* mutations in MDS and AML.^{2,21} The Genie public dataset was mostly generated using high-throughput short-read sequencing methods that are not sensitive in detecting SVs and CNVs. Although the prevalence of SNV/MNV and small indels may be accurate in the Genie dataset, the reported SVs and CNVs are underestimated.

Prognostic Implications of *TP53* Mutations in Myeloid Neoplasms

Numerous studies have demonstrated that genetic abnormalities of *TP53* in myeloid neoplasms are associated with chemotherapy resistance and poor clinical outcomes, with some subtle differences observed in the results of different studies.^{22–25} AML with *TP53* mutation is commonly observed in older adults. Although patients with AML carrying *TP53* mutations display no unique clinical presentations or pathological features compared with other forms of AML, they respond poorly to conventional anthracycline-based (7 + 3) combined chemotherapy, hypomethylating agent-based regimens, and venetoclax-based therapies.²⁶ The *TP53* mutation was recognized as the most significant poor prognostic factor in the IPSS-M for MDS.³ A *TP53* VAF $\geq 10\%$ and multiple *TP53* mutations were also associated with significantly poor

survival in MDS patients who received HSCT.¹⁹ These clinical studies formed the basis for WHO-HAEM5 and ICC to promote *TP53* as one of the molecular genetic abnormalities defining certain subtypes of myeloid neoplasms. However, as demonstrated in the presented case vignette, there are still challenges to applying *TP53* mutation in clinical diagnosis and classification of myeloid neoplasms. Although considered a separate entity in myeloid neoplasms, there were no significant differences in *TP53* mutation patterns in tMN compared with de novo MDS/AML.¹⁸ Similar to de novo MDS/AML, *TP53* mutations have been associated with a complex karyotype and inferior overall survival in tMN.¹⁸ A poorer survival associated with the presence of *TP53* mutations was also observed in tMDS patients receiving HSCT, whereas tMDS patients without *TP53* mutations had similar survival to primary MDS patients.¹⁹

A study on the mechanism of tMN suggested that cytotoxic therapy-induced DNA damage may not be the major cause of tMN. *TP53* mutations present in hematopoietic stem/progenitor cells (HSPCs) prior to cytotoxic chemotherapy or radiation therapy likely contribute to the development of tMN.²⁷ *TP53* mutations have been identified as age-related mutations in clonal hematopoiesis of indeterminate potential (CHIP),²⁸ and it was predicted that 44% of healthy individuals aged 50 years may have at least 1 HSPC that carries a randomly generated, functional *TP53* mutation.²⁷ CHIP has been associated with a proinflammatory state and linked to an increased risk of cardiovascular diseases.^{28,29} *TP53* mutation-mediated CHIP was confirmed to confer increased risk for atherosclerotic disease by an animal study.³⁰ However, at low allele frequencies, *TP53* mutations do not increase the risk of developing myeloid neoplasms.^{31,32} Rare HSPCs carrying age-related *TP53* mutations may be resistant to cytotoxic therapy and expand preferentially after treatment, thereby inducing the development of tMN.²⁷ These varied consequences of *TP53* mutations at low allele frequencies further complicate the interpretation of *TP53* mutations in clinical cases.

The Concept and Practical Utility of Biallelic or Multihit *TP53* Mutations

Based on the assumption that biallelic rather than single *TP53* hits are directly leukemogenic,³³ WHO-HAEM5 uses the term biallelic *TP53* inactivation to define a category of high-risk MDS. The molecular definition of biallelic mutations is the presence of 2 mutations in separate alleles of a gene. When more than 1 mutation is detected involving *TP53*, there can be several patterns of multiple hits. Although a biallelic mutation is the most likely pattern, it is also possible that 2 mutations occur on the same allele (cis mutations), and mutations occur in separate subclones harboring 1 mutation (mosaicism). Unless the 2 mutations occur close enough on the DNA sequence to be identified within a single sequencing read, the current molecular genetic tests available in clinical laboratories cannot reliably recognize biallelic mutations/alterations. When 2 or more different mutations occur in separate cells, subclonal mosaicism cannot be consistently recognized, unless single-cell sequencing is performed. In this sense, using the term multihit mutations to report test results is more accurate for clinical diagnostic laboratories. Furthermore, unless the test methods reliably detect all mutations affecting p53 function, identifying only a single mutation in *TP53* does not always indicate a monoallelic mutation. Multihit mutations may be missed when the VAF or the percentage of neoplastic subclones is low. A typical

example is the failure to detect low percentage loss of heterozygosity (LOH) by an SNV array when the clonal size is below the limit of analytic sensitivity. Additionally, as found in LFS studies, many missense mutations in *TP53* function as dominant negative proteins, impairing the activity of the remaining WT protein. A mutant p53 with GOF may also have a dominant effect. In these situations, a biallelic mutation may not be required to alter the p53 function.

In the published literature,²⁴ multihit alterations are assumed to be biallelic when the following abnormalities are present: (1) 2 or more alterations with combined VAF >50% (monoallelic *cis* mutations are disregarded); (2) at least 1 mutation coexists with del(17p), 17p LOH, or uniparental disomy (UPD), or monosomy 17; and (3) 1 mutation with allele frequency higher than 55%. Bahaj et al³⁴ reported 36% of *TP53*-mutated MDS and AML patients had single hits, whereas 64% exhibited double hits; patients with *TP53* double-hit mutations, whether missense and/or truncated, had a worse overall survival (OS) than those with single *TP53* hits. The difference in OS is more obvious in MDS cases. To fine-tune the VAF cutoff to separate the questionable cases into likely monoallelic vs likely biallelic, the study applied a random forest regression analysis, using survival as a surrogate marker for *TP53* allelic status, and found that a combined VAF cutoff of 23% was optimal for separating monoallelic and biallelic *TP53* mutations. The study proposed to separate *TP53* mutation status into 3 groups based on VAF: A, “obligatory” biallelic ($\geq 50\%$); B, “probable biallelic” 23% to <50%; and C, “probable monoallelic” combined <23%. Groups A and B were both associated with poor prognosis compared with the WT group, whereas the prognosis of group C was in between. In addition to VAFs, the association between mutation types and their functional and clinical consequences has been studied. Irrespective of the genetic configuration, *TP53* mutations were associated with worse OS. However, no significant differences were observed in OS between truncated and missense *TP53* mutations, or between canonical and noncanonical missense *TP53* mutations. In another study, by Dutta et al,³⁵ the functional impact of different types of *TP53* mutations was assessed in AML using 4 different scoring systems: (1) missense vs other types (nonsense, splice site, insertions, and deletions); (2) “disruptive” vs “nondisruptive,” whereas disruptive was defined by a premature stop or mutations occurred within DNA binding domain and replacement of an amino acid from a polarity/charge category by an amino acid from another category, and nondisruptive mutations were those occurring outside the binding domains or within the domains but with no change in polarity/charge category; (3) based on the evolutionary action score (EAp53) for missense mutations; and (4) relative fitness score (RFS), developed specifically for *TP53* mutations in the DNA-binding domain based on in vitro growth assays.³⁶ They found that only RFS was significantly associated with OS and event-free survival rates. Another study by Kanagal-Shamanna et al³⁷ found that EAp53 was associated with the clinical outcome of MDS. Although more studies are required to reach a consensus on interpreting the functional and clinical significance of specific types of *TP53* mutations, multihit mutations are not always required as driver mutations or to inactivate p53 function. Studies have confirmed that double hits are not necessary for association with poor prognosis in AML.³⁸ Therefore, when interpreting *TP53* mutation results, it is important to recognize that each mutation may have different effects, which may also be influenced by clinical and other genetic background of a specific patient.

In summary, the definition of biallelic *TP53* inactivation has not been standardized. “Multihit *TP53* mutation” is a more accurately descriptive

term for clinical laboratories until advances in technology make it possible to accurately recognize most, if not all, biallelic *TP53* mutations. To aid oncologists in achieving a better understanding of the mutation status, the allele frequencies of each mutation should be reported, and the likely functional consequences discussed in the mutation profiling report whenever possible.

Practical Approaches to Laboratory Testing of *TP53* Mutations for Samples of Myeloid Neoplasms

Given the various types and patterns of *TP53* mutations resulting in the disruption or GOF of the p53 protein, none of the single-molecule genetic test methods routinely available in clinical laboratories can detect all significant *TP53* mutations. To establish the most suitable approach for *TP53* mutation testing in myeloid neoplasms, a comprehensive understanding of the strengths, limitations, overall clinical performance, and cost-effectiveness of available molecular genetic test methods is necessary.

Cytogenetic Methods

Despite its low resolution and suboptimal analytic sensitivity, conventional G-band karyotyping remains the standard method for detecting complex karyotypic abnormalities. Fluorescence in situ hybridization (FISH) has higher analytic sensitivity in identifying del(17p) or monosomy 17; however, it does not provide a comprehensive genome-level profile and may not fully detect complex karyotypes. Several studies have indicated that when karyotyping yields satisfactory results for 20 cells, FISH does not significantly enhance the sensitivity of detecting chromosome abnormalities in MDS and AML.

SNV-copy number (SNV-CN) arrays offer improved resolution for detecting CN abnormalities and have the unique advantage of being able to identify LOH or UPD. However, SNV-CN arrays have limitations in detecting balanced translocations when the genetic material loss falls below the resolution of these assays. Nevertheless, this limitation does not typically affect the detection of *TP53* allele loss. Optical genome mapping (OGM) is a novel molecular karyotyping method to evaluate MDS and AML. OGM has demonstrated excellent performance in detecting SVs, complex karyotypes, and copy-neutral LOH in a study involving 101 MDS patients.³⁹ A multicenter study involving 100 AML cases reported diagnostic outcomes equivalent to, and in some cases superior to, standard-of-care technologies (conventional karyotyping, FISH, and/or arrays) in identifying all clinically relevant SVs and CNVs when representative clones were present in >5% allelic fraction. OGM has also shown improved performance in detecting *TP53* allele loss in some cases.⁴⁰ Consequently, OGM has the potential to replace conventional karyotyping, FISH, and arrays as a molecular karyotyping method for MDS and AML.^{41,42}

Sequencing Methods

Previously, Sanger sequencing was considered the gold standard for detecting *TP53* mutations, particularly germline variants, including SNV, MNV, indels, and translocations. Sequencing the entire gene for clinical testing is unnecessary and impractical. Targeted Sanger sequencing of specific regions or using complementary DNA may identify nearly all clinically significant germline mutations. Nevertheless, the inadequate analytic sensitivity of Sanger sequencing in detecting somatic mutations with VAF <20% restricts its utility in MDS, AML, and

other malignancies. With the adoption of massive parallel sequencing technology in clinical diagnostic laboratories, NGS has become the new gold standard for detecting *TP53* and other gene mutations. It enables the detection of different types of mutations with high analytic and diagnostic sensitivity without compromising specificity. However, with a higher sequencing depth than whole exome sequencing (WES) or whole genome sequencing (WGS), NGS methods used in clinical laboratories typically target a panel of genes by short-read sequencing, which may have compromised performance in detecting large indels, SVs, and CNVs. Additionally, the analytic sensitivity of NGS, unless specifically designed with a paired bioinformatics pipeline, may miss subclones harboring mutations at low allele frequencies. When applying WES or WGS to detect all potential driver mutations in the human genome, the limit of detection is an important consideration.⁴³ For follow-up studies and MRD monitoring, deep sequencing with specialized informatics analysis or targeted polymerase chain reaction (PCR)-based methods may be required.

Another critical aspect of NGS is the interpretation of the clinical significance of the detected variants. For relatively common *TP53* mutations, evidence-based online databases, such as cBioPortal⁴⁴, OncoKB⁴⁵, and CKBboost⁴⁶, can provide well-vetted information to facilitate clinical interpretation. NGS tests can detect germline *TP53* mutations and often detect sequence variants that are not well documented or characterized, which are currently classified as variants of unknown significance (VUSs). VUSs encompass somatic and germline sequence variants with a broad spectrum of oncogenic potentials, ranging from likely benign to likely pathogenic, but lack sufficient evidence to support their oncogenicity. Interpreting the clinical significance of *TP53* mutations, including germline variants, based on current guidelines poses significant challenges.^{47–49} Considering the potential dire consequences of missing an oncogenic *TP53* mutation, we typically adopt an aggressive approach. When unable to distinguish a VUS from a benign variant, we tend to lean towards considering it as a VUS. Another challenge is the interpretation of low VAF *TP53* mutations, which may represent CHIP not directly related to the neoplastic process.²⁸ It is critical to effectively communicate these concepts to the clinical team and to clarify the decision regarding the reported *TP53* variants. In cases where a variant is considered potentially germline (with a VAF close to 50% or 100%), it is advisable to include a recommendation in the sequencing report to test the variant using cells uncontaminated by hematolymphoid cells, preferably cultured skin fibroblasts, to confirm or rule out a germline mutation.

Immunohistochemical Stains

Given that molecular genetic methods for detecting *TP53* mutations are typically time-consuming and tests aimed at detecting all *TP53* alterations are not widely available in clinical laboratories, the possibility of using IHC staining as a cost-effective alternative for rapid screening of *TP53* mutations has been studied by several groups. Strong correlations were observed between strong nuclear p53 staining in the bone marrow biopsy core and *TP53* alterations detected by molecular genetic methods, as demonstrated in our index case. Myeloid neoplasms with wild-type *TP53* usually display weak and heterogeneous staining in scattered cells.^{50–52} McGraw et al⁵³ studied 13 MDS and 9 AML cases with myelodysplasia-related change cases with *TP53* mutations detected by NGS and compared them to 27 MDS and 5 AML-myelodysplasia-related change patients without *TP53* mutations. The study found that

the sensitivity and specificity in predicting *TP53* mutation status were 59.1% and 100%, respectively, using an IHC score cutoff of 1.0%, and 77.3% and 100%, respectively, when using a cutoff of 0.5% positive cells. Furthermore, p53 expression was significantly associated with *TP53* mutant VAF in MDS cases. They proposed that both the percentage of positive cells and the staining intensity should be taken into account when interpreting the results. Fernandez-Pol et al⁵² studied 143 cases of AML for p53 expression and its concordance with *TP53* mutation status. At a threshold of >5%, the sensitivity was 0.83 and specificity approached 0.89, whereas at a 15% threshold, the sensitivity was 0.5 and specificity 0.94, respectively. Similarly, Ruzinova et al⁵⁴ studied 73 cases of MDS and AML receiving decitabine therapy and showed that immunostaining had a sensitivity of 75% and specificity of 91% in detecting *TP53* mutations at a cutoff value of >10% of p53-positive cells. Fitzpatrick et al⁵¹ evaluated 142 cases of newly diagnosed AML to correlate p53 immunostaining with the presence of *TP53* mutations. Receiver operating characteristic curve analysis revealed that ≥3% strongly stained cells had the highest overall performance in distinguishing *TP53*-mutated cases from *TP53* WT cases. A higher threshold of 7% positive strong nuclear staining provided 100% specificity and a positive predictive value, with a sensitivity of 67% and a negative predictive value of 90%. Surprisingly, digital analysis did not consistently provide a superior evaluation compared with manual microscopic examination.⁵⁵ Although *TP53* mutation VAF and the percentage of IHC-positive cells may not significantly correlate at the initial diagnosis, changes in the percentage of IHC-positive cells closely paralleled changes in *TP53* mutation VAF levels.⁵⁵ As observed in our index case, an abnormal staining pattern with an increased number of positive cells after treatment indicates likely residual disease.

IHC staining is routinely available in almost all anatomic pathology laboratories; however, the staining results are known to be influenced by various factors, such as laboratory settings, antigen retrieval methods, antibodies used, and experimental protocols. The threshold for positive p53 staining correlating with *TP53* mutations varies among laboratories. Previous studies have highlighted the importance of considering factors such as the percentage of positive cells, signal intensity, and immunostaining scores when interpreting p53 IHC results. Notably, approximately 12.6% of *TP53* variants are predicted to produce truncated proteins that may be undetectable by p53 IHC, and an additional 10% of *TP53* mutations occur at splice sites or untranslated regions, which could variably affect protein expression. Consequently, the incidence of mutations that are likely undetectable by IHC is estimated to be 20%–25%.⁵⁴ The absence of staining with different anti-p53 antibodies may be associated with either *TP53*-WT or truncating mutations.⁵¹

Laboratory Workflow Considerations

Conventional karyotyping, a method that requires viable cells to be cultured in vitro to generate metaphase chromosomes for analysis, is influenced by the proliferative potential of different malignant clones. Other molecular genetic methods that do not require viable cell culture are affected by the quality of the sample being analyzed. Techniques such as FISH, microarray, and NGS are performed directly on aspirate samples. In cases where the bone marrow has significant hemodilution, the percentage of the neoplastic myeloid population and blasts in the aspiration may not be representative, and the associated mutant allele frequency may not accurately represent the underlying myeloid neoplasm. There are also situations such as myeloid

sarcoma or extramedullary presentations of MDS and AML, where bone marrow aspirate samples contain no or rare neoplastic cells for molecular genetic testing. FISH, NGS, and PCR-based molecular tests can be performed effectively on formalin-fixed paraffin-embedded (FFPE) tissue sections. However, it is important to validate the test performance before applying the same test that has been established for fresh samples to FFPE tissue, ensuring that molecular genetic testing maintains its reliability and accuracy.

Given that none of the tests routinely available in clinical laboratories can reliably detect all genetic alterations involving *TP53* and affecting p53 protein function, each laboratory must establish a protocol for a reasonable workflow to identify *TP53* mutations in different sample types of myeloid neoplasms. Based on our experiences, we present practical approaches that combine different methods to detect *TP53* mutations:

1. For samples from cases suspected of myeloid neoplasms, chromosome analysis and NGS with a panel of genes targeting mutations frequently associated with myeloid neoplasms, including *TP53*, should be routinely performed.
2. After morphologic review and immunophenotypic analysis, if a diagnosis of MDS or AML is considered, IHC staining of p53 may be considered in selected cases that need quick screening of *TP53* mutations. Each laboratory should validate the staining protocol and performance parameters when using p53 expression as a surrogate marker for *TP53* alterations.
3. In cases with unsatisfactory chromosome analysis by G-band karyotyping (poor karyotype result, insufficient cells for karyotyping, etc), FISH tests for abnormalities frequently associated with myeloid neoplasms, including chromosome 17p probe to evaluate *TP53* copy number changes, are added.
4. Although not directly related to the detection of *TP53* mutations, in a subset of cases that require better evaluation of genetic profiles, SNP-CN array and/or OGM tests may be considered to add clinical sensitivity in detecting complex cytogenetic abnormalities.

To appropriately stratify available intensive therapy options, the National Comprehensive Cancer Network (NCCN) guideline for AML⁵⁶ requires expedited test results of molecular and cytogenetic analyses for immediate actionable mutations or chromosomal abnormalities in AML patients. A rapid turnaround time test (results available within 3-5 days of diagnosis) for mutations in a panel of genes critical to the early treatment decision for AML is desirable in tertiary medical centers or cancer centers. AML patients with mutated *TP53* are in the poor/adverse risk category. Although not yet a treatment target, *TP53* mutation is an important factor in guiding AML treatment and should be integrated into the rapid testing panel. It is also desirable to consider combined DNA and RNA-based NGS assays that not only cover mutations in *NPM1*, *IDH1*, *IDH2*, and *TP53*, but also common gene fusions that are usually detected by FISH-based methods. Notably, in the newest version of the NCCN guidelines for MDS⁵⁷, WES and WGS, although previously more used in clinical research settings, were included as recommended methods for additional molecular testing in a subset of patients with heritable hematologic malignancy predisposition. With the decreasing cost of NGS and advancements in sequencing coverage as well as data analysis pipelines, integration of WES and WGS in routine clinical testing may facilitate improvements in the molecular testing workflow.

Treatment Implications of *TP53* Mutations in Myeloid Neoplasms

Disruption of p53 function is associated with resistance to chemotherapy-induced cell death. As mentioned above, AML patients harboring *TP53* mutations respond poorly to standard intensive chemotherapy with cytarabine and anthracycline,⁵⁸ including the liposomal formulations Vyxeos⁵⁹ and FLAG.⁶⁰ Studies involving hypomethylation agents (HMAs) such as azacitidine, decitabine, or other investigational HMAs in the treatment of AML and MDS patients have yielded conflicting results. Some studies indicated that *TP53* mutations were associated with poor OS and had no significant impact on treatment response.⁶¹⁻⁶³ Other studies using decitabine demonstrated an improved response in *TP53*-mutated patients, although single-agent decitabine treatment failed to show significantly better durable overall survival than those without *TP53* mutations.^{64,65} A study on the predictors of response to azacitidine treatment revealed that posttreatment neoplastic clonal size is highly predictive of clinical outcome.⁶⁶ In most studies, the addition of the BCL2 inhibitor venetoclax to HMAs failed to show significant improvements in response rates and OS in *TP53*-mutated AML.^{26,67-71} A meta-analysis of multiple studies confirmed the limited clinical benefits of HMA or HMA + venetoclax in newly diagnosed treatment-naïve patients with *TP53* mutated AML.⁷² Similar results were observed in a limited number of MDS patients studied so far.⁷³ The conclusion for HMA + venetoclax in treatment-naïve or refractory/relapsed, *TP53*-mutated MDS will be revealed in larger clinical trials.^{73,74}

Allogeneic HSCT (alloHSCT) remains the only curative treatment for MDS and should be considered for all eligible patients when an appropriate donor can be identified. Post-alloHSCT survival in *TP53*-mutated MDS patients was significantly worse.¹⁹ Zhang et al⁷⁵ conducted a study on MDS patients in the Center for International Blood and Marrow Transplant Research (CIBMTR) registration with WGS data and found that among all the recurrent somatic mutations, *TP53* variants were the only factor associated with inferior OS. In the sensitivity analysis of 301 patients, they identified a set of 7 novel genomic regions that were associated with inferior OS; this set of genes was significantly enriched in the *TP53*-centered pathway. A few studies on alloHSCT for *TP53*-mutated AML also revealed a lower probability of survival compared with *TP53* WT cases.^{76,77} However, in a multicenter study of AML patients,⁷⁸ the probability of survival after alloHSCT did not significantly differ between patients with or without *TP53* mutations prior to transplant.^{19,78} Complete remission on day 100 posttransplant and the presence of chronic graft-vs-host disease are indicators of a better probability of survival. *TP53* mutations with concurrent complex karyotypes were associated with worse alloHSCT outcome.⁷⁹ Early disease recurrence is the main cause of posttransplant mortality in individuals with *TP53* mutations. Most patients with concurrent complex karyotypes relapsed within 12 months post-alloHSCT.⁷⁹ In patients who received allogeneic transplant after azacitidine treatment, postazacitidine clonal size <10% determined by *TP53* mutation appears to indicate a sustainable long-term survival.⁶⁶

Given the poor clinical outcomes of traditional chemotherapy, HMA, and venetoclax treatment available for MDS and AML, *TP53*-mutated MDS and AML patients ineligible for alloHSCT should be strongly recommended for enrollment in clinical trials with novel therapeutic agents. Currently, 2 major options for clinical trials are available for *TP53*-mutated MDS and AML: reactivation of p53 and related pathway, and promotion of immune-mediated killing of neoplastic cells.

Reactivating p53 and inducing apoptosis with eprenetapopt (APR-246), a small-molecule p53 activator, has shown promising results in early-phase clinical trials.^{80–82} A better response was associated with the absence of concurrent mutations in other genes, higher p53 expression determined by IHC, and posttreatment clearance of *TP53* mutations (VAF <5%).⁸⁰ However, a recent phase 3 trial of eprenetapopt (APR-246) + azacitidine vs azacitidine alone in patients with *TP53*-mutated MDS failed to meet the primary endpoint.^{83,84} In a phase 2 multicenter open-label clinical trial, eprenetapopt (APR-246) combined with azacitidine as maintenance therapy after allo-HCT in patients with mutated *TP53* AML or MDS was well tolerated and showed promising improvements in median OS.⁸⁵ Disruption of the interaction between p53 and MDM2 to activate the p53 pathway using the small molecular inhibitor idasanutlin (RG7388) is considered a targeting therapy option in AML with *TP53* mutation.⁸⁶ Early clinical trials combined with cytarabine⁸⁷ or venetoclax⁸⁸ reported marginal effects. Further studies on reactivating p53 pathway function with this approach are required.⁸⁹

Promoting immune activity against neoplastic myeloid cells is based on the finding that AML with mutated *TP53* displayed changes in the microenvironment and overexpression of immune checkpoint proteins.^{90–92} Clinical trials of immune checkpoint inhibitors have reported limited benefits so far.^{93,94} Although not specific, antibodies against CD47, TIM-3, and hybrid anti-CD3 and CD123 have shown promising results. Early clinical trials using magrolimab, an anti-CD47 immunoglobulin G4 monoclonal antibody, combined with azacitidine to synergistically promote phagocytosis of leukemic cells, with or without venetoclax, have shown promising responses for *TP53*-mutated AML.^{95–97} An early clinical trial using the TIM-3 antibody, sabatolimab, achieved a good response rate in high-risk MDS patients, including *TP53*-mutated cases.⁷³ Individuals with *TP53*-mutated AML showed a better response to immunotherapy with the hybrid CD3xCD123 antibody flotetuzumab than AML patients with WT *TP53*,⁹¹ although the number of cases was limited. Clinical trials for these antibodies are ongoing.

Although novel therapeutic agents targeting *TP53* mutations or promoting immune activity against neoplastic cells are being actively explored, clearly effective treatment for *TP53*-mutated MDS and AML is yet to be identified. It is crucial for clinicians to consider personalized approaches in enrolling these challenging cases of AML and MDS in clinical trials, with comprehensive knowledge of the molecular features of *TP53* mutations in each patient.

Conclusions and Future Perspectives

TP53 mutations have consistently been correlated with poor response to chemotherapy and dismal long-term survival outcomes. As advancements in therapeutic strategies are being developed to address these challenges,^{74,98} it has become imperative for molecular pathologists and hematopathologists to gain a comprehensive understanding of the various aspects of genetic alterations involving *TP53*. Despite extensive research and clinical investigations on *TP53* mutations in myeloid neoplasms, questions remain regarding whether *TP53* mutations represent a distinct pathobiology in the development of these malignancies. Current clinical inquiries have predominantly focused on multihit mutations and the association between mutant allele burden and clinical outcomes. Classification of myeloid neoplasms based on *TP53* mutations has primarily revolved around their prognostic implications. Clearance of some ambiguities in the definition of the subclassification,

particularly in the context of myeloid neoplasms characterized by prominent erythroid proliferation, is required for clinical practice.

The technical complexities inherent in *TP53* mutations and related genetic alterations that affect protein expression, structural integrity, and functional capacity present significant challenges. Currently, clinical diagnostic laboratories struggle to provide a comprehensive analysis of *TP53* mutations and related genetic alterations within a reasonable turnaround time. The future trajectory points toward the refinement and implementation of high-fidelity long-read sequencing, cost-effective WES and WGS, integration of microarray technologies, and OGM at a reasonable cost to overcome these hurdles.

The existing treatment for MDS and AML, including conventional chemotherapy, hypomethylation agents, the *BCL2* inhibitor venetoclax, and alloHSCT, has proven largely inadequate to achieve enduring remission and prolonged survival in *TP53*-mutated cases. Clinical trials exploring strategies to reactivate p53 function and enhance the immune-mediated clearance of neoplastic myeloid cells have demonstrated only marginal improvements in treatment efficacy within the limited datasets available in the literature. There is an urgent need to develop substantive therapeutic agents and targeted therapies tailored to the specific molecular pathobiology underlying *TP53* mutations in myeloid neoplasms. With the rapid advancement of molecular genetic technologies and improved prediction of protein functionality based on amino acid information, particularly in the context of drug development, it is reasonable to anticipate substantial progress in establishing standardized laboratory testing protocols to cover all *TP53* mutations and alterations involving *TP53* and refine the standard of care for clinical management of myeloid neoplasms with *TP53* mutations.

Conflict of Interest Disclosure

The authors have nothing to disclose.

REFERENCES

- Ley TJ, Miller C, Ding L, et al. Cancer Genome Atlas Research Network. Genomic and epigenomic landscapes of adult de novo acute myeloid leukemia. *N Engl J Med*. 2013;368(22):2059–2074. <https://doi.org/10.1056/NEJMoa1301689>
- Bernard E, Nannya Y, Hasserjian RP, et al. Implications of *TP53* allelic state for genome stability, clinical presentation and outcomes in myelodysplastic syndromes. *Nat Med*. 2020;26(10):1549–1556. <https://doi.org/10.1038/s41591-020-1008-z>
- Bernard E, Tuechler H, Greenberg PL, et al. Molecular international prognostic scoring system for myelodysplastic syndromes. *NEJM Evid*. 2022;1(7):EVIDoaa2200008. <https://doi.org/10.1056/EVIDoaa2200008>
- Khoury JD, Solary E, Abla O, et al. The 5th edition of the World Health Organization classification of haematolymphoid tumours: myeloid and histiocytic/dendritic neoplasms. *Leukemia*. 2022;36(7):1703–1719. <https://doi.org/10.1038/s41375-022-01613-1>
- Arber DA, Orazi A, Hasserjian RP, et al. International consensus classification of myeloid neoplasms and acute leukemias: integrating morphologic, clinical, and genomic data. *Blood*. 2022;140(11):1200–1228. <https://doi.org/10.1182/blood.2022015850>
- Wang W, Haferlach T. Acute erythroid leukaemia. Blue books online. 2022. Accessed May 9, 2024. <https://tumourclassification.iarc.who.int/chaptercontent/63/58>

7. Monti P, Menichini P, Speciale A, et al. Heterogeneity of TP53 mutations and p53 protein residual function in cancer: does it matter? *Front Oncol.* 2020;10:593383. <https://doi.org/10.3389/fonc.2020.593383>
8. AACR Project GENIE Consortium. AACR Project GENIE: powering precision medicine through an international consortium. *Cancer Discov.* 2017;7(8):818-831. <https://doi.org/10.1158/2159-8290.CD-17-0151>
9. Gao J, Aksoy BA, Dogrusoz U, et al. Integrative analysis of complex cancer genomics and clinical profiles using the cBioPortal. *Sci Signal.* 2013;6(269):pl1. <https://doi.org/10.1126/scisignal.2004088>
10. Cerami E, Gao J, Dogrusoz U, et al. The cBio cancer genomics portal: an open platform for exploring multidimensional cancer genomics data. *Cancer Discov.* 2012;2(5):401-404. <https://doi.org/10.1158/2159-8290.CD-12-0095>
11. Kratz CP, Freycon C, Maxwell KN, et al. Analysis of the Li-Fraumeni spectrum based on an international germline TP53 variant data set: an International Agency for Research on Cancer TP53 database analysis. *JAMA Oncol.* 2021;7(12):1800-1805. <https://doi.org/10.1001/jamaoncol.2021.4398>
12. National Cancer Institute (NCI) of the National Institutes of Health. *The TP53 Database.* (R20, July 2019). Accessed February 15, 2024. <https://tp53.isb-cgc.org>.
13. Kato S, Han SY, Liu W, et al. Understanding the function-structure and function-mutation relationships of p53 tumor suppressor protein by high-resolution missense mutation analysis. *Proc Natl Acad Sci U S A.* 2003;100(14):8424-8429. <https://doi.org/10.1073/pnas.1431692100>
14. Vaddavalli PL, Schumacher B. The p53 network: cellular and systemic DNA damage responses in cancer and aging. *Trends Genet.* 2022;38(6):598-612. <https://doi.org/10.1016/j.tig.2022.02.010>
15. Chen X, Zhang T, Su W, et al. Mutant p53 in cancer: from molecular mechanism to therapeutic modulation. *Cell Death Dis.* 2022;13(11):974. <https://doi.org/10.1038/s41419-022-05408-1>
16. Fang J, Yang Y, Xie L, Yin W. Immunological role of TP53 somatic mutation classification in human cancers. *J Oncol.* 2023;2023:1904309. <https://doi.org/10.1155/2023/1904309>
17. Verma T, Papadantonakis N, Peker Barclift D, Zhang L. Molecular genetic profile of myelofibrosis: implications in the diagnosis, prognosis, and treatment advancements. *Cancers (Basel).* 2024;16(3):514. <https://doi.org/10.3390/cancers16030514>
18. Ok CY, Patel KP, Garcia-Manero G, et al. TP53 mutation characteristics in therapy-related myelodysplastic syndromes and acute myeloid leukemia is similar to de novo diseases. *J Hematol Oncol.* 2015;8:45. <https://doi.org/10.1186/s13045-015-0139-z>
19. Lindsley RC, Saber W, Mar BG, et al. Prognostic mutations in myelodysplastic syndrome after stem-cell transplantation. *N Engl J Med.* 2017;376(6):536-547. <https://doi.org/10.1056/NEJMoa1611604>
20. Marmouset V, Decroocq J, Garcia S, et al; UNIHEM, French Network of Pharmacovigilance Centers, ALFA, FILO, and GFM. Therapy-related myeloid neoplasms following PARP inhibitors: real-life experience. *Clin Cancer Res.* 2022;28(23):5211-5220. <https://doi.org/10.1158/1078-0432.CCR-22-1622>
21. Bejar R, Stevenson K, Abdel-Wahab O, et al. Clinical effect of point mutations in myelodysplastic syndromes. *N Engl J Med.* 2011;364(26):2496-2506. <https://doi.org/10.1056/NEJMoa1013343>
22. Döhner H, Wei AH, Appelbaum FR, et al. Diagnosis and management of AML in adults: 2022 recommendations from an international expert panel on behalf of the ELN. *Blood.* 2022;140(12):1345-1377. <https://doi.org/10.1182/blood.2022016867>
23. Shah MV, Tran ENH, Shah S, et al. TP53 mutation variant allele frequency of $\geq 10\%$ is associated with poor prognosis in therapy-related myeloid neoplasms. *Blood Cancer J.* 2023;13(1):51. <https://doi.org/10.1038/s41408-023-00821-x>
24. Grob T, Al Hinai ASA, Sanders MA, et al. Molecular characterization of mutant TP53 acute myeloid leukemia and high-risk myelodysplastic syndrome. *Blood.* 2022;139(15):2347-2354. <https://doi.org/10.1182/blood.2021014472>
25. DiNardo CD, Erba HP, Freeman SD, Wei AH. Acute myeloid leukaemia. *Lancet.* 2023;401(10393):2073-2086. [https://doi.org/10.1016/S0140-6736\(23\)00108-3](https://doi.org/10.1016/S0140-6736(23)00108-3)
26. Kim K, Maiti A, Loghavi S, et al. Outcomes of TP53-mutant acute myeloid leukemia with decitabine and venetoclax. *Cancer.* 2021;127(20):3772-3781. <https://doi.org/10.1002/cncr.33689>
27. Wong TN, Ramsingh G, Young AL, et al. Role of TP53 mutations in the origin and evolution of therapy-related acute myeloid leukaemia. *Nature.* 2015;518(7540):552-555. <https://doi.org/10.1038/nature13968>
28. Jaiswal S, Fontanillas P, Flannick J, et al. Age-related clonal hematopoiesis associated with adverse outcomes. *N Engl J Med.* 2014;371(26):2488-2498. <https://doi.org/10.1056/NEJMoa1408617>
29. Marnell CS, Bick A, Natarajan P. Clonal hematopoiesis of indeterminate potential (CHIP): linking somatic mutations, hematopoiesis, chronic inflammation and cardiovascular disease. *J Mol Cell Cardiol.* 2021;161:98-105. <https://doi.org/10.1016/j.yjmcc.2021.07.004>
30. Zekavat SM, Viana-Huete V, Matesanz N, et al. TP53-mediated clonal hematopoiesis confers increased risk for incident atherosclerotic disease. *Nat Cardiovasc Res.* 2023;2:144-158. <https://doi.org/10.1038/s44161-022-00206-6>
31. Malcovati L, Galli A, Travaglino E, et al. Clinical significance of somatic mutation in unexplained blood cytopenia. *Blood.* 2017;129(25):3371-3378. <https://doi.org/10.1182/blood-2017-01-763425>
32. Weeks LD, Niroula A, Neuberg D, et al. Prediction of risk for myeloid malignancy in clonal hematopoiesis. *NEJM Evid.* 2023;2(5):1. <https://doi.org/10.1056/evidoa2200310>
33. Donehower LA, Soussi T, Korkut A, et al. Integrated analysis of TP53 gene and pathway alterations in the Cancer Genome Atlas. *Cell Rep.* 2019;28(5):1370-1384.e5. <https://doi.org/10.1016/j.celrep.2019.07.001>
34. Bahaj W, Kewan T, Gurnari C, et al. Novel scheme for defining the clinical implications of TP53 mutations in myeloid neoplasia. *J Hematol Oncol.* 2023;16(1):91. <https://doi.org/10.1186/s13045-023-01480-y>
35. Dutta S, Pregartner G, Rucker FG, et al. Functional classification of TP53 mutations in acute myeloid leukemia. *Cancers.* 2020;12(3):637. <https://doi.org/10.3390/cancers12030637>
36. Kotler E, Shani O, Goldfeld G, et al. A systematic p53 mutation library links differential functional impact to cancer mutation pattern and evolutionary conservation. *Mol Cell.* 2018;71(1):178-190.e8. <https://doi.org/10.1016/j.molcel.2018.06.012>
37. Kanagal-Shamanna R, Montalban-Bravo G, Class C, et al. Evolutionary action (EA) score of TP53 mutations defines prognostic subsets within TP53 mutated myelodysplastic syndromes and acute myeloid leukemia. *Blood.* 2019;134(suppl 1):1719. <https://doi.org/10.1182/blood-2019-130545>
38. Prochazka KT, Pregartner G, Rucker FG, et al. Clinical implications of subclonal TP53 mutations in acute myeloid leukemia. *Haematologica.* 2019;104(3):516-523. <https://doi.org/10.3324/haematol.2018.205013>
39. Yang H, Garcia-Manero G, Sasaki K, et al. High-resolution structural variant profiling of myelodysplastic syndromes by optical genome mapping uncovers cryptic aberrations of prognostic and therapeutic significance. *Leukemia.* 2022;36(9):2306-2316. <https://doi.org/10.1038/s41375-022-01652-8>
40. Gerding WM, Tembrink M, Nilius-Elliliwi V, et al. Optical genome mapping reveals additional prognostic information compared to conventional cytogenetics in AML/MDS patients. *Int J Cancer.* 2022;150(12):1998-2011. <https://doi.org/10.1002/ijc.33942>
41. He R, Wiktor AE, Hanson CA, et al. Conventional karyotyping and fluorescence in situ hybridization: an effective utilization strategy in diagnostic adult acute myeloid leukemia. *Am J Clin Pathol.* 2015;143(6):873-878. <https://doi.org/10.1309/AJCPP6LVMQG4LNCK>

42. Wheeler FC, Kim AS, Mosse CA, Shaver AC, Yenamandra A, Seegmiller AC. Limited utility of fluorescence in situ hybridization for recurrent abnormalities in acute myeloid leukemia at diagnosis and follow-up. *Am J Clin Pathol*. 2018;149(5):418-424. <https://doi.org/10.1093/ajcp/aqy002>
43. Miura T, Yasuda S, Sato Y. A simple method to estimate the in-house limit of detection for genetic mutations with low allele frequencies in whole-exome sequencing analysis by next-generation sequencing. *BMC Genom Data*. 2021;22(1):8. <https://doi.org/10.1186/s12863-020-00956-x>
44. Memorial Sloan Kettering Cancer Center (MSK). *The cBioPortal for Cancer Genomics*. Accessed May 9, 2024. <https://www.cbioportal.org/>
45. Memorial Sloan Kettering Cancer Center (MSK). *OncoKB™*. Updated 2024. Accessed May 9, 2024. <https://www.oncokb.org/>
46. The Jackson Laboratory. *CKB Boost™*. 2018-2024. Accessed May 9, 2024. <https://ckbhome.jax.org>
47. Horak P, Griffith M, Danos AM, et al. Standards for the classification of pathogenicity of somatic variants in cancer (oncogenicity): joint recommendations of Clinical Genome Resource (ClinGen), Cancer Genomics Consortium (CGC), and Variant Interpretation for Cancer Consortium (VICC). *Genet Med*. 2022;24(5):986-998. <https://doi.org/10.1016/j.gim.2022.01.001>
48. Li MM, Datto M, Duncavage EJ, et al. Standards and guidelines for the interpretation and reporting of sequence variants in cancer. *J Mol Diagn*. 2017;19(1):4-23. <https://doi.org/10.1016/j.jmoldx.2016.10.002>
49. Fortuno C, Lee K, Olivier M, et al; ClinGen TP53 Variant Curation Expert Panel. Specifications of the ACMG/AMP variant interpretation guidelines for germline TP53 variants. *Hum Mutat*. 2021;42(3):223-236. <https://doi.org/10.1002/humu.24152>
50. Loghavi S, Al-Ibraheemi A, Zuo Z, et al. TP53 overexpression is an independent adverse prognostic factor in de novo myelodysplastic syndromes with fibrosis. *Br J Haematol*. 2015;171(1):91-99. <https://doi.org/10.1111/bjh.13529>
51. Fitzpatrick MJ, Boiocchi L, Fathi AT, Brunner AM, Hasserjian RP, Nardi V. Correlation of p53 immunohistochemistry with TP53 mutational status and overall survival in newly diagnosed acute myeloid leukaemia. *Histopathology*. 2022;81(4):496-510. <https://doi.org/10.1111/his.14726>
52. Fernandez-Pol S, Ma L, Ohgami RS, Arber DA. Immunohistochemistry for p53 is a useful tool to identify cases of acute myeloid leukemia with myelodysplasia-related changes that are TP53 mutated, have complex karyotype, and have poor prognosis. *Mod Pathol*. 2017;30(3):382-392. <https://doi.org/10.1038/modpathol.2016.206>
53. McGraw KL, Nguyen J, Komrokji RS, et al. Immunohistochemical pattern of p53 is a measure of TP53 mutation burden and adverse clinical outcome in myelodysplastic syndromes and secondary acute myeloid leukemia. *Haematologica*. 2016;101(8):e320-e323. <https://doi.org/10.3324/haematol.2016.143214>
54. Ruzinova MB, Lee YS, Duncavage EJ, Welch JS. TP53 immunohistochemistry correlates with TP53 mutation status and clearance in decitabine-treated patients with myeloid malignancies. *Haematologica*. 2019;104(8):e345-e348. <https://doi.org/10.3324/haematol.2018.205302>
55. Rogers KJ, Abukhiran IM, Syrbu S, et al. Utilizing digital pathology and immunohistochemistry of p53 as an adjunct to molecular testing in myeloid disorders. *Acad Pathol*. 2023;10(1):100064. <https://doi.org/10.1016/j.acpath.2022.100064>
56. National Comprehensive Cancer Network (NCCN) Clinical Practice Guidelines in Oncology (NCCN Guidelines). *Acute myeloid leukemia*. Version 3.2024. May 17, 2024. Accessed June 13, 2024. https://www.nccn.org/professionals/physician_gls/pdf/aml.pdf
57. National Comprehensive Cancer Network (NCCN) Clinical Practice Guidelines in Oncology (NCCN Guidelines). *Myelodysplastic syndromes*. Version 2.2024. May 22, 2024. Accessed June 13, 2024. https://www.nccn.org/professionals/physician_gls/pdf/mds.pdf
58. Rucker FG, Schlenk RF, Bullinger L, et al. TP53 alterations in acute myeloid leukemia with complex karyotype correlate with specific copy number alterations, monosomal karyotype, and dismal outcome. *Blood*. 2012;119(9):2114-2121. <https://doi.org/10.1182/blood-2011-08-375758>
59. Goldberg AD, Talati C, Desai P, et al. TP53 mutations predict poorer responses to CPX-351 in acute myeloid leukemia. *Blood*. 2018;132(suppl 1):1433. <https://doi.org/10.1182/blood-2018-99-117772>
60. Vulaj V, Perissinotti AJ, Uebel JR, et al. The FOSSIL Study: FLAG or standard 7 + 3 induction therapy in secondary acute myeloid leukemia. *Leuk Res*. 2018;70:91-96. <https://doi.org/10.1016/j.leukres.2018.05.011>
61. Bally C, Adès L, Renneville A, et al. Prognostic value of TP53 gene mutations in myelodysplastic syndromes and acute myeloid leukemia treated with azacitidine. *Leuk Res*. 2014;38(7):751-755. <https://doi.org/10.1016/j.leukres.2014.03.012>
62. Takahashi K, Patel K, Bueso-Ramos C, et al. Clinical implications of TP53 mutations in myelodysplastic syndromes treated with hypomethylating agents. *Oncotarget*. 2016;7(12):14172-14187. <https://doi.org/10.18632/oncotarget.7290>
63. Montalban-Bravo G, Takahashi K, Garcia-Manero G. Decitabine in TP53-mutated AML. *N Engl J Med*. 2017;376(8):796-797. <https://doi.org/10.1056/NEJMc1616062>
64. Welch JS, Petti AA, Miller CA, et al. TP53 and decitabine in acute myeloid leukemia and myelodysplastic syndromes. *N Engl J Med*. 2016;375(21):2023-2036. <https://doi.org/10.1056/NEJMoa1605949>
65. Chang CK, Zhao YS, Xu F, et al. TP53 mutations predict decitabine-induced complete responses in patients with myelodysplastic syndromes. *Br J Haematol*. 2017;176(4):600-608. <https://doi.org/10.1111/bjh.14455>
66. Nannya Y, Tobiasson M, Sato S, et al. Post-azacitidine clone size predicts outcome of patients with myelodysplastic syndromes and related myeloid neoplasms. *Blood Adv*. 2023;7(14):3624-3636. <https://doi.org/10.1182/bloodadvances.2022009564>
67. Aldoss I, Zhang J, Pillai R, et al. Venetoclax and hypomethylating agents in TP53-mutated acute myeloid leukaemia. *Br J Haematol*. 2019;187(2):e45-e48. <https://doi.org/10.1111/bjh.16166>
68. DiNardo CD, Pratz K, Pullarkat V, et al. Venetoclax combined with decitabine or azacitidine in treatment-naïve, elderly patients with acute myeloid leukemia. *Blood*. 2019;133(1):7-17. <https://doi.org/10.1182/blood-2018-08-868752>
69. DiNardo CD, Maiti A, Rausch CR, et al. 10-day decitabine with venetoclax for newly diagnosed intensive chemotherapy ineligible, and relapsed or refractory acute myeloid leukaemia: a single-centre, phase 2 trial. *Lancet Haematol*. 2020;7(10):e724-e736. [https://doi.org/10.1016/S2352-3026\(20\)30210-6](https://doi.org/10.1016/S2352-3026(20)30210-6)
70. DiNardo CD, Jonas BA, Pullarkat V, et al. Azacitidine and venetoclax in previously untreated acute myeloid leukemia. *N Engl J Med*. 2020;383(7):617-629. <https://doi.org/10.1056/NEJMoa2012971>
71. Pollyea DA, Pratz KW, Wei AH, et al. Outcomes in patients with poor-risk cytogenetics with or without TP53 mutations treated with venetoclax and azacitidine. *Clin Cancer Res*. 2022;28(24):5272-5279. <https://doi.org/10.1158/1078-0432.CCR-22-1183>
72. Daver NG, Iqbal S, Renard C, et al. Treatment outcomes for newly diagnosed, treatment-naïve TP53-mutated acute myeloid leukemia: a systematic review and meta-analysis. *J Hematol Oncol*. 2023;16(1):19. <https://doi.org/10.1186/s13045-023-01417-5>
73. Zeidan AM, Borate U, Pollyea DA, et al. A phase 1b study of venetoclax and azacitidine combination in patients with relapsed or refractory myelodysplastic syndromes. *Am J Hematol*. 2023;98(2):272-281. <https://doi.org/10.1002/ajh.26771>
74. Pereira MP, Herrity E, Kim DDH. TP53-mutated acute myeloid leukemia and myelodysplastic syndrome: biology, treatment challenges, and upcoming approaches. *Ann Hematol*. 2024;103(4):1049-1067. <https://doi.org/10.1007/s00277-023-05462-5>

75. Zhang T, Auer P, Dong J, et al. Whole-genome sequencing identifies novel predictors for hematopoietic cell transplant outcomes for patients with myelodysplastic syndrome: a CIBMTR study. *J Hematol Oncol.* 2023;16(1):37. <https://doi.org/10.1186/s13045-023-01431-7>
76. Middeke JM, Herold S, Rücker-Braun E, et al; Study Alliance Leukaemia (SAL). TP53 mutation in patients with high-risk acute myeloid leukaemia treated with allogeneic haematopoietic stem cell transplantation. *Br J Haematol.* 2016;172(6):914-922. <https://doi.org/10.1111/bjh.13912>
77. Shahzad M, Tariq E, Chaudhary SG, et al. Outcomes with allogeneic hematopoietic stem cell transplantation in TP53-mutated acute myeloid leukemia: a systematic review and meta-analysis. *Leuk Lymphoma.* 2022;63(14):3409-3417. <https://doi.org/10.1080/10428194.2022.2123228>
78. Badar T, Atallah E, Shallis R, et al. Survival of TP53-mutated acute myeloid leukemia patients receiving allogeneic stem cell transplantation after first induction or salvage therapy: results from the Consortium on Myeloid Malignancies and Neoplastic Diseases (COMMAND). *Leukemia.* 2023;37(4):799-806. <https://doi.org/10.1038/s41375-023-01847-7>
79. Pasca S, Haldar SD, Ambinder A, et al. Outcome heterogeneity of TP53-mutated myeloid neoplasms and the role of allogeneic hematopoietic cell transplantation. *Haematologica.* 2024;109(3):948-952. <https://doi.org/10.3324/haematol.2023.283886>
80. Sallman DA, DeZern AE, Garcia-Manero G, et al. Eprenetapopt (APR-246) and azacitidine in TP53-mutant myelodysplastic syndromes. *J Clin Oncol.* 2021;39(14):1584-1594. <https://doi.org/10.1200/JCO.20.02341>
81. Mishra A, Tamari R, DeZern AE, et al. Phase II trial of eprenetapopt (APR-246) in combination with azacitidine (AZA) as maintenance therapy for TP53 mutated AML or MDS following allogeneic stem cell transplantation (SCT). *Blood.* 2021;138(suppl 1):409. <https://doi.org/10.1182/blood-2021-147962>
82. Garcia-Manero G, Goldberg AD, Winer ES, et al. Eprenetapopt combined with venetoclax and azacitidine in TP53-mutated acute myeloid leukaemia: a phase 1, dose-finding and expansion study. *Lancet Haematol.* 2023;10(4):e272-e283. [https://doi.org/10.1016/S2352-3026\(22\)00403-3](https://doi.org/10.1016/S2352-3026(22)00403-3)
83. Aprea Therapeutics. Aprea Therapeutics Announces Results of Primary Endpoint from Phase 3 Trial of Eprenetapopt in TP53 Mutant Myelodysplastic Syndromes (MDS). 2020. Accessed October 4, 2023. <https://ir.aprea.com/news-releases/news-release-details/aprea-therapeutics-announces-results-primary-endpoint-phase-3>
84. El Chaer F, Hourigan CS, Zeidan AM. How I treat AML incorporating the updated classifications and guidelines. *Blood.* 2023;141(23):2813-2823. <https://doi.org/10.1182/blood.2022017808>
85. Mishra A, Tamari R, DeZern AE, et al. Eprenetapopt plus azacitidine after allogeneic hematopoietic stem-cell transplantation for TP53-mutant acute myeloid leukemia and myelodysplastic syndromes. *J Clin Oncol.* 2022;40(34):3985-3993. <https://doi.org/10.1200/JCO.22.00181>
86. Khurana A, Shafer DA. MDM2 antagonists as a novel treatment option for acute myeloid leukemia: perspectives on the therapeutic potential of idasanutlin (RG7388). *Onco Targets Ther.* 2019;12:2903-2910. <https://doi.org/10.2147/OTT.S172315>
87. Konopleva MY, Röllig C, Cavenagh J, et al. Idasanutlin plus cytarabine in relapsed or refractory acute myeloid leukemia: results of the MIRROS trial. *Blood Adv.* 2022;6(14):4147-4156. <https://doi.org/10.1182/bloodadvances.2021006303>
88. Daver NG, Dail M, Garcia JS, et al. Venetoclax and idasanutlin in relapsed/refractory AML: a nonrandomized, open-label phase 1b trial. *Blood.* 2023;141(11):1265-1276. <https://doi.org/10.1182/blood.2022016362>
89. Montesinos P, Beckermann BM, Catalani O, et al. MIRROS: a randomized, placebo-controlled, phase III trial of cytarabine ± idasanutlin in relapsed or refractory acute myeloid leukemia. *Future Oncol.* 2020;16(13):807-815. <https://doi.org/10.2217/fo-2020-0044>
90. Asl ER, Rostamzadeh D, Duijif PHG, et al. Mutant P53 in the formation and progression of the tumor microenvironment: friend or foe. *Life Sci.* 2023;315:121361. <https://doi.org/10.1016/j.lfs.2022.121361>
91. Vadakekolathu J, Lai C, Reeder S, et al. TP53 abnormalities correlate with immune infiltration and associate with response to flotetuzumab immunotherapy in AML. *Blood Adv.* 2020;4(20):5011-5024. <https://doi.org/10.1182/bloodadvances.2020002512>
92. Sakuishi K, Apetoh L, Sullivan JM, Blazar BR, Kuchroo VK, Anderson AC. Targeting Tim-3 and PD-1 pathways to reverse T cell exhaustion and restore anti-tumor immunity. *J Exp Med.* 2010;207(10):2187-2194. <https://doi.org/10.1084/jem.20100643>
93. Daver N, Garcia-Manero G, Basu S, et al. Efficacy, safety, and biomarkers of response to azacitidine and nivolumab in relapsed/refractory acute myeloid leukemia: a nonrandomized, open-label, phase II study. *Cancer Discov.* 2019;9(3):370-383. <https://doi.org/10.1158/2159-8290.CD-18-0774>
94. Saxena K, Herbrich SM, Pemmaraju N, et al. A phase 1b/2 study of azacitidine with PD-L1 antibody avelumab in relapsed/refractory acute myeloid leukemia. *Cancer.* 2021;127(20):3761-3771. <https://doi.org/10.1002/cncr.33690>
95. Daver N, Senapati J, Maiti A, et al. Phase I/II Study of azacitidine (AZA) with venetoclax (VEN) and magrolimab (Magro) in patients (pts) with newly diagnosed (ND) older/unfit or high-risk acute myeloid leukemia (AML) and relapsed/refractory (R/R) AML. *Blood.* 2022;140(suppl 1):141-144. <https://doi.org/10.1182/blood-2022-170188>
96. Johnson L, Zhang Y, Li B, et al. Nature of clinical response and depth of molecular response in patients with TP53 mutant myelodysplastic syndromes (MDS) and acute myeloid leukemia (AML) treated with magrolimab with azacitidine. *Blood.* 2022;140(suppl 1):6934-6935. <https://doi.org/10.1182/blood-2022-160337>
97. DiNardo KW, LeBlanc TW, Chen H. Novel agents and regimens in acute myeloid leukemia: latest updates from 2022 ASH Annual Meeting. *J Hematol Oncol.* 2023;16(1):17. <https://doi.org/10.1186/s13045-023-01411-x>
98. Daver NG, Maiti A, Kadia TM, et al. TP53-mutated myelodysplastic syndrome and acute myeloid leukemia: biology, current therapy, and future directions. *Cancer Discov.* 2022;12(11):2516-2529. <https://doi.org/10.1158/2159-8290.CD-22-0332>

Diagnostic value of serum STIP1 in HCC and AFP-negative HCC

Haiqing Sun, MD¹, Ning Liu, PhD¹, Jinli Lou, PhD¹

¹Department of Clinical Laboratory Center, Beijing Youan Hospital, Capital Medical University, Beijing, China. Corresponding author: Jinli Lou; loujinli@ccmu.edu.cn

Key words: STIP1; hepatocellular carcinoma; AFP-negative hepatocellular carcinoma; diagnostic value

Abbreviations: STIP1, stress-induced phosphoprotein 1; HCC, hepatocellular carcinoma; AFP, alpha-fetoprotein; ANHC, AFP-negative HCC; ROC, receiver operating characteristic; DCP, des- γ -carboxy prothrombin; CT, computed tomography; MRI, magnetic resonance imaging; GP73, Golgi protein 73; HCCR-1, human cervical pro-oncogene 1; AUC, area under the curve; ALT, alanine aminotransferase; AST, aspartate aminotransferase; TBIL, total bilirubin; ALB, albumin; GGT, γ -glutamyl transferase; BCLC, Barcelona Clinic Liver Cancer

Laboratory Medicine 2024;55:700-707; <https://doi.org/10.1093/labmed/lmae033>

ABSTRACT

Objective: This study aimed to investigate the diagnostic value of stress-induced phosphoprotein 1 (STIP1) in serum for hepatocellular carcinoma (HCC) and alpha-fetoprotein (AFP)-negative HCC (ANHC).

Methods: In this study, serum samples were collected from 158 HCC patients and 63 non-HCC patients. Logistic regression analysis was performed to identify independent risk factors associated with HCC and ANHC. The diagnostic values of each index for HCC and ANHC were analyzed using receiver operating characteristic (ROC) curve analysis.

Results: The STIP1, des- γ -carboxy prothrombin (DCP), and AFP levels were higher in the HCC groups than in the non-HCC groups ($P < .05$). Age, DCP, STIP1, and hepatitis B virus infection were independent predictors of HCC ($P < .05$). The diagnostic value of STIP1 for HCC was higher than that of DCP. Additionally, age, STIP1, and hepatitis B virus infection were independent predictors for ANHC patients. The ROC curve exhibited an area under the curve value of 0.919 for STIP1, with a diagnostic cutoff value of 68.5 U/mL. Moreover, 36 ANHC patients and 19 AFP-negative non-HCC patients were included to validate the diagnostic model. A total of 20 patients had STIP1 levels greater than 68.5 U/mL, resulting in diagnostic accuracy of 67.3%, sensitivity of 55.6%, and specificity of 89.5%.

Conclusion: STIP1 demonstrates excellent diagnostic value for HCC and ANHC.

Introduction

Hepatocellular carcinoma (HCC) is one of the most malignant tumors, with a high morbidity and high mortality.^{1,2} Every year, HCC causes the deaths of more than 700,000 individuals worldwide.² Accounting for around 90% of primary liver cancers, HCC is the most common type and is especially prevalent in Asian countries, contributing to 75%-80% of cases globally.³ Despite a substantial decline in cancer mortality rates since 1991, the number of deaths related to HCC is still on the rise. The main factors contributing to the risk of developing HCC are liver cirrhosis and hepatitis B virus infection.⁴ Although surgical removal of the tumor and liver transplantation have shown efficacy in the management of HCC,⁵ the 5-year overall survival rate is still only 7%.⁶ The early detection of HCC remains a formidable challenge, invariably leading to poor patient outcomes. An accurate and timely diagnosis can enhance treatment effectiveness considerably and alleviate patient suffering.⁷ Currently, early diagnosis of HCC relies on the utilization of imaging techniques and serological examination.⁸ The National Comprehensive Cancer Network clinical practice guidelines suggest that high-risk HCC patients, specifically those with cirrhosis of any cause, should undergo abdominal ultrasound and alpha-fetoprotein (AFP) monitoring twice annually. Although ultrasound is the primary radiological screening technique, its effectiveness can be affected by the operator's proficiency.⁹ It can be challenging to distinguish between malignant and benign nodules in cirrhotic liver, especially in cases where the nodules are small. The diagnostic accuracy of HCC has significantly improved due to the emergence of computed tomography (CT) and magnetic resonance imaging (MRI) methods. However, these techniques are costly and may not be suitable for mass screening.¹⁰

Alpha-fetoprotein was introduced in the 1960s as a serum marker for HCC. It remains the most commonly used biomarker for HCC worldwide.¹¹ However, the sensitivity of AFP for diagnosing HCC is approximately 60% to 70%. Even with a low cutoff value (10-20 ng/mL), its specificity remains inadequate, resulting in many HCC patients being missed (30%-40%).¹² In the case of AFP-negative HCC (ANHC), characterized by smaller tumor masses, imaging examinations are also prone to missing the diagnosis.¹³

ANHC accounts for approximately 30% to 40% of HCC. Its early diagnosis mainly relies on imaging tests such as ultrasound, CT, and MRI. However, ANHC mainly presents as a small HCC, often with mild clinical symptoms, lack of specificity, and inconspicuous imaging characteristics. This makes it more challenging to achieve early diagnosis and treatment in affected patients.¹⁴ ANHC currently lacks ideal biomarkers for early detection. However, the prognosis for patients in this group is generally favorable when treated promptly.¹² Therefore, increasing emphasis on ANHC and actively exploring more effective diagnostic methods are crucial.

In recent years, significant progress has been made in identifying potential serum markers for ANHC diagnosis. Researchers have reported promising findings regarding the utility of des- γ -carboxy prothrombin (DCP), AFP-L3, Golgi protein 73 (GP73), and human cervical pro-oncogene 1 (HCCR-1), among others. DCP is an abnormal prothrombin molecule produced by an acquired defect in the posttranslational carboxylation of the prothrombin precursor in malignant cells. AFP-L3 is a specific form of AFP that binds to lectin *Lens culinaris* agglutinin.¹² These markers hold great potential in improving the accuracy and early detection of ANHC. Further studies and exploration of novel serum markers are warranted to enhance our understanding and clinical management of this disease.¹⁵ Currently, the primary serum markers used in clinical practice for diagnosing and monitoring HCC are DCP and AFP-L3. DCP is an adjunctive marker to AFP and is elevated in certain HCC patients with low AFP levels or who test negative for AFP.¹⁶ A clinical combination test of DCP and AFP has shown the potential to enhance the diagnostic accuracy of ANHC.¹⁷ However, the use of DCP in clinical diagnosis also has its limitations, such as the risk of elevated DCP levels in benign liver diseases and other forms of cancer, which may necessitate additional tests combining multiple diagnostic indicators and imaging exams. Additionally, there are cases where DCP levels do not increase in specific individuals.¹⁷ Therefore, finding new tumor markers to diagnose ANHC is still necessary.

Phosphorylation stress-induced protein 1 (also known as stress-induced phosphoprotein 1 or STIP1) is emerging as a research breakthrough in diagnostic markers for HCC. STIP1, also called the tissue protein of heat shock protein 70/90, serves as a cochaperone, facilitating the transfer of client proteins from heat shock protein 70 to the heat shock protein 90 chaperone system.¹⁸ STIP1 is crucial in various essential processes besides its role as a tissue protein. It is actively involved in transcription regulation, cell cycle regulation, signal transduction, protein folding, and cell division.¹⁹ Previous studies have consistently demonstrated that elevated expression of STIP1 is commonly associated with an unfavorable prognosis in various malignant tumors, including HCC, pancreatic cancer, colorectal cancer, gastric cancer, and ovarian cancer.²⁰ The diagnostic value of STIP1 in HCC and ANHC has not been reported. Our study aims to investigate the levels of STIP1 in the serum of HCC patients and explore its potential as a diagnostic marker in both HCC and ANHC.

Methods

Patients

The study collected serum samples from 158 HCC patients and 63 non-HCC patients (including 29 patients with chronic hepatitis, 19 healthy individuals, and 15 patients with liver cirrhosis) who were treated

at Beijing Youan Hospital in August 2019. The diagnosis of HCC was based on the diagnostic criteria outlined in the Diagnosis and Treatment Guidelines for Primary Liver Cancer (2022 edition) issued by the National Health Commission of China. This study was approved by the Ethics Committee of Beijing Youan Hospital, and the utilization of residual serum samples from human subjects was exempted from informed consent (approval number: LL-2019-184-K). All procedures were conducted according to the 1964 Helsinki Declaration and its later amendments, or comparable ethical standards.

Diagnostic Criteria for Primary Liver Cancer

- AFP \geq 400 ng/mL in serum, which could exclude pregnancy, germ cell tumors, active liver disease, and metastatic liver cancer, and ultrasound or abdominal CT indicating a liver mass
- AFP <400 ng/mL in serum, and both ultrasound and abdominal CT indicating a liver mass, as well as ruling out other causes of elevated AFP, including pregnancy, active liver disease, germ cell tumors, and metastatic liver cancer
- Surgical and pathological confirmation of primary liver cancer

Inclusion Criteria

- Age >18 years, with no limitations on sex, ethnicity, and region
- The diagnosis of HCC followed the Diagnosis and Treatment Guidelines for Primary Liver Cancer (2022 edition)
- Complete clinical medical records were available

Exclusion Criteria

- Serum samples were deteriorated or less than 1 mL
- Patients who did not meet the diagnostic criteria
- Other diseases that could significantly affect the results of laboratory routine tests include severe infectious diseases, blood system diseases, immune-related diseases, and severe cardio-pulmonary-kidney diseases
- Incompleteness of medical records

Collection of Clinical Data

Clinical data on patients, including sex, age, liver function (aspartate aminotransferase [AST], alanine aminotransferase [ALT], total bilirubin, serum albumin, γ -glutamyl transferase [GGT]) (using Siemens ADVIA2400), hepatitis virus markers (Roche cobas e801), serum tumor marker AFP (Roche cobas e601), DCP (Fujirebio Lumipulse G120), imaging examinations (CT, MRI), and pathological histology examinations, were collected from the hospital information management system of Beijing Youan Hospital, affiliated with Capital Medical University. The collected data were entered into an Excel spreadsheet. Additionally, 1 mL of fasting venous blood was collected from all patients, centrifuged at 1610g for 20 minutes to separate the serum, and stored at -80°C for future use.

Detection of STIP1 in Serum

The STIP1 levels were measured using the human STIP1 ELISA kit (BIM) following these steps: Duplicate samples and standards were added to the micro ELISA strip plate. Protein standards were added appropriately,

with the blank condition containing no sample. A total of 100 mL enzyme-labeled reagent was added to the standard and sample wells, followed by incubation at 37°C for 60 minutes. The MicroELISA plate was washed 4 times. A total of 50 µL coloring agent A and agent B were added to each well, gently mixed, and incubated at 37°C for 15 minutes. Then, 50 µL of stop solution was added to each well. The optical density at 450 nm was measured within 15 minutes using a Multiscan MK3 (Thermo Fisher Scientific).

Statistical Methods

All statistical analyses were conducted using SPSS 21.0 software (IBM). Continuous variables were presented as mean plus or minus the standard error of the mean. The χ^2 test, Fisher exact probability test, and Student *t*-test were used to determine significant differences between groups. The nonparametric Mann-Whitney *U* test was applied if the data were not homogeneous. Logistic regression analysis was performed to evaluate the significance of STIP1 in predicting HCC. The receiver operating characteristic (ROC) curve analysis was conducted to assess the value of serum STIP1 levels in predicting HCC. The Delong test was used to perform a significance test for the area under the curve (AUC). Data were considered statistically significant at $P < .05$.

Results

General Data Analysis

This study included 158 HCC and 63 non-HCC patients. In the HCC group, 76.6% were male, aged 27 to 85 years. Among them, 117 patients were infected with hepatitis B. In the non-HCC group, 69.8% were

male, with an age range of 22 to 85 years, and 31 patients were infected with hepatitis B. There were no significant differences in age or sex between the 2 groups ($P > .05$). The general data of the patients, including ALT, AST, total bilirubin, albumin, GGT, AFP, DCP, STIP1, and whether they were infected with the hepatitis B virus, were subjected to statistical analysis. The results showed significant differences between the 2 groups regarding AFP, DCP, STIP1, and hepatitis B virus infection ($P < .05$), as shown in **TABLE 1** and **FIGURE 1**.

Univariate and Multivariate Logistic Regression Analysis Between HCC and Non-HCC Groups

The multivariate logistic regression analysis included the factors that showed statistical significance in the univariate analysis ($P < .05$). The results showed that age, DCP, STIP1, and hepatitis B virus infection were independent predictors of HCC, and the differences were statistically significant ($P < .05$), as shown in **TABLE 2**.

Evaluation of the Diagnostic Value of STIP1 and DCP in HCC

The ROC curve was used to evaluate the diagnostic value of STIP1, DCP, and their combined indexes in HCC. The results showed that the diagnostic value of STIP1 in HCC was significantly higher than that of DCP ($P < .05$), and the diagnostic cutoff value was 78.85 U/mL. Notably, the combined index of STIP1+DCP had the largest area under the ROC curve, measuring 0.937, with a sensitivity of 84.8% and specificity of 98%, as shown in **FIGURE 2** and **TABLE 3**. It is worth noting that the diagnostic value of STIP1 alone is not lower than that of multi-index combined detection, although the difference is not statistically significant ($Z = 1.152, P = .249$). Moreover, we divided the HCC group into 2 subgroups based on the cutoff value of STIP1 and showed that high

TABLE 1. General Data Analysis of the Non-HCC and HCC Groups

Variable	Non-HCC (n = 63)	HCC (n = 158)	$\chi^2/t/Z$	<i>P</i>
Age, y, mean \pm SD				
≤ 50	38.72 \pm 1.46	42.10 \pm 1.10	1.846	.071
> 50	60.29 \pm 1.28	62.99 \pm 0.65	1.883	.065
Sex, n (%)			1.082	.192
Male	44 (69.8)	121 (76.6)		
Female	19 (30.2)	37 (23.4)		
ALT, IU/L	27 (18, 43)	24 (17, 37)	1.314	.189
AST, IU/L	28 (22, 56)	31 (23, 43)	0.077	.939
TBIL, μ mol/L	19 (14.3, 29.3)	19.45 (12.78, 31.75)	0.203	.839
ALB, g/L	39.35 \pm 1.087	38.53 \pm 0.523	0.677	.5
GGT, U/L	45 (23, 104)	48 (30.75, 95.5)	0.919	.358
HBsAg				
Negative, n (%)	32 (50.79)	41 (25.94)	12.568	.000 ^a
Positive, n (%)	31 (49.21)	117 (74.05)		
AFP, ng/mL	3.94 (2.5, 10.17)	8.43 (3.41, 192.95)	3.819	.000 ^a
DCP, mAU/mL	48 (34, 93)	74 (33, 573.5)	2.607	.009 ^b
STIP1, U/mL	15.1 (8.6, 28.3)	405.85 (141.58, 554.9)	9.925	.000 ^a

AFP, alpha-fetoprotein; ALB, albumin; ALT, alanine aminotransferase; AST, aspartate aminotransferase; DCP, des- γ -carboxy prothrombin; GGT, γ -glutamyl transferase; HBsAg, hepatitis B surface antigen; HCC, hepatocellular carcinoma; STIP1, stress-induced phosphoprotein 1; TBIL, total bilirubin.

^aSignificant difference at $P < .001$.

^bSignificant difference at $P < .05$.

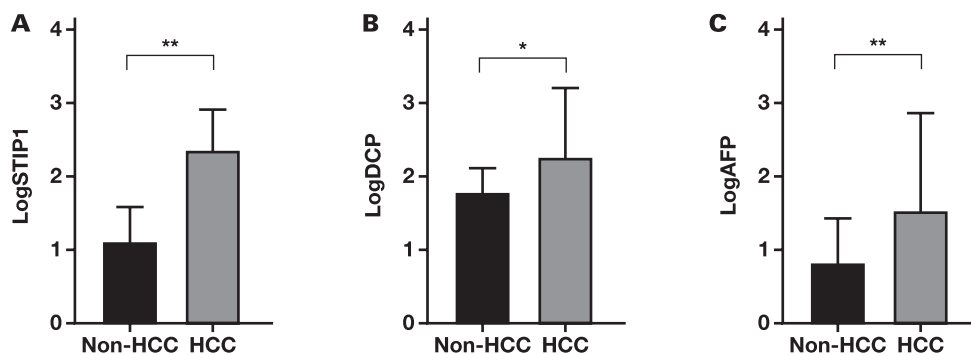


FIGURE 1. Comparison of HCC-related indicators between HCC and non-HCC groups. A, STIP1. B, DCP. C, AFP. AFP, alpha-fetoprotein; DCP, des- γ -carboxy prothrombin; HCC, hepatocellular carcinoma; STIP1, stress-induced phosphoprotein 1. *Significant difference at $P < .05$. **Significant difference at $P < .001$.

TABLE 2. Univariate and Multivariate Analysis Between the Non-HCC and HCC Groups

Variable	Univariate		Multivariate	
	Odds ratio (95% CI)	<i>P</i>	Odds ratio (95% CI)	<i>P</i>
Age	1.054 (1.027-1.082)	.000 ^a	1.061 (1.014-1.110)	.01 ^b
Sex	0.708 (0.369-1.359)	.299	—	—
ALT	0.989 (0.980-0.997)	.009 ^b	0.971 (0.936-1.008)	.121
AST	0.998 (0.995-1.001)	.185	—	—
Log AST	0.572 (0.217-1.507)	.258	—	—
TBIL	0.992 (0.984-1.000)	.048 ^b	1.002 (0.982-1.023)	.814
ALB	0.984 (0.944-1.026)	.447	—	—
GGT	0.999 (0.997-1.001)	.195	—	—
HBsAg	2.946 (1.603-5.414)	.001 ^a	7.069 (1.841-27.140)	.004 ^b
AFP	1.003 (1.000-1.007)	.079	—	—
Log AFP	2.061 (1.401-3.032)	.000 ^a	0.783 (0.302-2.028)	.614
DCP	1.002 (1.000-1.004)	.024 ^b	1.003 (1.001-1.006)	.016 ^b
STIP1	1.038 (1.017-1.059)	.000 ^a	1.037 (1.01-1.066)	.007 ^b

AFP, alpha-fetoprotein; ALB, albumin; ALT, alanine aminotransferase; AST, aspartate aminotransferase; DCP, des- γ -carboxy prothrombin; GGT, γ -glutamyl transferase; HBsAg, hepatitis B surface antigen; STIP1, stress-induced phosphoprotein 1; TBIL, total bilirubin.

^aSignificant difference at $P < .001$.

^bSignificant difference at $P < .05$.

levels of STIP1 may have a significant impact on AFP levels and nodule size, while the impact on tumor staging may not be significant, shown in Supplemental Table 1.

Univariate and Multivariate Analysis of Variance Between ANHC and Non-HCC Groups

Among the 73 patients with ANHC (<7 ng/mL), 83.56% were male, 83.6% were over 50 years old, and 23.3% were hepatitis B virus-infected. Univariate analysis revealed statistically significant differences between the 2 groups regarding age, ALT, AST, GGT, AFP, STIP1, and hepatitis B virus infection ($P < .05$). Further multivariate logistic analysis showed that age, STIP1, and hepatitis B virus infection were independent predictors of ANHC, as demonstrated in TABLE 4.

Diagnostic Value of STIP1 in ANHC

In 73 ANHC patients, the diagnostic value of STIP1 for ANHC was evaluated using ROC curves. The findings demonstrated that STIP1 exhibited a strong diagnostic capability for ANHC ($P < .001$). The area under the ROC curve was 0.919, the diagnostic cutoff value was

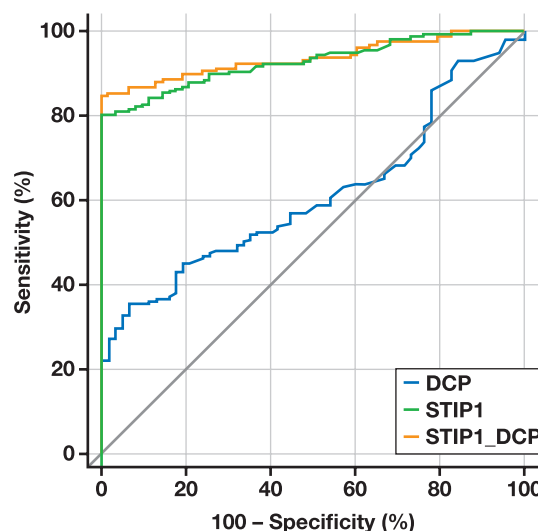


FIGURE 2. ROC curves of STIP1 and DCP for the diagnosis of HCC. DCP, des- γ -carboxy prothrombin; HCC, hepatocellular carcinoma; ROC, receiver operating characteristic; STIP1, stress-induced phosphoprotein 1.

TABLE 3. ROC Curve Parameters for STIP1, DCP, and Combined Tests

Variance	Sensitivity (%)	Specificity (%)	Youden index	AUC	95% CI	P
DCP	35.44	93.65	0.2909	0.612	0.545-0.677	.0032 ^a
STIP1	80.4	98	0.784	0.928	0.885-0.958	<.001 ^b
STIP1+DCP	84.8	98	0.828	0.937	0.896-0.965	<.001 ^b

AUC, area under the curve; DCP, des- γ -carboxy prothrombin; ROC, receiver operating characteristic; STIP1, stress-induced phosphoprotein 1.

^aSignificant difference at P < .05.

^bSignificant difference at P < .001.

TABLE 4. Univariate and Multivariate Analysis Between Non-HCC Groups and ANHC

Variance	Non-HCC (n = 63)	ANHC (n = 73)	Univariate		Multivariate	
			Odds ratio (95% CI)	P	Odds ratio (95% CI)	P
Sex, male, %	69.84	83.56	0.456 (0.201-1.034)	.06	—	—
Age, y, n (%)						
<50	25 (39.7)	12 (16.4)	3.344 (1.505-7.433)	.003 ^a	1.079 (1.008-1.155)	.028 ^b
>50	38 (60.32)	61 (83.6)				
ALT, IU/L	27 (18, 43)	22 (16, 32)	0.979 (0.963-0.995)	.013 ^a	0.958 (0.875-1.048)	.349
AST, IU/L	28 (22, 56)	26 (19.5, 35)	0.978 (0.960-0.996)	.018 ^a	1.001 (0.987-1.015)	.925
TBIL, μ mol/L	19 (14.3, 29.3)	19.4 (11.8, 32.65)	0.992 (0.983-1.002)	.127	—	—
ALB, g/L	39.35 \pm 1.09	38.6 \pm 0.82	0.988 (0.945-1.032)	.575	—	—
GGT, U/L	45 (23, 104)	42 (28, 70)	0.995 (0.991-1.000)	.031 ^a	1.005 (0.992-1.017)	.470
HBsAg, n (%)			3.4 (1.632-7.083)	.001 ^b	13.790 (1.871-101.667)	.01 ^a
Negative	32 (50.8)	56 (76.7)				
Positive	31 (49.2)	17 (23.3)				
AFP, ng/mL	3.94 (2.5, 10.17)	3.33 (2.36, 4.155)	0.837 (0.716-0.978)	.025 ^a	0.848 (0.589-1.220)	.374
DCP, mAU/mL	48 (34, 93)	45 (29, 111)	1.001 (1.000-1.003)	.140	—	—
STIP1, U/mL	19.03 \pm 1.96	364.58 \pm 28.29	1.041 (1.015-1.067)	.002 ^a	1.077 (1.023-1.133)	.005 ^a

AFP, alpha-fetoprotein; ALB, albumin; ALT, alanine aminotransferase; ANHC, AFP-negative HCC; AST, aspartate aminotransferase; DCP, des- γ -carboxy prothrombin; GGT, γ -glutamyl transferase; HBsAg, hepatitis B surface antigen; HCC, hepatocellular carcinoma; STIP1, stress-induced phosphoprotein 1; TBIL, total bilirubin.

^aSignificant difference at P < .05.

^bSignificant difference at P < .001.

68.5U/mL, and the sensitivity and specificity were 76.71% and 100%, respectively, as shown in **FIGURE 3**.

Validation of the Diagnostic Model of STIP1 for ANHC

In addition, 36 cases of ANHC patients and 19 cases of ANHC non-HCC patients were selected for model validation. There were statistically significant differences in STIP1 levels and hepatitis B virus infection between the 2 groups, as shown in **TABLE 5**. Among the 36 patients, 20 patients had STIP1 levels greater than 68.5 U/mL, resulting in diagnostic accuracy of 67.3%, sensitivity of 55.6%, and specificity of 89.5%.

Discussion

HCC is one of the most common malignancies of the digestive system, with high morbidity and mortality. Its early diagnosis is crucial for timely treatment and improved survival rate. Although ultrasound, MRI, and other imaging techniques have greatly improved the accuracy of HCC diagnosis, its application is limited by its high cost, invasiveness, and insensitivity to small tumors. Therefore, the convenient, inexpensive, noninvasive, and reproducible detection of serum biomarkers plays an essential role in diagnosing HCC.¹⁶ AFP is a widely used biomarker for the diagnosis of HCC. However, its diagnostic accuracy is limited due

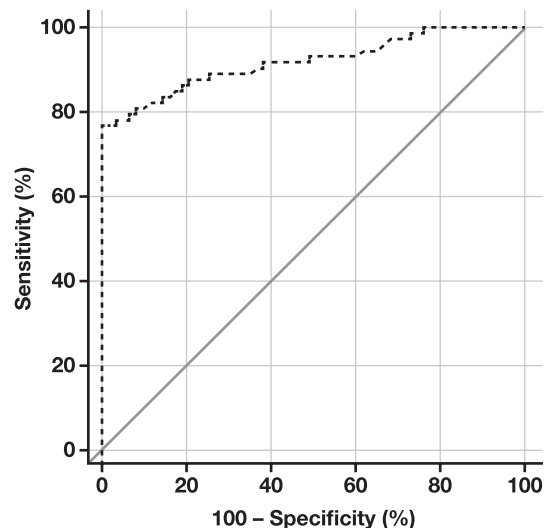


FIGURE 3. ROC curves of STIP 1 for diagnosis of ANHC. ANHC, alpha-fetoprotein-negative hepatocellular carcinoma; ROC, receiver operating characteristic; STIP1, stress-induced phosphoprotein 1. Sensitivity = 76.71%; specificity = 100%; area under the curve = 0.919.

TABLE 5. Analysis of General Data for Non-HCC Groups and ANHC Groups

	Non-HCC (n = 19)	ANHC (n = 36)	$\chi^2/t/z$	P
Age, y, mean \pm SD	50.68 \pm 3.117	57.08 \pm 2.124	1.731	.089
Sex, n (%)				
Male	10 (52.6)	26 (72.2)	2.111	.233
Female	9 (47.4)	10 (27.8)		
HBSAg, n (%)				
Negative	18 (94.7)	12 (33.3)	18.912	.000 ^a
Positive	1 (5.3)	24 (66.7)		
AFP	3.274 \pm 0.377	3.205 \pm 0.278	0.147	.884
STIP1	12.7 (9.1, 28.3)	252.6 (9.35, 604.75)	2.231	.026 ^b

AFP, alpha-fetoprotein; ANHC, AFP-negative HCC; HBSAg, hepatitis B surface antigen; HCC, hepatocellular carcinoma; STIP1, stress-induced phosphoprotein 1.

^aSignificant difference at $P < .001$.

^bSignificant difference at $P < .05$.

to its high false-negative rate in detecting small and early-stage tumors. Zhang et al²¹ demonstrated that an AFP threshold of 400 ng/mL yielded a summary sensitivity of 0.32 (95% CI, 0.31-0.34) and specificity of 0.99 (95% CI, 0.98-0.99) by analyzing 29,828 articles from Medline and Embase databases. Marrero et al²² found that AFP >20 ng/mL had a sensitivity of 53% and a specificity of 90% for the early diagnosis of HCC. This means that even with a low cutoff value (eg, 10-20 ng/mL), there is a risk of misdiagnosing patients with ANHC.²³ Furthermore, AFP may be elevated in some benign liver diseases, such as chronic hepatitis and cirrhosis without HCC. Currently, the use of AFP for early screening of HCC has been controversial.^{24,25} As a supplement to AFP, DCP has been used in clinical practice. It has been reported that a DCP level of \geq 40 mAU/mL has a sensitivity of 64% and specificity of 89% in diagnosing early-stage liver cancer. The overall accuracy of this diagnostic approach is reported to be 86.3%.²⁶ In the case of very early Barcelona Clinic Liver Cancer (BCLC 0) and early (BCLCA) HCC, the percentage of DCP (55.6% and 61.1%, respectively) was significantly higher than AFP (22.2% and 16.7%, respectively). In the middle and advanced stages of HCC (BCLCB/C), DCP also exhibited higher levels than AFP, although the difference was relatively minor.¹⁶

In our study, AFP and DCP were tested in 158 HCC patients. The results showed that the levels of AFP and DCP were significantly higher in the HCC group than the non-HCC group. Univariate analysis confirmed a strong correlation between log AFP and DCP with HCC. Furthermore, multivariate analysis revealed that DCP was an independent predictive factor for HCC. Results from the ROC curve analysis demonstrated that DCP had a specificity of 93.65% and a sensitivity of 35.44%. Our study also confirmed that AFP >400 ng/mL is consistent with the diagnosis of pathological examination in HCC ($\kappa = 0.042$, $P = .013$), with a specificity of approximately 100% and a sensitivity of 20.3% (Supplemental Table 2). In addition, we found that the specificity for diagnosing HCC with tumor nodules <2 cm when AFP > 400 ng/mL was 100%, whereas the sensitivity was 4%, due to a small sample size in the control group (Supplemental Table 3). These results emphasize the limitations of using AFP alone to diagnose HCC, particularly given a certain missed rate of ANHC.²⁷ Patients with ANHC have a better prognosis than AFP-positive HCC patients. Studies have found that the 1-year, 3-year, and 5-year recurrence-free survival rates for the ANHC group were 78.1%, 57.5%, and 40.6%, respectively, whereas those for the AFP-positive

group were 61.8%, 37.7%, and 31.4%, respectively. Correspondingly, the overall survival rates for the ANHC group were 94.4%, 83.8%, and 62.3%, respectively, and those for the AFP-positive group were 87.2%, 60.0%, and 36.7%, respectively.²⁵ Therefore, diagnosing ANHC is essential to improving prognosis for HCC patients. Currently, the detection methods for ANHC are divided into serum biomarkers and imaging examinations. China's Diagnosis and Treatment Guidelines for Primary Liver Cancer (2022), issued by the National Health Commission, recommends combining AFP-L3 and DCP to improve the diagnosis rate of early HCC. In our study, we screened a total of 73 ANHC patients, and no difference was found in DCP levels between the ANHC and non-HCC groups, which may be due to the limited sample size in the experiment.

Scholars have been actively dedicated to identifying ANHC biomarkers with significant diagnostic value. Shu et al²⁸ used serum proteomics technology to discover 5 HCC biomarkers. Among these biomarkers, the combination of haptoglobin demonstrates significant diagnostic value for ANHC, with an impressive AUC of 0.763. Zhu et al²⁹ revealed that serum heparin-binding cytokines exhibit an 80% positivity rate in ANHC. Furthermore, there is also some diagnostic value in ANHC for inhibitors of the Wnt pathway, such as Dickkopf1,³⁰ adenyl cyclase-associated protein 2,³¹ and latent transforming growth factor-beta-binding protein 1.³² However, more extensive research is required to confirm the diagnostic potential of these biomarkers in ANHC.

STIP1 is a multifunctional protein that plays a crucial role in various cellular processes. Encoded by the STIP1 gene, it is widely expressed in different tissues and cells. STIP1 has been identified as a key player in cancer development and metastasis. Studies suggest that STIP1 regulates tumor cell growth and invasiveness, contributing to tumor progression.³³ Furthermore, STIP1 is also implicated in cancer-related factors such as drug resistance and poor prognosis. Ma et al¹⁸ conducted studies and found that STIP1 levels were significantly elevated in the HCC group, suggesting its potential as an early diagnostic marker for HCC. Chen et al³³ reported that serum STIP1 level was positively correlated with the malignancy degree and tumor size in HCC, indicating STIP1 as a potential biomarker for HCC diagnosis and prognostic evaluation.

Our study revealed that the STIP1 level was significantly higher in the HCC group than in the non-HCC group. Univariate analysis demonstrated that STIP1 and tumor markers log AFP and DCP were

associated factors of HCC, whereas multivariate logistic analysis showed STIP1 and DCP as independent predictors of HCC. Further results from the ROC curve analysis demonstrated that STIP1 combined with DCP exhibited a sensitivity of 84.8% and specificity of 100%. Interestingly, this experiment revealed that the diagnostic value of STIP1 alone was comparable to that of multi-index combination detection, although without statistical significance ($Z = 1.152$, $P = .249$). In conclusion, STIP1 holds significant diagnostic value in HCC. We classified 158 HCC patients based on different levels of STIP1 and observed that a majority of those with high STIP1 levels were in the subgroup with AFP <400 ng/mL and nodules >2 cm, indicating that STIP1 might hold greater diagnostic value for HCC patients with low AFP levels. Previous research shows that larger nodules may indicate a higher degree of tumor invasiveness, thereby suggesting a potential role for STIP1 in the progression of HCC. For the first time, our study confirmed the significant diagnostic value of STIP1 in ANHC. We screened 73 ANHC patients and found that age, ALT, AST, GGT, AFP, STIP1, and hepatitis B virus infection were significantly associated with ANHC. At the same time, DCP did not show such an association, possibly due to the small sample size. Multivariate analysis demonstrated that STIP1 was also an independent predictor of ANHC. The ROC curve results indicated that STIP1 exhibited excellent diagnostic value for ANHC ($P < .0001$). The area under the ROC curve was 0.919, with a diagnostic cutoff value of 68.5 U/mL, sensitivity of 76.71%, and specificity of 100%. Additionally, the validation of the ANHC diagnostic model yielded a diagnostic accuracy of 67.3%, sensitivity of 55.6%, and specificity of 89.5%.

In conclusion, STIP1 shows significant potential as a diagnostic biomarker for HCC and ANHC, providing a new theoretical foundation for diagnosing such diseases. However, further validation and expansion of the sample size are necessary to confirm the diagnostic value of STIP1 and establish a new laboratory basis for the early clinical diagnosis of HCC.

Acknowledgments

The authors thank Dr Zheng Guanghui (Beijing Tiantan Hospital) for his valuable input in the conception of this article.

Funding

This study was funded by Beijing Youan Hospital, Capital Medical University (BJYAYY-CY2019-09).

Conflict of Interest Disclosure

The authors have nothing to disclose.

REFERENCES

- Gao T, Zhi J, Mu C, et al. One-step detection for two serological biomarker species to improve the diagnostic accuracy of hepatocellular carcinoma. *Talanta*. 2018;178:89-93. <https://doi.org/10.1016/j.talanta.2017.09.011>
- Cadier B, Bulsei J, Nahon P, et al; ANRS CO12 CirVir and CHANGH groups. Early detection and curative treatment of hepatocellular carcinoma: a cost-effectiveness analysis in France and the United States. *Hepatology*. 2017;65(4):1237-1248. <https://doi.org/10.1002/hep.28961>
- Llovet JM, Zucman-Rossi J, Pikarsky E, et al. Hepatocellular carcinoma. *Nat Rev Dis Primers*. 2016;2:16018. <https://doi.org/10.1038/nrdp.2016.18>
- Brown ZJ, Tsilimigras DI, Ruff SM, et al. Management of hepatocellular carcinoma: a review. *JAMA Surg*. 2023;158(4):410-420. <https://doi.org/10.1001/jamasurg.2022.7989>
- Forner A, Reig M, Bruix J. Hepatocellular carcinoma. *Lancet*. 2018;391(10127):1301-1314. [https://doi.org/10.1016/S0140-6736\(18\)30010-2](https://doi.org/10.1016/S0140-6736(18)30010-2)
- Ruan DY, Lin ZX, Wang TT, et al. Nomogram for preoperative estimation of long-term survival of patients who underwent curative resection with HCC beyond Barcelona clinic HCC stage A1. *Oncotarget*. 2016;7(38):61378-61389. <https://doi.org/10.18632/oncotarget.11358>
- Marrero JA, Kulik LM, Sirlin CB, et al. Diagnosis, staging, and management of hepatocellular carcinoma: 2018 practice guidance by the American Association for the Study of Liver Diseases. *Hepatology*. 2018;68(2):723-750. <https://doi.org/10.1002/hep.29913>
- Clark T, Maximin S, Meier J, Pokharel S, Bhargava P. Hepatocellular carcinoma: review of epidemiology, screening, imaging diagnosis, response assessment, and treatment. *Curr Probl Diagn Radiol*. 2015;44(6):479-486. <https://doi.org/10.1067/j.cpradiol.2015.04.004>
- Tzartzeva K, Obi J, Rich NE, et al. Surveillance imaging and alpha fetoprotein for early detection of HCC in patients with cirrhosis: a meta-analysis. *Gastroenterology*. 2018;154(6):1706-1718.e1. <https://doi.org/10.1053/j.gastro.2018.01.064>
- Villanueva A, Minguez B, Forner A, Reig M, Llovet JM. Hepatocellular carcinoma: novel molecular approaches for diagnosis, prognosis, and therapy. *Annu Rev Med*. 2010;61:317-328. <https://doi.org/10.1146/annurev.med.080608.100623>
- Wun YT, Dickinson JA. Alpha-fetoprotein and liver ultrasonography for HCC screening in patients with chronic hepatitis B. *Cochrane Database Syst Rev*. 2012;2012(9):CD002799. <https://doi.org/10.1002/14651858.CD002799>
- Luo P, Wu S, Yu Y, et al. Current status and perspective biomarkers in AFP negative HCC: towards screening for and diagnosing HCC at an earlier stage. *Pathol Oncol Res*. 2020;26(2):599-603. <https://doi.org/10.1007/s12253-019-00585-5>
- Li B, Liu H, Shang HW, Li P, Li N, Ding HG. Diagnostic value of glypican-3 in alpha-fetoprotein negative HCC patients. *Afr Health Sci*. 2013;13(3):703-709.
- Li J, Cheng ZJ, Liu Y, et al. Serum thioredoxin is a diagnostic marker for hepatocellular carcinoma. *Oncotarget*. 2015;6(11):9551-9563. <https://doi.org/10.18632/oncotarget.3314>
- Zhang Z, Zhang Y, Wang Y, Xu L, Xu W. Alpha-fetoprotein-L3 and Golgi protein 73 may serve as candidate biomarkers for diagnosing alpha-fetoprotein-negative hepatocellular carcinoma. *Onco Targets Ther*. 2016;9:123-129. <https://doi.org/10.2147/OTT.S90732>
- Feng H, Li B, Li Z, Wei Q, Ren L. PIVKA-II serves as a potential biomarker that complements AFP for the diagnosis of hepatocellular carcinoma. *BMC Cancer*. 2021;21(1):401. <https://doi.org/10.1186/s12885-021-08138-3>
- Piñero F, Dirchwolf M, Pessôa MG. Biomarkers in hepatocellular carcinoma: diagnosis, prognosis and treatment response assessment. *Cells*. 2020;9(6):1370. <https://doi.org/10.3390/cells9061370>
- Ma XL, Tang WG, Yang MJ, et al. Serum STIP1, a novel indicator for microvascular invasion, predicts outcomes and treatment response in hepatocellular carcinoma. *Front Oncol*. 2020;10:511. <https://doi.org/10.3389/fonc.2020.00511>
- Huang L, Zhai E, Cai S, et al. Stress-inducible protein-1 promotes metastasis of gastric cancer via the Wnt/ β -catenin signaling pathway. *J Exp Clin Cancer Res*. 2018;37(1):6. <https://doi.org/10.1186/s13046-018-0676-8>
- Lin CY, Chen SH, Tsai CL, Tang YH, Wu KY, Chao A. Intracellular targeting of STIP1 inhibits human cancer cell line growth. *Transl Cancer Res*. 2021;10(3):1313-1323. <https://doi.org/10.21037/tcr-20-3333>

21. Zhang J, Chen G, Zhang P, et al. The threshold of alpha-fetoprotein (AFP) for the diagnosis of hepatocellular carcinoma: a systematic review and meta-analysis. *PLoS One*. 2020;15(2):e0228857. <https://doi.org/10.1371/journal.pone.0228857>
22. Marrero JA, Feng Z, Wang Y, et al. Alpha-fetoprotein, des-gamma carboxyprothrombin, and lectin-bound alpha-fetoprotein in early hepatocellular carcinoma. *Gastroenterology*. 2009;137(1):110-118. <https://doi.org/10.1053/j.gastro.2009.04.005>
23. Trevisani F, D'Intino PE, Morselli-Labate AM, et al. Serum alpha-fetoprotein for diagnosis of HCC in patients with chronic liver disease: influence of HBsAg and anti-HCV status. *J Hepatol*. 2001;34(4):570-575. [https://doi.org/10.1016/s0168-8278\(00\)00053-2](https://doi.org/10.1016/s0168-8278(00)00053-2)
24. Choi JY, Jung SW, Kim HY, et al. Diagnostic value of AFP-L3 and PIVKA-II in HCC according to total-AFP. *World J Gastroenterol*. 2013;19(3):339-346. <https://doi.org/10.3748/wjg.v19.i3.339>
25. Wang T, Zhang KH. New blood biomarkers for the diagnosis of AFP-negative hepatocellular carcinoma. *Front Oncol*. 2020;10:1316.
26. De J, Shen Y, Qin J, Feng L, Wang Y, Yang LA. Systematic review of des- γ -carboxy prothrombin for the diagnosis of primary hepatocellular carcinoma. *Medicine (Baltimore)*. 2016;95(17):e3448. <https://doi.org/10.1097/MD.0000000000003448>
27. Xu Y, Lu X, Mao Y, et al. Clinical diagnosis and treatment of alpha-fetoprotein-negative small hepatic lesions. *Chin J Cancer Res*. 2013;25(4):382-388. <https://doi.org/10.3978/j.issn.1000-9604.2013.08.12>
28. Shu H, Kang X, Guo K, et al. Diagnostic value of serum haptoglobin protein as HCC candidate marker complementary to α fetoprotein. *Oncol Rep*. 2010;24(5):1271-1276. https://doi.org/10.3892/or_00000982
29. Zhu WW, Guo JJ, Guo L, et al. Evaluation of midkine as a diagnostic serum biomarker in hepatocellular carcinoma. *Clin Cancer Res*. 2013;19(14):3944-3954. <https://doi.org/10.1158/1078-0432.CCR-12-3363>
30. Shen Q, Fan J, Yang XR, et al. Serum DKK1 as a protein biomarker for the diagnosis of hepatocellular carcinoma: a large-scale, multicentre study. *Lancet Oncol*. 2012;13(8):817-826. [https://doi.org/10.1016/S1470-2045\(12\)70233-4](https://doi.org/10.1016/S1470-2045(12)70233-4)
31. Chen M, Zheng T, Han S, et al. A preliminary study of plasma cyclase-associated protein 2 as a novel biomarker for early stage and alpha-fetoprotein negative HCC patients. *Clin Res Hepatol Gastroenterol*. 2015;39(2):215-221. <https://doi.org/10.1016/j.clinre.2014.08.006>
32. Cao B, Yang L, Rong W, et al. Latent transforming growth factor-beta binding protein-1 in circulating plasma as a novel biomarker for early detection of hepatocellular carcinoma. *Int J Clin Exp Pathol*. 2015;8(12):16046-16054.
33. Chen Z, Xu L, Su T, et al. Autocrine STIP1 signaling promotes tumor growth and is associated with disease outcomes in hepatocellular carcinoma. *Biochem Biophys Res Commun*. 2017;493(1):365-372. <https://doi.org/10.1016/j.bbrc.2017.09.016>

Interference of hemoglobin variants with HbA1c measurements by six commonly used HbA1c methods

Mingyang Li¹, Song Ge¹, Xin Shu², Xiongjun Wu³, Haiyan Liu², Anping Xu¹, Ling Ji¹

¹Clinical Laboratory, DongYang People's Hospital, Dongyang, China. *To whom correspondence should be addressed: 15958490336@139.com.

Keywords: FMEA, emergency complete blood count, laboratory turnaround time, phlebotomy skills, quality control, morphology training

Abbreviations: FMEA, failure mode and effects analysis; CBC, complete blood count; RPN, risk priority number; TAT, turnaround time; ISO, International Organization for Standardization; CRP, C-reactive protein; S, severity; O, probability of occurrence; D, fault detection; IQR, interquartile range

Laboratory Medicine 2024;54:574-581; <https://doi.org/10.1093/labmed/lmad002>

ABSTRACT

Objective: Failure mode and effects analysis (FMEA) was used to identify factors that contribute to quality management deficiencies in laboratory testing of emergency complete blood count (CBC).

Methods: Improvements included instrument updates, personnel training, and laboratory information system optimization. We used operational data from January 2021 (control group) and January 2022 (FMEA group) to compare the risk priority number (RPN) of FMEA, emergency CBC laboratory turnaround time (TAT), error report rate, and specimen failure rate.

Results: After the implementation of FMEA, the average RPN dropped from 36.24 ± 9.68 to 9.45 ± 2.25 , ($t = 20.89$, $P < .05$). Additionally, the median TAT for emergency CBCs decreased from 23 min to 11 min as did the interquartile distance (17-34 min to 8-16 min) ($P < .05$). The rate of emergency CBC error reports decreased from 1.39% to 0.71% ($P < .05$), and the specimen failure rate decreased from 0.95% to 0.32% ($P < .05$). Patient satisfaction also increased from 43% to 74% ($P < .05$), and the technician-performed morphology assessment pass rate increased from 16.7% to 100% ($P < .05$).

Conclusion: Improving the emergency CBC testing process with FMEA can shorten emergency CBC laboratory TAT and reduce

specimen failure rates and reporting error rates. The FMEA can be used to improve quality management in emergency CBC laboratories.

Emergency complete blood count (CBC) analysis is commonly requested during emergency medical care. Indicators such as hemoglobin, neutrophils, monocytes, and eosinophils can reflect early signs of many systemic diseases such as leukemia, anemia, systemic lupus erythematosus, tuberculosis, and acute aortic syndrome among others.¹⁻⁶ A CBC is usually the initial test of choice in emergency pediatric settings to differentiate between bacterial and viral infections.⁷ Recent studies have shown that CBCs also have had an early warning effect during the global COVID-19 pandemic.⁸⁻¹⁰ Timely and correct reporting is the basis for reliable medical disposition,¹¹ and establishing correct and effective laboratory quality indicators is the key to ensuring that test reports are timely and correct.

Quality indicators are one of the tools for quantifying the quality of a certain aspect of a laboratory's services. The International Organization for Standardization (ISO) 15189:2012 guidelines state "[L]aboratories should establish quality indicators to monitor and evaluate the key links in the pre-test, inspection and post-test process." The Chinese Health and Family Planning Commission issued 15 medical quality control indicators for clinical laboratory specialties (2015 edition). Using these 15 indicators combined with the characteristics of our laboratory, we selected 9 of them as the quality indicators for this emergency CBC laboratory. They are the specimen failure rate in the pretest process, laboratory turnaround time (TAT) during inspection, error reporting rate in the posttest process, and the rates of specimen type error, container error, specimen loss, specimen coagulation, hemolysis, and insufficient collection, which are the main reasons for specimen failure. Quantitative assessment of the errors in the entire process of testing was carried out using the above indicators. Although the use of quality indicators can help laboratories quantify and monitor risks throughout the workflow of emergency CBCs, the guidelines of ISO and the Chinese Health and Family Planning Commission do not provide specific methods for risk identification and management.

Failure mode and effects analysis (FMEA) is a management tool that proactively identifies potential failures and assesses their causes and effects, thereby preventing their occurrence.¹²⁻¹⁴ Liu et al¹⁴ showed that

FMEA has high utility in improving health care quality and reducing errors, and this method has already been widely used to improve health care processes in hospitals, including clinical practices¹⁵ such as chemotherapy,¹⁶ pediatrics,¹⁷ intensive care,¹⁸ paramedical technology,^{19,20} reproductive health medicine,²¹ hospital infection control,²² and others.

The FMEA has been successfully used to improve the quality of various clinical procedures and processes in hospital systems; however, its specific application to quality management in emergency CBC laboratories is rare, and it is not very common to use FMEA for process improvement to optimize laboratory quality management. At the same time, owing to the diversity of laboratory test lists and the consideration of time and effort costs, it is not easy to conduct extensive laboratory quality management assessments in this way. Therefore, we used emergency CBC as an example to conduct an FMEA study. The objective of this study was to (1) evaluate the effectiveness of improving emergency CBC quality management by applying the FMEA model, (2) identify improvement measures, and (3) provide a reference for quality management in other laboratories.

Materials and Methods

General Materials

The study was conducted at a 1700-bed general tertiary hospital in China. The selected emergency laboratory was certified by ISO15189 in 2014. We used operational data from all emergency CBC samples tested in emergency laboratories in January 2021 as the control group ($n = 9680$) and the same data in January 2022 as the FMEA group ($n = 10,352$). The FMEA improvement period was from February 2021 to December 2021. The data were obtained from the Emergency Laboratory Information System (LIS). Some emergency CBCs appeared in combination with C-reactive protein (CRP) level testing in the report. The original emergency CBC testing instrument was the BC 6800 Auto Hematology Analyzer (Mindray), which was replaced by the XN-2000 Hematology Analyzer (Sysmex) as part of the improvements. The CRP detection instrument used was the Aristo Specific Protein Analyzer (Goldsite), which was replaced by the PA990pro Specific Protein Analyzer (Lifotronic) after improvement. The study was approved by the hospital review board.

FMEA Team Formation

The FMEA team was multidisciplinary, consisting of 6 people—1 laboratory director, 1 FMEA guidance expert, 1 laboratory quality statistical analyst, 2 resident personnel of the emergency laboratory, and 1 specimen recipient—who were key to emergency CBC quality management. Under the auspices of the director, the FMEA guidance expert trained team members on FMEA models. The department regularly held FMEA meetings to analyze the quality defects in the emergency CBC process from reception to reporting, assessing risks, summarizing the causes, formulating improvement measures, and supervising implementation.

FMEA Analysis

Team members listed all the steps of emergency CBC analysis in detail, beginning from receipt of the sample in the laboratory to the issuance of the report, which was divided into receipt of specimen, preinspection processing, instrument testing, and final report based on the time recorded by the LIS (FIGURE 1). By consulting the literature and the

process characteristics of our hospital's emergency CBC,^{23,24} we listed 6 failure modes in the emergency CBC testing process that could cause quality defects, which were specimens not being processed in a timely manner after receipt, many unqualified specimens, congestion during peak periods, the instrument running slowly, reports not being sent in a timely manner, and error reporting. We discussed and analyzed the causes and outcomes of the failures, then scored them based on the severity (S), probability of occurrence (O), and fault detection (D), and summarized the scores of the 6 members, expressed as averages. To reduce subjective errors, we developed the scoring criteria of O, S, and D after discussion (TABLE 1). Based on the International Joint Commission guidelines of 2010,²¹ the risk priority number (RPN) was calculated as $O \times S \times D$. Finally, the risk was sorted according to the RPN, and the risks of failure were positively correlated with the RPN. Referring to the characteristics of this scoring and the introduction of the literature, we determined that an $RPN \geq 30$ indicated a high-risk factor and prioritized a failure mode above $S \geq 4$ for improvement; if the $RPN < 30$, but any of the values in O or $D \geq 4$, the factor was also considered to be high risk.^{25–27} According to the above rules, 6 failure modes were found in need of improvement. The risks from highest to lowest were as follows: the instrument running slowly, many unqualified specimens, congestion during peak periods, error reporting, specimens not being processed in a timely manner after receipt, and reports not being sent in a timely manner (TABLE 2).

FMEA Improvement Process

1. The instrument runs slowly (RPN: 46.24; S:4.00; O:4.33). This extended the laboratory TAT because of the high failure rate of CRP instruments; a single CBC instrument could not meet the daily workload. We therefore purchased the Sysmex blood routine assembly line, including 2 CBC detectors, a fully automatic staining instrument. We also updated and added 2 CRP detectors for alternative use to reduce failure rate.
2. There are many unqualified specimens of quality (RPN: 40.35; S:4.00; O:4.33). Here, the cause of the failure was the unqualified quality of specimens caused by insufficient phlebotomy skills. We created a phlebotomy training plan for all phlebotomists who had been trained and assessed every 6 months and set a monthly quality target for each phlebotomist. We then publicized the completions of the target. The Medical Department conducts a quarterly phlebotomy skills satisfaction survey.
3. Congestion during peak periods (RPN: 37.28; S:4.00; O:4.00), the failure was due to high specimen volume during peak periods; therefore, we increased the emergency laboratory staff during peak times (9:00 to 11:00 AM, 4:00 to 6:00 PM).
4. Error reporting (RPN: 21.36.28; S:4.00; O:2.67). Here, the cause of the failure was unfamiliar reporting rules. In response, we set the blood routine reexamination rules in the LIS: a report that does not trigger the reexamination rules is automatically sent by the system, the report that triggers the reexamination rules is sent after manual review, and the difficult results (such as leukemia) that cannot be automatically classified by the instrument are manually classified by microscopy. We also created a blood cell morphology training plan with a teaching group, and the morphology experts in the department served as teachers.

FIGURE 1. Emergency complete blood count laboratory turnaround process.

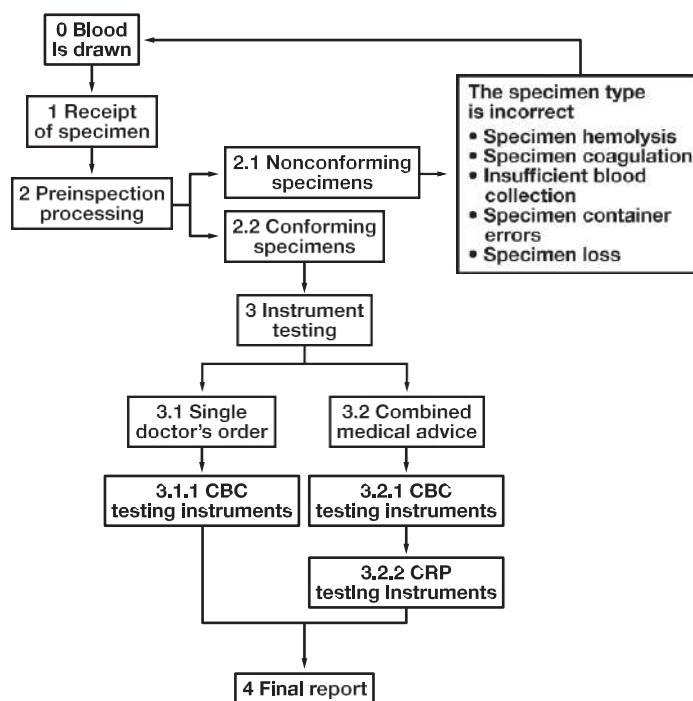


TABLE 1. Scoring of Factors That Influence the Failure Modes and Effects Analysis Performance

Score	Description
Occurrence (O)	
1	Rarely occurs
2	Occurs quarterly
3	Occurs monthly
4	Occurs daily
5	Occurs continuously
Severity (S)	
1	No effect; processing time <5 min
2	Minor; processing time 5-10 min
3	Major; processing time 10-15 min
4	Serious; processing time 15-30 min
5	Very serious; processing time >30 min
Detection (D)	
1	When blood is drawn
2	Specimen collection phase
3	Before instrument testing
4	Inspection before report is issued
5	Unable to detect

Monthly morphology training and quarterly assessments were planned for young employees with less than 5 years of seniority, and employees with 5 to 10 years of seniority who had a certain morphological foundation were scheduled to be evaluated every 6 months. We set the qualifying score at 90 points. Employees

could stop the morphological assessments in advance if they passed the assessments 4 times in a row.

- Failure to process promptly after receipt (RPN: 24.56; S:2.83; O:4.00). This failure was caused by the fact that the specimen acceptance site was located at a distance from the laboratory, resulting in the extension of the reporting TAT. The improvement measures we took consisted of relocating the sampling site and setting up sampling points in the laboratory to shorten the time from specimen sampling to testing.
- Reports are not sent in a timely manner (RPN: 16.98; S:1.50; D:4.00). This failure was due to the large workload in the emergency laboratory, resulting in the extension of the laboratory TAT. To improve this, we set up a TAT reminder service on LIS to remind laboratory personnel to prioritize the processing of long reports of the TAT.

Finally, the team members then developed an emergency CBC test standard operating procedure based on the improvement measures for performance. Emergency department personnel were required to operate strictly according to these standardized procedures. These FMEA improvements were implemented between February 2021 and December 2021, followed by a second round of FMEA analysis of emergency CBC quality management in January 2022.

Evaluation

The RPN and changes in laboratory TAT were used to assess changes in processes before and after improvement. The specimen failure rate and the satisfaction of phlebotomy skills were used to evaluate phlebotomy skills; the error reporting rate and morphological assessment pass rate were used to evaluate the reporting ability.

TABLE 2. Risk Assessment Form for Quality Deficiencies in Emergency CBC Laboratory Management

Process Step	Potential Failure Mode	Cause	Impact on Quality Indicators	S	O	D	RPN	Prioritization	Improvement Measure
1. Receipt of specimen	Specimens are not processed in a timely manner after receipt	The specimen collection location is far from the detection location	Laboratory TAT increases	2.83	4.00	2.17	24.56	6	Relocation of sample collection sites; set the specimen collection point in the laboratory
2. Preinspection processing	There are many rejected specimens owing to quality	Insufficient phlebotomy skills	The quality failure rate increases, and the specimen is re-extracted	4.00	4.33	2.33	40.35	2	Train the phlebotomists in phlebotomy skills and set a target value for each person to pass the phlebotomy per month; finally, announce the completion of the target
3. Instrument testing	Congestion during peak periods	Large specimen volume	Laboratory TAT increases	4.00	4.00	2.33	37.28	3	Increased availability of personnel from 9:00 to 11:00 AM and from 4:00 to 6:00 PM to cope with the peak period of specimens
	The instrument runs slowly	Insufficient testing instruments	Laboratory TAT increases	4.00	4.33	2.67	46.24	1	The introduction of Sysmex blood routine assembly line, including 2 CBC detectors and an automatic dyeing instrument
4. Final report	Reports are not sent in a timely manner	Large specimen volume	Laboratory TAT increases	1.50	2.83	4.00	16.98	6	Set the TAT preset value in the LIS to detect when a report was unintentionally missed
	Error reporting	Lack of well-established reexamination system for reporting blood routines, and the morphological ability of the reporting was inadequate	Report recovery rates increased	4.00	2.67	2.00	21.36	4	We established a blood routine re-examination system and regularly train personnel in blood cell morphology

CBC, complete blood count; D, detectability of failure occurrence; LIS, laboratory information system; O, the possibility of the failure; RPN, risk priority number (1 to 6 from highest to lowest priority); S, the severity of the failure; TAT, turnaround time.

RPN

After the FMEA improvement, we obtained the RPN in the same way as before the improvement.

Laboratory TAT

We divided TAT into 4 subdivisions: (1) laboratory TAT, which was clock started when the specimen reached the laboratory and was first accessioned by the LIS and clock stopped when the result was finalized in the LIS; (2) peak hour TAT, that is, the laboratory TAT during the maximum specimen volume time period (9:00 to 11:00 AM, 4:00 to 6:00 PM); (3) single doctor's order TAT, which means a laboratory TAT that only contains a single item of the emergency CBC in the medical order; and (4) combination doctor's order TAT, which refers to the laboratory TAT, including emergency CBC and CRP level testing. We used median and interquartile range (IQR) to describe the changes in TAT before and after FMEA.

Error Report Rate

The error report rate was the number of emergency CBC error reports recovered by LIS divided by the total number of emergency CBC specimens in the month.

Specimen Failure Rate

The specimen failure rate is considered the number of rejected specimens divided by the total number of emergency CBC specimens in the month. The reasons for failure were divided into specimen type error, container error, specimen loss, hemolysis, coagulation, and insufficient collection amount, and the proportion of rejection reasons was compared.

Phlebotomy Skills Satisfaction

A questionnaire was compiled by the hospital medical department and distributed to patients every quarter. The satisfaction level was divided into unsatisfactory, average, satisfactory, and very satisfied. The content of the survey included the patient's satisfaction with environment, phlebotomy skills, infrastructure construction, and so on, and combined with the service attitude of the phlebotomists. Results were quantified thus: phlebotomy skills satisfaction = very satisfied + satisfied/total number of cases × 100%. We compared the results of questionnaires in the fourth quarter of 2020 (control group, collected in January 2021) before and after improvement in the fourth quarter of 2021 (FMEA group, collected in January 2022) to identify changes in patient satisfaction.

Morphological Assessment Pass Rate

The assessment content was divided into theoretical examination and practical assessment. The theory consisted of 50 cell morphological maps. The practical assessment consisted of manually classifying 5 blood cell smears stained by Wright's staining within 30 min. The specimens used for the assessment were from healthy people, platelet aggregates, leukemia, inflammatory infection patients, and others. Results were quantified as pass rate = number of qualified people/total number of people assessed × 100%. The total score was 100 points, and 90 points and above represented a passing grade.

Statistical Analysis

We used SPSS statistical software version 26.0 (IBM) for statistical analysis and processing. Continuous variables containing normally distributed data are expressed as the mean and standard deviation.

Nonnormally distributed data are represented as the median and interquartile range. We used χ^2 tests to compare categorical variables. We performed the Student's *t*-test and the Mann-Whitney *U* test to compare parametric and nonparametric continuous variables, respectively. A *P* value < .05 was considered statistically significant.

Results

There was no statistically significant difference (*P* > .05) in the sex and age or the proportion of disease types between the 2021 and 2022 groups (TABLE 3).

After the implementation of FMEA, the average RPN dropped from 36.24 ± 9.68 to 9.45 ± 2.25 , (*t* = 20.89, *P* < .05). (TABLE 4).

After FMEA improvements, the median TAT (11 min) and IQR (8-16 min) in the emergency CBC laboratories were significantly shorter than those before (23 min and 17-34 min), and the peak TAT, single doctor's order TAT, and combination doctor's order TAT were significantly (*P* < .01) shorter than those before (TABLE 5).

TABLE 3. Characteristics of Patients from Whom Samples Were Obtained

Item	Control Group	FMEA Group	χ^2/t	<i>P</i> Value
Sex (F/M)	4530/5150	4943/5409	1.81	.18
Age, y, $\bar{X} \pm SD$	46.31 \pm 26.20	49.43 \pm 23.48	-1.60	.112
Diagnostic categories	9680	10,352	14.27	.01
Presence of fever	3274	3409	1.78	.18
Surgical cases	3370	3818	9.29	<.05
Internal medicine cases	3036	3125	3.25	.07

FMEA, failure modes and effects analysis; SD, standard deviation; *X*, mean.

TABLE 4. Changes in RPN before and after FMEA

Potential Failure Mode	RPN		Reduction in RPN (%)
	Before	After	
The instrument runs slowly	46.24	10.68	76.90
Instrument congestion during peak periods	37.28	9.32	75.00
There are many rejected specimens due to quality	40.35	9.32	76.90
Error reporting	21.36	8.00	62.55
High review rate	42.47	12.75	69.98
Specimens are not processed in a timely manner after receipt	24.56	6.14	75.00
Reports are not sent in a timely manner	16.98	6.00	64.66
Average value ($\bar{X} \pm SD$)	36.24 \pm 9.68	9.45 \pm 2.25 ^a	71.57

FMEA, failure mode and effects analysis; RPN, risk priority number.

^aCompared with before, *t* = 20.89, *P* < .05.

TABLE 5. Decreases in Turnaround Time at Different Stages before and after FMEA

	Median (IQR), min		<i>Z</i> Value	<i>P</i> Value
	Control Group (2021)	FMEA Group (2022)		
Laboratory TAT	23 (17-34)	11 (8-16)	-63.79	<.05
Peak TAT	45 (37-71)	38 (33-49)	-3.95	<.05
Single doctor's order TAT	12 (7-27)	9 (6-15)	-67.08	<.05
Combination doctor's order TAT	24 (18-34)	11 (8-16)	-7.57	<.05

FMEA, failure mode and effects analysis; IQR, interquartile range; TAT, turnaround time.

^aLaboratory TAT is the TAT for laboratory from specimen receipt to report generation. T3 is the peak TAT, the lab TAT of maximum time period for specimen volume (9:00 to 11:00 AM, 4:00 to 6:00 PM). Single doctor's order TAT is the doctor's order includes only laboratory TAT at the time of emergency complete blood count (CBC) testing. The combination doctor's order TAT is the physician's order includes laboratory TAT for emergency CBC and C-reactive protein level testing.

The error reporting rate decreased from 1.39% to 0.71% ($\chi^2 = 23.14$, *P* < .05) and the specimen failure rate decreased from 0.95% to 0.32% ($\chi^2 = 10.63$, *P* < .05), and the proportion of all causes of nonconformity decreased after improvement; especially of note was that the incidence of container error and specimen loss was 0, which was a significant improvement, as shown in TABLE 6.

After the phlebotomists received training, the patient satisfaction rate with regard to phlebotomy skills increased from 43% to 74%, ($\chi^2 = 19.79$, *P* < .05), which was statistically significant (TABLE 7).

During the morphology training of reporters, the pass rate of the assessment increased from 16.7% in the first quarter to 100% in the fourth quarter of 2021, and the difference was statistically significant (*P* < .05) (TABLE 8).

Discussion

In this study, we categorized the main processes involved in emergency CBC procedures into receipt of specimen, preinspection processing,

TABLE 6. Emergency CBC Reporting Error Recovery Rate and Specimen Quality Analysis before and after FMEA

	No. (%)		χ^2	P Value
	Control Group (n = 9680)	FMEA Group (n = 10,352)		
Reporting error recovery rate	135 (1.39)	73 (0.71)	23.14 ^a	<.05
Total rejection rate of emergency CBC specimens	92 (1.12)	33 (0.41)	10.63 ^b	.04
The specimen type is incorrect	17 (0.17)	9 (0.09)	3.03 ^a	<.05
Specimen container errors	10 (0.10)	0 (0)	10.70 ^b	<.05
Specimen loss	7 (0.07)	0 (0)	7.49 ^b	<.05
Specimen hemolysis	18 (0.18)	11 (0.11)	29.99 ^a	<.05
Specimen coagulation	34 (0.35)	8 (0.07)	17.95 ^a	<.05
Insufficient blood collection	23 (0.24)	11 (0.1)	5.09 ^a	.02

CBC, complete blood count; FMEA, failure mode and effects analysis.

^aPearson χ^2 .

^bFisher exact probability.

TABLE 7. Patient Satisfaction of Blood Collection before and after Improvement^a

	Not Satisfied	Generally	Satisfied	Very Satisfied	Satisfaction
Control group (n = 200)	50 (25%)	64 (32%)	64 (32%)	22 (11%)	43%
FMEA group (n = 200)	16 (8%)	36 (18%)	94 (47%)	54 (27%)	74%

^aThe control group shows the results of a blood collection satisfaction survey for the fourth quarter of 2020. The failure mode and effects analysis (FMEA) group shows the results of a blood collection satisfaction survey for the fourth quarter of 2021. Satisfaction is calculated as very satisfied + satisfied/total number of cases \times 100%. $\chi^2 = 19.79$; $P < .05$.

TABLE 8. Changes in Morphology Test Pass Rates^a

Employees with Less than 10 Years of Service	Examination Score			
	1st Quarter	2nd Quarter	3rd Quarter	4th Quarter
A	72	89	98 (pass)	100 (pass)
B	68	84	92 (pass)	98 (pass)
C	82	90 (pass)	92 (pass)	100 (pass)
D	90 (pass)	95 (pass)	100 (pass)	100 (pass)
E	78	96 (pass)	100 (pass)	98 (pass)
F	77	86	92 (pass)	100 (pass)
G		88		92 (pass)
H		90 (pass)		96 (pass)
J		91 (pass)		94 (pass)
Pass rate	16.7%	55.6% ^b	100% ^b	100% ^b

^aA to F indicates employees within 5 years of seniority who are evaluated quarterly in morphology. G to J indicates employees with 5 to 10 years of seniority who had a certain morphological foundation and were scheduled to be evaluated every 6 months. A score of 90 or more will be awarded a pass. The pass rate is the number of passes/total number of people taking the exam \times 100%.

^bCompared with the first quarter, $P < .05$.

instrument testing, preliminary examination, and final report. Failure patterns that caused laboratory quality defects at each step were investigated, and interventions were developed to address them. Using FMEA, we identified 6 failure modes that could lead to emergency CBC quality defects and sorted them by rectification priority. These failure modes were divided into the following: the instrument runs slowly, there are many unqualified specimens of quality, congestion during peak periods, error reporting, specimens are not processed in a timely manner after receipt, and reports are not sent in a timely manner.

The instrument runs slowly had the largest RPN in our risk assessment, in which the failure mode was instrument detection in the

inspection; therefore, we updated and increased the number of our testing instruments for CBC and CRP level. We purchased the Sysmex XN2800 pipeline system, which included 2 XN2000 blood cell detectors and a fully automatic staining instrument to replace the previously improved single blood cell detection mode. Additionally, as emergency CBC and CRP level testing often exist in combination orders, we also added new CRP detectors to increase the speed of our analysis. After this improvement, both the laboratory TAT and the combined doctor's order TAT were shortened by half, and the single doctor's order TAT was also significantly shortened. Although we did not compare instrument characteristics of CBC and CRP before and after the improvement, the

significantly shortened TAT illustrated the benefits of replacing the instrument. Updating and adding testing equipment also solved the problem of specimen accumulation caused by insufficient equipment. However, congestion due to large specimen volumes during peak periods remained a problem. The failure mode of congestion during peak periods, which was the same as specimens are not processed in a timely manner after receipt, would lead to the extension of laboratory TAT. The causes of failure also overlapped partially, mainly owing to the large number of specimens and insufficient manpower during peak hours. In particular, the specimens are not processed in a timely manner after receipt failure category had an additional cause: the specimen acceptance site was located at a distance from the laboratory. Therefore, the relocation of the specimen receiving area to the laboratory effectively solved the problem. To improve congestion during peak periods we increased the emergency laboratory staff during peak times (9:00 to 11:00 AM, 4:00 to 6:00 PM). As the peak period TAT was shortened significantly after improvement, the effectiveness of the measure was demonstrated. However, the changes in this TAT were not as obvious as other TAT changes, possibly because of other fault factors, such as the occupation of resources by nonemergency specimens, which was also mentioned in the 738 Chinese laboratory surveys conducted by Zhang et al.²⁸

Another important indicator of the quality of emergency CBC laboratories was the specimen failure rate, which was manifested in several aspects: specimen type error, container error, specimen coagulation, hemolysis, insufficient collection, and specimen loss. We implemented further training in phlebotomy skills while setting each phlebotomist a monthly target for quality qualification and the completion of the target value was publicized. Owing to the continuous enhancement of phlebotomy skills, simple collection errors, such as container errors, were directly avoided and dropped to zero after improvements. The specimen coagulation, hemolysis, and insufficient amount of collection were also significantly reduced. However, in the process of phlebotomy, it is difficult to avoid the phenomenon of unqualified specimens due to the fact that some patients' blood vessels are relatively hidden, or the patient's blood itself is in a hypercoagulable state and incorrect pretreatment process outside the laboratory. For the improvement of specimen loss, the solution was to separate the placement areas for inspected and uninspected specimens. This stopped the phenomenon of random placement of uninspected specimens with the completed specimens, and the incidence of specimen loss after improvement decreased to zero, which shows that a reasonable laboratory layout can reduce the frequency of adverse events. This was similar to the conclusions of Tsai et al.²⁹

To address the error reporting failure category, we rectified both LIS and personnel. We also added blood routine review rules to LIS, which could be automatically issued for normal reports that do not trigger the rules, whereas reports that trigger retest rules need to be manually reviewed. Reports that cannot be automatically sorted by the instrument would be sent through manual classification. At the same time, regular blood cell morphology training was carried out for personnel to improve the detection and accuracy of difficult blood cell reports. Although the decline in the error reporting rate showed that this rectification was effective, the application of the automatic report sending system requires further improvements and supervision in the later stage. Finally, to address the reports are not sent in a timely manner failure category, we set up a TAT reminder service on the LIS, which effectively reminds the staff to review and deliver the report on time.

Similar to other efforts to employ FMEAs, our analysis may be subjective and depends on the experience and skills of the team members. We only targeted process improvements within the emergency CBC laboratory and did not address the relevant process factors outside the laboratory, which should be investigated in future research.

In summary, we optimized the testing process of emergency CBC laboratory from the aspects of instrument update, personnel training, and LIS optimization and improved their quality management capabilities.

Conclusion

Improving the emergency CBC testing process through FMEA can shorten laboratory TAT and reduce specimen failure rates and report recovery rates, thereby improving laboratory quality management.

Conflict of Interest Disclosure

The authors have nothing to disclose.

REFERENCES

1. Lee E, Kim M, Jeon K, et al. Mean platelet volume, platelet distribution width, and platelet count, in connection with immune thrombocytopenic purpura and essential thrombocytopenia. *Lab Med*. 2019;50(3):279–285.
2. Park CH, Yun JW, Kim HY, et al. Myelodysplastic syndrome/ myeloproliferative neoplasm with ring sideroblasts and thrombocytosis with cooccurrent SF3B1 and MPL gene mutations: a case report and brief review of the literature. *Lab Med*. 2020;51(3):315–319.
3. Jeon YL, Lee WI, Kang SY, et al. Neutrophil-to-monocyte-plus-lymphocyte ratio as a potential marker for discriminating pulmonary tuberculosis from nontuberculosis infectious lung diseases. *Lab Med*. 2019;50(3):286–291.
4. Peirovy A, Malek Mahdavi A, Khabbazi A, et al. Clinical usefulness of hematologic indices as predictive parameters for systemic lupus erythematosus. *Lab Med*. 2020;51(5):519–528.
5. Moon SY, Lee HS, Park MS, Kim I-S, Lee SM. Evaluation of the barricor tube in 28 routine chemical tests and its impact on turnaround time in an outpatient clinic. *Ann Lab Med*. 2021;41(3):277–284. doi:10.3343/alm.2021.41.3.277.
6. Morello F, Cavalot G, Giachino F, et al. White blood cell and platelet count as adjuncts to standard clinical evaluation for risk assessment in patients at low probability of acute aortic syndrome. *Eur Heart J Acute Cardiovasc Care*. 2017;6(5):389–395.
7. Tamelytė E, Vaičekauskienė G, Dagys A, et al. Early blood biomarkers to improve sepsis/bacteremia diagnostics in pediatric emergency settings. *Medicina (Kaunas)*. 2019;55(4):E99.
8. Urrechaga E, Ponga C, Fernández M, et al. Diagnostic potential of leukocyte differential and cell population data in prediction of COVID-19 among related viral and bacterial infections at emergency department. *Clin Chem Lab Med*. 2022;60(5):e104–e107.
9. Cabitza F, Campagner A, Ferrari D, et al. Development, evaluation, and validation of machine learning models for COVID-19 detection based on routine blood tests. *Clin Chem Lab Med*. 2021;59(2):421–431.
10. Ye W, Chen G, Li X, et al. Dynamic changes of D-dimer and neutrophil-lymphocyte count ratio as prognostic biomarkers in COVID-19. *Respir Res*. 2020;21(1):169.
11. Huang Y, Zhang X, Fei Y, et al. Investigation on the turnaround time of the whole process of clinical testing blood projects. *J Clin Examination*. 2018;36(7):528–531.
12. Woodhouse S. Engineering for safety: use of failure mode and effects analysis in the laboratory. *Lab Med*. 2005;36(1):16–18.

13. Hammerling JA. A review of medical errors in laboratory diagnostics and where we are today. *Lab Med*. 2012;43(2):41–44.
14. Liu HC, Zhang LJ, Ping YJ, Wang L. Failure mode and effects analysis for proactive healthcare risk evaluation: a systematic literature review. *J Eval Clin Pract*. 2020;26(4):1320–1337.
15. Lee H, Lee H, Baik J, et al. Failure mode and effects analysis drastically reduced potential risks in clinical trial conduct. *Drug Des Devel Ther*. 2017;11(19):3035–3043.
16. Cheng CH, Chou CJ, Wang PC, et al. Applying HFMEA to prevent chemotherapy errors. *J Med Syst*. 2012;36(3):1543–1551.
17. Anjalee JAL, Rutter V, Samaranyake NR. Application of failure mode and effects analysis (FMEA) to improve medication safety in the dispensing process—a study at a teaching hospital, Sri Lanka. *BMC Public Health*. 2021;21(1):1430.
18. Lin L, Wang R, Chen T, et al. Failure mode and effects analysis on the control effect of multi-drug-resistant bacteria in ICU patients. *Am J Transl Res*. 2021;13(9):10777–10784.
19. Wexler A, Gu B, Goddu S, et al. FMEA of manual and automated methods for commissioning a radiotherapy treatment planning system. *Med Phys*. 2017;44(9):4415–4425. doi:10.1002/mp.12278.
20. Jiang Y, Jiang H, Ding S, Liu Q. Application of failure mode and effects analysis in a clinical chemistry laboratory. *Clin Chim Acta*. 2015;448(25):80–85. doi:10.1016/j.cca.2015.06.016.
21. Rienzi L, Bariani F, Dalla Zorza M, et al. Comprehensive protocol of traceability during IVF: the result of a multicentre failure mode and effect analysis. *Hum Reprod*. 2017;32(8):1612–1620. doi:10.1093/humrep/dex144.
22. Xu Y, Wang W, Li Z, et al. Effects of healthcare failure mode and effect analysis on the prevention of multi-drug resistant organisms infections in oral and maxillofacial surgery. *Am J Transl Res*. 2021;13(4):3674–3681.
23. Duan M, Kang F, Zhao H, et al. Analysis and evaluation of the external quality assessment results of quality indicators in laboratory medicine all over China from 2015 to 2018. *Clin Chem Lab Med*. 2019;57(6):812–821.
24. Biljak VR, Lapić I, Vidranski V, et al. Policies and practices in the field of laboratory hematology in Croatia—a current overview and call for improvement. *Clin Chem Lab Med*. 2022;60(2):271–282.
25. Karadağ C, Demirel NN. Continual improvement of the pre-analytical process in a public health laboratory with quality indicators-based risk management. *Clin Chem Lab Med*. 2019;57(10):1530–1538.
26. Hoof VV, Bench S, Soto AB, et al. Failure mode and effects analysis (FMEA) at the preanalytical phase for POCT blood gas analysis: proposal for a shared proactive risk analysis model. *Clin Chem Lab Med*. 2022;60(8):1186–1201.
27. Donald M. Powers, PhD. Laboratory quality control requirements should be based on risk management principles. *Lab Med*. 2005;36(10):633–638.
28. Zhang X, Fei Y, Wang W, et al. National survey on turnaround time of clinical biochemistry tests in 738 laboratories in China. *J Clin Lab Anal*. 2018;32(2):e22251.
29. Tsai ER, Tintu AN, Demirtas D, et al. A critical review of laboratory performance indicators. *Crit Rev Clin Lab Sci*. 2019;56(7):458–471.

Diagnostic Performance of 10 Mathematical Formulae for Identifying Blood Donors with Thalassemia Trait

Egarit Noulsri, PhD,^{1,*} Surada Lerdwana, BSc,² Duangdao Palasuwan, PhD,³ and Attakorn Palasuwan, PhD³

¹Research Division, ²Biomedical Research Incubator Unit, Faculty of Medicine Siriraj Hospital, Mahidol University, Bangkok, Thailand, ³Oxidation in Red Cell Disorders Research Unit, Department of Clinical Microscopy, Faculty of Allied Health Sciences, Chulalongkorn University, Bangkok, Thailand. *To whom correspondence should be addressed: egarit.nou@mahidol.ac.th; egarit@hotmail.com.

Keywords: thalassemia trait, RBC indices, complete blood count, blood donor, transfusion medicine, basic science

Abbreviations: IDA, iron deficiency anemia; Hb CS, Hb constant spring; G6PD, glucose-6-phosphate dehydrogenase; HCT, hematocrit

Laboratory Medicine 2023;54:593-597; <https://doi.org/10.1093/labmed/lmad011>

ABSTRACT

Objective: To compare the diagnostic performance of 10 mathematical formulae for identifying thalassemia trait in blood donors.

Methods: Complete blood counts were conducted on peripheral blood specimens using the UniCel DxH 800 hematology analyzer. Receiver operating characteristic curves were used to evaluate the diagnostic performance of each mathematical formula.

Results: In the 66 donors with thalassemia and 288 subjects with no thalassemia analyzed, donors with thalassemia trait had lower values for mean corpuscular volume and mean corpuscular hemoglobin than subjects without thalassemia donors (77 fL vs 86 fL [$P < .001$]; 25 pg vs 28 pg [$P < .001$]). The formula developed by Shine and Lal in 1977 showed the highest area under the curve value, namely, 0.9. At the cutoff value of <1812, this formula had maximum specificity of 82.35% and sensitivity of 89.58%.

Conclusions: Our data indicate that the Shine and Lal formula has remarkable diagnostic performance in identifying donors with underlying thalassemia trait.

Thalassemia is an inherited hematological disorder that has been reported in many countries.¹ Patients can have thalassemia in different

degrees of severity, ranging from asymptomatic to severe anemia.² Patients with severe anemia require blood transfusions, whereas silent carriers of thalassemia trait have no symptoms and do not require therapy. In several countries, individuals with thalassemia trait can still donate blood if their hemoglobin levels meet the minimum criteria established in blood donor selection guidelines.³

Certain study reports^{4,5} have stated that the spectrum of β gene mutations varies among ethnic groups. Given the wide range of independent mutations that affect different populations regionally and donor selection criteria, blood donors with underlying thalassemia trait may have little effect in some areas, such as the United States and North America. In Thailand, a previous study⁶ examined the prevalence of donors with thalassemia, and the investigators found that 20% of transfusion donors were carriers of this trait. Despite advanced research on donors with thalassemia trait, a recent published review⁷ noted that studies would be required to investigate the quality of blood products prepared from these donors, as well as the quality of life of healthy donors who have underlying thalassemia trait. Given the prevalence of thalassemia in selected geographic locations, an approach to identifying thalassemia is required. This strategy will help to minimize adverse donor events during and after blood donations.

A variety of approaches have been used to identify individuals with thalassemia, such as the use of CBC parameters or hemoglobin typing using high-performance liquid chromatography (HPLC), which is the criterion standard.^{8,9} In addition to these strategies, mathematical formulae have been used to identify individuals suspected of carrying β -thalassemia or those with hypochromic microcytic anemia. Sinvastava¹⁰ and Mentzer¹¹ published reports of the first attempt, which used algorithms to calculate mean corpuscular hemoglobin (MCH), mean corpuscular volume (MCV), and red blood cell (RBC) concentration. Subsequently, Shine and Lal¹² developed another calculation by multiplying MCV by MCH and then dividing the result by 100; they reported that this approach could detect 137 heterozygous thalassemia traits. The findings of several studies¹³⁻¹⁶ have confirmed the reliability of the Shine and Lal formula.

Later, other formulae were proposed to improve the accuracy and reliability of the mathematical formulae by including other complete blood count (CBC) parameters in the calculations.¹⁷⁻²⁰ Bordbar et al²¹ applied the formula $|80 - \text{MCV}| \times |27 - \text{MCH}|$ to screen couples who had children younger than 18 years who had β -thalassemia and reported that the formula had high sensitivity and specificity in differentiating people carrying β -thalassemia (thalassemia carriers) from individuals with microcytic hypochromic anemia.

Further, Schoorl et al²² incorporated 4 hematological parameters, including hemoglobin (Hb), RBC, and mean corpuscular hemoglobin concentration (MCHC), into a mathematical formula for distinguishing iron deficiency anemia (IDA) from thalassemia. Their findings showed that the algorithm has sensitivity and specificity of 79% and 97%, respectively. Several studies, such as Roth et al¹³ and Bordbar et al,²¹ have evaluated these formulae, and the results regarding the detection of thalassemia carriers in the general population have varied. However, little is known about the performance of these formulae in transfusion laboratories in identifying donors with thalassemia. In the current study, we performed CBC and thalassemia screening tests on 354 blood donors to assess the practical use of the proposed mathematical formulae for identifying donors with thalassemia trait.

Materials and Methods

Ethics Statement

This study was approved by the International Review Board of the Faculty of Medicine Siriraj Hospital, Mahidol University, Bangkok, Thailand (COA No. Si395/2016). The donors who participated in the current study were referred by the Department of Transfusion. All experimental procedures were performed in accordance with the ethics standards of the Declaration of Helsinki.

Blood Specimen Collection and Thalassemia Screening

The following were our requirements for recruiting blood donors: donors must be between the ages of 17 and 70 years and weigh more than 45 kg; volunteer donors must have a minimum Hb concentration of 13 g/dL for males and 12.5 g/dL for females; and donors were screened for Hb using a copper sulfate (CuSO₄)–specific gravity approach, and those who had a drop of blood that floated or took too long to sink in CuSO₄ solution were deferred and excluded from the current study.

After written informed consent was obtained from each participant, 3 mL of peripheral blood was collected into a BD Vacutainer tube (Becton Dickinson) containing the anticoagulant K₂EDTA. Hemoglobin typing was performed using HPLC. The percentage of Hb was determined, and patients whose HbA2 levels were >3.5% were identified as having β-thalassemia trait. The multiplex gap-polymerase chain reaction was used to detect α-globin gene variants.

Automated Hematology Analyzer

The CBCs were determined using a UniCel DxH 800 hematology analyzer (Beckman Coulter) according to the routine procedure of the Department of Transfusion, Faculty of Medicine, Siriraj Hospital. Before being used to analyze the specimens, the instrument underwent inter- and intralaboratory validation. The CBC data set obtained included RBC, Hb, hematocrit (HCT), MCV, MCH, MCHC, red cell distribution width (RDW), white blood cell (WBC) count, and platelet (PLT) count.

Mathematical Calculations

The hematological data from each donor were incorporated into each formula used, which included the following mathematical formulae: the Srivastava formula¹⁰: MCH/RBC; the Mentzler formula¹¹: MCV/RBC; the Shine and Lal formula¹²: (MCV² × MCH)/100; the Green and King formula¹⁷: (MCV² × RDW)/(Hb × 100); the D’Onofrio et al

formula¹⁸: MCV/MCH; the Ehsani et al formula¹⁹: (MCV – 10 × RBC); the Sirdah et al formula²³: (MCV – RBC – 3 × Hb); the Sirachainan et al formula²⁰: 1.5 × Hb – 0.05 × MCV; the Bordbar et al formula²¹: |80 – MCV| × |27 – MCH|; and the Schoorl et al formula²²: (Hb × RDW × 100)/(RBC² × MCHC).

Statistical Analysis

The data were analyzed and graphed using GraphPad Prism software, version 5.0. The Kolmogorov-Smirnov normality test was used to assess the distribution of the variables. The results were expressed as mean, SE, and range (minimum–maximum). For each formula, a receiver operating characteristic (ROC) curve was plotted to calculate the area under the curve (AUC), sensitivity, and specificity, all of which were considered when determining the optimal cutoff values. The AUC is represented as a value between 0 and 1, and the ideal ROC curve has an AUC of 1.0, indicating the outstanding ability of the test to distinguish between patients with and without the disease. The optimal cutoff value is determined by the maximum sensitivity and specificity of the model. An unpaired *t* test was used to compare the differences in hematological data between the 2 groups. *P* ≤ .05 was considered statistically significant.

RESULTS

Donor Characteristics, Hemoglobin Analysis, and CBC Parameters

In the current cross-sectional study, we examined data from 354 transfusion donors, 66 of whom had thalassemia trait, and 288 of whom did not have thalassemia trait. The mean age of the donors with thalassemia trait was 35 (1.4) years, and the mean age of the donors without thalassemia was 36 (0.69) years. In the thalassemia group, the female/male (F/M) ratio was 26/40, and in the non-thalassemia group, it was 147/141. The donors with thalassemia were classified as having hemoglobin E trait (*n* = 34); 3.7-kb deletion (*n* = 20); Hb constant spring (Hb CS) (*n* = 5); β-thalassemia trait (*n* = 3); and other Hb types, which included 4.2-kb deletion (*n* = 1), homozygous Hb E (*n* = 1), Southeast Asian (SEA) deletion (*n* = 1), and Hb Pakse (*n* = 1).

TABLE 1 summarizes the hematological parameters of donors with and without thalassemia trait. Those with thalassemia trait had MCV and MCH values significantly lower than those without thalassemia. However, donors with thalassemia trait had higher RDW and RBC values than donors without thalassemia. A slight but statistically significant difference in MCHC was found between the donor groups. There were no statistically significant differences between the groups in the levels of Hb, HCT, WBC, or PLT.

AUC, Sensitivity, and Specificity of Each Mathematical Formula

The CBC parameters were incorporated into each mathematical formula, and diagnostic performance was compared using ROC analysis. **TABLE 2** summarizes the results regarding AUC values, sensitivities, and specificities. Five formulae had an AUC >0.8, with the Shine and Lal formula having the highest AUC value: 0.9. The Shine and Lal formula also had the highest sensitivity, 83.58%, and specificity, 82.35%, at a cutoff value of 1812; the other formulae had sensitivities and specificities ranging from 70%–81%.

TABLE 1. Hematological Parameters of Donors with and without Thalassemia Trait

Parameter	Mean (SE) (Minimum–Maximum)		P Value
	Donors with Thalassemia Trait (n = 66)	Donors without Thalassemia Trait (n = 288)	
Hb (g/dL)	14 (0.12) (12–16)	14 (0.07) (11–18)	.08
RBCs ($\times 10^6$ cells/ μ L)	5.4 (0.06) (4.36–7.17)	4.92 (0.02) (3.98–6.84)	<.001 ^a
HCT (%)	42 (0.35) (36–47)	42 (0.21) (34–54)	.24
MCV (fL)	77 (0.71) (57–87)	86 (0.34) (56–96)	<.001 ^a
MCH (pg)	25 (0.24) (20–29)	28 (0.13) (18–33)	<.001 ^a
MCHC (g/dL)	33 (0.1) (30–35)	33 (0.05) (30–36)	.05 ^a
RDW (%)	15 (0.13) (13–18)	14 (0.06) (12–21)	<.001 ^a
WBCs ($\times 10^3$ cells/ μ L)	7.55 (0.21) (4.27–12.54)	7.31 (0.09) (3.77–13.97)	.29
PLTs ($\times 10^3$ cells/ μ L)	252 (7) (141–413)	266 (3.66) (33–415)	.09

Hb, hemoglobin; HCT, hematocrit; MCH, mean corpuscular hemoglobin; MCHC, mean corpuscular hemoglobin concentration; MCV, mean corpuscular volume; PLT, platelet; RBC, red blood cell; RDW, red cell distribution width; WBC, white blood cell.

^aIndicates statistically significant difference.

TABLE 2. Area Under the Curve (AUC) Values, Cutoff, Sensitivity, and Specificity of Mathematical Formulae

Formula	Mean (95% CI)			
	AUC	Cutoff Value	Sensitivity, %	Specificity, %
Srivastava ¹⁰	0.85 (0.8–0.9)	<5.29	80.6 (69.58–88.29)	74.05 (68.7–78.76)
Mentzer ¹¹	0.84 (0.8–0.89)	<15.62	73.13 (61.48–82.28)	80.97 (76.05–85.08)
Shine and Lal ¹²	0.9 (0.87–0.93)	<1812	83.58 (72.94–90.58)	82.35 (77.54–86.32)
Green and King ¹⁷	0.74 (0.67–0.8)	<68.94	64.18 (52.22–74.6)	67.13 (61.52–72.29)
D'Onofrio et al ¹⁸	0.58 (0.5–0.65)	>3.05	56.72 (44.81–67.9)	55.02 (49.25–60.65)
Ehsani et al ¹⁹	0.86 (0.82–0.91)	<30.45	74.63 (63–83.51)	79.93 (74.93–84.14)
Sirdah et al ²³	0.82 (0.77–0.88)	<34.51	73.13 (61.48–82.28)	80.62 (75.68–84.77)
Sirachainan et al ²⁰	0.52 (0.45–0.6)	<16.39	52.24 (40.49–63.75)	52.25 (46.5–57.94)
Bordbar et al ²¹	0.61 (0.54–0.69)	>7.17	59.7 (47.74–70.61)	61.94 (56.22–67.34)
Schoorl et al ²²	0.76 (0.7–0.82)	<22.73	68.66 (56.80–78.49)	67.82 (62.23–72.94)

Discussion

The current study investigated the diagnostic performance of 10 mathematical equations used to identify donors with thalassemia trait. Among these formulae, the Shine and Lal algorithm had the best diagnostic performance in identifying donors with underlying thalassemia that had not yet been recognized.

Our main findings are as follows. First, there were no statistically significant differences in Hb values between donors with and without thalassemia. This finding confirmed the thalassemia trait characteristics of the individuals recruited into the current study and implied that traditional practices, such as the CuSO₄ method, may be unable to identify donors with thalassemia trait.²⁴ Second, the Shine and Lal formula had the highest AUC, at 0.9, which suggests a strong capacity for discrimination between donors with and without thalassemia. Third, the Shine and Lal formula demonstrated the highest sensitivity and specificity—each more than 80%—which means that this formula produces few false-negative and false-positive results.

Taken together, our findings suggest that the Shine and Lal formula could be useful as an initial indicator of the need for further extensive investigation of a specific donor, to protect donors from undue harm during blood donation.²⁵ Given that automatic CBC analysis is less expensive than HPLC testing, this simple technique could lower the cost of identifying large numbers of transfusion donors in transfusion laboratories.

Another finding of ours was that donors with thalassemia trait had lower MCV and MCH levels than donors without thalassemia. This observation is consistent with those of earlier studies^{26,27} that examined the most commonly used erythrocyte indices and concluded that MCV and MCH are the most essential criteria for identifying thalassemia trait. This finding is also consistent with our previous observation regarding the Shine and Lal formula having the highest performance. This formula multiplies MCV by MCH, resulting in a noticeable difference when compared to the results of formulas that lack similar qualities in their formulations. Although MCV and MCH values may be used to differentiate between donors with and without thalassemia, multiplying these parameters may increase the strength of the discrimination and minimize erroneous results compared to using MCV or MCH by themselves. Previously, Carlos et al²⁸ reported decreased RBC values, including those for Hb, MCV, MCH, MCHC, and RDW, in patients with IDA who also had thalassemia. Other studies^{29,30} assessing the prevalence of IDA in blood donors found sensitivity and specificity of more than 80% when using the Mentzer algorithm to screen these groups of blood donors. The variability in the performance of each formula might be explained by interpopulation variances, various mutations, and the degree of anemia affecting RBC parameters.

Despite the good performance of the Shine and Lal formula, the variations between our study findings and those of other studies regarding

the detected sensitivity and specificity might be due to a distinct mutation that influences the pathophysiology of thalassemia or the use by other studies of different criteria to group individuals.^{23,31} Further, the discrepancies in performance suggest that each laboratory should determine its own cutoff level for identifying donors with thalassemia trait.

It is also worth mentioning that RBC levels were higher in donors with thalassemia than in healthy volunteer donors in the study. However, both levels were within normal ranges.³² In addition to the formulae examined in this study, algorithms that have diagnostic performance regarding IDA and thalassemia carriers have been reported in the general population.^{26,33} As a result, further studies should be conducted to analyze these proposed equations to find better algorithms for identifying donors with thalassemia.

In terms of cutoff values, a previous study¹² reported the performance of the Shine and Lal formula for diagnosing thalassemia with a cutoff value of 1530. Another study found that the Shine and Lal formula had excellent diagnostic performance (AUC = 0.94) for diagnosing thalassemia with a cutoff value of 1110.²¹ Variability in cutoff values, sensitivity, and specificity may be attributed to various gene mutations in different geographical groups or an underlying cause of anemia, such as iron or B12 deficiency, which affects RBC indices.^{4,5} Also, variation in cutoff levels implies that each laboratory should determine its own values. It might also be argued that screening requires a high-sensitivity approach. However, other underlying diseases, such as IDA, may be associated with hematological characteristics that were not included in the current investigation. Given this context, a reliable screening strategy is necessary to minimize false positives and false negatives. As a result, we chose the optimal cutoff values for maximum sensitivity and specificity.

The current study has several limitations. First, we examined only donors with thalassemia. However, 2 previous study reports^{6,34} stated that glucose-6-phosphate dehydrogenase (G6PD) deficiency was common in transfusion donors. Therefore, because our investigation might have included donors with G6PD deficiency, additional studies should examine the application of mathematical formulae to identify donors who are deficient in G6PD.

The second drawback is that we did not test for IDA. Given its prevalence in various countries, including Thailand, the presence of IDA might have been a factor in the decreased levels of MCV and MCH we observed in this study.^{35,36}

Third, we examined conventional RBC parameters. Earlier study reports^{37,38} have stated that expanded RBC characteristics from multiple automated hematological analyzers may be used to detect individuals who are carriers of thalassemia. Further studies should be conducted to identify whether these extended RBC measures surpass conventional RBC parameters in identifying blood donors with thalassemia. Finally, the reliability of the mathematical calculations could have been limited if the donors had mutations that had no effect on their RBC characteristics.^{39,40}

Our findings support the reliability and accuracy of the Shine and Lal formula in identifying donors with thalassemia trait. Implementing this easy, low-cost technique can help to assure the safety of voluntary donors, particularly those with undisclosed underlying thalassemia.

Acknowledgments

This research was funded by Chulalongkorn University (CU-GES-60-05-30-01). The authors thank the Faculty of Medicine of Siriraj Hospital, Mahidol University, for supporting this research project.

Conflicts of Interest

The authors have nothing to disclose.

REFERENCES

1. Clegg JB, Weatherall DJ. Thalassemia and malaria: new insights into an old problem. *Proc Assoc Am Physicians*. 1999;111(4):278–282. doi:10.1046/j.1525-1381.1999.99235.x
2. Olivieri NF, Pakbaz Z, Vichinsky E. Hb E/beta-thalassaemia: a common & clinically diverse disorder. *Indian J Med Res*. 2011;134(4):522–531.
3. World Health Organization: Guidelines Review Committee. *Blood Donor Selection: Guidelines on Assessing Donor Suitability for Blood Donation*. World Health Organization; 2012.
4. De Sanctis V, Kattamis C, Canatan D, et al. β -Thalassemia distribution in the Old World: an ancient disease seen from a historical standpoint. *Mediterr J Hematol Infect Dis*. 2017;9(1):e2017018. doi:10.4084/MJHID.2017.018
5. Rezaee AR, Banoei MM, Khalili E, Houshmand M. Beta-thalassemia in Iran: new insight into the role of genetic admixture and migration. *Sci World J*. 2012;2012:635183. doi:10.1100/2012/635183
6. Kittisares K, Palasuwan D, Nulsri E, Palasuwan A. Thalassemia trait and G6PD deficiency in Thai blood donors. *Transfus Apher Sci*. 2019;58(2):201–206. doi:10.1016/j.transci.2019.03.009
7. Nulsri E, Lerdwana S. Blood donors with thalassaemic trait, glucose-6-phosphate dehydrogenase deficiency trait, and sickle cell trait and their blood products: current status and future perspective. *Lab Med*. 2023;54(1):6–12. doi:10.1093/labmed/lmac061
8. Brancialeoni V, Di Pierro E, Motta I, Cappellini MD. Laboratory diagnosis of thalassemia. *Int J Lab Hematol*. 2016;38(Suppl 1):32–40. doi:10.1111/ijlh.12527
9. Khera R, Singh T, Khuana N, Gupta N, Dubey AP. HPLC in characterization of hemoglobin profile in thalassemia syndromes and hemoglobinopathies: a clinicohematological correlation. *Indian J Hematol Blood Transfus*. 2015;31(1):110–115.
10. Srivastava PC. Differentiation of thalassaemia minor from iron deficiency. *Lancet*. 1973;2(7821):154–155. doi:10.1016/s0140-6736(73)93104-8
11. Mentzer WC Jr. Differentiation of iron deficiency from thalassaemia trait. *Lancet*. 1973;1(7808):882. doi:10.1016/s0140-6736(73)91446-3
12. Shine I, Lal S. A strategy to detect β -thalassaemia minor. *Lancet*. 1977;1(8013):692–694. doi:10.1016/S0140-6736(77)92128-6
13. Roth IL, Lachover B, Koren G, Levin C, Zalman L, Koren A. Detection of β -thalassaemia carriers by red cell parameters obtained from automatic counters using mathematical formulas. *Mediterr J Hematol Infect Dis*. 2018;10(1):e2018008. doi:10.4084/MJHID.2018.008
14. Sahli CA, Bibi A, Ouali F, et al. Red cell indices: differentiation between β -thalassaemia trait and iron deficiency anemia and application to sickle-cell disease and sickle-cell thalassaemia. *Clin Chem Lab Med*. 2013;51(11):2115–2124. doi:10.1515/ccclm-2013-0354
15. Beyan C, Kaptan K, Ifran A. Predictive value of discrimination indices in differential diagnosis of iron deficiency anemia and beta-thalassaemia trait. *Eur J Haematol*. 2007;78(6):524–526. doi:10.1111/j.1600-0609.2007.00853.x
16. Rathod DA, Kaur A, Patel V, et al. Usefulness of cell counter-based parameters and formulas in detection of beta-thalassaemia trait in areas of high prevalence. *Am J Clin Pathol*. 2007;128(4):585–589. doi:10.1309/R1YL4B4BT2WCQDGV
17. Green R, King R. A new red cell discriminant incorporating volume dispersion for differentiating iron deficiency anemia from thalassaemia minor. *Blood Cells*. 1989;15(3):481–491; discussion 492–485.
18. d'Onofrio G, Zini G, Ricerca BM, Mancini S, Mango G. Automated measurement of red blood cell microcytosis and hypochromia in iron deficiency and beta-thalassaemia trait. *Arch Pathol Lab Med*. 1992;116(1):84–89.

19. Ehsani MA, Shahgholi E, Rahiminejad MS, Seighali F, Rashidi A. A new index for discrimination between iron deficiency anemia and beta-thalassemia minor: results in 284 patients. *Pak J Biol Sci.* 2009;12(5):473–475. doi:10.3923/pjbs.2009.473.475
20. Sirachainan N, Iamsirirak P, Charoenkwan P, et al. New mathematical formula for differentiating thalassemia trait and iron deficiency anemia in thalassemia prevalent area: a study in healthy school-age children. *Southeast Asian J Trop Med Public Health.* 2014;45(1):174–182.
21. Bordbar E, Taghipour M, Zucconi BE. Reliability of different RBC indices and formulas in discriminating between β -thalassemia minor and other microcytic hypochromic cases. *Mediterr J Hematol Infect Dis.* 2015;7(1):e2015022. doi:10.4084/mjhid.2015.022
22. Schooli M, Schooli M, van Pelt J, Bartels PCM. Application of innovative hemocytometric parameters and algorithms for improvement of microcytic anemia discrimination. *Hematol Rep.* 2015;7(2):5843.
23. Sirdah M, Tarazi I, Al Najjar E, Al Haddad R. Evaluation of the diagnostic reliability of different RBC indices and formulas in the differentiation of the beta-thalassaemia minor from iron deficiency in Palestinian population. *Int J Lab Hematol.* 2008;30(4):324–330. doi:10.1111/j.1751-553x.2007.00966.x
24. Antwi-Baffour S, Annor DK, Adjei JK, Kyeremeh R, Kpentey G, Kyei F. Anemia in prospective blood donors deferred by the copper sulphate technique of hemoglobin estimation. *BMC Hematol.* 2015;15:15. doi:10.1186/s12878-015-0035-3
25. Figueiredo MS. Anemia and the blood donor. *Rev Bras Hematol Hemoter.* 2012;34(5):328–329. doi:10.5581/1516-8484.20120085
26. Hoffmann JJML, Urrechaga E, Aguirre U. Discriminant indices for distinguishing thalassemia and iron deficiency in patients with microcytic anemia: a meta-analysis. *Clin Chem Lab Med.* 2015;53(12):1883–1894. doi:10.1515/cclm-2015-0179
27. Clarke GM, Higgins TN. Laboratory investigation of hemoglobinopathies and thalassemias: review and update. *Clin Chem.* 2000;46(8 Pt 2):1284–1290.
28. Carlos AM, Souza BMB, Souza RAV, Resende GAD, Pereira GA, Moraes-Souza H. Causes of microcytic anaemia and evaluation of conventional laboratory parameters in the differentiation of erythrocytic microcytosis in blood donors candidates. *Hematology.* 2018;23(9):705–711. doi:10.1080/10245332.2018.1446703
29. Tiwari AK, Chandola I, Ahuja A. Approach to blood donors with microcytosis. *Transfus Med.* 2010;20(2):88–94. doi:10.1111/j.1365-3148.2009.00980.x
30. Sundh A, Kaur P, Palta A, Kaur G. Utility of screening tools to differentiate beta thalassemia trait and iron-deficiency anemia - do they serve a purpose in blood donors? *Blood Res.* 2020;55(3):169–174. doi:10.5045/br.2020.2020219
31. Nienhuis AW, Nathan DG. Pathophysiology and clinical manifestations of the β -thalassemias. *Cold Spring Harb Perspect Med.* 2012;2(12):a011726. doi:10.1101/cshperspect.a011726
32. Besarab A, Frinak S, Yee J. What is so bad about a hemoglobin level of 12 to 13 g/dL for chronic kidney disease patients anyway? *Adv Chronic Kidney Dis.* 2009;16(2):131–142. doi:10.1053/j.ackd.2008.12.007
33. Hoffmann JJML, Urrechaga E. Verification of 20 mathematical formulas for discriminating between iron deficiency anemia and thalassaemia in microcytic anemia. *Lab Med.* 2020;51(6):628–634. doi:10.1093/labmed/lmaa030
34. Noulis E, Lerdwana S, Palasuwan D, Palasuwan A. Cell-derived microparticles in blood products from blood donors deficient in glucose-6-phosphate dehydrogenase. *Lab Med.* 2021;52(6):528–535. doi:10.1093/labmed/lmab007
35. Brimson S, Suwanwong Y, Brimson JM. Nutritional anemia predominant form of anemia in educated young Thai women. *Ethn Health.* 2019;24(4):405–414. doi:10.1080/13557858.2017.1346188
36. Jammok J, Sanchaisuriya K, Sanchaisuriya P, Fucharoen G, Fucharoen S, Ahmed F. Factors associated with anaemia and iron deficiency among women of reproductive age in Northeast Thailand: a cross-sectional study. *BMC Public Health.* 2020;20(1):102. doi:10.1186/s12889-020-8248-1
37. Urrechaga E. The new mature red cell parameter, low haemoglobin density of the Beckman-Coulter LH750: clinical utility in the diagnosis of iron deficiency. *Int J Lab Hematol.* 2010;32(1 pt 1):e144–e150. doi:10.1111/j.1751-553X.2008.01127.xCitations
38. Ng EHY, Leung JHW, Lau YS, Ma ESK. Evaluation of the new red cell parameters on Beckman Coulter DxH800 in distinguishing iron deficiency anaemia from thalassaemia trait. *Int J Lab Hematol.* 2015;37(2):199–207. doi:10.1111/ijlh.12262
39. Maragoudaki E, Kanavakis E, Traeger-Synodinos J, et al. Molecular, haematological and clinical studies of the $-101\text{ C} \rightarrow \text{T}$ substitution in the beta-globin gene promoter in 25 β -thalassaemia intermedia patients and 45 heterozygotes. *Br J Haematol.* 1999;107(4):699–706. doi:10.1046/j.1365-2141.1999.01788.x
40. Perseu L, Satta S, Moi P, et al. *KLF1* gene mutations cause borderline HbA₂. *Blood.* 2011;118(16):4454–4458. doi:10.1182/blood-2011-04-345736

Evaluation of methods to eliminate analytical interference in multiple myeloma patients with spurious hyperphosphatemia

Xin Tian, MD,^{1,*} Li Zhao, MD,^{1,*} Jin Ma, MD,¹ Jie Lu, MD,¹ Tian-yi Zhu, MD,¹ Yan Liu, MD,¹ Hong-xun Sun, MD¹

¹Department of Laboratory Medicine, The Third Hospital of Hebei Medical University, Shijiazhuang, China. Corresponding author: Hong-xun Sun; 18533112710@163.com. *First authors.

Keywords: paraprotein interference, spurious hypophosphate, multiple myeloma

Abbreviations: TCA, trichloroacetic acid; H₂O, deionized water, NS, normal saline; bias%, bias percentage; Ig, immunoglobulin; MM, multiple myeloma

Laboratory Medicine 2023;54:598-602; <https://doi.org/10.1093/labmed/lmad012>

ABSTRACT

Objective: The acid/molybdate assay performed on the Beckman Coulter AU5821 could be subject to paraprotein interference, which potentially results in spurious hyperphosphatemia. We attempted to find a reliable solution to eliminate paraprotein interference in laboratory test results and discuss the causes of paraprotein interference.

Methods: We observed 50 multiple myeloma patients with serum paraproteins. We used the trichloroacetic acid (TCA) deproteinizing method to confirm that paraproteins indeed interfered with phosphate detection in the serum acid/molybdate assay. Furthermore, we used the dry chemical method (Vitros 5.1 FS, Johnson) and deionized water (H₂O), normal saline (NS), and healthy human serum as alternative diluents. We assessed the clinical acceptability of the 4 methods by evaluating a bias percentage (bias%) lower than 10% under the premise of TCA treatment as a serum phosphate reference method.

Results: In total, comparing the results of the TCA treatment on the Beckman Coulter AU5821, 3/50 (6%) multiple myeloma patients exhibited phosphate pseudo-elevation (bias% >10%). Additionally, we found pseudo-hypophosphate only in immunoglobulin (Ig)G-kappa paraprotein samples, and all were above 50 g/L. The bias% between TCA and dry chemical method for the 3 patients was below 10%. The maximum acceptable dilutions for patient 22 were 8-fold H₂O, 4-fold H₂O, and 2-fold serum; those for patient 45 were 16-fold H₂O, 16-fold

H₂O, and 2-fold serum. However, the bias% of patient 40 was beyond the acceptable range in all 3 dilution groups.

Conclusion: High concentrations of IgG kappa-type paraproteins are more likely to interfere with serum phosphorous detection. Both the TCA and dry chemical method can effectively eliminate paraprotein interference.

Paraproteins are monoclonal immunoglobulins (Igs) or immunoglobulin fractions present in the blood or urine produced by a clonal population of B-cell lineage cells, most commonly plasma cells. The presence of paraproteins may signify a variety of underlying conditions, ranging from a benign process known as monoclonal gammopathy of unknown significance to plasma cell malignancy, that is, multiple myeloma (MM).¹ It has been reported that paraproteins often interfere with biochemical immunoassays and result in inaccurate test results.^{2,3} In particular, there have been several reports indicating that serum phosphate concentrations may be erroneously high in patients with paraproteinemia if the method of phosphate measurement is based on a direct reaction with molybdate in an acid medium.⁴ However, the method information sheet accompanying the current phosphate method kit does not explicitly mention the possibility of interference by paraproteins. Therefore, the presence of pseudo-hyperphosphorus interference by paraprotein effects could be more widespread than realized due to current laboratory testing method limitations.

Hyperphosphatemia occurs in hypoparathyroidism, acute rhabdomyolysis, and metabolic acidosis. Hyperphosphatemia also occurs in secondary renal damage caused by B-cell neoplasia, such as MM or Waldenström's macroglobulinemia.⁵ If incorrect serum phosphate results are reported to clinicians, they could lead to unnecessary investigations and changes to patient treatment. Therefore, in the current study, serum phosphate concentrations were measured in 50 MM patients with serum paraproteins to study how paraproteins interfered with phosphate detection in the serum direct acid/molybdate method. We attempted to find a reliable and simple solution to eliminate paraprotein interference for laboratory serum phosphate examination and further explore the causes of paraprotein interference by using the trichloroacetic acid (TCA) deproteinizing method to remove paraproteins to accurately assay the serum phosphate and used deionized water (H₂O), normal saline (NS), and healthy low-value human serum as alternative diluents.

Materials and Methods

Ethics Statement

All procedures performed in the study involving human participants were in accordance with the ethical standards of the institutional and/or national research committee and with the 1964 Helsinki Declaration and its later amendments or comparable ethical standards. The study protocol was approved by Hebei Medical University ethical committee (W2021-095-1). Written informed consent was obtained from each participant.

Study Subjects

Subjects meeting the following criteria were enrolled in the study: (1) Chinese patients who met the diagnosis standard for MM according to the Revised International Myeloma Working Group criteria (IMWG 2014)⁶; and (2) MM patients with a monoclonal immunoglobulin band identified by serum protein electrophoresis. Patients whose serum samples were lipemic, icteric, or hemolytic or those who were treated with phosphate therapy were excluded.

Paraprotein Typing and Concentration Detection

Identified paraproteins were typed by immunofixation electrophoresis as IgM, IgG, IgE, IgA, or IgD, and light chain type (kappa or lambda). The paraprotein concentration was detected by the immunoturbidimetric method on the Beckman Coulter IMMAGE 800 Specific Protein Analyzer.

Methods for Serum Phosphate Concentration Detection

Beckman Coulter AU5821 Determination Method

Serum phosphate concentrations were analyzed using a Beckman Coulter AU5821 and an ammonium molybdate-based method in which inorganic phosphorus reacted with ammonium molybdate in the presence of sulfuric acid to form an unreduced phosphomolybdate complex, which was measured as an end-point reaction at 340 nm (reference interval: 0.85–1.51 mmol/L).

TCA Deproteinizing Method

Samples were deproteinized using TCA (Deproteinizing Sample Preparation Kit, Bio Vision). The protocol included: (1) Protein precipitation, in which 150 μ L sample was mixed with 15 μ L cold TCA in a 1.5 mL microcentrifuge tube. The sample was kept on ice for 15 min, then centrifuged at 12,000g for 5 min. Supernatant was carefully transferred to another tube. (2) Sample neutralization, in which 10 μ L cold neutralization solution was added to the collected supernatant. The sample was placed on ice for 5 min and directly measured with the Beckman Coulter AU5821 analyzer for the phosphate concentrations. We defined the serum phosphate results by the TCA deproteinizing method and removal of paraproteins as the true result and compared them with the original results to confirm whether there were pseudo-hyperphosphatemia test results in patients with MM with paraproteins, where the relative bias (bias%) between the 2 assays was more than 10%. We analyzed the relationship between paraprotein-interfered serum phosphate determination samples and paraprotein concentrations and immunoglobulin typing.

Methods for Removing Paraprotein Interference

Vitros 5.1 FS Detection Method

Serum phosphate concentrations were analyzed using the dry chemical method (Vitros 5.1 FS, Johnson). Vitros 5.1 FS analysis requires the use

of a slide-based method for the reaction of inorganic phosphorus with ammonium molybdate to form a phosphomolybdate complex. This complex was then reduced by p-methyl-aminophenol sulfate, an organic reductant, to form a stable heteropoly molybdenum blue chromophore. The phosphate concentration was then estimated by reflectance spectrophotometry at 670 nm.

Dilution Methods

Diluents included H₂O, NS, and healthy low-value serum phosphorus samples; the original serum samples containing paraproteins were diluted by the various diluents, and serum phosphate was remeasured on the AU5821 analyzer.

Separately, we compared the results by the multiple methods for removing paraprotein interference with the results by TCA treatment, where a bias% <10% was the judgment criterion, to determine the most desirable method to detect serum phosphorus interference by paraproteins in daily practice.

Statistical Methods

Continuous variables conforming to a normal distribution are described as mean \pm SD; otherwise, they are described as median and interquartile range (P₂₅–P₇₅). Categorical variables are described as frequencies and percentages (%).

The absolute bias was defined by the difference between the serum phosphate results by the TCA deproteinizing method and the original serum phosphate concentrations by AU5821. The relative bias (bias%) denoted the absolute bias divided by the original serum phosphate concentrations by AU5821. If the bias% was more than 10%, there was a difference; that is, there was pseudo-hyperphosphorus interference by paraprotein effects in the AU5821 analyzer.

Results

Patient Characteristics and Paraprotein Typing

In the current study, 50 different MM patients were included, 23 females and 27 males. The median age was 63 years (interquartile range, 43–80 years). Of the study patients, 27 had IgG typing paraproteins (9 IgG lambda and 18 IgG kappa), 18 had IgA paraproteins (10 IgA lambda and 8 IgA kappa), and 5 had IgM paraproteins (4 IgM kappa and 1 IgM lambda). The paraprotein concentration range was 5.62 to 74.90 g/L with a median of 23.9 (12.06–40.31) g/L (TABLE 1).

Original Serum Phosphate Results and TCA Treatment Results

Of the 50 paraprotein-positive samples, 3 (6%) showed a bias% greater than 10% and phosphate pseudo-elevation. In addition, we found pseudo-hyperphosphate only in IgG kappa-type paraprotein samples. The concentrations of paraproteins in the 3 cases were all above 50 g/L, and serum total protein was above 100 g/L (TABLE 1 and TABLE 2).

Comparison of the Results of the Dilution Group and Vitros Group with TCA

The maximum dilutions of patient 22 were 8-fold H₂O, 4-fold NS, and 2-fold low-value phosphate serum; those for patient 45 were 16-fold

TABLE 1. Basic Characteristics of 50 Patients with Multiple Myeloma

Patient No.	AU5821	TCA	Bias%	Paraprotein type	Paraprotein concentration (g/L)	Patient No.	AU5821	TCA	Bias%	Paraprotein type	Paraprotein concentration (g/L)
1	1.41	1.38	2%	IgG kappa	18.64	26	0.91	0.93	-2%	IgM kappa	8.26
2	1.50	1.46	3%	IgG lambda	8.53	27	1.34	1.39	-4%	IgG lambda	11.82
3	1.29	1.21	6%	IgA kappa	5.62	28	0.92	0.91	1%	IgG lambda	31.27
4	2.28	2.18	5%	IgM lambda	7.15	29	1.27	1.30	-2%	IgG lambda	17.16
5	1.34	1.45	-8%	IgG kappa	43.85	30	0.90	0.93	-3%	IgA lambda	34.20
6	0.99	0.92	7%	IgA lambda	31.90	31	1.18	1.20	-2%	IgG kappa	23.70
7	1.33	1.24	7%	IgG kappa	31.3	32	1.18	1.23	-4%	IgA lambda	55.70
8	1.48	1.34	10%	IgG kappa	38.39	33	1.32	1.26	4%	IgG kappa	25.47
9	1.31	1.28	3%	IgG kappa	13.54	34	0.92	0.99	-7%	IgA kappa	23.90
10	1.42	1.33	7%	IgA lambda	38.91	35	1.26	1.26	0%	IgA kappa	25.00
11	1.04	1.00	4%	IgA lambda	15.3	36	0.96	1.00	-4%	IgG kappa	8.70
12	1.79	1.61	10%	IgA lambda	57.4	37	1.00	1.00	0%	IgG kappa	15.40
13	1.34	1.25	7%	IgA kappa	60.42	38	0.69	0.63	9%	IgM kappa	7.5
14	1.05	1.13	-7%	IgG lambda	16.73	39	0.93	0.96	-3%	IgG kappa	8.9
15	0.83	0.88	-5%	IgA kappa	10.77	40	5.50	2.25	59%	IgG kappa	73.90
16	1.63	1.61	1%	IgA lambda	13.78	41	1.27	1.38	-8%	IgA kappa	60.3
17	1.34	1.35	-1%	IgA lambda	12.62	42	1.61	1.54	5%	IgA lambda	37.1
18	1.35	1.43	-6%	IgG kappa	74.90	43	0.74	0.75	-1%	IgG lambda	19.09
19	1.30	1.23	6%	IgA lambda	26.28	44	1.49	1.44	4%	IgG kappa	53.9
20	1.50	1.48	2%	IgM kappa	38.12	45	3.19	1.56	51%	IgG kappa	50.10
21	1.83	1.86	-2%	IgG lambda	34.20	46	1.41	1.46	-4%	IgG kappa	6.97
22	2.96	1.56	47%	IgG kappa	59.90	47	1.45	1.46	-1%	IgA kappa	12.3
23	2.50	2.26	10%	IgG kappa	46.65	48	1.46	1.36	7%	IgG kappa	41.7
24	1.42	1.43	0%	IgM kappa	8.07	49	1.53	1.41	8%	IgA kappa	9.5
25	1.35	1.26	6%	IgG lambda	22.79	50	1.47	1.46	1%	IgG lambda	49.3

AU5821, the serum phosphate concentration(mmol/L) result measured on the AU5821 analyzer; TCA, the serum phosphate concentration(mmol/L) result measured on AU5821 after TCA precipitation method.

TABLE 2. Patient Characteristics Associated with Spurious Hyperphosphatemia and Results After Dilution

Characteristic	Patient No.		
	22	40	45
Sex	M	M	M
Age (y)	57	62	66
Monoclonal component type	IgG kappa	IgG kappa	IgG kappa
Monoclonal component (g/L)	59.90	73.90	50.10
Serum total protein (g/L)	118.09	121.29	118.56
Serum creatinine (mmol/L)	57.16	544.79	99.92
Serum calcium (mmol/L)	2.18	2.88	2.17
Serum phosphorus by AU5821 (mmol/L)	2.96	5.50	3.19
Serum phosphorus by TCA (mmol/L)	1.56	2.25	1.75
Serum phosphorus by Vitros (mmol/L)	1.69	2.43	1.81

IgG, immunoglobulin.

H₂O, 16-fold NS, and 2-fold serum. However, the bias% of patient 40 was beyond the acceptable range in the 3 dilution groups. The bias% of the Vitros 5.1 FS method compared with the TCA method was less than 10% in these 3 cases (TABLE 3).

Discussion

Hyperphosphatemia is usually secondary to hypoparathyroidism or advanced renal failure. Pseudo-hyperphosphatemia, a rare condition, is most commonly associated with paraproteinemia but is also seen in other conditions, such as hyperlipidemia, hyperbilirubinemia, and hemolysis. Pseudo-hyperphosphatemia is found in MM samples, caused by the interaction of the paraprotein with molybdate reagent in the acid molybdate-based assay.⁷⁻¹¹ Indeed, in the current study, we discovered 3 cases of pseudo-hyperphosphatemia in our laboratory from April 2021 to January 2022, all of them IgG kappa-type MM. However, the available studies do not suggest that the pseudo-increased serum phosphorus has a significant correlation with paraprotein types. Sinclair et al¹² reported IgA and IgG with pseudo-increased blood phosphorus in MM patients. In 2007, Kiki et al⁹ reported another pseudo-elevation in serum phosphorus in IgG MM. In 2015, Made et al¹³ found pseudo-hyperphosphatemia in an IgA kappa MM patient. Additionally, the study results are discrepant about whether the paraprotein concentration is related to the spurious increase in phosphorus. In the current study, we found that the paraprotein concentration of 3 cases was more than 50 g/L, indicating that high concentrations of paraprotein are more likely to cause interference. Some experts also believe that paraprotein interference is more likely to occur at high paraprotein concentrations.¹⁴

TABLE 3. Recovery Rate of Serum Phosphate on the AU 5821 Analyzer at Various Dilutions

Dilution	H ₂ O			NS			Serum			
	Expected value (mmol/L)	Obtained value (mmol/L)	Bias (%)	Expected value (mmol/L)	Obtained value (mmol/L)	Bias (%)	Expected value (mmol/L)	Obtained value (mmol/L)	Bias (%)	
Patient 22	Original	1.56	—	1.56	—	—	1.56	—	—	
	2×	0.78	0.78	0.78	0.85	8.97 ^a	0.78	0.82	5.13 ^a	
	4×	0.39	0.37	-5.13 ^a	0.39	0.36	-7.69 ^a	0.39	0.34	-12.82
	8×	0.20	0.18	-7.69 ^a	0.20	0.16	-17.95	0.20	0.16	-17.95
	16×	0.10	0.08	-17.95	0.10	0.08	-17.95	0.10	0.07	-28.21
Patient 40	Original	2.25	—	2.25	—	—	2.25	—	—	
	2×	1.13	3.16	180.89	1.13	3.34	196.89	3.97	252.89	
	4×	0.56	2.20	291.11	0.56	1.19	111.56	1.16	105.99	
	8×	0.28	0.76	170.22	0.28	0.74	163.11	0.66	133.29	
	16×	0.14	0.18	28.00	0.14	0.18	28.00	0.16	14.13	
Patient 45	Original	1.75	—	1.75	—	—	1.75	—	—	
	2×	0.88	0.96	9.71 ^a	0.88	0.95	8.57 ^a	0.94	7.43 ^a	
	4×	0.44	0.46	5.14 ^a	0.44	0.43	-1.71 ^a	0.39	-10.86	
	8×	0.22	0.20	-8.57 ^a	0.22	0.20	-8.57 ^a	0.18	-17.71	
	16×	0.11	0.10	-8.57 ^a	0.11	0.10	-8.57 ^a	0.09	-17.71	

^aIndicates that the bias% is within the acceptable range.

However, Roy¹ insisted that there is no significant correlation between paraprotein interference and concentration or type.

Furthermore, it has been reported that artifactual laboratory abnormalities are uncommon; percentage of abnormalities were found to be 1.2% and 1.5% in 2 studies.^{10,11} We found that of the 50 paraprotein-positive samples, 3 (6%) exhibited phosphate pseudo-elevation. The incidence of such a phenomenon is not accurately known and may be even higher than generally appreciated. It is important for clinicians to be aware of the possibility and recognize artifactual errors in laboratory parameters so that unnecessary tests and erroneous conclusions can be avoided. The wide variation in reported incidences of pseudo-hyperphosphatemia may be due to different definitions of the phenomenon in different studies. We defined any phosphate value measured on the AU5821 that was 10% different from the result obtained on TCA as being pseudo-hyperphosphatemia. Because TCA could completely eliminate the paraproteins, we treated the TCA result as the real result. There was no significant difference in the serum phosphate values between the TCA treatment and the Vitros 5.1 FS dry chemical analyzer method, indicating that both methods had a similar ability to resist paraprotein interference in the clinical laboratory. The Vitros 5.1 FS method is reported to be interference-free because the sample has to penetrate several slide layers before reaching the reaction layer, although the method is based on the reaction of phosphate with ammonium molybdate. This may therefore have the effect of filtering out any interfering compounds.¹⁵ Finally, we attempted the dilution method commonly used in eliminating analytical interference and compared it with the TCA method. The maximum acceptable dilutions of patient 22 were 8-fold H₂O, 4-fold NS, and 2-fold low-value phosphate serum and those of patient 45 were 16-fold H₂O, 16-fold NS, and 2-fold serum. The only exception was patient 40, whose results lacked linearity. This patient's phosphate concentrations measured on the AU5821 system were 5.5 mmol/L and the overestimated values were absurdly high. In addition, the patient had severe renal impairment (creatinine: 544.79 mmol/L). As a result, this sample is not linear with the TCA method regardless of dilution method. However, the TCA treatment result of this sample was 2.25 mmol/L, and the dry chemical result was 2.43 mmol/L. These results are a more realistic reflection of the patient's physiological state.

The purpose of the current study was to analyze the clinical laboratory abnormalities caused by paraproteins to improve awareness of the possibility of such interference and avoid unnecessary erroneous conclusions in practical work. When suspicious results appear, the TCA method is preferred for processing samples. If a laboratory does not have a deproteinizing reagent, the dry chemical (Vitros) method is reliable. Through a series of dilutions, the results were also close to the real results except for an unexpectedly high concentration of phosphorus. It is very important to provide clinicians and patients with more accurate results, which can assist clinicians in making accurate diagnoses.

Conclusion

A high concentration of paraproteins is more likely to cause interference, and IgG kappa-type paraproteins are more likely to interfere with phosphorous detection. Both the TCA and dry chemical methods can effectively eliminate paraprotein interference. Paraprotein interference cannot be completely eliminated by dilution, especially with very high paraprotein concentrations.

Funding

This work was supported by the Health Commission of Hebei Province (20211034) and the Hebei Education Department (ZD2015040).

Conflict of Interest Disclosure

The authors have nothing to disclose.

Data Availability

The datasets used and/or analyzed during the current study are available from the corresponding author on reasonable request.

REFERENCES

1. Roy V. Artfactual laboratory abnormalities in patients with paraproteinemia. *South Med J*. 2009;102(2):167–170.
2. Oren S, Feldman A, Turkot S, Lugassy G. Hyperphosphatemia in multiple myeloma. *Ann Hematol*. 1994;69:41–43. doi:10.1007/BF01757346
3. Sinclair D, Smith H, Woodhead P. Spurious hyperphosphataemia caused by an IgA paraprotein: a topic revisited. *Ann Clin Biochem*. 2004;41(pt 2):119–124. doi:10.1258/000456304322879999
4. McClure D, Lai LC, Cornell C. Pseudohyperphosphataemia in patients with multiple myeloma. *J Clin Pathol*. 1992;45:731–732. doi:10.1136/jcp.45.8.731
5. Endres DB, Rude RK. Bone and mineral metabolism. In: Burtis CA, Ashwood ER, Bruns DE, eds. *Tietz Textbook of Clinical Chemistry and Molecular Diagnostics*. 4th ed. St Louis, MO: Elsevier; 2006:1905–1909.
6. Rajkumar SV, Dimopoulos MA, Palumbo A, et al. International Myeloma Working Group updated criteria for the diagnosis of multiple myeloma. *Lancet Oncol*. 2014;15:e538–e548. doi:10.1016/S1470-2045(14)70442-5
7. Lee Y, Koo T, Yi JH, et al. Pseudohyperphosphatemia in a patient with multiple myeloma. *Electrolyte Blood Press*. 2007;5:131–135. doi:10.5049/EBP.2007.5.2.131
8. Umeda M, Okuda S, Izumi H, et al. Prognostic significance of the serum phosphorus level and its relationship with other prognostic factors in multiple myeloma. *Ann Hematol*. 2006;85:469–473. doi:10.1007/s00277-006-0095-3
9. Kiki I, Gundogdu M, Kaya H. Spuriously high phosphate level which is promptly resolved after plasmapheresis in a patient with multiple myeloma. *Transfus Apher Sci*. 2007;37:157–159. doi:10.1016/j.transci.2007.07.005
10. Izzedine H, Camous L, Bourry E, Azar N, Leblond V, Deray G. Make your diagnosis: multiple myeloma associated with spurious hyperphosphatemia. *Kidney Int*. 2007;72:1035–1036. doi:10.1038/sj.ki.5002485
11. Mavrikakis M, Vaiopoulos G, Athanassiades P, Antoniadis L, Papamichael C, Dimopoulos MA. Pseudohyperphosphatemia in multiple myeloma. *Am J Hematol*. 1996;51:178–179. doi:10.1002/(SICI)1096-8652(199602)51:2<178::AID-AJH22>3.0.CO;2-D
12. Sinclair D, Smith H, Woodhead P. Spurious hyperphosphataemia caused by an IgA paraprotein: a topic revisited. *Ann Clin Biochem*. 2004;41(pt 2):119–124. doi:10.1258/000456304322879999
13. Maden M, Emel Pamuk G, Asoglu V, Nuri Pamuk O. The rapid resolution of pseudohyperphosphatemia in an IgA κ multiple myeloma patient after therapy with a bortezomib-containing regimen: report of the first case. *J Cancer Res Ther*. 2015;11(4):1043.
14. García-González E, González-Tarancón R, Aramendía M, Rello L. Analytical interference by monoclonal immunoglobulins on the direct bilirubin AU Beckman Coulter assay: the benefit of unsuspected diagnosis from spurious results. *Clin Chem Lab Med*. 2016;54:1329–1335. doi:10.1515/cclm-2015-0608
15. Sonntag O. Dry chemistry analysis with carrier-bound reagents. In: Van der Vliet PC, ed. *Laboratory Techniques in Biochemistry and Molecular Biology*. Vol 25. London, UK: Elsevier; 1993:57–59.

The importance of the trisomy 21 local cutoff value evaluation for prenatal screening in the second trimester of pregnancy

Yiming Chen, MBBS^{1,2,*}, Yijie Chen, MD^{2,*}, Long Sun, MD³, Liyao Li, MM¹, Wenwen Ning, MM, MS²

¹Departments of Prenatal Diagnosis and Screening Center and ³Clinical Laboratory, Hangzhou Women's Hospital (Hangzhou Maternity and Child Health Care Hospital), Hangzhou, China, ²Department of the Fourth School of Clinical Medical, Zhejiang Chinese Medical University, Hangzhou, China. Corresponding author: Yiming Chen; cxy40344@163.com. *Contributed equally.

Key words: alpha-fetoprotein; free beta subunit of human chorionic gonadotropin; trisomy 21; the local cutoff value; the inline cutoff value; second-trimester

Abbreviations: LCV, local cutoff value; ICV, the inline cutoff value; DS, Down syndrome; ROC, receiver operating characteristic; AFP, alpha-fetoprotein; free β -hCG, free beta human chorionic gonadotropin; uE3, unconjugated estriol; FPR, false-positive rate; MoM, multiple of the median; AUC, area under the curve; SEN, sensitivity; PRs, positive rates; PPV, positive predictive value.

Laboratory Medicine 2023;54:603-607; <https://doi.org/10.1093/labmed/lmad015>

ABSTRACT

Objective: The aim of this work was to compare different local cutoff values (LCV) and inline cutoff values (ICV) in pregnant women in the second trimester at high risk for carrying fetuses with trisomy 21.

Methods: This retrospective cohort study analyzed prenatal screening outcomes in pregnant women ($n = 311,561$). The receiver operating characteristic curve was used to evaluate the diagnostic significance of the trisomy 21 risk value, alpha-fetoprotein, and free beta human chorionic gonadotropin multiple of the median for predicting trisomy 21 risk. The cutoff value corresponding to the maximal Youden index was taken as the LCV. The screening efficiency of both cutoff values was compared.

Results: The LCV cutoff value was lower than the ICV cutoff value (1/643 vs 1/270). The sensitivity increased by 19.80%, the positive predictive value decreased by 0.20%, and the false-positive rate increased by 6.50%.

Conclusion: The LCV should be used to determine trisomy 21 risk, which can increase the detection rate of trisomy 21 in the second trimester.

Aneuploidy is the presence or the absence of one or more extra chromosomes.¹ Persons who have an extra chromosome 21 are diagnosed with Down syndrome (DS), one of the most common fetal chromosomal abnormalities, with a prevalence of approximately 1/800 to 1/600 live births.² Most individuals with trisomy 21 cannot take care of themselves due to severe mental and physical disabilities. The risk of a pregnant woman giving birth to a newborn with trisomy 21 increases from 1/1480 at 20 years of maternal age to 1/85 at 40 years of maternal age. As there is no treatment for trisomy 21, individuals with DS can create serious economic burdens on families and health care systems. As such, all pregnant women should undergo prenatal screening and counseling,³⁻⁵ which can help patients and families decide whether or not to continue the pregnancy. Furthermore, counseling should be nondirective in nature, and clinicians should support patients and families, regardless of the decision that is made.⁶

Comprehensive indicator screening between 10 and 13 weeks of gestation can detect approximately 82% to 87% of fetuses with trisomy 21, whereas screening between 15 and 21 weeks of gestation can detect approximately 81% of fetuses with the abnormality. The positive detection rate of trisomy 21 is higher in women in early pregnancy that underwent serum panel testing or integrated screening (ie, ultrasound combined with serum panel testing) than that in women that underwent single biomarker testing.⁷ Noninvasive prenatal testing, a high-performance screening approach for determining trisomy 21 risk with a detection rate of 99%, can be used initially or subsequently in the follow-up of abnormal results in the first or second trimester of pregnancy.⁸ Diagnostic testing to confirm positive results includes chorionic villus sampling at 10 to 13 weeks of gestation or amniocentesis after 15 weeks of gestation.⁷ Triple screening of serum indicators, namely, alpha-fetoprotein (AFP), free beta human chorionic gonadotropin (free β -hCG), and unconjugated estriol (uE3), is routinely carried out in pregnant women in the second trimester, which usually yields the lowest positive detection rate and the highest false-positive rate (FPR). Another advantage of triple screening is that it can detect neural tube defects when screening for trisomy 21 and 18.^{9,10}

Presently, there is no agreement on the cutoff value for predicting trisomy 21 risk in the second trimester of pregnancy. The cutoff value is 1/250 in France and Finland,^{11,12} 1/300 in the UK and Germany,^{13,14} and 1/270 in China and other Asian countries.^{15,16} As such, it is important to establish the trisomy 21 cutoff value in prenatal screening.

The aim of our study was to explore the diagnostic significance of the local cutoff value (LCV) in dual-marker prenatal screening of trisomy 21 in the second trimester. This retrospective cohort study analyzed 311,561 young pregnant women, including 136 cases of trisomy 21, and compared the diagnostic significance of the LCV with the inline cutoff value (ICV) for predicting trisomy 21 risk.

Materials and Methods

Participants

This was a retrospective study of young women undergoing routine second trimester aneuploidy screenings (15 to 20 weeks and 6 days of gestation) at 48 prenatal health community centers in Hangzhou Women's Hospital (Hangzhou Maternity and Child Health Care Hospital) China, from January 2015 to October 2019. There were 136 pregnant women carrying fetuses with trisomy 21, including high-risk and low-risk cases, and 311,425 pregnant women carrying healthy fetuses. The fetuses with trisomy 21 were diagnosed according to results of karyotype analysis of amniotic fluid cells and ultrasound examinations.

Inclusion and Exclusion Criteria

The inclusion criteria were as follows: pregnant women at 15 to 20 weeks and 6 days of gestation, with a singleton pregnancy, voluntarily undergoing prenatal screening for determining trisomy 21 risk in the second trimester. The exclusion criteria were as follows: patients with a history of smoking, diabetes mellitus, chromosomal abnormalities and congenital malformations, pregnancy complications or other related conditions, fetuses conceived in vitro, or plural gestations. This study was approved by the Medical Ethics Committee of Hangzhou Women's Hospital [2021] Medical Ethics Review A (3) - 02.

Reagents and Instruments

The 1235 Automatic Immunoassay System (Perkin Elmer) and double labeling kit (AFP/free β -hCG, catalog number 644147, Wallac Oy) were used in this study.

Detection Methods

Materials and Test Indicators

Fasting venous blood (2–3 mL) was collected from pregnant women at 15 to 20 weeks and 6 days of gestation. Serum specimens were stored in a refrigerator at 2°C to 8°C and transported to the Prenatal Screening Laboratory of Hangzhou Women's Hospital (Hangzhou Maternity and Child Health Hospital) within 1 week from collection.

MoM Calculation

AFP and free β -hCG were expressed as the multiple of the median (MoM) for variables, such as gestational age and maternal weight, as previously reported.¹⁷

Quality Control

Quality control serum specimens (catalog number 39180; Bio-Rad) were classified as low value, medium value, or high value. The certificate of

conformity, which describes the activities organized by the Clinical Laboratory Center of the National Health Commission of China 3 times a year, was obtained. All personnel received training and obtained certification from the relevant health authorities before the start of testing and analysis.

Inline Cutoff Value

Life Cycle 4.0 software (Wallac Oy) was used to calculate the ICV of trisomy 21 after adjusting for maternal age, maternal weight, and gestational age at testing. If the trisomy 21 risk value was $\geq 1:270$, then the fetus was at high risk of trisomy 21, with all other values indicating that the fetus was at low risk of the abnormality.¹⁸ According to the ROC, the cutoff value corresponding to the maximal Youden index was taken as the LCV with the largest area under the curve (AUC) and the best screening efficacy.

Prenatal Diagnosis

Pregnant women underwent ultrasound-guided amniocentesis at 17 to 20 weeks of gestation after providing written informed consent. In brief, the amniotic tank was positioned and <30 mL of amniotic fluid was collected by puncture through the abdomen with a 20-gauge needle and transferred to a sterile centrifuge tube. Specimens were centrifuged at 2500 rpm for 10 min. Cells were resuspended in medium and cultured in an incubator at 37°C with 5% CO₂, and cell proliferation was observed. Thirty mitotic phases were counted under a microscope, and 5 karyotypes were analyzed. Additionally, chromosomal G-banding and karyotype analyses were performed according to the International Nomenclature System of Human Genetics. The number of abnormal karyotypes was increased, adding C and N banding, if necessary.¹⁹

Data Analysis

IBM SPSS 24.0 software (IBM Corp) was used for statistical analysis. The one-sample Kolmogorov-Smirnov test was used to assess the normality. The maternal age, gestational age at testing, and maternal weight in the second trimester of pregnancy were expressed as percentiles [M (P_{2.5}, P_{97.5})]. Skewed data were compared within or between groups using the Mann-Whitney *U* test. The positive rates (PRs) of the 2 methods were compared using the χ^2 test. To assess the diagnostic significance of AFP MoM and free β -hCG MoM, as well as the trisomy 21 risk calculation, cutoff values and AUCs were determined using receiver operator characteristic (ROC) curves. The sensitivity (SEN) and the FPR were used to evaluate the efficacy of trisomy 21 screening. The SEN was calculated as follows: number of true positives/(number of true positives + number of false negatives) \times 100%. The FPR was calculated as follows: number of false positives/(number of true negatives + number of false positives) \times 100% \div number of gold standard. *P* < .05 was considered statistically significant.

Results

Comparison of Patient Characteristics

The maternal age at testing in the second trimester was significantly higher in the trisomy 21 group than in the control group (*Z* = 9.470, *P* < .001), whereas the gestational age at testing was lower in the trisomy 21 group than in the control group (*Z* = 2.579, *P* = 0.010). No significant difference in the maternal weight between the groups was noted (*P* > 0.05) (TABLE 1).

TABLE 1. Comparison of Clinical Data Between the Control and the Trisomy 21 Group^a

Variable	Control (n = 311,425)	Trisomy 21 (n = 136)	Z	P
Maternal age (y)	28.80 (21.62–37.61)	33.34 (23.43–44.35)	9.470	<.001
Maternal weight (kg)	55.00 (43.00–75.00)	55.10 (45.00–75.00)	0.745	.456
Gestational age (d)	118.00 (109.00–133.00)	117.00 (109.00–131.00)	2.579	.010
Trisomy 21 risk value	1/4377 (1/121–1/68176)	1/132 (1/5–1/7983)	16.422	<.001
Trisomy 18 risk value	1/56,383 (1/2303–1/100,000)	1/18,498 (1/442–1/100,000)	7.820	<.001
AFP MoM	0.98 (0.54–1.86)	0.73 (0.40–1.51)	9.310	<.001
Free β-hCG MoM	0.99 (0.33–3.62)	2.23 (0.44–12.64)	11.994	<.001

AFP, alpha-fetoprotein; free β-hCG, free beta subunit of human chorionic gonadotropin; MoM, multiple of the median.

^aData are presented as median ($P_{2.5}$ – $P_{97.5}$).

TABLE 2. Diagnostic Significance of the Trisomy 21 Risk Value, AFP MoM, and Free β-hCG MoM for Predicting Trisomy 21 Risk

Screening Indicator	AUC	95% CI	P	SEN	SPE	Youden Index	LCV Cutoff	High Risk (n)	PR	ICV Cutoff	High Risk (n)	PR	χ^2	P
Trisomy 21 risk value	0.907	0.878–0.935	<.001	0.816	0.880	0.697	1/643	37357	0.120	1/270	17171	0.055	8189.394	<.001
AFP MoM	0.730	0.683–0.778	<.001	0.559	0.819	0.378	0.75	56419	0.181	0.50	4781	0.015	48315.275	<.001
Free β-hCG MoM	0.797	0.755–0.839	<.001	0.713	0.774	0.488	1.56	70370	0.226	2.50	22798	0.073	28560.839	<.001

AFP, alpha-fetoprotein; free β-hCG, free beta subunit of human chorionic gonadotropin; ICV, inline cutoff value; LCV, local cutoff value; MoM, multiple of the median; PR, positive rate; SEN, sensitivity; SPE, specificity.

Determination of the Trisomy 21 Risk Value, AFP MoM, and Free β-hCG MoM

The trisomy 21 risk value (1/132) was significantly higher in the trisomy 21 group than in the control group ($Z = 16.442$, $P < .001$), whereas the trisomy 18 risk value (1/18498) was significantly higher in the trisomy 21 group than in the control group ($Z = 7.820$, $P < .001$). The AFP MoM was 0.73 in the trisomy 21 group, which was significantly lower than in the control group (0.98, $Z = 9.310$, $P < .001$). The free β-hCG MoM was 2.23 in the trisomy 21 group, which was significantly higher than in the control group (0.99, $Z = 11.994$, $P < .001$) (TABLE 1).

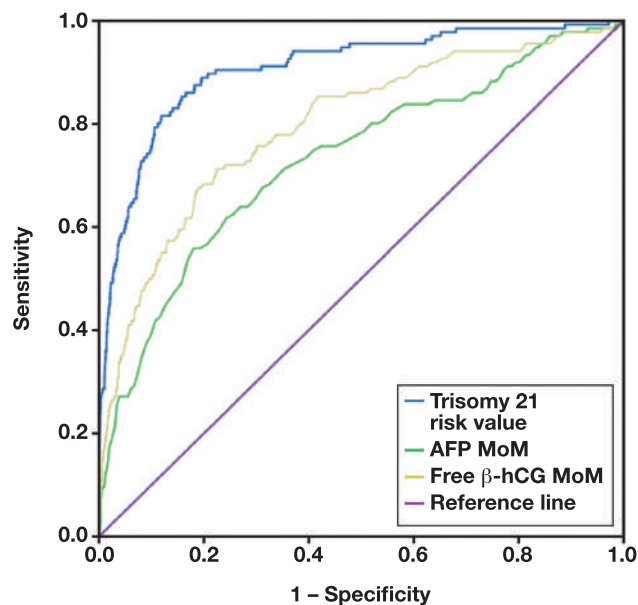
Diagnostic Value of the Trisomy 21 Risk Value, AFP MoM, and Free β-hCG MoM for Predicting Trisomy 21 Risk Using Local and Inline Cutoff Values

The LCV for predicting trisomy 21 risk, the AUC, the cutoff value and SEN of the trisomy 21 risk calculation, AFP MoM, and free β-hCG MoM were 0.907, 1/643 and 0.816; 0.730, 0.75 MoM and 0.559; 0.797, 1.56 MoM and 0.713, respectively (TABLE 2 and FIGURE 1).

The PRs of the LCVs for predicting the trisomy 21 risk value, AFP MoM, and free β-hCG MoM were all higher than those of the ICVs (0.120, 0.181, and 0.226 vs 0.055, 0.015, and 0.073, respectively), and differences were statistically significant ($\chi^2 = 8189.394$, $\chi^2 = 48315.275$, and $\chi^2 = 28560.839$, all $P < .001$) (TABLE 2). The LCV cutoff value was lower than the ICV cutoff value (1/643 vs 1/270), whereas the SEN increased by 19.80% (0.816 vs 0.618), the positive predictive value (PPV) decreased by 0.20% (0.005 vs 0.003), and the FPR increased by 6.50% (0.120 vs 0.055) (TABLE 3).

Discussion

The main findings of our study were as follows: differences in the trisomy 21 risk value, AFP MoM, and free β-hCG MoM between trisomy 21 and control groups were statistically significant ($P < .001$), and the PRs of the LCVs for predicting the trisomy 21 risk value, AFP MoM, and

FIGURE 1. Receiver operating characteristic curve for predicting trisomy 21 risk. AFP, alpha-fetoprotein; free β-hCG, free beta subunit of human chorionic gonadotropin; MoM, multiple of the median.

free β-hCG MoM were all higher than the PRs of the respective ICVs ($P < .001$). The LCV cutoff value was 1/643, the SEN increased by 19.80% (0.816 vs 0.618), the PPV decreased by 0.20% (0.005 vs 0.003), and the FPR increased by 6.50% (0.120 vs 0.055), which was lower than the ICV cutoff value (1/270).

Prenatal screening, a safe, simple, and economical approach used in prenatal health centers worldwide, is critical in pregnant women at risk for carrying fetuses with congenital defects such as trisomy 21. In Europe, the prevalence of trisomy 21 is 22/10,000.²⁰ Our study

TABLE 3. Diagnostic Significance of LCV and ICV for Predicting Trisomy 21 Risk

Screening Model	Cutoff	SEN	SPE	PPV	NPV	FPR	FNR
ICV	1/270	0.618	0.945	0.005	1.000	0.055	0.382
LCV	1/643	0.816	0.88	0.003	1.000	0.120	0.184

FNR, false negative rate; FPR, false positive rate; ICV, inline cutoff value; LCV, local cutoff value; NPV, negative predictive value; PPV, positive predictive value; SEN, sensitivity; SPE, specificity.

shows statistically significant differences in the PRs of cutoff values for predicting trisomy 21 risk. We wanted to understand whether LCV is suitable in the local laboratory and the prenatal screen value of LCV for trisomy 21 fetuses. In our study, LCV reduced the misdiagnosis rate compared with ICV and improved the detection rate. Furthermore, our results showed that the AUC of the trisomy 21 risk value was higher than that of AFP MoM and free β -hCG MoM alone (0.907 vs 0.704 and 0.797). The SEN of the trisomy 21 risk value was 0.816, which was higher than that of AFP MoM (0.559) and free β -hCG MoM (0.713), consistent with previous studies.²¹ Liu et al²¹ demonstrated that the AUC of AFP MoM + free β -hCG MoM was 0.748 (95% CI: 0.635–0.860), whereas Guo et al²² illustrated that the AUC of the trisomy 21 risk value was 0.935 (95% CI: 0.879–0.991), indicating that the screening efficacy of AFP MoM + free β -hCG MoM was better than that of AFP MoM and free β -hCG MoM alone. Guo et al²² also reported that when the FPR was 0.047, the cutoff value and the SEN were 1/265 and 0.778, respectively. However, when the FPR was 0.223, the cutoff value and the SEN were 1/1000 and 0.889.

Hwa et al²³ showed that when the FPR was 0.178, the cutoff value of the ROC was 1/499 and the SEN was 0.900. However, when the FPR was 0.120, the cutoff value was 1/332 and the SEN was 0.800.^{23, 24} In our study, the PRs of the LCVs for predicting the trisomy 21 risk value, AFP MoM, and free β -hCG MoM were all higher than those of the respective ICVs.

As such, a reasonable FPR is key to determining the cutoff value. However, our results illustrated that trisomy 21 risk value, AFP MoM, and free β -hCG MoM were variable with different FPRs. Therefore, the LCV should be used to determine the trisomy 21 risk in different settings. In addition, we acknowledge the limitations of our study. First, there were only 136 cases of trisomy 21 among 311,561 pregnant women. Although the incidence of trisomy 21 in our study was too low to bias the results, compared with the prevalence of 1/800 to 1/600 fetuses, additional studies with a larger population of trisomy 21 cases are needed. Second, the FPR increased by 6.50% (0.120 vs 0.055) compared with the previous screening (3% to 5%), and the former required the next prenatal diagnosis. Finally, from 2015 to 2019, the local medical system in China only paid for AFP and free β -hCG double screening; uE3 is not included in medical insurance. Therefore, this study only uses data from double screening instead of a AFP, free β -hCG, and uE3 triple screening.

In summary, prenatal health centers should use LCV to determine the trisomy 21 risk in the second trimester of pregnancy, which can reduce the misdiagnosis rate, increase the detection rate, and eliminate unnecessary interventions, thereby increasing the efficacy of prenatal screening.

Acknowledgments

The authors are grateful to all participants and contributors. We thank Songhe Chen from Hangzhou Women's Hospital for assistance in

collecting the data. We also thank Xiao Lu and Shaolei Lv of the Data Analysis Department of Zhejiang Biosan Biochemical Technologies for their contribution to data matching and model building. We also thank International Science Editing (<http://www.internationalscienceediting.com>) for editing this manuscript. The datasets used and/or analyzed during the current study are available from the corresponding author on reasonable request.

Funding

This study was supported by The Joint Fund Project of Zhejiang Provincial Natural Science Foundation of China under Grant No. LB23H200009.

Conflicting of Interest Disclosure

The authors have nothing to disclose.

REFERENCES

- Chitayat D, Langlois S, Wilson RD. No. 261-Prenatal screening for fetal aneuploidy in singleton pregnancies. *J Obstet Gynaecol Can.* 2017;39(9):e380–e394.
- The American College of Obstetricians and Gynecologists' Committee on Practice Bulletins—Obstetrics, Committee on Genetics, and the Society for Maternal–Fetal Medicine, Nancy CR, Brian MM. Practice bulletin No. 163 summary: screening for fetal aneuploidy. *Obstet Gynecol.* 2016;127(5):979–981.
- Webster A, Schuh M. Mechanisms of aneuploidy in human eggs. *Trends Cell Biol.* 2017;27(1):55–68.
- Li T, Zhao H, Han X, et al. The spontaneous differentiation and chromosome loss in iPSCs of human trisomy 18 syndrome. *Cell Death Dis.* 2017;8(10):e3149.
- Wang S, Hassold T, Hunt P, et al. Inefficient crossover maturation underlies elevated aneuploidy in human female meiosis. *Cell.* 2017;168(6):977–989.
- Johnston J, Farrell RM, Parens E. Supporting women's autonomy in prenatal testing. *N Engl J Med.* 2017;377(6):505–507.
- LeFevre NM, Sundermeyer RL. Fetal aneuploidy: screening and diagnostic testing. *Am Fam Physician.* 2020;101(8):481–488.
- Cheng Y, Leung WC, Leung TY, et al. Women's preference for non-invasive prenatal DNA testing versus chromosomal microarray after screening for Down syndrome: a prospective study. *BJOG.* 2018;25(4):451–459.
- Metcalfe A, Hippman C, Pastuck M, Johnson JA. Beyond trisomy 21: additional chromosomal anomalies detected through routine aneuploidy screening. *J Clin Med.* 2014;3(2):388–415.
- Palomaki GE, Bupp C, Gregg AR, Norton ME, Oglesbee D, Best RG. Laboratory screening and diagnosis of open neural tube defects, 2019 revision: a technical standard of the American College of Medical Genetics and Genomics (ACMG). *Genet Med.* 2020;22(3):462–474.
- Royère D. The impact of introducing combined first-trimester trisomy 21 screening in the French population. *Eur J Public Health.* 2016;26(3):492–497.

12. Peuhkurinen S, Laitinen P, Honkasalo T, Ryyanen M, Marttala J. Comparison of combined, biochemical and nuchal translucency screening for Down syndrome in first trimester in Northern Finland. *Acta Obstet Gyn Scan.* 2013;92(7):769–774.
13. Snijders RJ, Noble P, Sebire N, Souka A, Nicolaides KH. UK multicentre project on assessment of risk of trisomy 21 by maternal age and fetal nuchal-translucency thickness at 10-14 weeks of gestation. Fetal medicine foundation first trimester screening group. *Lancet (London).* 1998;352(9125):343–346.
14. Hörmansdörfer C, Scharf A, Golatta M, et al. Comparison of prenatal risk calculation (PRC) with PIA fetal database software in first-trimester screening for fetal aneuploidy. *Ultrasound Obstet Gynecol.* 2009;33(2):147–151.
15. Lan RY, Chou CT, Wang PH, Chen RC, Hsiao CH. Trisomy 21 screening based on first and second trimester in a Taiwanese population. *Taiwan J Obstet Gynecol.* 2018;57(4):551–554.
16. Shaw SW, Lin SY, Lin CH, et al. Second-trimester maternal serum quadruple test for Down syndrome screening: a Taiwanese population-based study. *Taiwan J Obstet Gynecol.* 2010;49(1):30–34.
17. Bock JL. Current issues in maternal serum alpha-fetoprotein screening. *Am J Clin Pathol.* 1992;97(4):541–554.
18. Huang T, Alberman E, Wald N, Summers AM. Triploidy identified through second-trimester serum screening. *Prenatal Diag.* 2005;25(3):229–233.
19. Ordulu Z, Wong KE, Currall BB, Ivanov AR, Pereira S, Althari S, Gusella JF, Talkowski ME. Describing sequencing results of structural chromosome rearrangements with a suggested next-generation cytogenetic nomenclature. *Am J Hum Genet.* 2014;94(5):695–709.
20. Loane M, Morris JK, Addor MC, et al. Twenty-year trends in the prevalence of Down syndrome and other trisomies in Europe: impact of maternal age and prenatal screening. *Eur. J. Hum. Genet.* 2013;21(1):27–33.
21. Liu F, Liang H, Jiang X, et al. Second trimester prenatal screening for Down's syndrome in mainland Chinese subjects using double-marker analysis of α -fetoprotein and β -human chorionic gonadotropin combined with measurement of nuchal fold thickness. *Ann Acad Med Singap.* 2011;40(7):315–318.
22. Guo F, Xiao KC, Lin LH, et al. Assessment of risk cut-off values for Down syndrome screening in midtrimester. *Chin J Eugen Genet.* 2014;22(02):50–51.
23. Hwa HL, Ko TM, Hsieh FJ, Yen MF, Chou KP, Chen TH. Risk prediction for Down's syndrome in young pregnant women using maternal serum biomarkers: determination of cutoff risk from receiver operating characteristic curve analysis. *J Eval Clin Pract.* 2007;13(2):254–258.
24. Yu D Y, Fu P, Zhang Z H, et al. Evaluation of Down's syndrome screening methods using maternal serum biochemistry in the second trimester pregnancy. *Zhonghua Yi Xue Yi Chuan Xue Za Zhi.* 2011;28(3):332–335.

Serum aspartate aminotransferase is an adverse prognostic indicator for patients with resectable pancreatic ductal adenocarcinoma

Meifang He, MD^{1,2,*}, Yin Liu, MS^{1,*}, Hefei Huang, MS¹, Jiali Wu, MS¹, Juehui Wu, MS¹, Ruizhi Wang, MD¹, Dong Wang, MD¹

¹Division of Laboratory Medicine and ²Laboratory of General Surgery, the First Affiliated Hospital of Sun Yat-sen University, Guangzhou, China. Corresponding author: Dong Wang; cwdong@mail.sysu.edu.cn. *Contributed equally.

Key words: aspartate aminotransferase; prognosis; overall survival; nomogram; TNM stage; pancreatic ductal adenocarcinoma

Abbreviations: OS, overall survival; ALT, alanine aminotransferase; AST, aspartate aminotransferase; PDAC, pancreatic ductal adenocarcinoma; GGT, γ -glutamyltransferase; ALP, alkaline phosphatase; LDH, lactate dehydrogenase; HR, hazard ratio

Laboratory Medicine 2023;54:608-612; <https://doi.org/10.1093/labmed/lmad014>

ABSTRACT

Objective: In this study, the association between preoperative levels of serum liver enzymes and overall survival (OS) was evaluated in patients with resectable pancreatic cancer.

Methods: Preoperative serum levels of alanine aminotransferase (ALT), aspartate aminotransferase (AST), γ -glutamyltransferase, alkaline phosphatase, and lactate dehydrogenase of 101 patients with pancreatic ductal adenocarcinoma (PDAC) were collected. Univariate and multivariate Cox hazard models were used to identify independent variables associated with OS in this cohort.

Results: Patients with elevated AST levels had significantly worse OS than patients with lower AST levels. A nomogram was created using TNM staging and AST levels and was shown to be more accurate in prediction than the American Joint Committee on Cancer 8th edition standard method.

Conclusion: Preoperative AST levels could be a novel independent prognostic biomarker for patients with PDAC. The incorporation of AST levels into a nomogram with TNM staging can be an accurate predictive model for OS in patients with resectable PDAC.

Pancreatic cancer has a high mortality rate and is the fourth leading cause of cancer-related deaths globally, and the incidence has been increasing year after year. Pancreatic ductal adenocarcinoma (PDAC) is the most common type of pancreatic cancer. The 5-year overall survival rate for patients with PDAC is less than 9%, and median survival is less than 1 year.¹ Although 20% to 30% of patients with resectable PDAC receive active therapeutic interventions, postoperation survival periods vary from patient to patient. The median survival among surgically resected cases is less than 2 years, and the 5-year survival rate is only around 20% to 25%.² Therefore, it is imperative to identify biomarkers that facilitate improved disease prognosis for these patients.

As routine clinical indexes, serum levels of liver enzymes, including alanine aminotransferase (ALT), aspartate aminotransferase (AST), γ -glutamyltransferase (GGT), alkaline phosphatase (ALP), and lactate dehydrogenase (LDH), are informative biomarkers of liver injury and predictors of all-cause mortality. Aspartate aminotransferase is a key enzyme of amino acid metabolism that catalyzes the reversible transfer of the amine group from L-aspartate to 2-oxoglutarate. Aspartate aminotransferase is primarily expressed in mitochondria and is present in all tissues except bone, with the highest expression levels in liver and skeletal muscle. When liver cells are damaged, the mitochondria disintegrate, causing AST to be released into the circulation. Aspartate aminotransferase is a specific indicator of abnormal liver function and has prognostic value for different types of hepatitis, cancer, and other diseases.

Recently, it has been reported that liver enzymes might serve as biomarkers for prognostic monitoring and recurrence in different cancers, including metastatic colorectal cancer,³ metastatic breast cancer,⁴ advanced urothelial carcinoma,⁵⁻⁸ and advanced PDAC.^{9,10} Serum levels of GGT, LDH, ALP, and ALT have been shown to be independent prognostic indicators of advanced PDAC,¹⁰⁻¹³ and preoperative serum levels of LDH and ALP have been identified as independent prognostic factors for disease-free survival and overall survival for patients with resectable PDAC.¹⁴ Nevertheless, the contributions of other liver enzymes, such as ALT and AST, to disease prognosis for patients with resectable PDAC have yet to be established.⁹ Therefore, the relationship between the serum liver enzymes, including AST and ALT, and prognosis of early stage PDAC merits elucidation.

In this study, we performed a retrospective analysis to explore the feasibility of using serum liver enzymes as prognostic biomarkers to predict patient survival in PDAC. We constructed a prognostic nomogram for

resectable PDAC based on clinicopathological parameters and evaluated whether use of this model resulted in a more accurate prediction of outcome for patients with PDAC.

Materials and Methods

Patients

This study was approved by the Human Research Ethics Committees of the First Affiliated Hospital of Sun Yat-sen University (approval No. [2020]339), in accordance with the Helsinki Declaration.

A total of 101 adult patients diagnosed with PDAC (62 males and 39 females) who underwent curative resection at the First Affiliated Hospital of Sun Yat-sen University from 2003 to 2011 and received standard treatment with no chemotherapy or radiotherapy before or after surgery were enrolled and analyzed retrospectively in this study. Follow-up was based on electronic hospital charts and physician records. In general, patients were followed up every 3 months in the first year, every 6 months for the next 2 years, and annually thereafter. Recurrence was defined as disease recurrence locally or in distant organs. Patients who did not experience recurrence, cancer-specific death, or any-cause death were censored at last follow-up. The inclusion and exclusion criteria were as follows: (1) pathological diagnosis of PDAC; (2) no radiotherapy, chemotherapy, or medication before surgery; (3) complete clinical data and follow-up data present; (4) did not receive any drugs known to affect indicators of liver function or surgery before enrollment; (5) not diagnosed with liver disease, cardiovascular disease, diabetes, or metabolic syndrome; (6) no history or concurrence of other cancers; and (7) no concurrence of other severe diseases. Routine clinic data including sex, age, tumor size, histological differentiation, and TNM stage were collected from patient records.

Laboratory Measurements

Serum biochemical tests were performed on the first visit to the hospital. Blood was collected between 7 AM and 8 AM and centrifuged at 3500 rpm for 5 minutes to collect serum samples. The serum levels of ALT, AST, GGT, ALP, and LDH were evaluated by enzyme method (such as the malate dehydrogenase method for AST and LDH method for ALT) on an AU5800 automated analyzer (Beckman Coulter) and the corollary reagents. Accuracy and precision of all methods were performed in accordance with the relevant guidelines and regulations.

Statistical Analysis

Statistical analyses were performed by SPSS software version 22 (IBM). Overall survival was calculated from the date of tumor resection to the time of death. Patients who were lost to follow-up or died from causes unrelated to PDAC were treated as censored events. Cox proportional-hazard regression model was used for univariate and multivariate analysis. Significant prognostic factors identified by univariate analysis were further evaluated by multivariate Cox regression analysis. Survival curves were plotted using the Kaplan-Meier method, and differences between survival curves were analyzed using the log rank test. The χ^2 test was used to analyze the correlation between AST and clinical characteristics. The prognostic nomogram was performed using the R package. The predictive performance of the prognostic nomogram was assessed by C-index and receiver operating characteristic curve for overall survival (OS). All

statistical tests were 2-sided, and a *P* value of ≤ 0.05 was considered to be statistically significant.

Results

Clinical Pathological Characteristics

A cohort of 101 patients with pathologically confirmed PDAC was enrolled in this study. Patient characteristics are listed in **TABLE 1**. There were 62 males and 39 females with an average age of 59.5 years. The median follow-up time was 32 months with a range from 1 to 56 months. Regarding tumor differentiation, 25 patients had tumors with poor differentiation and 76 patients had tumors with moderate or well-defined differentiation. The number of patients diagnosed at stage I-II and III-IV were 66 (65.3%) and 35 (34.7%), respectively.

Prognostic Significance of AST in PDAC

The clinical data above and levels of serum liver enzymes (ALT, AST, ALP, GGT, and LDH) were included in Cox regression analysis for evaluation of OS. Univariate analysis indicated that higher levels of ALT (hazard

TABLE 1. Baseline Characteristics in Patients with PDAC

Characteristic	No. of Cases (%)
Sex	101
Male	62 (61.4)
Female	39 (38.6)
Age, y	101
≤ 60	47 (46.5)
> 60	54 (53.5)
Tumor size, cm	101
≤ 2	14 (13.9)
> 2	87 (86.1)
Differentiation	101
Poor	25 (24.8)
Moderate/well	76 (75.2)
TNM stage	101
I-II	66 (65.3)
III-IV	35 (34.7)
Lymphatic spread	101
Yes	37 (36.6)
No	64 (63.4)
Metastasis	101
Yes	14 (13.9)
No	87 (86.1)
CEA, $\mu\text{g/L}$	94
≤ 3.1	46 (48.9)
> 3.1	48 (51.1)
CA125, U/mL	87
≤ 19.5	49 (56.3)
> 19.5	38 (43.7)
CA199, U/mL	95
≤ 371.5	55 (57.9)
> 371.5	40 (42.1)

ratio [HR]: 1.002, 95% CI = 1.001–1.004, $P = .007$) and AST (HR: 1.003, 95% CI = 1.001–1.005, $P = .003$) were significantly associated with higher mortality in PDAC patients (TABLE 2). Variables with $P < .05$ in the univariate analysis were further evaluated in multivariate analysis to

TABLE 2. Univariate and Multivariate Analysis of Factors Associated with OS^a

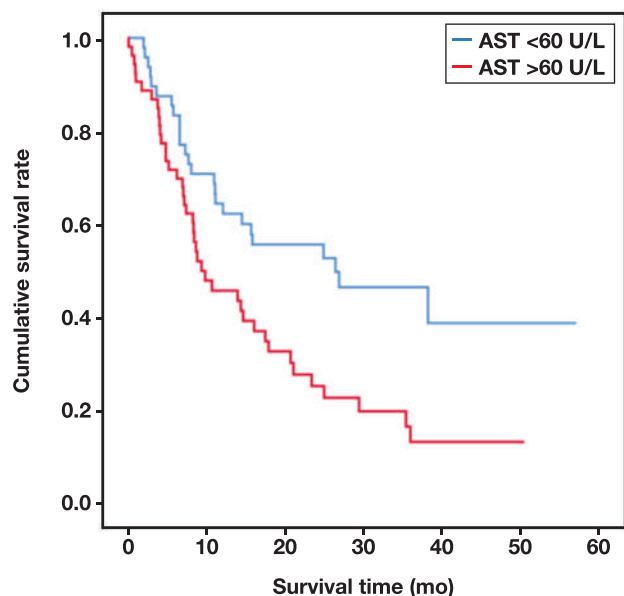
Clinical variables	No. of cases	HR (95% CI) ^b	P value ^b
Univariate analysis			
Sex (M vs F)	62/39	1.211 (0.733–2.002)	.455
Age (>60 y vs ≤60 y)	54/47	1.497 (0.811–2.761)	.197
Tumor size (>3 cm vs ≤3 cm)	87/14	1.031 (0.745–1.426)	.853
Differentiation (poor vs well and moderate)	25/86	1.409 (1.090–1.823)	.009
TNM stage (III/IV vs I/II)	45/66	1.344 (1.052–1.715)	.018
Lymphatic spread (yes vs no)	30/71	1.304 (1.020–1.667)	.034
Metastasis (yes vs no)	40/61	1.425 (1.050–1.934)	.023
Serum ALT	NA	1.002 (1.001–1.004)	.007
Serum AST	NA	1.003 (1.001–1.005)	.003
Serum GGT	NA	1.000 (1.000–1.001)	.519
Serum ALP	NA	1.001 (1.000–1.002)	.177
Serum LDH	NA	1.002 (1.000–1.005)	.065
Multivariate analysis			
TNM stage (III/IV vs I/II)	45/66	1.736 (1.064–2.833)	.027
Serum AST	NA	1.003 (1.001–1.005)	.005

ALP, alkaline phosphatase; ALT, alanine aminotransferase; AST, aspartate aminotransferase; GGT, γ -glutamyltransferase; LDH, lactate dehydrogenase; NA, not applicable; OS, overall survival; PDAC, pancreatic ductal adenocarcinoma.

^aAnalysis was conducted on 101 cases.

^bHR (hazard ratio) and P values were calculated using univariate or multivariate Cox proportional hazards regression. P values < .05 are shown in bold.

FIGURE 1. Overall survival curve of patients with pancreatic ductal adenocarcinoma according to aspartate aminotransferase (AST) levels ($P = .005$). Kaplan-Meier survival curves indicated that higher AST level was significantly related to shorter survival.



exclude the confounder effect, confirming that TNM stage (HR: 1.736, 95% CI = 1.064–2.833, $P = .027$) and AST (HR: 1.003, 95% CI = 1.001–1.005, $P = .005$) were independent predictors for OS. These data suggest that serum AST levels are a reliable prognostic indicator for PDAC.

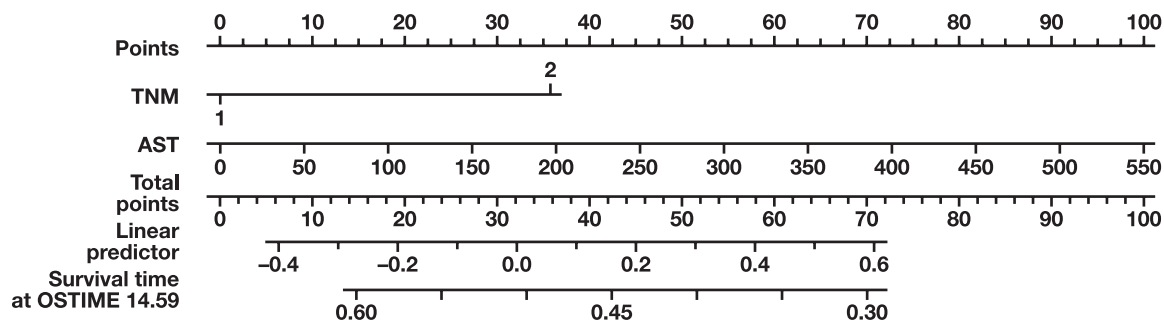
TABLE 3. Relationship between AST Levels and Clinical Characteristics in Patients with PDAC

Variable	AST (U/L)		Total cases	P value ^a
	≤60	>60		
Sex				
Male	28	34	62	.683
Female	20	19	39	
Age, y				
≤60	24	23	47	.553
>60	24	30	54	
Tumor size, cm				
≤2	5	9	14	.398
>2	43	44	87	
Differentiation				
Poor	7	15	22	.147
Moderate/well	41	38	79	
TNM stage				
I–II	31	35	66	1.000
III–IV	17	18	35	
Lymphatic spread				
Yes	12	25	37	.024
No	36	28	64	
Metastasis				
Yes	11	15	26	.650
No	37	38	75	
CEA, μ g/L				
≤3.1	23	23	46	.680
>3.1	21	27	48	
CA125, U/mL				
≤19.5	20	29	49	.288
>19.5	20	18	38	
CA199, U/mL				
≤371.5	27	28	55	.540
>371.5	17	23	40	
Death				
Yes	25	41	66	.012
No	23	12	35	
ALT				
	48	53	101	.000
AST				
	48	53	101	.000
GGT				
	48	53	101	.000
ALP				
	48	53	101	.160
LDH				
	48	53	101	.879

ALP, alkaline phosphatase; ALT, alanine aminotransferase; AST, aspartate aminotransferase; CEA, carcinoembryonic antigen; GGT, γ -glutamyltransferase; LDH, lactate dehydrogenase; PDAC, pancreatic ductal adenocarcinoma.

^aP values of nominal variables and continuous variables were calculated using the χ^2 test and t-test, respectively. P values < .05 are shown in bold.

FIGURE 2. Prognostic nomogram for pancreatic ductal adenocarcinoma (PDAC). The nomogram predicts overall survival (OS) in patients with PDAC. A patient's value for each variable is located on the respective axis; the top axis is used to measure the score of each variable. The sum of these scores is located on the total points axis, and the bottom line is the survival axes to determine the likelihood of 14.59-month OS.



Next, X-tile software was used to determine the optimal cut-off value of 60 U/L AST levels in the Kaplan-Meier survival analysis. Based on this cut-off value, the associations between serum AST levels and clinical pathologic factors in patients were analyzed (TABLE 3). The χ^2 test revealed that higher AST levels (>60 U/L) were associated with histological differentiation ($P = .042$) and death ($P = .006$). Moreover, Kaplan-Meier analysis revealed that higher AST level (>60 U/L) was significantly associated with decreased OS (FIGURE 1). The OS in patients with lower AST levels was 13.8 months longer than in patients with higher AST levels.

Nomogram Construction and Prognostic Value in PDAC

To predict the mortality of patients with PDAC, a prognostic nomogram was constructed using multivariate Cox regression model analysis, which integrated the 2 independent prognostic indicators for OS, AST, and TNM (FIGURE 2). The Harrell's C-index for mortality prediction was 0.802 (95% CI = 0.66–0.82), which was significantly higher than TNM stage alone (0.756). The calibration plot for the probability of mortality demonstrates an optimal agreement between the prediction by nomogram and actual observation.

Discussion

Pretreatment serum AST level and its relative indexes are significantly associated with OS of patients with advanced PDAC.^{9,15} However, the relationship between the pretreatment serum AST levels and survival of patients with resectable early-stage PDAC has not previously been reported. Therefore, the aim of this study was to explore the role of serologic AST levels in disease prognosis for patients with resectable PDAC. Here, we attempted to identify serum liver enzymes that could be informative prognostic indicators for patients with resectable PDAC. We analyzed data from routine blood test results of liver enzymes from 101 patients with PDAC. We used univariate and multivariate analysis to determine that serum AST levels and TNM stage were independent prognostic factors for patients with surgically treated PDAC. We found that higher AST levels are generally associated with shorter survival time. To evaluate the prognostic power of AST, we established a predictive nomogram model for patients with PDAC. The C-index of the nomogram model predicted OS with an accuracy of 0.802 (95% CI, 0.66–0.82). Interestingly, this nomogram displayed improved accuracy compared to the current TNM classification system (C-index = 0.756).

We suggest a potential mechanism for how the established nomogram based on AST can improve prognostic assessment of patients

with PDAC. First, in pancreatic cancer, tumor cells invading the adjacent biliopancreatic ducts obstruct bile and damage hepatocytes, which impairs liver function and contributes to elevated AST levels. In addition, PDAC is usually accompanied by a proinflammatory state. Inflammation is an essential promoter of pancreatic cancer development and is involved in PDAC initiation, progression, and metastasis.^{16,17} A prolonged state of inflammation can cause lasting damage to the pancreas and release AST into the blood. In addition to the release of cellular content caused by tissue damage, AST itself plays a key role in cancer cell metabolism in PDAC. Cancer cells are often adapted to glycolytic metabolism as a principle mode of energy production. In addition, PDAC cancer cells strongly depend on glutamine to supply biomass and energy for cell growth and replication. Aspartate derived from glutamine is transported to the cytoplasm and converted to oxaloacetate by AST (GOT1), which is subsequently converted to malic acid and, finally, pyruvate. Aspartate aminotransferase is an important regulator in this metabolic pathway, which increases the nicotinamide adenine dinucleotide phosphate hydrogen/nicotinamide adenine dinucleotide phosphate ratio and maintains reactive oxygen species balance in PDAC cells.^{18,19}

Prognostic biomarkers are needed to better understand the progression of PDAC and to develop personalized treatment strategies for early stage disease. It is necessary to identify readily assessable and efficient prognostic biomarkers for PDAC. Liver function tests are common laboratory tests, and previous studies have noted the association between AST and the risk of malignancy.^{20–23} Based on the function of AST in PDAC development and the value of serum AST level in prognosis of advanced PDAC,^{9,15} we therefore hypothesized that serum AST levels might also be a prognostic marker for patients with resectable early stage PDAC. Our data confirming that TNM stage and differentiation are significant prognostic factors for PDAC are consistent with other reports.^{24,25} In addition, among the 101 patients in our study cohort, patients with high preoperative serum AST levels had significantly poorer OS than patients with low serum AST levels. This finding suggests a possible prognostic role for AST in predicting survival for patients with resected early-stage PDAC.

The established nomogram based on serum AST levels could predict survival more precisely for patients with resectable PDAC than current methods. However, there are several limitations to this study. First, this was a retrospective study carried out in a single center in China. A large-scale and multicenter prospective study is needed to eliminate selectivity bias and validate the conclusion. Further studies using another dataset to verify this prognostic model may shed more light on

the clinical application of serum AST levels for prognostic prediction in PDAC. Second, the AST cut-off value in this study may not be applicable in other studies, and it may be necessary to determine the most appropriate AST cut-off value through a meta-analysis that includes various AST validated studies. Despite these limitations, this model provides an effective tool for predicting OS of patients with PDAC and can be helpful when making individualized treatment decisions for patients.

In summary, our data indicated that preoperative serum AST levels, but not levels of ALT, LDH, ALP or GGT, are an independent prognostic factor of resectable PDAC. Aspartate aminotransferase is an effective and available serum biomarker and may be a reliable prognostic predictor for survival in patients with resected early-stage PDAC. Compared to the TNM staging system alone, a prognostic monogram composed of serum AST and TNM stage could provide more accurate prognostic prediction for patients with resectable PDAC.

Data Availability

The datasets generated for this study are available on reasonable request to the corresponding author.

Funding

This work was financially supported by the National Natural Science Foundation of China (No. 81972750) to Ruizhi Wang.

Conflict of Interest Disclosure

The authors have nothing to disclose.

REFERENCES

1. Siegel RL, Miller KD, Jemal A. Cancer statistics, 2020. *CA Cancer J Clin.* 2020;70(1):7–30. doi:10.3322/caac.21590.
2. Hackert T, Buchler MW. Pancreatic cancer: advances in treatment, results and limitations. *Dig Dis.* 2013;31(1):51–56. doi:10.1159/000347178.
3. Wei Y, Xu H, Dai J, et al. Prognostic significance of serum lactic acid, lactate dehydrogenase, and albumin levels in patients with metastatic colorectal cancer. *Biomed Res Int.* 2018;2018:1804086. doi:10.1155/2018/1804086.
4. Staudigl C, Concin N, Grimm C, et al. Prognostic relevance of pretherapeutic gamma-glutamyltransferase in patients with primary metastatic breast cancer. *PLoS One.* 2015;10(4):e0125317. doi:10.1371/journal.pone.0125317.
5. Takemura K, Fukushima H, Ito M, et al. Prognostic significance of serum gamma-glutamyltransferase in patients with advanced urothelial carcinoma. *Urol Oncol.* 2019;37(2):108–115. doi:10.1016/j.urolonc.2018.11.002.
6. Lakshmanan M, Kumar V, Chaturvedi A, et al. Role of serum HE4 as a prognostic marker in carcinoma of the ovary. *Indian J Cancer.* 2019;56(3):216–221. doi:10.4103/ijc.IJC_305_18.
7. McCartney A, Biagioni C, Schiavon G, et al. Prognostic role of serum thymidine kinase 1 activity in patients with hormone receptor-positive metastatic breast cancer: analysis of the randomised phase III Evaluation of Faslodex versus Exemestane Clinical Trial (EFECT). *Eur J Cancer.* 2019;114:55–66. doi:10.1016/j.ejca.2019.04.002.
8. Wan Z, Zhang X, Yu X, Hou Y. Prognostic significance of serum soluble DR5 levels in small-cell lung cancer. *Int J Med Sci.* 2019;16(3):403–408. doi:10.7150/ijms.28814.
9. Riedl JM, Posch F, Prager G, et al. The AST/ALT (De Ritis) ratio predicts clinical outcome in patients with pancreatic cancer treated

with first-line nab-paclitaxel and gemcitabine: post hoc analysis of an Austrian multicenter, noninterventional study. *Ther Adv Med Oncol.* 2020;12:1758835919900872. doi:10.1177/1758835919900872.

10. Xiao Y, Lu J, Chang W, et al. Dynamic serum alkaline phosphatase is an indicator of overall survival in pancreatic cancer. *BMC Cancer.* 2019;19(1):785. doi:10.1186/s12885-019-6004-7.
11. Xiao Y, Yang H, Lu J, Li D, Xu C, Risch HA. Serum gamma-glutamyltransferase and the overall survival of metastatic pancreatic cancer. *BMC Cancer.* 2019;19(1):1020. doi:10.1186/s12885-019-6250-8.
12. Xiao Y, Chen W, Xie Z, et al. Prognostic relevance of lactate dehydrogenase in advanced pancreatic ductal adenocarcinoma patients. *BMC Cancer.* 2017;17(1):25. doi:10.1186/s12885-016-3012-8.
13. Deng QL, Dong S, Wang L, et al. Development and validation of a nomogram for predicting survival in patients with advanced pancreatic ductal adenocarcinoma. *Sci Rep.* 2017;7(1):11524. doi:10.1038/s41598-017-11227-8.
14. Ji F, Fu SJ, Guo ZY, et al. Prognostic value of combined preoperative lactate dehydrogenase and alkaline phosphatase levels in patients with resectable pancreatic ductal adenocarcinoma. *Medicine (Baltimore).* 2016;95(27):e4065e4065. doi:10.1097/md.0000000000004065.
15. Stocken DD, Hassan AB, Altman DG, et al. Modelling prognostic factors in advanced pancreatic cancer. *Br J Cancer.* 2008;99(6):883–893. doi:10.1038/sj.bjc.6604568.
16. Yamada S, Fujii T, Yabusaki N, et al. Clinical implication of inflammation-based prognostic score in pancreatic cancer: Glasgow prognostic score is the most reliable parameter. *Medicine (Baltimore).* 2016;95(18):e3582e3582. doi:10.1097/md.0000000000003582.
17. Lu H, Ouyang W, Huang C. Inflammation, a key event in cancer development. *Mol Cancer Res.* 2006;4(4):221–233. doi:10.1158/1541-7786.MCR-05-0261.
18. Son J, Lyssiotis CA, Ying H, et al. Glutamine supports pancreatic cancer growth through a KRAS-regulated metabolic pathway. *Nature.* 2013;496(7443):101–105. doi:10.1038/nature12040.
19. Holt MC, Assar Z, Beheshti Zavareh R, et al. Biochemical characterization and structure-based mutational analysis provide insight into the binding and mechanism of action of novel aspartate aminotransferase inhibitors. *Biochemistry.* 2018;57(47):6604–6614. doi:10.1021/acs.biochem.8b00914.
20. Yuk HD, Jeong CW, Kwak C, Kim HH, Ku JH. De Ritis ratio (aspartate transaminase/alanine transaminase) as a significant prognostic factor in patients undergoing radical cystectomy with bladder urothelial carcinoma: a propensity score-matched study. *Dis Markers.* 2019;2019:6702964. doi:10.1155/2019/6702964.
21. Miyake H, Matsushita Y, Watanabe H, et al. Significance of De Ritis (aspartate transaminase/alanine transaminase) ratio as a significant prognostic but not predictive biomarker in Japanese patients with metastatic castration-resistant prostate cancer treated with cabazitaxel. *Anticancer Res.* 2018;38(7):4179–4185. doi:10.21873/anticancer.12711.
22. Kang M, Yu J, Sung HH, et al. Prognostic impact of the pretreatment aspartate transaminase/alanine transaminase ratio in patients treated with first-line systemic tyrosine kinase inhibitor therapy for metastatic renal cell carcinoma. *Int J Urol.* 2018;25(6):596–603. doi:10.1111/iju.13574.
23. Lee H, Lee SE, Byun SS, Kim HH, Kwak C, Hong SK. De Ritis ratio (aspartate transaminase/alanine transaminase ratio) as a significant prognostic factor after surgical treatment in patients with clear-cell localized renal cell carcinoma: a propensity score-matched study. *BJU Int.* 2017;119(2):261–267. doi:10.1111/bju.13545.
24. Imamura T, Yamamoto Y, Sugiura T, et al. The prognostic relevance of the new 8th edition of the Union for International Cancer Control Classification of TNM Staging for ampulla of Vater carcinoma. *Ann Surg Oncol.* 2019;26(6):1639–1648. doi:10.1245/s10434-019-07238-6.
25. Wen S, Zhan B, Feng J, et al. Non-invasively predicting differentiation of pancreatic cancer through comparative serum metabolomic profiling. *BMC Cancer.* 2017;17(1):708. doi:10.1186/s12885-017-3703-9.

Serum expression of tumor marker CA242 in patients with different gynecological diseases

Jing Zhu, BS¹, Huidan Li, PhD²

¹Department of Laboratory Medicine, Jiading Branch of Shanghai General Hospital, Shanghai Jiao Tong University School of Medicine, Shanghai, China,

²Department of Clinical Laboratory, Shanghai General Hospital, Shanghai, China. Corresponding author: Huidan Li; lhdlucky@163.com

Key words: tumor marker; CA242; gynecological diseases; clinical diagnosis

Abbreviations: ROC, receiver operating characteristic; AUC, area under the curve; CIN, cervical intraepithelial neoplasia

Laboratory Medicine 2023;54:613-617; <https://doi.org/10.1093/labmed/lmad017>

ABSTRACT

Objective: The aim of this study was to investigate the serum levels of CA242 in different types of gynecological diseases and its clinical significance.

Methods: A total of 1021 patients with gynecological diseases and 499 healthy female controls were included in the study. The serum CA242 levels were detected and median value, $-\log_{10} P$ value, and positive rate were calculated. Serum CA125 and HE4 levels of patients with ovarian lesions were measured, and the predictive value for ovarian cancer was statistically analyzed.

Results: Higher serum CA242 levels were observed in patients with mature teratoma, ovarian cancer, and other gynecological tumor diseases than in healthy controls. In contrast, the CA242 levels in patients with cervical intraepithelial neoplasia, uterine polyps, or endometrial hyperplasia were comparable to that of controls. Moreover, serum CA242 expression was increased in malignant uterine and ovarian diseases compared with benign ones ($P < .05$). Specifically, combining CA242, CA125, and HE4 yielded a higher area under the receiver operating characteristic curve than single biomarkers ($P < .05$).

Conclusion: Heterogeneous increases in tumor marker CA242 expression levels are observed in different gynecological diseases, suggesting its potential value for clinical diagnosis.

Tumor-associated antigen CA242 is a new sialic acid-containing carbohydrate, present on the cell surface as a glycoprotein/glycolipid or in the

serum as an O-linked enriched glycoprotein (mucin). Elevated CA242 levels have long been used clinically as serological diagnostic markers for intestinal diseases, especially pancreatic cancer.¹⁻³ However, given its high expression in some gynecologic tumors,⁴⁻⁷ an increasing body of evidence suggests that CA242 has significant value as a screening marker for cancer in females.⁸ To the best of our knowledge, few reports have hitherto compared serum CA242 levels in different populations of female tumor and nontumor patients. Therefore, this study sought to analyze serum CA242 levels in female patients with different gynecological diseases and assess its diagnostic value.

Materials and Methods

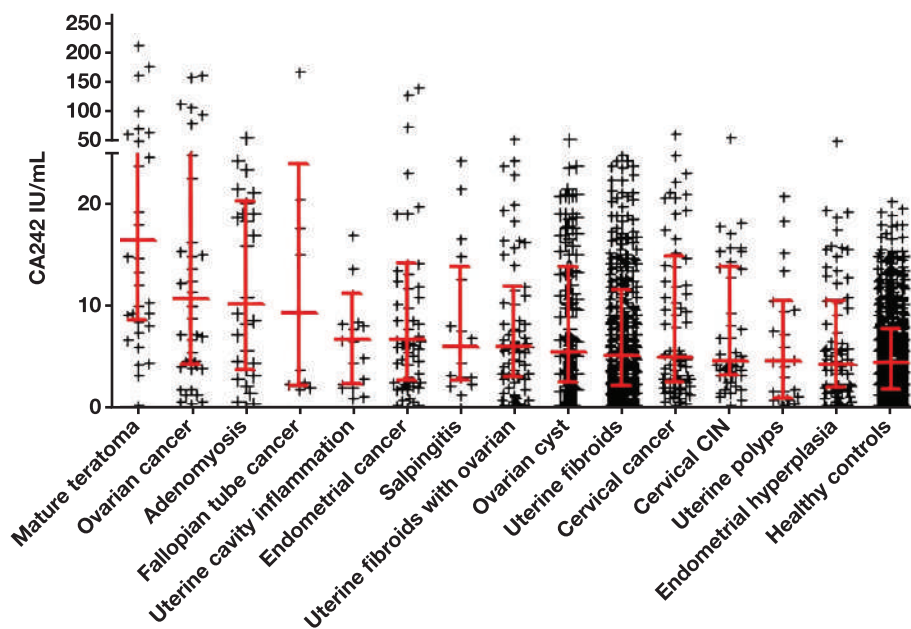
All clinical data were collected from 1371 patients admitted to the gynecological ward of Shanghai General Hospital from March 2019 to November 2019. All patients were informed of the study and agreed to undergo serum CA242 quantitative analysis before diagnosis.

All included tumor patients had newly diagnosed cases and had not received chemotherapy, radiotherapy, or other antitumor treatments. The diagnosis was confirmed by postoperative histopathology. Patients with other benign diseases were confirmed by pathology, imaging, and laboratory examinations. We excluded patients with comorbidities such as autoimmune diseases, mental disorders, severe liver and kidney dysfunction, and other cancers (pancreatic cancer, colorectal cancer, etc). Using these inclusion and exclusion criteria, 1021 patients were enrolled and divided into 14 groups according to the disease type. In addition, 499 healthy females that underwent blood testing during the same period were included in the control group.

All blood samples were collected 1 day after admission. The serum was separated by centrifugation at 3000 rpm for 10 min. The serum CA242 was detected using the Beijing Kemei CHEMCLIN1500 Immunoassay System. The serum CA125 and HE4 in the ovarian cancer group were measured using the Beckman Coulter's Dxl 800 Immunoassay System and the Roche E170 Immunoassay System, respectively. The CA242 reference range was 0 to 25 U/mL, CA125 reference range was 0 to 35 U/mL, and the HE4 reference range was 0 to 140 pmol/L. A finding of CA242 >25 U/mL is regarded as positive.

All data were analyzed by IBM SPSS Statistics for Windows, version 21. The Kolmogorov-Smirnov test was used to test for normality. Because the data were nonnormally distributed, pairwise comparisons between groups were statistically analyzed using the Mann-Whitney U test with $P < .05$ being considered as statistically significant. The $-\log_{10} P$ value was used to compare the difference in P values between diseases. The receiver

FIGURE 1. The expression levels of serum CA242 in 14 different gynecological diseases. The data are sorted in descending order of median value. The concentration of CA242 within the range of lower quartile (25%), median (50%), and upper quartile (75%) in each type are shown.



operating characteristic (ROC) curve was used to calculate the sensitivity and specificity of the biomarkers and determine their diagnostic efficacy.

Results

After statistical analysis of the data, we calculated and listed the median value, $-\log_{10} P$ value, and positive rate of serum CA242 levels in 14 gynecological diseases and healthy controls. The median serum CA242 values were higher in 9 diseases than in healthy controls. The highest median serum CA242 value (16.57 U/mL) was observed in mature teratoma. The median serum CA242 levels were higher in patients with ovarian cancer (10.80 U/mL), adenomyosis (10.25 U/mL), and fallopian tube cancer (9.46 U/mL) than in other gynecological diseases and healthy controls. The median serum CA242 values in patients with cervical intraepithelial neoplasia (CIN) (4.71 U/mL), uterine polyps (4.64 U/mL), and endometrial hyperplasia (4.45 U/mL) did not increase significantly compared with healthy controls (FIGURE 1). Among the 4 gynecological malignancies (ovarian, fallopian tube, endometrial, and cervical cancers), the median and positive rates of serum CA242 were higher in fallopian tube and ovarian cancers. In contrast, the median (5.15 U/mL) and the positive rate (8.97%) of serum CA242 in cervical cancer was relatively low (TABLE 1).

Compared with healthy controls, the CA242 $-\log_{10} P$ value level heat map of 14 different diseases showed a $-\log_{10} P$ value >1.3 for 9 diseases, suggesting that $-\log_{10} P$ value has a significant diagnostic value for at least 8 gynecological diseases, such as teratoma, ovarian cancer, ovarian cyst, and adenomyosis (FIGURE 2).

The highest positive rate was observed in mature teratoma (38.89%) followed by ovarian and endometrial cancers. The positive rates of serum CA242 in ovarian cysts and adenomyosis were also relatively high. In contrast, the positive rate of serum CA242 in uterine fibroids with ovarian cysts (8%) was lower than in ovarian cysts (8.81%) but higher

than in simple uterine fibroids (4.37%). Among them, the positive rates of serum CA242 in CIN, uterine fibroids, endometrial diseases, and uterine polyps were relatively low (TABLE 1).

As shown in TABLE 2, a comparison of serum CA242 levels between benign and malignant lesions of the same site showed that serum CA242 levels in malignant uterine lesions were higher than in benign lesions. Also, the serum CA242 levels in malignant ovarian lesions were higher than in benign ovarian lesions. There was a significant difference between benign/malignant lesions of the uterus and ovary ($P < .05$).

The area under the ROC curve for the diagnosis of ovarian cancer using CA242, CA125, and HE4 was 0.631 (sensitivity 64.3% and specificity 59.7%), 0.703 (sensitivity 78.6% and specificity 59.1%), and 0.839 (sensitivity 66.7% and specificity 90.6%) (TABLE 3), respectively. The area under the ROC curve of the combination of CA125 and CA242 in the diagnosis of ovarian cancer was 0.759 (sensitivity 83.3% and specificity 60.4%), which yielded better diagnostic performance than single biomarkers. The area under the ROC curve of CA125 combined with HE4 for the diagnosis of ovarian cancer was 0.858 (sensitivity 71.4% and specificity 88.7%). When CA242 was added to the above combination, the area under the curve (AUC) was 0.887, yielding a relatively higher sensitivity of 78.6% than CA125 combined with HE4 detection and high specificity of 86.8% (FIGURE 3).

Discussion

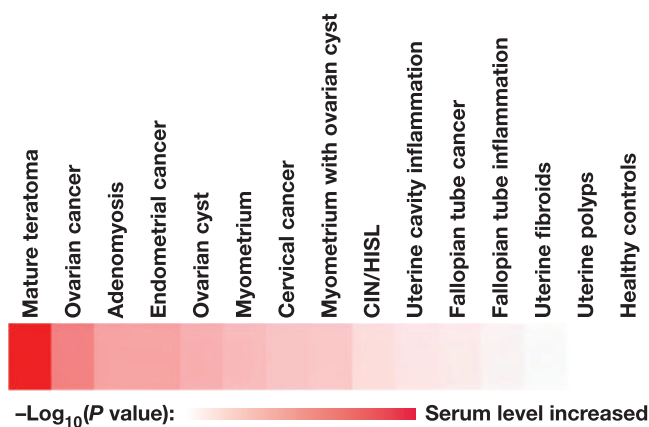
In 1985, Lindholm isolated the sialylated glycoprotein CA242 by immunizing mice with the human colorectal cancer cell line COLO205, which has similar antigenic determinant epitopes to CA199 and CA50 both. However, its antigenic determinant structure differs from CA199 and CA50 and cannot react with sialylated galactosides.⁹ With its low expression levels in healthy people and benign diseases,

TABLE 1. Comparison of Serum CA242 Levels in Between 14 Different Gynecological Diseases and Healthy Controls

Group	n	M (P25, P75)	Median difference (95% CI)	$-\log_{10}$ (P value)	Positive rate, n (%) ^a
Mature teratoma	36	16.57 (9.05, 39.93)	12.08 (7.77–19.39)	12.11	14 (38.89)
Ovarian cancer	42	10.80 (4.45, 27.59)	6.31 (2.89–9.11)	5.54	11 (26.19)
Adenomyosis	30	10.25 (4.15, 19.89)	5.76 (2.55–10.49)	4.01	3 (10.00)
Fallopian tube cancer	10	9.46 (2.46, 19.85)	4.97 (–0.62–14.01)	0.99	2 (20)
Uterine cavity inflammation	19	6.85 (2.75, 9.91)	2.36 (–0.22–4.41)	1.08	2 (10.53)
Endometrial cancer	63	6.76 (2.96, 14.27)	2.27 (1.25–4.44)	3.99	10 (15.87)
Salpingitis	17	6.18 (3.18, 12.71)	1.69 (–0.75–3.98)	0.71	0 (0)
Uterine fibroids with ovarian cyst	75	6.12 (3.30, 11.90)	1.63 (0.43–2.90)	2.25	6 (8.00)
Ovarian cyst	159	5.64 (2.72, 13.78)	1.15 (0.61–2.36)	3.34	14 (8.81)
Uterine fibroids	343	5.17 (2.38, 11.69)	0.68 (0.35–1.59)	2.84	15 (4.37)
Cervical cancer	78	5.15 (2.69, 14.59)	0.66 (0.48–2.91)	2.42	7 (8.97)
Cervical intraepithelial neoplasia	47	4.71 (3.32, 13.83)	0.22 (0.04–2.55)	1.38	3 (6.38)
Uterine polyps	27	4.64 (1.21, 10.18)	0.15 (1.30–2.32)	0.09	2 (7.41)
Endometrial hyperplasia	75	4.45 (2.16, 10.57)	–0.04 (–0.61–1.26)	0.31	3 (4.00)
Healthy controls	499	4.49 (1.94, 7.89)			

^aPositive rate: CA242 >25 U/mL is regarded as positive.

FIGURE 2. The $-\log_{10}$ P values of CA242 in 14 different gynecological diseases compared with the normal control group.



CA242 is a relatively new tumor marker extensively used in clinical practice.¹⁰ Overwhelming evidence substantiates that serum CA242 is a good diagnostic marker for pancreatic and colorectal cancers.^{11–13} Lei et al¹⁴ reported that the CA242 value has the highest specificity (80.14%) and positive predictive value (69.71%) in diagnosing pancreatic cancer. Moreover, when CA242 is combined with CA199, CEA, and CA125, the diagnostic sensitivity and specificity for pancreatic cancer were improved to 90.4% and 93.8%, respectively, which is significantly higher than single tumor markers.¹⁵ Further studies confirmed that the positive detection rate of CA242 was high and assisted in diagnosing lung, breast, and other cancers.^{16–19} Meanwhile, numerous studies^{5,20–22} reported that the combination of CA242, CA199, and CA125 has high application value in the differential diagnosis of ovarian cancer, cervical cancer, and other gynecological cancers, as well as in dynamic observation during tumor treatment.

This study showed that the serum levels of CA242 in ovarian, cervical, and other gynecological tumor diseases were high, consistent with previous reports.^{5,23} The median value and positive rate of CA242 in ovarian, endometrial, and fallopian tube cancer were significantly higher than in cervical cancer, followed by nonmalignant diseases such as adenomyosis, uterine cavity inflammation, and ovarian cysts. The me-

dian and $-\log_{10}$ P values of serum CA242 levels in ovarian cancer were significantly higher than those of ovarian cysts. Moreover, the serum CA242 levels in endometrial and cervical cancers were higher than in endometrial hyperplasia and CIN respectively. These results indicate that the higher the degree of malignancy of the gynecological disease, the higher the serum CA242 level. We used $-\log_{10}$ P value to show the CA242 serum levels of 14 gynecological diseases. Mature teratomas and ovarian cancer exhibited the highest expression levels compared with healthy controls, followed by ovarian cysts, adenomyosis, and endometrial cancer. Eight diseases had $-\log_{10}$ P values > 1.3, indicating that CA242 expression can be used as a tumor marker for these 8 diseases. However, there was no significant difference in intrauterine inflammation, fallopian tube cancer, tubal inflammation, endometrial hyperplasia and uterine polyps ($P > .05$).

According to the grouping of benign and malignant lesions at the same sites, the results showed that serum CA242 was significantly higher in serum of malignant lesions at uterine and ovarian sites than at benign sites ($P < .05$). For the fallopian tube site, although the median value of CA242 was higher in the serum of malignant lesions compared with benign lesions ($P > .05$), there was no significant difference between the two, probably due to the small number of cases of tubal lesions in this study. We also analyzed the diagnostic performance of CA242, CA125, and HE4 alone and in combination for ovarian cancer. The area under the ROC curve of CA242 combined with CA125 in diagnosing ovarian cancer was 0.759, with a sensitivity of 83.3% and a specificity of 60.4%, higher than the single marker. The AUC of CA125 combined with HE4 in the diagnosis of ovarian cancer was 0.858, with a sensitivity of 71.4%, which was inferior to that of CA242 combined with CA125. In contrast, its specificity of 88.7% was significantly higher than that of CA242 combined with CA125. The AUC of the combination of the three tumor markers in the diagnosis of ovarian cancer was 0.887, with a sensitivity of 78.6% and a specificity of 86.8%, which was higher than the combination of CA125 and HE4. However, the sensitivity was inferior to that of the combination of CA242 and CA125, indicating that the sensitivity of CA242 combined with the other two indicators was significantly higher. A good specificity was also observed, suggesting the combination of CA242, CA125, and HE4 has diagnostic value for ovarian cancer.

In this study, we also found that the median value, positive rate, and $-\log_{10}$ P value of serum CA242 in patients with mature teratoma were

TABLE 2. The Expression Levels of CA242 in Benign and Malignant Lesions of the Same Site

Group ^a	n	Median (25%, 75%) (U/mL)
Uterine benign lesions	475	5.17 (2.24, 11.97)
Uterine malignant lesions	63	6.67 (2.78, 14.31) ^b
Ovarian benign lesions	159	5.64 (2.67, 13.91)
Ovarian malignant lesions	42	10.80 (4.35, 28.52) ^b
Cervical benign lesions	47	4.71 (3.31, 13.84)
Cervical malignant lesions	78	5.14 (2.64, 14.89)
Benign fallopian tube lesions	17	6.18 (2.78, 13.87)
Malignant fallopian tube lesions	10	9.46 (2.30, 23.96)

^aBenign uterine lesions include adenomyosis, uterine polyps, endometrial hyperplasia, and uterine fibroids. Uterine malignant lesions include endometrial cancer. Ovarian benign lesions include ovarian cysts. Ovarian malignant lesions include ovarian cancer. Cervical benign lesions include cervical intraepithelial neoplasia (CIN). Cervical malignant lesions include cervical cancer. Benign fallopian tube lesions include salpingitis. Malignant fallopian tube lesions include fallopian tube cancer. Comparison of benign and malignant lesions is at the same site.

^bP < .05.

FIGURE 3. The receiver operating characteristic curve of CA242, CA125, and HE4 alone and in combination for the diagnosis of ovarian cancer.

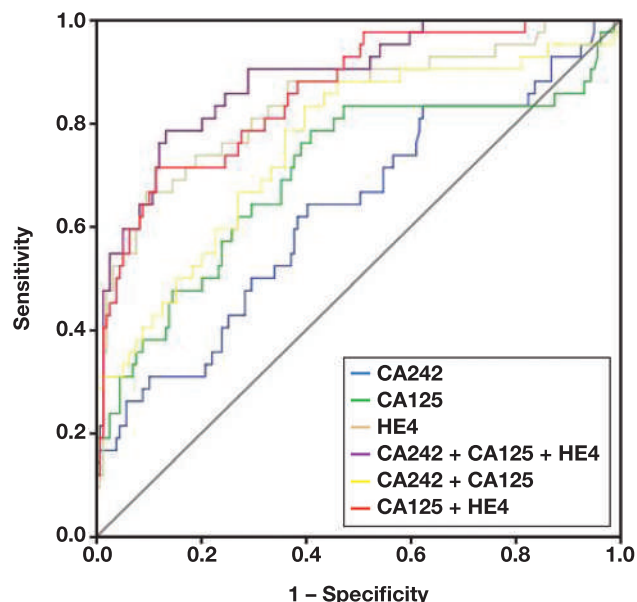


TABLE 3. Comparison of the Diagnostic Efficacy of CA242, CA125, and HE4 Alone and in Combination for Ovarian Cancer

Tumor marker	AUC	95% CI	Sensitivity	Specificity	P value
CA242	0.631	0.531~0.731	0.643	0.597	<.05
CA125	0.703	0.600~0.805	0.786	0.591	<.05
HE4	0.839	0.764~0.915	0.667	0.906	<.05
CA242+CA125	0.759	0.671~0.847	0.833	0.604	<.05
CA125+HE4	0.858	0.794~0.922	0.714	0.887	<.05
CA242+CA125+HE4	0.887	0.831~0.944	0.786	0.868	<.05

AUC, area under the curve.

the highest among the 14 gynecological diseases. Teratoma is a germ cell tumor, and mature teratomas correlate with a lower risk of malignant transformation. In contrast, relatively immature teratomas are usually associated with higher levels of necrotic components.^{24,25} Interestingly, Wang et al²⁴ and Suh et al²⁶ founded that the combination of CA199 and CA125 can differentiate mature cystic teratoma from other malignant tumors. Chen et al²⁷ and Gomes et al²⁸ showed that the combination of tumor markers has significant value in the differential diagnosis of immature and mature ovarian teratomas. However, few studies have assessed the value of CA242 in the clinical diagnosis of teratoma. Our future studies will focus on more in-depth stratified study with a larger sample size to provide more valuable laboratory data for clinical practice.

In summary, heterogeneous increases in tumor marker CA242 expression levels are observed in different gynecological diseases. The CA242 levels are increased in chronic diseases and malignant tumors of the uterus and ovary. Further studies are warranted to assess its clinical application value.

Funding

This study was supported by the National Natural Science Foundation of China (Grant No. 81801582) and the Key Medical Discipline of Shanghai Jiading District (Grant No. 2020-jdyxzdxx-13).

Conflict of Interest Disclosure

The authors have nothing to disclose.

REFERENCES

- Su J, Wang Y, Shao H, You X, Li S. Value of multi-detector computed tomography combined with serum tumor markers in diagnosis, preoperative, and prognostic evaluation of pancreatic cancer. *World J Surg Oncol.* 2022;20(1):323. PMID: 36175918.
- Ge L, Pan B, Song F, et al. Comparing the diagnostic accuracy of five common tumour biomarkers and CA19-9 for pancreatic cancer: a protocol for a network meta-analysis of diagnostic test accuracy. *BMJ Open.* 2017;7(12):e018175. PMID: 29282264.
- Sun LQ, Peng LS, Guo JF, et al. Validation of serum tumor biomarkers in predicting advanced cystic mucinous neoplasm of the pancreas. *World J Gastroenterol.* 2021; 27(6): 501–512. PMID: 33642824.
- Luo H, Shen K, Li B, Li R, Wang Z, Xie Z. Clinical significance and diagnostic value of serum NSE, CEA, CA19-9, CA125 and CA242 levels in colorectal cancer. *Oncol Lett.* 2020;20(1):742–750. PMID: 32566000.
- Dou H, Sun G, Zhang L. CA242 as a biomarker for pancreatic cancer and other diseases. *Prog Mol Biol Transl Sci.* 2019;162:229–239. PMID: 30905452.
- Zhu Y, Chen N, Chen M, et al. Circulating tumor cells: a surrogate to predict the effect of treatment and overall survival in gastric

- adenocarcinoma. *Int J Biol Markers* 2021;36(1): 28–35. PMID: 33499715.
7. Wang YF, Feng FL, Zhao XH, et al. Combined detection tumor markers for diagnosis and prognosis of gallbladder cancer. *World J Gastroenterol* 2014;20(14): 4085–4092. PMID: 24744600.
 8. Zhang Y, Li C, Luo S, et al. Retrospective study of the epidemiology, pathology, and therapeutic management in patients with mucinous ovarian tumors. *Technol Cancer Res Treat*. 2020;19: 1533033820946423 PMID: 32783505.
 9. Gui JC, Yan WL, Liu XD. CA19-9 and CA242 as tumor markers for the diagnosis of pancreatic cancer: a meta-analysis. *Clin Exp Med*. 2014;14(2):225–233. PMID: 23456571.
 10. Dong D, Jia L, Zhang L, et al. Periostin and CA242 as potential diagnostic serum biomarkers complementing CA19.9 in detecting pancreatic cancer. *Cancer Sci*. 2018;109(9): 2841–2851 PMID: 29945294.
 11. Zhang Y, Yang J, Li H, Wu Y, Zhang H, Chen W. Tumor markers CA19-9, CA242 and CEA in the diagnosis of pancreatic cancer: a meta-analysis. *Int J Clin Exp Med*. 2015;8(7):11683–11691. PMID: 26380005.
 12. Liu Y, Chen J. Expression levels and clinical significance of serum miR-497, CEA, CA24-2, and HBsAg in patients with colorectal cancer. *Biomed Res Int*. 2022;2022:3541403. PMID: 35993056.
 13. Tao L, Zhou J, Yuan C, et al. Metabolomics identifies serum and exosomes metabolite markers of pancreatic cancer. *Metabolomics*. 2019;15(6):86. PMID: 31147790.
 14. Lei XF, Jia SZ, Ye J, et al. Application values of detection of serum CA199, CA242 and CA50 in the diagnosis of pancreatic cancer. *J Biol Regul Homeost Agents*. 2017;31(2): 383–388. PMID: 28685541.
 15. Gu YL, Lan C, Pei H, Yang SN, Liu YF, Xiao LL. Applicative value of serum CA19-9, CEA, CA125 and CA242 in diagnosis and prognosis for patients with pancreatic cancer treated by concurrent chemoradiotherapy. *Asian Pac J Cancer Prev*. 2015;16(15):6569–6573. PMID: 26434876.
 16. Wang X, Zhang Y, Sun L, et al. Evaluation of the clinical application of multiple tumor marker protein chip in the diagnostic of lung cancer. *J Clin Lab Anal* 2018;32(8): e22565. PMID: 29736949.
 17. Xu MX, Cui HJ, Yao TL, Gui YF. Clinical value of combined tests for tumor markers for gastric cancer. *J Biol Regul Homeost Agents*. 2018;32(2):263–268. PMID: 29685004.
 18. Liang L, Fang J, Han X, et al. Prognostic value of CEA, CA19-9, CA125, CA724, and CA242 in serum and ascites in pseudomyxoma peritonei. *Front Oncol*. 2021;11:594763.PMID: 34733775.
 19. Zhao H, Lu B. Prediction of multiple serum tumor markers in hepatolithiasis complicated with intrahepatic cholangiocarcinoma. *Cancer Manag Res*. 2022;14:249–255. PMID: 35082529.
 20. Deng H, Chen M, Guo X, et al. Comprehensive analysis of serum tumor markers and BRCA1/2 germline mutations in Chinese ovarian cancer patients. *Mol Genet Genomic Med*. 2019;7(6):e672. PMID: 30972954.
 21. Li X, Li S, Zhang Z, Huang D. Association of multiple tumor markers with newly diagnosed gastric cancer patients: a retrospective study. *PeerJ*. 2022;10:e13488. PMID: 35611170.
 22. Ge L, Wang S, Liu H, Shi X, Shi J, Feng R. Intralobar pulmonary sequestration with aspergillus infection and elevated serum CA19-9 and CA242: a case report. *Transl Cancer Res*. 2021;10(2):1169–1176. PMID: 35116444.
 23. Bian J, Li B, Kou XJ, Wang XN, Sun XX, Ming L. Clinical applicability of multi-tumor marker protein chips for diagnosing ovarian cancer. *Asian Pac J Cancer Prev*. 2014;15(19):8409–8411. PMID: 25339038.
 24. Wang YQ, Xia WT, Wang F, Zhuang XX, Zheng FY, Lin F. Use of cancer antigen 125, cancer antigen 19-9, and the neutrophil-to-lymphocyte ratio to diagnose mature cystic teratoma with torsion. *Int J Gynaecol Obstet*. 2017;137(3):332–337. PMID: 28273351.
 25. Fan JT, Yan HQ, Malla S, et al. The clinical significance of CA19-9 in ovarian mature cystic teratoma. *Clin Exp Obstet Gynecol*. 2016;43(4): 522–525. PMID: 29734540.
 26. Suh DS, Moon SH, Kim SC, Joo JK, Park WY, Kim KH. Significant simultaneous changes in serum CA19-9 and CA125 due to prolonged torsion of mature cystic teratoma of the ovary. *World J Surg Oncol*. 2014;12:353. PMID: 25416055.
 27. Chen JM, Gao HY, Wang Q, Li Q. Expression and clinical significance of tumor markers in ovarian mature cystic teratoma. *Clin Exp Obstet Gynecol*. 2016;43(3):397–400. PMID: 27328499.
 28. Gomes TA, Campos EA, Yoshida A, Sarian LO, Andrade L, Derchain SF. Preoperative differentiation of benign and malignant non-epithelial ovarian tumors: clinical features and tumor markers. *Rev Bras Ginecol Obstet*. 2020;42(9):555–561. PMID: 32992358.

A population-based characterization study of anti-mitochondrial M2 antibodies and its consistency with anti-mitochondrial antibodies

En-yu Liang, MD,^{1,2} Miao Liu, MBBS,¹ Pei-feng Ke, MM,¹ Guang Han, MM,¹ Cheng Zhang, MM,¹ Li Deng, MBBS,¹ Yun-xiu Wang, MM,¹ Hui Huang, MM,¹ Wu-jiao Huang, MM,¹ Rui-ping Liu, MBBS,¹ Guo-hua Li, MM,¹ Ze-min Wan, MM,¹ Yi-ting He, MD,³ Min He, MD,^{1,2,4,*} Xian-zhang Huang, MD^{1,2,4,*}

¹Department of Laboratory Medicine, ²State Key Laboratory of Dampness Syndrome of Chinese Medicine, ³Intellectual Property Management and Transfer Center, and ⁴Guangdong Provincial Key Laboratory of Chinese Medicine for Prevention and Treatment of Refractory Chronic Diseases, the Second Affiliated Hospital of Guangzhou University of Chinese Medicine, Guangzhou, China. Corresponding author: Min He; minhe@gzucm.edu.cn. *Contributed equally.

Keywords: antimitochondrial antibody subtype M2 (AMA-M2); primary biliary cholangitis; population characteristics; risk factors

Abbreviations: AMA, antimitochondrial antibody; AMA-M2, AMA M2 subtype; PBC, primary biliary cholangitis; EASL, European Association for the Study of the Liver; ACG, American College of Gastroenterology; ALP, alkaline phosphatase; IIF, indirect immunofluorescence; ELISA, enzyme-linked immunosorbent assay; ALT, alanine aminotransferase; AST, aspartate aminotransferase; GGT, gamma-glutamyl transferase; ALB, albumin; TP, total protein; TBIL, total bilirubin; PA, prealbumin; Ig, immunoglobulin; C3/C4, complement 3/4; RF, rheumatoid factor; ASO, antistreptolysin O; BMI, body mass index; CHE, cholinesterase; ULN, upper limit of normal; DBIL, direct bilirubin

Laboratory Medicine 2023;54:618-625; <https://doi.org/10.1093/labmed/lmad018>

ABSTRACT

Objective: This study aims to estimate the prevalence of anti-mitochondrial antibody subtype M2 (AMA-M2) and assess its consistency with AMA in a general population.

Methods: A total of 8954 volunteers were included to screen AMA-M2 using enzyme-linked immunosorbent assay. Sera with AMA-M2 >50 RU/mL were further tested for AMA using an indirect immunofluorescence assay.

Results: The population frequency of AMA-M2 positivity was 9.67%, of which 48.04% were males and 51.96% were females. The AMA-M2 positivity in males had a peak and valley value of 7.81% and 16.88% in those aged 40 to 49 and ≥70 years, respectively, whereas it showed a balanced age distribution in females. Transferrin and immunoglobulin

M were the risk factors for AMA-M2 positivity and exercise was the only protective factor. Of 155 cases with AMA-M2 >50 RU/mL, 25 cases were AMA-positive, with a female-to-male ratio of 5.25:1. Only 2 people, with very high AMA-M2 of 760 and >800 RU/mL, met the diagnostic criteria of primary biliary cholangitis (PBC), making the prevalence of PBC 223.36 per million in southern China.

Conclusion: We found that AMA-M2 has a low coincidence rate with AMA in the general population. A new decision-making point for AMA-M2 is needed to improve consistency with AMA and diagnostic accuracy.

Introduction

Primary biliary cholangitis (PBC), previously named primary biliary cirrhosis, is a chronic autoimmune cholestatic liver disease with progressive histological lesions as nonsuppurative lymphocytic or granulomatous interlobular bile duct cholangitis.^{1,2} Primary biliary cholangitis has been reported to be more prevalent in Europe and North America than in the Asia Pacific region.³⁻⁵ During the last decade, there has been a marked increase in the number of PBC cases in China.⁶ This may be largely attributed to the awareness and availability of early screening of PBC, especially for the application of autoantibody testing like antimitochondrial antibodies (AMA). However, most of the reported prevalence of PBC was based on the combined case-finding and case ascertainment strategy,⁷ which probably underestimated the PBC prevalence in the whole population and neglected preclinical and asymptomatic persons. Thus, epidemiological data on the prevalence of PBC based on the general population strategy in China is desirable.

Primary biliary cholangitis typically progresses slowly and insidiously to cirrhosis, hepatobiliary malignancies, and eventually to liver-related mortality. Therefore, early diagnosis and intervention are essential for delaying the development of this disease. Antimitochondrial antibodies are serological hallmarks of PBC and are present in more than 95% of PBC patients.⁸ They may antedate other biochemical markers, histological changes, and clinical manifestations for several years and persist throughout the whole course of the disease.⁹ As suggested by the European Association for the Study of the Liver (EASL)¹⁰ and the American College of Gastroenterology (ACG),¹¹ a diagnosis of PBC can be made

with the presence of AMA and elevated alkaline phosphatase (ALP), even without a liver biopsy. This makes the AMA test particularly attractive for assessing the extent of the PBC spectrum on a population scale. Currently, the standard method for detecting AMA in many clinical laboratories is indirect immunofluorescence (IIF), which is based on tissue sections. However, the costly, lengthy process and observer dependence limit its large-scale clinical application. Recently, quantitative detection of its specific subtype, M2 (AMA-M2), by enzyme-linked immunosorbent assay (ELISA) is widely used in clinical practice, especially those using recombinant proteins such as MIT3 targeting immunodominant portions of PDC-E2, BCOADC-E2, and OGDC-E2.¹² However, increasing research has reported that ELISA is slightly more sensitive but less specific than IIF in biopsy-proven PBC. Its application can turn 90% of the PBC-negative tests for AMA by the conventional IIF method into positives.¹³ As suggested by a large-scale characterization study, nearly half of prospectively detected AMA in clinical practice was not related to a diagnosis of PBC.⁹ Because AMA-M2 and AMA have advantages and disadvantages, the issue is whether they share the same prevalence in the general population.

Herein, we report on a population-based epidemiological study to estimate the prevalence of PBC and analyze the natural distribution of AMA-M2 in both sampled populations and individuals undergoing health checkups. Moreover, the related risk factors of AMA-M2, including biochemical, immunological, and lifestyles, were analyzed. Our rationale was that the natural distribution and sources of variations of AMA-M2 in the general population would promote the efficiency of early screening and accurate diagnosis of PBC.

Methods

Subjects

This was a cross-sectional study conducted in Guangzhou from August 2010 to June 2014, including 2 cohorts. The volunteers in cohort 1 (n = 3755) were recruited using a stratified sampling method based on the regional population distribution and the proportion of urban and rural residents from the sixth national census data of the Guangzhou resident population. Adult citizens who lived in Guangzhou for at least 5 years and lived at the sampling points for at least 1 year were included in this study. The participants were invited to complete a questionnaire on medical history before they were enrolled. General information, living habits, health status, and physical examinations were recorded

in a secure database with restricted access. Participants in cohort 2 (n = 5197) were consecutively enrolled from those who underwent a health checkup at the Second Affiliated Hospital of Guangzhou University of Chinese Medicine. Overall, of the 8952 volunteers recruited in the study, 4582 (51.2%) were males and 4354 (48.8%) were females. The age of participants ranged from 18 to 93 years with a male-to-female ratio of 1.05:1, which reflects the general sex distribution in Guangzhou (1.08:1) as reported in the sixth national census data of the Guangzhou resident population.

Ethical Approval

This study followed the tenets of the Helsinki Declaration. All human subjects signed informed consent about using their medical data and blood specimens for research purposes before they were enrolled in this study. This study was approved by the hospital ethical committee (2013-127-2).

Laboratory Testing

The laboratory indices included clinical chemical analytes, immunoassay, and infection markers. The clinical chemical analytes included alanine aminotransferase (ALT), aspartate aminotransferase (AST), ALP, gamma-glutamyl transferase (GGT), albumin (ALB), total protein (TP), and total bilirubin (TBIL), which were measured by Roche Modular P 800 automatic biochemical analyzer (Roche Diagnostics). The immunoassays included prealbumin (PA), immunoglobulin (Ig)G, IgA, IgM, complement 3 (C3), C4, rheumatoid factor (RF), antistreptolysin O (ASO), and transferrin and were quantified by Roche Modular P or Siemens BNII. The serum infection markers of hepatitis B or hepatitis C viruses were detected using the cobas e602 analyzer (Roche Diagnostics).

Detection of AMA-M2

Antimitochondrial antibody subtype M2 was measured using an ELISA kit (Shanghai Kexin Biotech). The manufacturer's cutoff was established at 25 RU/mL.¹⁴ According to the resulting concentrations of AMA-M2, patients were categorized into three subgroups for further analysis: group 1, AMA-M2 ≤25 RU/mL; group 2, 25 < M2 ≤50 RU/mL; and group 3, AMA-M2 >50 RU/mL (twice the cutoff value).

IIF Assay for AMA

Sera with AMA-M2 >50 RU/mL were additionally tested for AMA (the quadruple tissue matrix; Euroimmun).¹⁵ Positivity and patterns were evaluated by 2 independent evaluators using fluorescence microscopy, and titer equal to or higher than 1:100 was considered positive.

TABLE 1. Positive Rates of AMA-M2 by Sex and Age Groups

Age, y	Cohort 1 (n = 3755)		Cohort 2 (n = 5197)		Total (n = 8952)	
	Male	Female	Male	Female	Male	Female
18-29	29/290 (10.00%) ^{a,b}	41/337 (12.17%)	98/1086 (9.02%)	78/777 (10.04%)	127/1376 (9.23%) ^{a,b}	119/1114 (10.68%)
30-39	23/286 (8.04%) ^{a,b}	37/298 (12.41%)	67/653 (10.26%)	58/559 (10.38%)	90/939 (9.58%) ^{a,b,c}	95/857 (11.09%)
40-49	25/320 (7.81%) ^b	45/403 (11.17%)	27/436 (6.19%)	37/455 (8.13%)	52/756 (6.88%) ^b	82/858 (9.56%) ^d
50-59	35/399 (8.77%) ^{a,b}	35/413 (8.47%)	25/378 (6.61%)	34/308 (11.04%)	60/777 (7.72%) ^{a,b}	69/721 (9.57%)
60-69	34/295 (11.53%) ^{a,b}	33/335 (9.85%)	16/167 (9.58%)	14/181 (7.73%)	50/462 (10.82%) ^{a,c}	47/516 (9.11%)
≥70	27/160 (16.88%) ^a	31/219 (14.16%)	10/112 (8.93%)	7/69 (10.14%)	37/272 (13.60%) ^c	38/288 (13.19%)
Total	173/1750 (9.89%)	222/2005 (11.07%)	243/2832 (8.58%)	228/2349 (9.71%)	416/4582 (9.08%)	450/4354 (10.34%)

^{a,b,c}Compared with the different age groups in the same cohort and with the same sex, no statistically significant difference exists between the 2 groups with any identical superscript footnote.

^aCompared with males in the same age group, P < .01.

TABLE 2. Physical and Laboratory Characteristics of 3755 Participants Categorized with AMA-M2 Concentrations^a

Measurement parameters	Group 1 M2 ≤25 RU/mL (n = 3360)	Group 2 25 RU/mL < M2 ≤50 RU/mL (n = 240)	Group 3 M2 >50 RU/mL (n = 155)	P ^{1b}	P ^{2b}	P ^{3b}
Age (y)	47.74 ± 15.78	49.38 ± 16.95	47.6 ± 17.16	NS	NS	NS
Height (m)	1.62 ± 0.08	1.62 ± 0.09	1.61 ± 0.08	NS	NS	NS
Weight (kg)	59.78 ± 10.65	59.38 ± 10.76	57.6 ± 10.76	NS	.017	NS
BMI (kg/m ²)	22.79 ± 3.13	22.64 ± 2.98	22.07 ± 3.06	NS	.010	NS
Waistline (cm)	81.51 ± 23.19	80.47 ± 9.03	78.70 ± 9.29	NS	.004	NS
Hipline (cm)	94.42 ± 7.13	94.30 ± 6.68	93.14 ± 7.44	NS	.040	NS
ALT (U/L)	20.42 ± 15.35	21.49 ± 31.67	19.6 ± 17.05	NS	NS	NS
AST (U/L)	22.26 ± 8.11	24.50 ± 28.02	23.2 ± 13.51	NS	NS	NS
ALP (U/L)	72.24 ± 21.43	71.64 ± 20.33	78.3 ± 65.59	NS	NS	NS
GGT (U/L)	28.26 ± 27.92	34.23 ± 75.99	31.8 ± 61.37	NS	NS	NS
CHE (U/L)	9268.32 ± 1799.03	9271.32 ± 1730.66	8629.8 ± 1566.07	NS	.040	.016
TP (g/L)	76.70 ± 4.49	77.27 ± 4.83	76.95 ± 4.96	NS	NS	NS
ALB (g/L)	47.63 ± 2.84	47.75 ± 3.40	47.38 ± 3.05	NS	NS	NS
TBIL (μmol/L)	10.83 ± 5.02	10.81 ± 5.51	10.94 ± 7.62	NS	NS	NS
DBIL (μmol/L)	3.47 ± 2.02	3.48 ± 1.75	3.93 ± 6.02	NS	NS	NS
IgA (g/L)	2.55 ± 1.04	2.52 ± 0.96	2.60 ± 1.01	NS	NS	NS
IgG (g/L)	13.08 ± 2.47	13.39 ± 2.37	13.60 ± 3.33	NS	NS	NS
IgM (g/L)	1.23 ± 0.63	1.29 ± 0.71	1.58 ± 1.41	NS	.002	.030
C3 (g/L)	1.09 ± 0.18	1.11 ± 0.16	1.10 ± 0.20	NS	NS	NS
C4 (g/L)	0.28 ± 0.09	0.29 ± 0.09	0.28 ± 0.13	NS	NS	NS
RF (IU/mL)	12.09 ± 27.64	12.38 ± 12.69	16.0 ± 53.51	NS	NS	NS
ASO (IU/mL)	69.12 ± 78.76	56.70 ± 53.65	77.0 ± 83.14	NS	NS	NS
Transferrin (mg/L)	2.60 ± 0.38	2.59 ± 0.35	2.74 ± 0.44	NS	.045	.009
PA (mg/L)	282.03 ± 53.51	286.74 ± 56.24	283.9 ± 56.95	NS	NS	NS
Questionnaire survey						
Sex						
Male	1577 (46.93)	112 (46.67)	61 (39.35)	NS	NS	NS
Female	1783 (53.07)	128 (53.33)	94 (60.65)			
Habitation						
Urban	2470 (73.51)	165 (68.75)	112 (72.26)	NS	NS	NS
Rural	890 (26.49)	75 (31.25)	43 (27.74)			
Exercise						
Less	1921 (57.17)	127 (52.92)	106 (68.39)	NS	.008	.008
More	1439 (42.83)	113 (47.08)	49 (31.61)			
Fatigue						
No	2450 (72.92)	180 (75.00)	112 (72.26)	NS	NS	NS
Yes	910 (27.08)	60 (25.00)	43 (27.74)			
Smoke						
Nonsmoking	2621 (78.01)	183 (76.25)	126 (81.29)	NS	NS	NS
Abstinence	221 (6.58)	15 (6.25)	4 (2.58)			
Smoker	518 (15.42)	42 (17.50)	25 (16.13)			
Drink						
Teetotaler	2647 (78.78)	187 (77.92)	127 (81.94)	NS	NS	NS
Abstinence	411 (12.23)	30 (12.50)	17 (10.97)			
Alcoholic	302 (8.99)	23 (9.58)	11 (7.10)			

ALB, albumin; ALP, alkaline phosphatase; ALT, alanine aminotransferase; AMA, antimitochondrial antibody; ASO, antistreptolysin O; AST, aspartate aminotransferase; BMI, body mass index; CHE, cholinesterase; DBIL, direct bilirubin; GGT, gamma-glutamyl transferase; NS, nonsignificant; PA, prealbumin; RF, rheumatoid factor; TBIL, total bilirubin; TP, total protein.

^aData are given as mean ± SD or No. (%).

^bP1, P2, and P3 were the P values for M2 ≤25 RU/mL vs 25 RU/mL < M2 ≤50 RU/mL, M2 ≤25 RU/mL vs M2 >50 RU/mL, 25 RU/mL < M2 ≤50 RU/mL vs M2 >50 RU/mL, respectively.

FIGURE 1. Forest plot of various risk factors. A, The risk factors and odds ratio (OR) between M2 ≤25 RU/mL and M2 >50 RU/mL groups. B, The risk factors and OR between 25 RU/mL < M2 ≤50 RU/mL and M2 >50 RU/mL group. BMI, body mass index; CHE, cholinesterase.

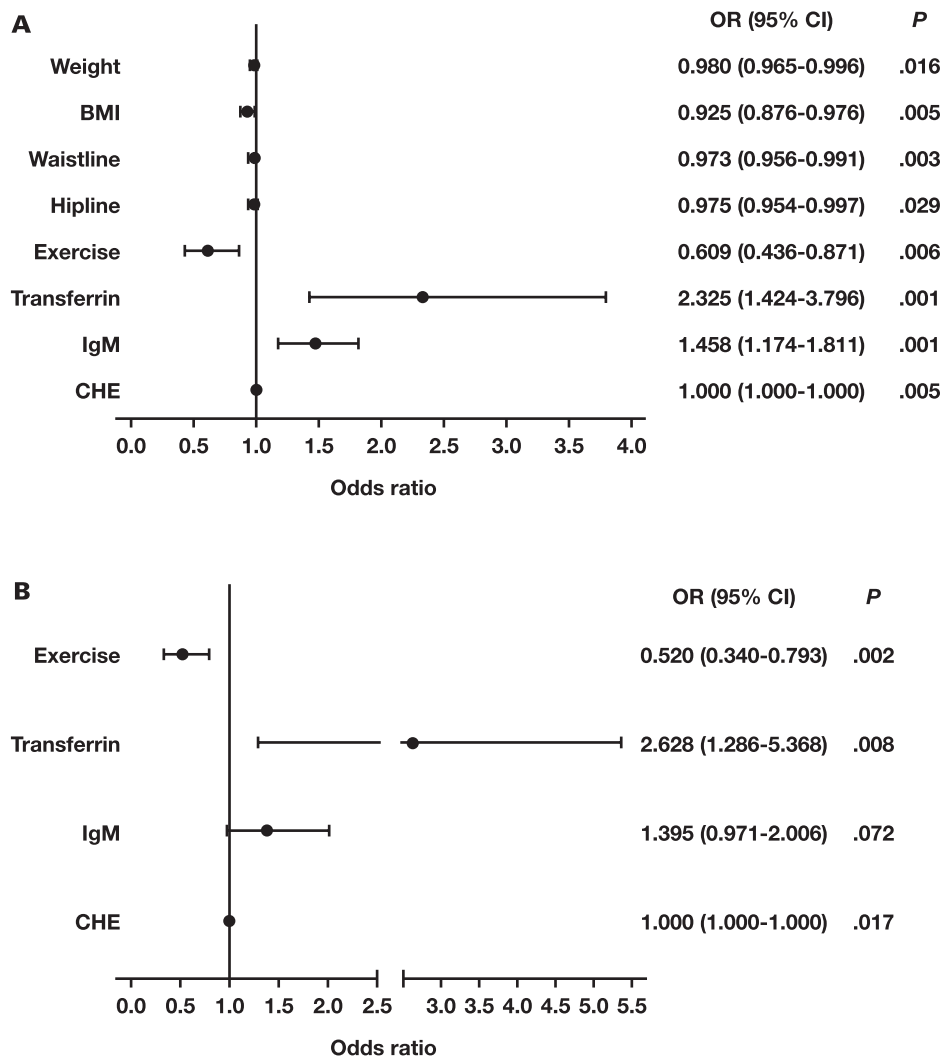


FIGURE 2. The distribution characteristics of the antimitochondrial antibody (AMA)-positive population. A, The positive rates of AMA were categorized by sex and age groups. B, The correlation of AMA with quantitative AMA-M2, sex, and age. The black circles around the dots represented that the participant had an elevated alkaline phosphatase (ALP) up to 2× the upper limit of normal. The numbers above or next to the dots represented the concentration of AMA-M2 in cases with positive AMA.

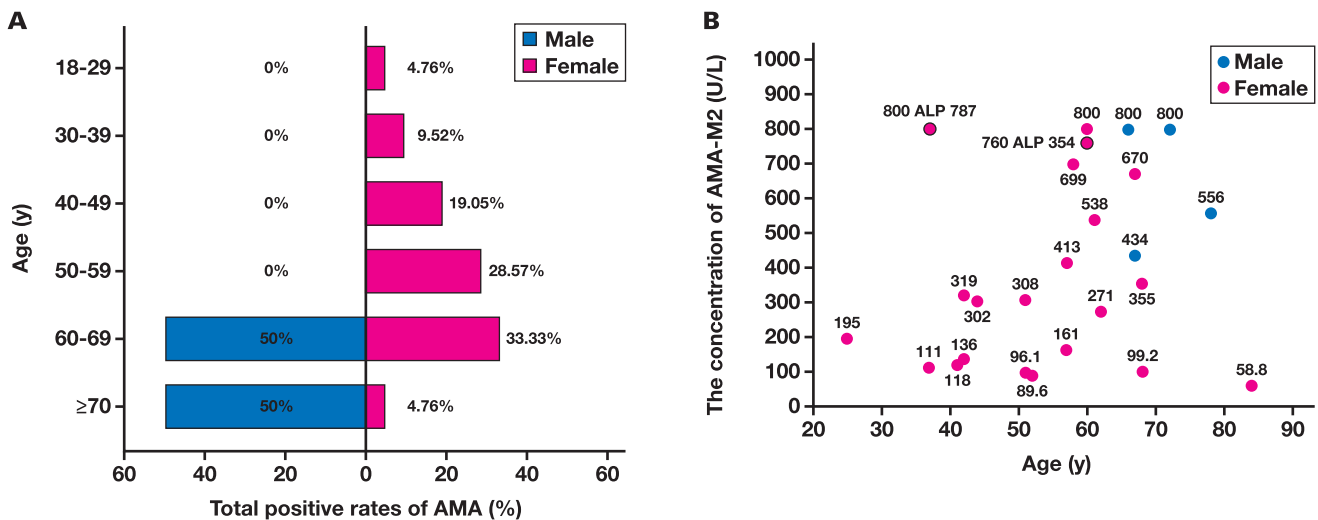


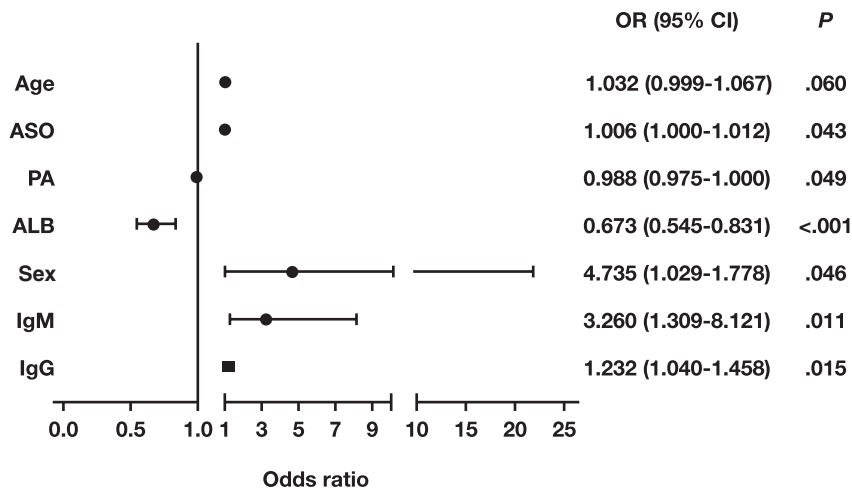
TABLE 3. Physical and Laboratory Characteristics of 155 Participants Categorized by AMA^a

Measurement parameters	AMA- (n = 140)	AMA+ (n = 15)	P
Age (y)	46.78 ± 17.27	55.73 ± 14.24	.041
Height (m)	1.62 ± 0.08	1.57 ± 0.07	.054
Weight (kg)	58.09 ± 10.86	52.18 ± 6.94	.138
BMI (kg/m ²)	22.11 ± 3.09	21.16 ± 2.28	.670
Waistline (cm)	78.86 ± 9.51	76.57 ± 6.85	.600
Hipline (cm)	93.27 ± 7.19	90.21 ± 7.49	.391
ALT (U/L)	19.12 ± 16.16	24.71 ± 24.87	.213
AST (U/L)	22.18 ± 8.73	33.93 ± 34.71	.235
ALP (U/L)	72.50 ± 22.40	135.43 ± 203.51	.259
GGT (U/L)	25.37 ± 22.92	96.86 ± 183.64	.440
CHE (U/L)	8699.78 ± 1583.71	7580.75 ± 782.26	.100
TP (g/L)	76.77 ± 4.45	79.11 ± 8.43	.419
ALB (g/L)	47.72 ± 2.78	44.49 ± 3.75	<.001
TBIL (μmol/L)	10.42 ± 4.90	16.23 ± 19.86	.444
DBIL (μmol/L)	3.38 ± 1.65	9.48 ± 18.99	.560
IgA (g/L)	2.50 ± 0.92	3.35 ± 1.45	.095
IgG (g/L)	13.24 ± 2.67	16.37 ± 6.18	.033
IgM (g/L)	1.37 ± 0.62	3.28 ± 3.58	.001
C3 (g/L)	1.09 ± 0.19	1.17 ± 0.28	.869
C4 (g/L)	0.29 ± 0.13	0.24 ± 0.05	.125
RF (IU/mL)	16.91 ± 57.05	9.75 ± 3.48	.942
ASO (IU/mL)	69.97 ± 77.67	108.78 ± 87.85	.025
Transferrin (mg/L)	2.71 ± 0.39	3.00 ± 0.67	.473
PA (mg/L)	288.35 ± 56.57	253.74 ± 53.18	.044
Questionnaire survey			
Sex			
Male	59 (42.14)	2 (13.33)	.048
Female	81 (57.86)	13 (86.67)	
Habitation			
Urban	100 (71.43)	12 (80.00)	.558
Rural	40 (28.57)	3 (20.00)	
Exercise			
Less	99 (70.71)	7 (46.67)	.078
More	41 (29.29)	8 (53.33)	
Fatigue			
No	104 (74.29)	8 (53.33)	.125
Yes	36 (25.71)	7 (46.67)	
Smoke			
Nonsmoking	112 (80.00)	14 (93.33)	.325
Abstinence	4 (2.86)	0 (0.00)	
Smoker	24 (17.14)	1 (6.67)	
Drink			
Teetotaler	113 (80.71)	14 (93.33)	1.000
Abstinence	16 (11.43)	1 (6.67)	
Alcoholic	11 (7.86)	0 (0.00)	

ALB, albumin; ALT, alanine aminotransferase; ALP, alkaline phosphatase; AMA, antimitochondrial antibody; ASO, antistreptolysin O; AST, aspartate aminotransferase; BMI, body mass index; CHE, cholinesterase; DBIL, direct bilirubin; GGT, gamma-glutamyl transferase; PA, prealbumin; RF, rheumatoid factor; TBIL, total bilirubin; TP, total protein.

^aData are given as mean ± SD or No. (%).

FIGURE 3. Forest plot of risk factors with odds ratio (OR) in the antimitochondrial antibody-positive population. ALB, albumin; ASO, antistreptolysin O; PA, prealbumin.



Statistical Analysis

Descriptive statistics were expressed as mean \pm SD and percentage (%). The continuous variables were compared by 1-way analysis of variance or Mann-Whitney *U* test according to the distributions of the data, whereas the categorical variables were compared using the χ^2 or Fisher exact test. The significant variables were submitted to logistic regression analysis to calculate the odds ratio (OR) and the 95% CI. The forest plots of various risk factors were drawn using GraphPad Prism 8.0. The statistical analysis was performed using SPSS 19.0 with a 2-sided statistically significant *P* value $<$.05.

Results

Demographic Characteristics of AMA-M2 Antibody

To improve representativeness and investigate the prevalence of AMA-M2, 3755 participants recruited by stratified sampling (cohort 1) and 5197 participants enrolled from health checkups (cohort 2) were included in our study. The quantitative distribution of positive results for males and females in each age group is shown in **TABLE 1**. The AMA-M2 positive rate of cohort 1 was a little higher than that of cohort 2 (10.52% vs 9.06%). In cohort 1, only the positive rates of AMA-M2 of males showed a different age distribution with the peak and valley values being 7.81% and 16.88% in those 40 to 49 years old and \geq 70 years old, respectively (**TABLE 1**). There was no other difference between age groups, sex, and cohorts. Overall, the population frequency of AMA-M2 was 9.67% (866/8952), accounting for 9.08% of males and 10.34% of females. The age distribution of abnormal AMA-M2 displayed a parabolic model with the lowest point at 40 to 49 years where the positive rates of AMA-M2 in females (82/858) were 28.03% higher than that in males (52/756) (*P* = .006) (**TABLE 1**).

Risk Factors for Quantitative AMA-M2

Complete laboratory data and lifestyle parameters were available for cohort 1. Thus, a subgroup analysis was performed based on AMA-M2 concentrations to define the risk factors. All variables of the participants did not differ between group 1 ($M_2 \leq 25$ RU/mL) and group 2 (25 RU/mL $<$ $M_2 \leq 50$ RU/mL) but a significant difference was found when

compared with group 3 ($M_2 > 50$ RU/mL). The volunteers in group 3 ($M_2 > 50$ RU/mL) had a significantly lower weight, smaller body mass index (BMI), waistline, hipline, and a lower exercise frequency, whereas cholinesterase (CHE), IgM, and transferrin were markedly increased (**TABLE 2**). Unexpectedly, no sex differences were found among these 3 groups (**TABLE 2**). Finally, the variables with statistical significance were included in the next risk assessments. The results showed that transferrin was the most significant risk factor in group 3, with an OR of 2.325 and 2.628 when compared with group 1 and 2, respectively. Immunoglobulin M was a significant risk factor for group 3, with an OR of 1.458 when compared with group 1, whereas it was unremarkable between group 2 and group 3. The ORs of weight, BMI, waistline, and hipline were too close to 1 to be defined as a protective factor. Exercise was the only protective factor in group 3 (**FIGURE 1**).

Correlation of Quantitative AMA-M2 with AMA

The population characteristics in group 3 were remarkably different from those in group 1 and group 2. Therefore, sera with AMA-M2 > 50 RU/mL (155 cases from cohort 1 and 180 cases from cohort 2) were further tested for AMA using an IIF assay. There were 25 cases (15 cases from cohort 1 and 10 cases from cohort 2) in the AMA-M2-positive population that were concurrently AMA-positive, in which 21 cases were female and 4 cases were male, accounting for the high female-to-male ratio of 5.25:1. The females with positive AMA showed an increasing trend with age and more than 80% of these cases were found at 40 to 69 years old. The males with positive AMA were over 60 years old (**FIGURE 2A**). In these 25 cases, only 2 cases had an elevated ALP up to 2 times upper limit of normal who had a very high AMA-M2, 760 RU/mL and > 800 RU/mL (**FIGURE 2B**). According to EASL¹⁰ and ACG,¹¹ these 2 individuals (2/8936, 0.022%) met the diagnostic criteria of PBC, increasing speculation about the approximate prevalence of PBC, which was 223.81 per million in southern China.

Characteristic and Risk Factor Assessment of Various Parameters Categorized by AMA

We also explored whether population characteristics were more distinctive when categorized by AMA. First, the patients in cohort 1

with AMA-M2 concentrations >50 RU/mL were further categorized into 2 groups: AMA+/M2+ and AMA-/M2+. Unlike the characteristics categorized with AMA-M2 concentrations, the populations differed significantly when classified by AMA. The AMA-positive population tended to have low ALB and PA, increased IgG and IgM, and a sex ratio imbalance. The female-to-male ratio was 6.5:1 with an OR of 4.735 (TABLE 3, FIGURE 3). Also, the increased IgG and IgM were significant high-risk factors, with OR of 1.232 and 3.260, respectively, whereas ALB was a protective factor for the AMA-positive population (FIGURE 3).

Discussion

We conducted a population-based study to screen for PBC with its specific autoantibodies in representative Guangzhou residents. We started from the natural distribution of quantitative AMA-M2 and semi-quantitative AMA to their associated risk factors.

It is reported that PBC displayed substantial geographical disparity. In the Asia-Pacific region, the estimated overall prevalence of PBC was 204.87 per million in China, 221.01 per million in Japan, 99.6 per million in New Zealand, and 39.09 per million in Australia and South Korea.⁵ Even in China, the prevalence of PBC varied greatly, ranging from 56.4 to 492 per million inhabitants.¹⁶⁻¹⁸ The apparent inconsistency between different studies is due not only to geographical variations but to the research methodologies. Some of these studies were based on the case-finding and case ascertainment strategy and included only diagnosed patients, which might have underestimated the prevalence.¹⁹ Some studies were conducted on people who came to a hospital for a health checkup, which might not be the same as the general population and may have overestimated PBC prevalence. In this study, we recruited 2 cohorts of volunteers, a sampled population and those attending health checkups. The recruited individuals were almost equally distributed by age and sex, which represent the local population. Finally, 2 cases were diagnosed as PBC patients, which led to a point prevalence of PBC in southern China as 223.36 per million. These 2 cases were found in the sampled population, not in the health checkup group. However, this point prevalence was much lower than that in another Chinese report conducted only on people who came to a hospital for a health checkup.¹⁷

Although AMA-M2 is one of the serological markers of PBC, it is not disease-specific. The elevation of AMA-M2 had been found in various disorders, such as chronic hepatitis C virus infection,²⁰ autoimmune hepatitis,²¹ Sjögren syndrome,²² and hematological malignancies.²³ Thus, the population frequencies of AMA-M2 remained to be clarified. In this study, both cohorts showed similar distributions of AMA-M2 (10.52% vs 9.06% in cohort 1 vs cohort 2). The total positivity rate was much higher than that reported by a Chinese study as 0.73%.¹⁴ The assay methods and the selected population are the main reasons. It is noteworthy that the AMA-M2 levels of the 2 diagnostic PBC patients were 760 RU/mL and >800 RU/mL. These results are much higher than the cut-off value. Therefore, it seems that the currently used reference interval for AMA-M2 is not proper for the screen of PBC, let alone the diagnosis. As recommended by the American Association for the Study of Liver Diseases, liver biopsies were performed only in the presence of high titers of autoantibodies with signs suggestive of autoimmune liver disease.²⁴ Concerning the low prevalence of PBC, the application of AMA-M2 to the general population would lead to a very low positive predictive value. Thus, our study highlights the necessity to establish a diagnostic level for AMA-M2 for PBC diagnosis.

Primary biliary cholangitis predominantly affects women in their fifties and sixties.^{25,26} Unexpectedly, female predominance was not prominent when categorized with AMA-M2 concentrations. However, a sex ratio imbalance emerged when the AMA-M2-positive population was further categorized with AMA (male-to-female ratio, 1:6.5). Of note, the positive reactivity for AMA in this study was close to another study conducted in Guangzhou.¹⁷ Therefore, these findings imply that AMA-M2 (ELISA) and AMA (IIF) had tremendously different screening performances in different populations. Hu et al²⁷ suggested that although both AMA and AMA-M2 have favorable accuracy for the diagnosis of PBC, AMA would be a better and more comprehensive test than AMA-M2. Nevertheless, Han et al²⁸ suggested the use of IIF with high specificity as a first-line screening test for AMA detection and the use of a sensitive AMA-M2 assay as a confirmatory test. The combination of AMA-M2 and AMA was not only useful for IIF AMA-negative patients but also useful for low-titer AMA-positive patients.

Several prognostic models have been developed and validated for survival in untreated PBC patients, such as the Mayo score. Other than age and sex, several potential and significant risk factors for PBC have been included, such as IgM, ALB, IgG, etc. We tried to explore the risk factors related to elevated AMA-M2. Three subgroups were categorized according to serum AMA-M2 concentrations in cohort 1. Group 3 (AMA-M2 >50 RU/mL) exhibited a different population character, including lower weight, smaller BMI, waistline, hipline, higher transferrin, and IgM. Logistic regression analysis showed that transferrin had the highest OR, which was consistent with the findings of an early study that the serum level of transferrin in PBC was higher than in healthy blood donors, alcoholic cirrhosis, and fatty liver.²⁹ The significant elevation of transferrin in PBC patients might be caused by increased efflux through the disruptive cell membrane.³⁰ In addition, we also confirmed that ALB and exercise were protective factors for the AMA-M2-positive population. The ALB reduction in PBC is a signature of impaired liver synthesis, which usually indicates the development of cirrhosis.¹⁰ In the AMA-positive population, the risk effects of sex and IgM were more prominent than in the AMA-M2-positive population. Despite smoking cessation and limited or no alcohol consumption being recommended in the primary care guidelines for PBC,¹¹ our results indicated that the demographics of smoking and alcohol consumption had little association with AMA-M2 and AMA.

One of the strengths of our study is that the data are based on a population-based cohort of inhabitants that is representative of the southern China population. As one of the main limitations of this study, AMA-2 was not the only disease-specific autoantibody for PBC.³¹ Other autoantibodies, such as antinuclear antibodies to sp-100 or gp-210, are often identified in patients with PBC. Thus, a screening started from AMA-M2 might lead to underestimated prevalence. Second, we could not obtain follow-up data to learn about development or outcome of the participants with different concentrations of AMA-M2. Third, although PBC is reported to be almost exclusively a disease of adults,³² it would be more thorough to study all ages. Thus, further multicenter research to learn disease prevalence, geographic variations, heterogeneity, and differences in the sex ratio of PBC in China is desirable.

This study highlights different characteristics and reports on a risk assessment of the populations defined by AMA-M2 and AMA. These results indicate that more research should focus on the decision-making point for AMA-M2 to improve consistency with AMA and accuracy of diagnosis.

Funding

The study was supported by Science and Technology Projects in Guangzhou [202102021139]; Science and technology research project of traditional Chinese Medicine of Guangdong Provincial Hospital of Chinese Medicine [YN2019QL06]; Guangdong Basic and Applied Basic Research Foundation [2020A1515110329]; State Key Laboratory of Dampness Syndrome of Chinese Medicine [SZ2021ZZ24]; Guangdong Provincial Key Laboratory of Chinese Medicine for Prevention and Treatment of Refractory Chronic Diseases [2018B030322012].

Conflict of Interest Disclosure

The authors have nothing to disclose.

REFERENCES

- Shah RA, Kowdley KV. Current and potential treatments for primary biliary cholangitis. *Lancet Gastroenterol Hepatol*. 2020;5(3):306–315. doi:10.1016/S2468-1253(19)30343-7.
- Lv T, Chen S, Li M, Zhang D, Kong Y, Jia J. Regional variation and temporal trend of primary biliary cholangitis epidemiology: a systematic review and meta-analysis. *J Gastroenterol Hepatol*. 2021;36(6):1423–1434. doi:10.1111/jgh.15329.
- Yoshida EM, Mason A, Peltekian KM, et al. Epidemiology and liver transplantation burden of primary biliary cholangitis: a retrospective cohort study. *CMAJ Open*. 2018;6(4):E664–E670. doi:10.9778/cmajo.20180029.
- Boonstra K, Beuers U, Ponsioen CY. Epidemiology of primary sclerosing cholangitis and primary biliary cirrhosis: a systematic review. *J Hepatol*. 2012;56(5):1181–1188. doi:10.1016/j.jhep.2011.10.025.
- Zeng N, Duan W, Chen S, et al. Epidemiology and clinical course of primary biliary cholangitis in the Asia-Pacific region: a systematic review and meta-analysis. *Hepatol Int*. 2019;13(6):788–799. doi:10.1007/s12072-019-09984-x.
- Wang L, Gershwin ME, Wang FS. Primary biliary cholangitis in China. *Curr Opin Gastroenterol*. 2016;32(3):195–203. doi:10.1097/MOG.0000000000000257.
- Lleo A, Colapietro F. Changes in the epidemiology of primary biliary cholangitis. *Clin Liver Dis*. 2018;22(3):429–441. doi:10.1016/j.cld.2018.03.001.
- Lindor KD, Bowlus CL, Boyer J, Levy C, Mayo M. Primary biliary cholangitis: 2018 practice guidance from the American Association for the Study of Liver Diseases. *Hepatology*. 2019;69(1):394–419. doi:10.1002/hep.30145.
- Dahlqvist G, Gaouar F, Carrat F, et al; French Network of Immunology Laboratories. Large-scale characterization study of patients with antimitochondrial antibodies but nonestablished primary biliary cholangitis. *Hepatology*. 2017;65(1):152–163. doi:10.1002/hep.28859.
- European Association for the Study of the Liver. EASL clinical practice guidelines: the diagnosis and management of patients with primary biliary cholangitis. *J Hepatol*. 2017;67(1):145–172.
- Younossi ZM, Bernstein D, Shiffman ML, et al. Diagnosis and management of primary biliary cholangitis. *Am J Gastroenterol*. 2019;114(1):48–63. doi:10.1038/s41395-018-0390-3.
- Moteki S, Leung PS, Coppel RL, et al. Use of a designer triple expression hybrid clone for three different lipoyl domain for the detection of antimitochondrial autoantibodies. *Hepatology*. 1996;24(1):97–103. doi:10.1002/hep.510240117.
- Patel D, Egner W, Gleeson D, Wild G, Ward A. Detection of serum M2 anti-mitochondrial antibodies by enzyme-linked immunosorbent assay is potentially less specific than by immunofluorescence. *Ann Clin Biochem*. 2002;39(Pt 3):304–307. doi:10.1258/0004563021902008.
- Chen BH, Wang QQ, Zhang W, Zhao LY, Wang GQ. Screening of anti-mitochondrial antibody subtype M2 in residents at least 18 years of age in an urban district of Shanghai, China. *Eur Rev Med Pharmacol Sci*. 2016;20(10):2052–2060.
- Li X, Liu X, Cui J, et al. Epidemiological survey of antinuclear antibodies in healthy population and analysis of clinical characteristics of positive population. *J Clin Lab Anal*. 2019;33(8):e22965. doi:10.1002/jcla.22965.
- Trivedi PJ, Hirschfield GM. Recent advances in clinical practice: epidemiology of autoimmune liver diseases. *Gut*. 2021;70(10):1989–2003. doi:10.1136/gutjnl-2020-322362.
- Liu H, Liu Y, Wang L, et al. Prevalence of primary biliary cirrhosis in adults referring hospital for annual health check-up in Southern China. *BMC Gastroenterol*. 2010;10:100. doi:10.1186/1471-230X-10-100.
- Cheung KS, Seto WK, Fung J, Lai CL, Yuen MF. epidemiology and natural history of primary biliary cholangitis in the Chinese: a territory-based study in Hong Kong between 2000 and 2015. *Clin Transl Gastroenterol*. 2017;8(8):e116. doi:10.1038/ctg.2017.43.
- French J, van der Mei I, Simpson S Jr, et al. Increasing prevalence of primary biliary cholangitis in Victoria, Australia. *J Gastroenterol Hepatol*. 2020;35(4):673–679.
- Ramos-Casals M, Pares A, Jara LJ, et al., HISPAMEC Study Group. Antimitochondrial antibodies in patients with chronic hepatitis C virus infection: description of 18 cases and review of the literature. *J Viral Hepat*. 2005;12(6):648–654. doi:10.1111/j.1365-2893.2005.00642.x.
- Tomizawa M, Shinozaki F, Fugo K, et al. Anti-mitochondrial M2 antibody-positive autoimmune hepatitis. *Exp Ther Med*. 2015;10(4):1419–1422. doi:10.3892/etm.2015.2694.
- Zamfir O, Briaud I, Dubel L, Ballot E, Johanet C. Anti-pyruvate dehydrogenase autoantibodies in extrahepatic disorders. *J Hepatol*. 1999;31(5):964–965. doi:10.1016/s0168-8278(99)80302-x.
- Wakabayashi SI, Kimura T, Tanaka N, et al. Emergence of anti-mitochondrial M2 antibody in patient with angioimmunoblastic T-cell lymphoma. *Clin J Gastroenterol*. 2018;11(4):302–308. doi:10.1007/s12328-018-0831-y.
- Ravi S, Shoreibah M, Raff E, et al. Autoimmune markers do not impact clinical presentation or natural history of steatohepatitis-related liver disease. *Dig Dis Sci*. 2015;60(12):3788–3793. doi:10.1007/s10620-015-3795-5.
- Lleo A, Jepsen P, Morengi E, et al. Evolving trends in female to male incidence and male mortality of primary biliary cholangitis. *Sci Rep*. 2016;6:1–8. doi:10.1038/srep25906.
- Asselta R, Paraboschi EM, Gerussi A, et al; Canadian-US PBC Consortium. X Chromosome contribution to the genetic architecture of primary biliary cholangitis. *Gastroenterology*. 2021;160(7):2483–2495. e26. doi:10.1053/j.gastro.2021.02.061.
- Hu C, Deng C, Song G, et al. Prevalence of autoimmune liver disease related autoantibodies in Chinese patients with primary biliary cirrhosis. *Dig Dis Sci*. 2011;56(11):3357–3363. doi:10.1007/s10620-011-1756-1.
- Han E, Jo SJ, Lee H, et al. Clinical relevance of combined anti-mitochondrial M2 detection assays for primary biliary cirrhosis. *Clin Chim Acta*. 2017;464:113–117. doi:10.1016/j.cca.2016.11.021.
- Teppo AM, Maury CP. Serum prealbumin, transferrin and immunoglobulins in fatty liver, alcoholic cirrhosis and primary biliary cirrhosis. *Clin Chim Acta*. 1983;129(3):279–286. doi:10.1016/0009-8981(83)90030-x.
- Grytczuk A, Bauer A, Gruszewska E, Cylwik B, Chrostek L. Changed profile of serum transferrin isoforms in primary biliary cholangitis. *J Clin Med*. 2020;9(9):2894.
- Hu S, Zhao F, Wang Q, Chen WX. The accuracy of the anti-mitochondrial antibody and the M2 subtype test for diagnosis of primary biliary cirrhosis: a meta-analysis. *Clin Chem Lab Med*. 2014;52(11):1533–1542. doi:10.1515/cclm-2013-0926.
- Kitic I, Boskovic A, Stankovic I, Prokic D. Twelve-year-old girl with primary biliary cirrhosis. *Case Rep Pediatr*. 2012;2012:937150. doi:10.1155/2012/937150.

Serum Ribonucleotide Reductase Subunit M2 in Patients with Chronic Liver Diseases and Hepatocellular Carcinoma

Xuehang Jin, PhD,¹ Wei Yu, MD,¹ Ange Wang, MM,² and Yunqing Qiu, MM^{1,*}

¹State Key Laboratory for Diagnosis and Treatment of Infectious Disease, National Clinical Research Center for Infectious Diseases, Collaborative Innovation Center for Diagnosis and Treatment of Infectious Diseases, Zhejiang Provincial Key Laboratory for Drug Clinical Research and Evaluation, The First Affiliated Hospital, and ²Department of Geriatrics, School of Medicine, The First Affiliated Hospital, Zhejiang University, Hangzhou, China. *To whom correspondence should be addressed: qiyuq@zju.edu.cn.

Keywords: hepatitis B virus, hepatocellular carcinoma, chronic liver disease, ribonucleotide reductase, serum ribonucleotide reductase subunit M2 biomarker

Abbreviations: CHB, chronic hepatitis B; LC, liver cirrhosis; HBC, hepatitis B cirrhosis; RR, ribonucleotide reductase; AASLD, American Association for the Study of Liver Diseases; HBsAg, hepatitis B surface antigen; HBsAb, hepatitis B surface antibody; HbeAg, hepatitis B e antigen; APRI, aspartate aminotransferase-to-platelet ratio index; MELD, Model for End-Stage Liver Disease; TNM, tumor node metastasis classification; TBIL, total bilirubin; HBeAb, hepatitis B e antibody; PEIU, Paul-Ehrlich-Institut units; S/CO, signal to cutoff ratio; HBeAb, hepatitis B c antibody; FIB4, fibrosis-4 score; Lg, Log₁₀

Laboratory Medicine 2023;54:626-632; <https://doi.org/10.1093/labmed/lmad013>

ABSTRACT

Background: Ribonucleotide reductase subunit M2 (RRM2) plays a key role in cell and hepatitis B virus (HBV) replication. Nevertheless, its clinical implications for managing liver diseases have been inadequately studied.

Methods: A total of 412 participants were enrolled, including 60 healthy control individuals, 55 patients with chronic hepatitis B (CHB), 173 patients with cirrhosis, and 124 patients with hepatocellular carcinoma (HCC). Serum RRM2 was measured via ELISA.

Results: The level of serum RRM2 in patients with CHB, cirrhosis, and HCC was higher than that in healthy controls ($P < .05$). A large difference in serum RRM2 was found between HBV-related and non-HBV-related patients in the cirrhosis group ($P < .001$), compared with the difference between HBV-related HCC and non-HBV-related HCC

($P = .86$). In the HBV-related cirrhosis group, the serum RRM2 level showed significant positive correlations with HBV DNA, hepatitis B surface antigen, hepatitis B e antigen, Child-Pugh scores, and MELD scores and played a strong role in diagnosing HBV-related cirrhosis in CHB, compared with fibrosis-4 score and aspartate aminotransferase-to-platelet ratio index.

Conclusions: Serum RRM2 is a reliable biomarker for accurate HBV-related cirrhosis diagnosis and evaluation. Also, serum RRM2 could reflect the expression state of HBV replication in patients with HBV-related cirrhosis.

Hepatitis B virus (HBV) infection is endemic worldwide and is one of the leading causes of viral hepatitis in Southeast Asia. According to the World Health Organization, approximately 2 billion people worldwide have been infected with HBV, and the number of people with chronic HBV infection is approximately 350 million.¹ In China and Southeast Asian countries, most patients become infected with HBV during the perinatal period. Due to the immature immune function of young children, they cannot clear the virus in a timely manner and they become chronically infected with HBV as adults, when the immune system becomes able to effectively fight against the infection. As a result, the viral infection is usually acute and self-limiting. In some patients, the disease progresses to chronic hepatitis B (CHB), liver cirrhosis (LC), and HCC due to long-term inflammation. Approximately 20% of patients with CHB develop hepatitis B cirrhosis (HBC), and approximately 3% develop cirrhosis yearly.^{2,3}

Ribonucleotide reductase (RR) is present in all types of living cells; as the only enzyme catalyzing the reduction of ribonucleotides to the corresponding deoxyribonucleotides, it is involved in metabolizing nucleotides. Human RR consists mainly of large (RRM1) and small subunits (RRM2). These subunits play a key role in cell proliferation by providing not only various precursor deoxyribonucleotides but also regulating the balance of the content of various dNTPs in DNA synthesis and repair.⁴

DNA synthesis and repair heavily depend on the balance of the dNTP pool, and an imbalance in dNTP levels and their relative amounts can lead to cell death or abnormal genetic metabolism. As a DNA polymerase

substrate, dNTP affects all aspects of the replication process, and reduced RR activity decreases intracellular dNTPs levels, thereby inhibiting DNA synthesis and repair, resulting in cell-cycle arrest.⁵ Therefore, RR plays an important role in controlling cell proliferation and maintaining genome stability. Previous study reports, such as Li et al,⁶ have stated that the activity of this enzyme depends on the level of RRM2 protein.

Recent study results, such as those reported by Liu et al,⁷ have shown that RR has a crucial role in HBV replication and proliferation in hepatocytes. Shao et al¹¹ have suggested that RRM2 is a potential target against HBV replication, and its inhibitors are potential novel potential drugs against HBV and HCC. Also, Ricardo-Lax et al⁸ have reported that HBV can activate the production of RRM2 through the DNA damage pathway.

Based on its close relationship with HBV replication and propagation, RR is feasible in the study of chronic liver diseases, especially CHB and HCC. Therefore, we made a relevant analysis of RR in the diagnosis and evaluation of chronic liver diseases and liver cancer, to provide a theoretical basis for its practical application in the clinical setting and future antiviral therapy.

Materials and Methods

Study Population

A total of 412 participants were enrolled in our study. These included 60 healthy control individuals, 55 patients with CHB, 173 patients with cirrhosis (of whom 90 had HBV-related cirrhosis), and 124 patients with liver cancer (of whom 98 had HBV-related cancer). All included subjects were from inpatient and outpatient settings in our hospital, The First Affiliated Hospital, Zhejiang University, Hangzhou, China, from March 2018 through March 2020. Patients with CHB, cirrhosis, or liver cancer were diagnosed according to the recent guidelines of the American Association for the Study of Liver Diseases (AASLD).

We excluded patients infected with viruses other than HBV and other liver diseases; those with lung cancer, pancreatic cancer, and ovarian cancer, and other malignant tumors except liver cancer; those with other comorbidities, including heart diseases, systematic inflammation, chronic kidney disease, etc; and those who had undergone radiofrequency ablation and surgical procedures before blood specimen collection.

The study was performed in accordance with the Code of Ethics of the World Medical Association (Declaration of Helsinki) and was based on the ethical standards of our institution. All study participants provided written informed consent. The study was approved by the Ethics Committee of our hospital.

Data Detection and Collection

Peripheral venous blood was drawn from fasting patients in the early morning, and the blood specimens were numbered based on the order in which patient specimens were collected. The supernatant was removed after centrifugation and stored in a -80°C freezer. Circulating RRM2 levels were detected by Human RRM2 ELISA Kits (Shanghai Run-BioTech). The specimens had 3 biological repetitions, and the kit instructions were strictly followed during all operations.

Other blood tests and imaging examinations were provided by the Laboratory Department and Imaging Department of the First Affiliated Hospital of Zhejiang University, including aspartate aminotransferase

(AST), <40 U/L; alanine aminotransferase (ALT), <40 U/L; alkaline phosphatase (ALP), $40\text{--}150$ U/L; gamma-glutamyl transferase (GGT), $11\text{--}50$ U/L; total bilirubin (TBIL), <21 $\mu\text{mol/L}$; alpha-fetoprotein (AFP), <20 ng/mL; and HBV-related tests (HBV DNA, hepatitis B surface antigen [HBsAg], hepatitis B surface antibody [HBsAb], hepatitis B e antigen [HBeAg], hepatitis B e antibody [HBeAb], and hepatitis B c antibody [HBcAb]). We calculated the relevant index as follows: APRI = $([100 \times \text{AST}] / \text{upper limit of normal AST}) / \text{platelets (PLT)} (\times 10^9 / \text{L})^9$ fibrosis-4 (FIB4) = $(\text{age} \times \text{AST [U/L]}) / (\text{PLT } [10^9 / \text{L}] \times \text{ALT}^{1/2} [\text{U/L}])^{10}$

Statistical Analysis

We processed the data and specimens using SPSS Statistics software, version 25 (IBM) and GraphPad Prism 7 (GraphPad Software). Measurement data were expressed as mean (SD) ($\bar{x} \pm s$). Data between 2 groups were analyzed by independent sample *t* testing, area under the curve (AUC) comparisons between groups were made by *z* testing. Analysis of variance (ANOVA) was used among multiple data groups, with $P < .05$ indicating statistical significance. Independent variables potentially affecting RRM2 were screened by regression analysis; curves were fitted to predict the correlation between RRM2 and other indicators (correlation coefficient *R*).

Results

Clinical Characteristics of Participants

Depending on the type of HBV infection and final diagnosis, we divided the enrolled participants into 6 groups: healthy control, CHB, HBV-related cirrhosis, non-HBV-related cirrhosis, HBV-related HCC, and non-HBV-related HCC. As shown in **TABLE 1**, each group comprised more men than women. The average age of people in the healthy control, CHB, cirrhosis, and HCC groups was 47.3, 46.7, 52.7, and 61.6 years, respectively, which was consistent with the progression of chronic liver disease.

As we expected, healthy controls had good biochemical parameters. In contrast, patients in other groups had higher liver function indicators such as ALT and AST. Patients with CHB had the highest circulating HBV DNA virus, serum HBsAg, and HBeAg levels among patients infected with HBV.

Serum RRM2 Level in All Groups

The serum level of RRM2 in patients with liver disease and healthy controls is shown in **FIGURE 1**. All patients had higher circulating RRM2 levels than healthy controls (mean [SD], $378.5 [79.8]$ U/L). In particular, RRM2 levels in patients with HBV-related cirrhosis and HCC were higher than that in patients with CHB. We further divided the cirrhosis and liver cancer groups into hepatitis B-related and non-hepatitis-B-related groups and observed that the HBV-related cirrhosis group had higher serum RRM2 levels than the non-HBV-related groups ($3827.3 [3158.3]$ U/L vs $761.5 [898.9]$ U/L; $P < .001$); there was no significant difference in serum RRM2 levels between HBV-related HCC and non-HBV-related HCC groups ($3326.6 [2885.1]$ U/L vs $3173.5 [4737.8]$ U/L; $P = .86$).

Serum RRM2 Values in Cirrhosis

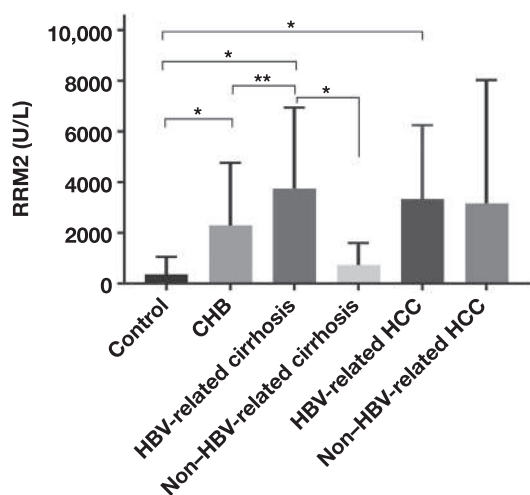
Because we found significantly higher serum RRM2 in the HBV-related cirrhosis group than that in the CHB group, we further analyzed the

TABLE 1. Characteristics of the Patients Enrolled in the Study

Variable	Control	CHB	HBV-related cirrhosis	Non-HBV-related cirrhosis	HBV-related HCC	Non-HBV-related HCC
Male/Female	32/28	37/18	68/22	50/33	84/14	18/8
Age (y), mean (SD)	47.3 (10.4)	46.7 (13.4)	50.0 (9.8)	55.6 (11.8)	60.9 (10.0)	61.6 (10.5)
ALT (IU/L), mean (SD)	23.9 (13.7)	278.3 (365.8)	75.0 (134.7)	72.1 (190.7)	82.5 (100.4)	72.7 (100.2)
AST (IU/L), mean (SD)	20.9 (7.2)	148.1 (168.2)	70.2 (107.8)	76.4 (124.0)	117.0 (216.3)	125.9 (241.3)
ALP (IU/L), mean (SD)	66.6 (22.0)	116.8 (101.1)	109.3 (91.4)	135.8 (113.7)	104.4 (77.5)	137.8 (107.6)
GGT (IU/L), mean (SD)	39.3 (25.5)	126.1 (125.7)	64.2 (81.1)	125.8 (137.4)	107.9 (138.4)	137.0 (176.5)
TBIL ($\mu\text{mol/L}$), mean (SD)	11.9 (7.9)	68.1 (104.4)	69.9 (104.3)	85.3 (127.2)	34.8 (62.0)	42.3 (72.2)
AFP, mean (SD)	4.0 (1.9)	17.2 (24.6)	67.7 (306.0)	5.0 (8.0)	4768.1 (5008.1)	5426.0 (18331.5)
HBV DNA (Log_{10} IU/mL), mean (SD)	—	4.0 (2.3)	2.6 (2.8)	—	1.6 (2.1)	—
HBsAg (IU/mL) $\times 10^5$, mean (SD)	—	121.2 (169.7)	10.1 (16.5)	—	2.5 (5.0)	—
HBsAb (mIU/mL), mean (SD)	—	7.1 (32.3)	35.7 (108.4)	—	0.6 (1.3)	—
HBeAg (PEIU/mL), mean (SD)	—	100.2 (164.1)	17.8 (67.2)	—	21.0 (8.9)	—
HBeAb (S/CO), mean (SD)	—	12.9 (20.7)	3.4 (10.3)	—	3.3 (2.2)	—
HBcAb (S/CO), mean (SD)	—	8.9 (1.9)	7.9 (3.7)	—	8.4 (1.0)	—

AFP, alpha-fetoprotein; ALP, alkaline phosphatase; ALT, alanine aminotransferase; AST, aspartate aminotransferase; GGT, gamma-glutamyl transferase; HBcAb, hepatitis B c antibody; HBeAb, hepatitis B e antibody; HBeAg, hepatitis B e antigen; HbsAb, hepatitis B surface antibody; HBsAg, hepatitis B surface antigen; HBV, hepatitis B virus; HCC, hepatocellular carcinoma; PEIU, Paul-Ehrlich-Institut units; S/CO, signal-to-cutoff ratio; TBIL, total bilirubin.

FIGURE 1. Serum ribonucleotide reductase subunit M2 (RRM2) in chronic liver disease and liver cancer. Comparison of serum RRM2 in healthy control individuals, as well as patients with chronic hepatitis B (CHB), hepatitis B virus (HBV)-related cirrhosis, non-HBV-related cirrhosis, HBV-related hepatocellular carcinoma (HCC), and non-HBV-related HCC. * $P < .001$; ** $P < .01$.



value of RRM2 in the diagnosis and clinical staging of patients with liver cirrhosis. We compared the diagnostic performance of serum RRM2 with widely used serum markers of fibrosis, namely, FIB4 and aspartate aminotransferase-to-platelet ratio index (APRI). We found that at the cutoff value of 1715.6 U/L, serum RRM2 provided a sensitivity and specificity of 87.5% and 66.6%, respectively, for diagnosing HBV-related cirrhosis from CHB. FIB4 demonstrated sensitivity and specificity of 95.4% and 59.4%, respectively, at the cutoff value of 1.04. In contrast, APRI showed sensitivity and specificity of 87.4% and 21.9%, respectively, at the cutoff value of 0.52.

ROC analysis showed that serum RRM2 had a similar diagnostic value as FIB4 (AUC, 0.684 vs 0.737; $P = .45$) and had better AUC scores than APRI (AUC, 0.684 vs 0.462; $P < .01$). The detailed data are shown in **TABLE 2**. Also, when we used combined measurements of serum RRM2, APRI, and FIB4, we detected a higher AUC value (AUC = 0.791).

Serum RRM2 was also shown to be a potential indicator to assess the severity of HBV-related cirrhosis. Decompensated cirrhosis in patients in the HBV group had higher serum RRM2 levels than compensated cirrhosis in patients with HBV (4525.4 [3555.1] vs 2908.9 [2232.9] U/L; $P = .009$). In contrast, there was no significant difference between the compensated and decompensated groups of patients with non-HBV-related cirrhosis (818.9 [1038.8] vs 729.0 [807.5] U/L; $P = .93$) (**FIGURE 2A**). Using the Child-Pugh classification to verify the severity of cirrhosis in patients with that disease, we also acquired significant results, given that patients with Child-Pugh C who had HBV-related cirrhosis had a higher serum RRM2 level than that in patients with Child-Pugh A ($P < .001$) and Child-Pugh B ($P = .01$; **FIGURE 2B**).

A correlation between serum RRM2 and Child-Pugh and Model for End-Stage Liver Disease (MELD) scores was further examined. A significant positive correlation was found between RRM2 and Child-Pugh scores ($R = 0.37$; $P < .001$). MELD scores also showed a positive and significant correlation with RRM2 ($R = 0.40$; $P < .001$) (**FIGURE 2C**, **FIGURE 2D**).

Correlation between Serum RRM2 and HCC Stage and Biomarkers

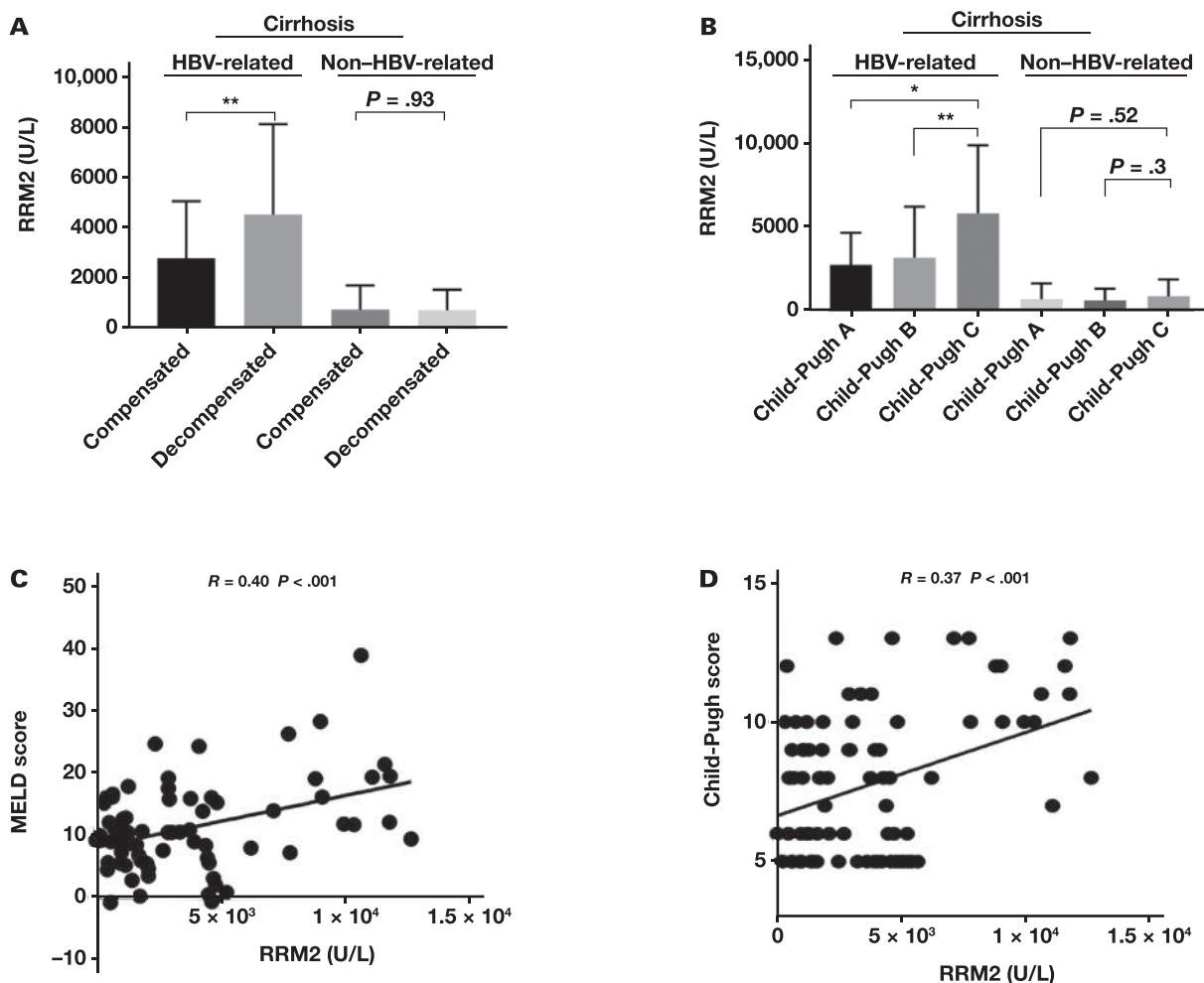
Participants in this study included 98 patients with HBV-associated HCC and 26 patients with non-HBV-associated HCC. Based on tumor node metastasis classification (TNM), among patients with HBV-related HCC, 44 patients had stage I disease, 33 patients had stage II/III, and 21 patients had stage IV. There was no significant difference in serum RRM2 among the aforementioned groups; the numbers of patients with

TABLE 2. Diagnostic Performance of RRM2, FIB4, and APRI, Separately and in Combination, in the Prediction of HBV-Related Cirrhosis

Analyte	AUC (%)	Sensitivity (%)	Specificity (%)	Cutoff	Youden index (%)	P value
RRM2	68.4	87.5	66.6	1715.6	54.2	.002
FIB4	73.7	95.4	59.4	1.0	36.0	<.001
APRI	46.2	87.4	21.9	0.5	21.4	.52
RRM2 + FIB4 + APRI	79.1	74.7	84.4	—	59.1	<.001

APRI, aspartate aminotransferase-to-platelet ratio index; FIB4, fibrosis-4 score; HBV, hepatitis B virus; RRM2, ribonucleotide reductase subunit M2.

FIGURE 2. Serum ribonucleotide reductase subunit M2 (RRM2) in cirrhosis. A, Serum RRM2 level in compensated and decompensated cirrhosis. B, Serum ribonucleotide reductase subunit M2 (RRM2) in cirrhosis. * $P < .001$; ** $P < .01$. Correlation analysis between RRM2 and MELD score (C) or Child-Pugh score (D).



stage I, II/III, and IV disease in the non-HBV-related group were 11, 9, and 6, respectively. The 1-way ANOVA results did not indicate a significant difference between the groups in patients in the HBV-related disease ($P = .42$) or non-HBV-related disease ($P = .72$) groups (Supplementary Figure 1).

A total of 57 patients with HCC underwent surgical resection or liver biopsy (9 in the non-HBV-related and 48 in the HBV-related groups). We obtained the immunohistochemical data of the tumors of these patients and made the correlation between these biomarkers with serum RRM2 levels. However, no obvious correlation was shown between serum RRM2 and immunohistochemical results (AFP and glypican-3). More details are shown in TABLE 3.

Linear Correlation between Serum RRM2 and HBV Markers

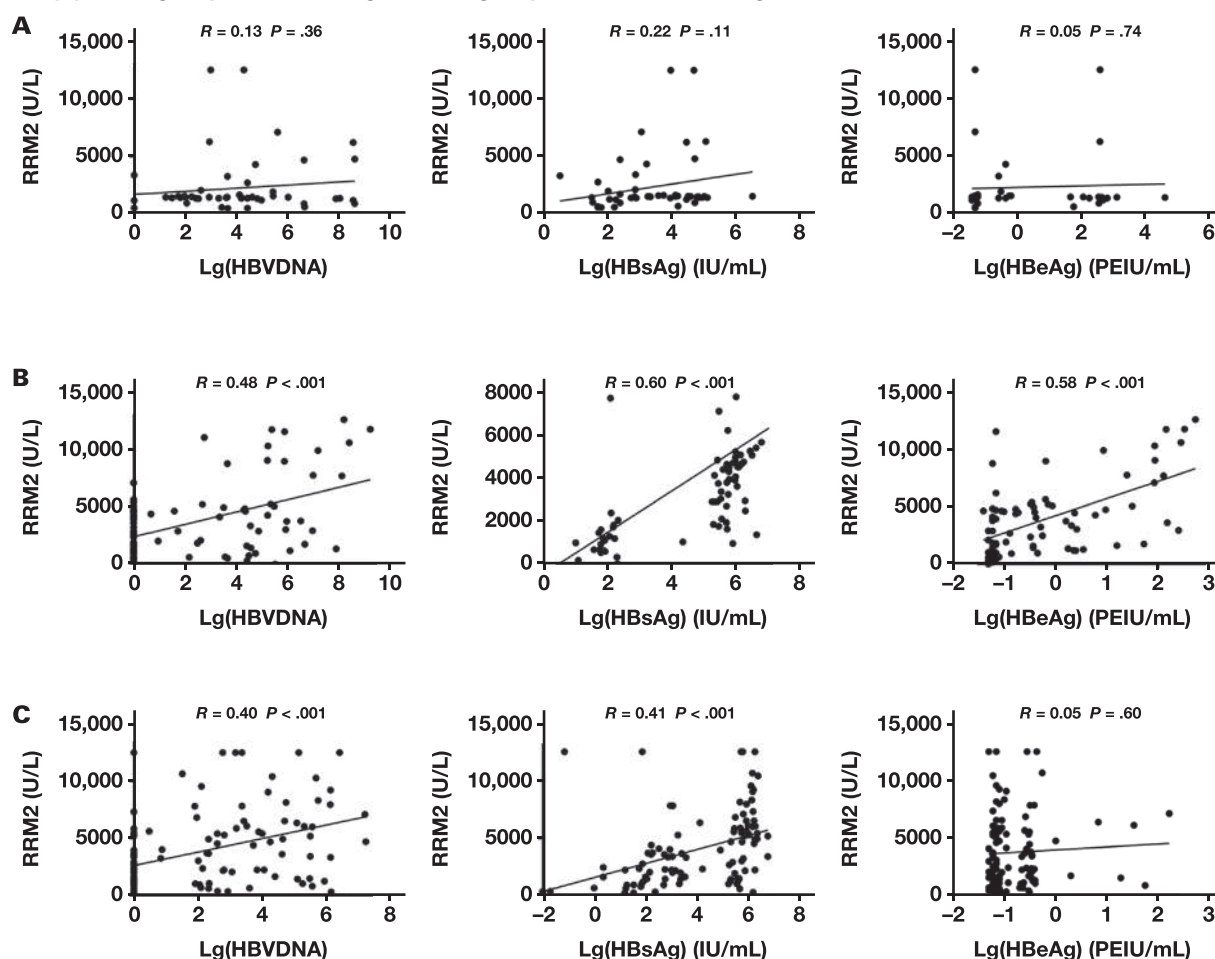
The results mentioned earlier herein demonstrated a strong association between serum RRM2 levels and HBV infection, especially in HBV-related cirrhosis. We used the Pearson correlation coefficient to analyze the linear correlation between RRM2 and HBV DNA, HBsAg, and HBeAg. There was no significant difference between serum RRM2 levels and HBV DNA, HBsAg, and HBeAg in the CHB group ($P > .05$; FIGURE 3A). The correlation coefficients between serum RRM2 level and HBV DNA, HBsAg, and HBeAg in patients with HBV-related cirrhosis were $R = 0.48$ ($P < .001$), $R = 0.60$ ($P < .001$), and $R = 0.58$ ($P < .001$), respectively (FIGURE 3B). In patients with HBV-related HCC,

TABLE 3. Correlation between RRM2 and Immunohistochemical Biomarkers in HCC

Variable	Result	HBV-related HCC			Non-HBV-related HCC		
		No.	RRM2	P value	No.	RRM2	P value
AFP	Negative	10	3104 (1797)	.88	5	3019 (4764)	—
	Positive	5	3368 (4568)		—	—	
GPC-3	Negative	4	2819 (3061)	.59	2	6350 (6150)	.35
	Positive	32	3821 (5079)		8	2394 (3999)	

AFP, alpha-fetoprotein; GPC-3, glypican-3; HBV, hepatitis B virus; HCC, hepatocellular carcinoma; RRM2, ribonucleotide reductase subunit M2.

FIGURE 3. Serum ribonucleotide reductase subunit M2 (RRM2) with hepatitis B virus (HBV). Linear relevance analysis between serum RRM2 and HBV-related indicators in chronic hepatitis B (A), HBV-related cirrhosis (B), and HBV-related hepatocellular carcinoma (C). HBeAg, hepatitis B e antigen; HBsAg, hepatitis B surface antigen; PEIU, Paul-Ehrlich-Institut units.



significant differences were found between circulating RRM2 and HBV DNA ($R = 0.40$; $P < .001$) and HBsAg ($R = 0.41$; $P < .001$) but not between RRM2 and HBeAg ($R = 0.05$; $P = .60$; **FIGURE 3C**).

We further performed a subgroup analysis in patients with HBV-related cirrhosis based on the level of ALT, AST, ALP, GGT, TBIL, and AFP. Patients with HBV-related cirrhosis with ALT, AST, TBIL, or AFP of twice the normal upper limit had higher RRM2 levels, compared with patients with those values in the normal ranges (**TABLE 4**). Also, better correlation performance was shown between RRM2 and HBV DNA, HBsAg, and HBeAg in patients with HBV-related cirrhosis whose ALT or ALP values were twice the normal upper limit (ALT-R value, HBV DNA:

0.58 vs 0.36; HBsAg: 0.71 vs 0.57; HBeAg: 0.59 vs 0.43; ALP-R value, HBV DNA: 0.82 vs 0.42; HBsAg: 0.72 vs 0.59; HBeAg: 0.76 vs 0.52).

Discussion

RR is an enzyme necessary for biological DNA synthesis and is one of the most highly conserved enzymes. It consists of a large subunit (RRM1) and a small subunit (RRM2), which are present at the site of substrate binding and metastable effectors and which control substrate specificity and enzyme activity. The contact inhibition region carried by RRM2 can control the substrate conversion function; hence, RRM2 has both

TABLE 4. Correlation between RRM2 and Biochemical Indicators in HBV-Related Cirrhosis

Analyte	Range	No.	RRM2	P value	R-Lg(HBV DNA)	R-Lg(HBsAg)	R-Lg(HBeAg)
ALT	NR	58	2980 (2208)	.008	0.36	0.57	0.43
	>2 ULN	17	5141 (4595)		0.58	0.71	0.59
AST	NR	51	2870 (272)	.001	0.33	0.72	0.34
	>2 ULN	24	5580 (933)		0.36	0.70	0.57
ALP	NR	67	3665 (349)	.52	0.42	0.59	0.52
	>2 ULN	13	4286 (1080)		0.82	0.72	0.76
GGT	NR	60	3366 (300)	.09	0.46	0.67	0.56
	>2 ULN	19	4705 (1041)		0.54	0.62	0.50
TBIL	NR	56	3088 (405)	.04	0.36	0.46	0.58
	>2 ULN	22	4644 (581)		0.51	0.60	0.54
AFP	NR	67	3305 (307)	.004	0.60	0.60	0.53
	>2 ULN	14	5981 (1304)		0.49	0.70	0.77

AFP, alpha-fetoprotein; ALP, alkaline phosphatase; ALT, alanine aminotransferase; AST, aspartate aminotransferase; GGT, gamma-glutamyl transferase; HBV, hepatitis B virus; NR, normal range; R-Lg(HBeAg), correlation between RRM2 level and the Log₁₀ of hepatitis B e antigen; R-Lg(HBsAg), correlation between RRM2 level and the Log₁₀ of hepatitis B surface antigen; R-Lg(HBV DNA), correlation between RRM2 level and the Log₁₀ of HBV DNA; RRM2, ribonucleotide reductase subunit M2; TBIL, total bilirubin; ULN, upper limit of normal.

catalytic and regulatory roles. The transcription of *RRM1* and *RRM2* is regulated by the cell cycle, and mRNA of *RRM1* and *RRM2* is not detected in G0/G1 phase cells; the mRNA expression of *RRM1* and *RRM2* reaches the maximum level in the S phase. *RRM1* has a half-life of 18–24 hours, and its level is almost constant in proliferating cells and relatively excessive throughout the cell cycle. In contrast, *RRM2* protein is specifically expressed in the S phase and synthesized in the late G1 or early S phase, with a shorter half-life of about 3–4 hours. It is rapidly degraded and then slowly accumulates in cells until late mitosis.¹¹ Therefore, the enzyme activity depends on the level of *RRM2* protein. Thus, in this study, the level of *RRM2* in the peripheral blood of patients was measured, to reflect the RR enzyme activity.

In our study, patients with CHB had significantly higher serum *RRM2* levels than healthy controls ($P < .001$). The same trend was observed in patients with cirrhosis, indicating that HBV can increase *RRM2* levels in hepatocytes, which is consistent with the findings of a previous study.⁸ In patients with cirrhosis, *RRM2* levels in the HBV-related group were obviously higher than those in healthy controls ($P < .001$) and CHB ($P < .01$); those levels in the non-HBV-related group were slightly higher than the levels in healthy controls ($P = .01$) but significantly lower compared with the levels in the CHB group ($P < .001$). The results of further correlation analysis showed the strong relevance between *RRM2* and HBV-related indicators (HBV DNA, HBsAg, and HBeAg) in the cirrhosis group. Our conclusion based on the aforementioned results is that cirrhosis and HBV infection could facilitate the serum *RRM2* level and had a synergistic effect on the rise of serum *RRM2*.

Because HBV does not carry RR genes, it cannot express RR enzyme and needs to rely on dNTPs in hepatocytes to complete the replication of its virions. HBV replication in primary rat hepatocytes has been reported to require HBV protein HBx to induce quiescent hepatocytes to exit the G0 phase and enter and arrest the G1 phase. Also, exiting the G0 and entering the G1 phase activates HBV polymerase and increases *RRM2* levels, enhancing HBV replication and providing a favorable cellular environment for HBV replication.¹²

These findings suggest that activation of *RRM2* production in hepatocytes by HBV was a potential cause of high serum *RRM2* levels in

patients with HBV. Results of the subgroup analysis revealed that patients with HBV-related cirrhosis with high ALT levels had higher *RRM2* levels and better correlations between *RRM2* and HBV-related indexes. These findings might partially be explained by the fact that in hepatocyte injury *RRM2* detected in the blood is more accurate and closer to the actual level of *RRM2* in hepatocytes and, as a result, more related to the secreted substances, such as HBV DNA, HBsAg, and HBeAg.

Previous study reports^{13–15} have stated that FIB4 may be more reliable than APRI for staging fibrosis in CHB and only moderately accurately and sensitively with both scoring systems, which is consistent with the findings from our study. We expand the literature by providing information regarding the accuracy of serum *RRM2* in diagnosing HBV-related cirrhosis and comparing it with currently widely used indicators. The ROC analysis revealed that serum *RRM2* achieved a similar diagnostic value to FIB4 and was better than APRI. Moreover, *RRM2* achieved the highest Youden index, which represented the best screening program. Circulating *RRM2* also acted as a good biomarker to assess the severity of liver cirrhosis. Compared with FIB4 and APRI, which comprise multiple indicators and require complex calculation formulas, *RRM2* is easy to apply and achieves similar clinical applications without a cumbersome calculation process.

Serum *RRM2* level was also high in patients with HBV-related HCC. Cancer cells rely on RR for dNTP biosynthesis; therefore, elevated RR expression is a feature of many types of cancer. The results of previous study^{16–18} have revealed *RRM2* overexpression in various malignancies, including oral, colorectal, and bladder cancers. Elford et al¹⁹ found a significant correlation between RR activity and tumor growth rate in a rat liver cancer model, with differences in RR enzyme activity of as high as 200-fold between fast-growing and slow-growing tumor cells. In our study findings, there was no significant trend in serum *RRM2* between HBV-associated cirrhosis and HBV-associated HCC or HBV-associated and non-HBV-associated HCC. These findings suggest that *RRM2* is not a biomarker of neoplastic transformation in chronic liver diseases.

There were some limitations to this experiment. First, the number of patients with various types of chronic liver diseases and liver cancers was quite small, and the study was somewhat biased; the results need to be further confirmed by larger samples and multicenter studies.

Second, there was a lack of pathological results; serum RRM2 may be unstable due to the influence of some unknown factors. Further testing of the pathological findings of the extent of liver fibrosis and intrahepatocellular RRM2 levels is needed to refine the conclusions.

Conclusions

RRM2 is a reliable biomarker for accurate diagnosis and evaluation of HBV-related cirrhosis. Moreover, the expression state of HBV replication in patients with cirrhosis and HBV can be indicated by serum RRM2.

Supplementary Data

Supplemental figures and tables can be found in the online version of this article at www.labmedicine.com.

Acknowledgments

The work was supported by the The First Affiliated Hospital of Zhejiang University, Hangzhou, China.

Conflict of Interest Disclosure

The authors have nothing to disclose.

REFERENCES

1. The Polaris Observatory Collaborators. Global prevalence, treatment, and prevention of hepatitis B virus infection in 2016: a modelling study. *Lancet Gastroenterol Hepatol*. 2018;3(6):383–403. doi: [10.1016/S2468-1253\(18\)30056-6](https://doi.org/10.1016/S2468-1253(18)30056-6)
2. Guan R, Lui HF. Treatment of hepatitis B in decompensated liver cirrhosis. *Int J Hepatol*. 2011;2011:918017. doi: [10.4061/2011/918017](https://doi.org/10.4061/2011/918017)
3. Hu KQ. A practical approach to management of chronic hepatitis B. *Int J Med Sci*. 2005;2(1):17–23. doi: [10.7150/ijms.2.17](https://doi.org/10.7150/ijms.2.17)
4. Guarino E, Salguero I, Kearsey SE. Cellular regulation of ribonucleotide reductase in eukaryotes. *Semin Cell Dev Biol*. 2014;30:97–103. doi: [10.1016/j.semcdb.2014.03.030](https://doi.org/10.1016/j.semcdb.2014.03.030)
5. Wijerathna SR, Ahmad MF, Xu H, et al. Targeting the large subunit of human ribonucleotide reductase for cancer chemotherapy. *Pharmaceuticals*. 2011;4(10):1328–1354. doi: [10.3390/ph4101328](https://doi.org/10.3390/ph4101328)
6. Li C, Zheng J, Chen S, et al. RRM2 promotes the progression of human glioblastoma. *J Cell Physiol*. 2018;233(10):6759–6767. doi: [10.1002/jcp.26529](https://doi.org/10.1002/jcp.26529)
7. Liu X, Xu Z, Hou C, et al. Inhibition of hepatitis B virus replication by targeting ribonucleotide reductase M2 protein. *Biochem Pharmacol*. 2016;103:118–128. doi: [10.1016/j.bcp.2016.01.003](https://doi.org/10.1016/j.bcp.2016.01.003)
8. Ricardo-Lax I, Ramanan V, Michailidis E, et al. Hepatitis B virus induces RNR-R2 expression via DNA damage response activation. *J Hepatol*. 2015;63(4):789–796. doi: [10.1016/j.jhep.2015.05.017](https://doi.org/10.1016/j.jhep.2015.05.017)
9. Wai C-T, Greenson JK, Fontana RJ, et al. A simple noninvasive index can predict both significant fibrosis and cirrhosis in patients with chronic hepatitis C. *Hepatology*. 2003;38(2):518–526. doi: [10.1053/jhep.2003.50346](https://doi.org/10.1053/jhep.2003.50346)
10. Sterling RK, Lissen E, Clumeck N, et al; APRICOT Clinical Investigators. Development of a simple noninvasive index to predict significant fibrosis in patients with HIV/HCV coinfection. *Hepatology*. 2006;43(6):1317–1325. doi: [10.1002/hep.21178](https://doi.org/10.1002/hep.21178)
11. Shao J, Liu X, Zhu L, Yen Y. Targeting ribonucleotide reductase for cancer therapy. *Expert Opin Ther Targets*. 2013;17(12):1423–1437. doi: [10.1517/14728222.2013.840293](https://doi.org/10.1517/14728222.2013.840293)
12. Cohen D, Adamovich Y, Reuven N, Shaul Y. Hepatitis B virus activates deoxynucleotide synthesis in nondividing hepatocytes by targeting the R2 gene. *Hepatology*. 2010;51(5):1538–1546. doi: [10.1002/hep.23519](https://doi.org/10.1002/hep.23519)
13. Kim BK, Kim DY, Park JY, et al. Validation of FIB-4 and comparison with other simple noninvasive indices for predicting liver fibrosis and cirrhosis in hepatitis B virus-infected patients. *Liver Int*. 2010;30(4):546–553. doi: [10.1111/j.1478-3231.2009.02192.x](https://doi.org/10.1111/j.1478-3231.2009.02192.x)
14. Mallet V, Dhalluin-Venier V, Roussin C, et al. The accuracy of the FIB-4 index for the diagnosis of mild fibrosis in chronic hepatitis B. *Aliment Pharmacol Ther*. 2009;29(4):409–415. doi: [10.1111/j.1365-2036.2008.03895.x](https://doi.org/10.1111/j.1365-2036.2008.03895.x)
15. Xiao G, Yang J, Yan L. Comparison of diagnostic accuracy of aspartate aminotransferase to platelet ratio index and fibrosis-4 index for detecting liver fibrosis in adult patients with chronic hepatitis B virus infection: a systemic review and meta-analysis. *Hepatology*. 2015;61(1):292–302. doi: [10.1002/hep.27382](https://doi.org/10.1002/hep.27382)
16. Morikawa T, Maeda D, Kume H, Homma Y, Fukayama M. Ribonucleotide reductase M2 subunit is a novel diagnostic marker and a potential therapeutic target in bladder cancer. *Histopathology*. 2010;57(6):885–892. doi: [10.1111/j.1365-2559.2010.03725.x](https://doi.org/10.1111/j.1365-2559.2010.03725.x)
17. Liu X, Zhang H, Lai L, et al. Ribonucleotide reductase small subunit M2 serves as a prognostic biomarker and predicts poor survival of colorectal cancers. *Clin Sci (Lond)*. 2013;124(9):567–578. doi: [10.1042/CS20120240](https://doi.org/10.1042/CS20120240)
18. Khor GH, Froemming GRA, Zain RB, Abraham MT, Thong KL. Screening of differential promoter hypermethylated genes in primary oral squamous cell carcinoma. *Asian Pac J Cancer Prev*. 2014;15(20):8957–8961. doi: [10.7314/apjcp.2014.15.20.8957](https://doi.org/10.7314/apjcp.2014.15.20.8957)
19. Elford HL, Freese M, Passamani E, Morris HP. Ribonucleotide reductase and cell proliferation: I. Variations of ribonucleotide reductase activity with tumor growth rate in a series of rat hepatomas. *J Biol Chem*. 1970;245(20):5228–5233.

Associations between apolipoprotein B/A1 ratio, lipoprotein(a), and the risk of metabolic-associated fatty liver diseases in a Korean population

Kyoung-Jin Park, MD, PhD¹ 

¹Department of Laboratory Medicine, Samsung Changwon Hospital, Sungkyunkwan University School of Medicine, Changwon, Republic of Korea. Corresponding author: Kyoung-Jin Park; unmar21@gmail.com.

Key words: metabolic-associated fatty liver disease (MAFLD); apolipoprotein B/A1 ratio; lipoprotein(a); Korean population

Abbreviations: MAFLD, metabolic-associated fatty liver disease; apo B/A1 apolipoprotein B/A1 ratio; NAFLD, nonalcoholic fatty liver disease; CVD, cardiovascular disease; BMI, body mass index; AST, aspartate aminotransferase; ALT, alanine aminotransferase; GGT, gamma-glutamyltransferase; HDL, high-density lipoprotein; LDL, low-density lipoprotein; HbA1c, hemoglobin A1c; hs-CRP, high-sensitivity C-reactive protein; HOMA-IR, homeostasis model assessment of insulin resistance; FIB-4, fibrosis-4; NFS, NAFLD fibrosis score; APRI, AST/platelet ratio index; APASL, Asian Pacific Association for the Study of the Liver

Laboratory Medicine 2023;54:633-637; <https://doi.org/10.1093/labmed/lmad021>

ABSTRACT

Objective: Metabolic-associated fatty liver disease (MAFLD) is new nomenclature for the fatty liver condition associated with metabolic dysfunction. This study aimed to investigate the association between apolipoprotein B/A1 (apo B/A1) ratio, lipoprotein(a), and MAFLD in a Korean population.

Methods: This study consisted of 14,419 subjects in the Korean population. Multivariate logistic regression was conducted to analyze the association between apo B/A1 ratio and MAFLD.

Results: The prevalence of MAFLD in the general Korean population was 34.5%. The apo B/A1 ratio (odds ratio: 3.913, $P = .019$) was independently associated with MAFLD. Lipoprotein(a) was significantly lower in patients with MAFLD with hepatic fibrosis ($P < .0001$).

Conclusion: Apolipoprotein B/A1 ratio and lipoprotein(a) have opposite associations with MAFLD. This study suggests that lipoprotein(a) should be used with caution as a biomarker for MAFLD, especially in patients with hepatic fibrosis.

Introduction

Nonalcoholic fatty liver disease (NAFLD) is one of the most common chronic liver diseases, with a global prevalence of 25%.¹ Metabolic abnormalities, including diabetes and dyslipidemia, are associated with NAFLD. Furthermore, NAFLD is significantly associated with an increased risk of cardiovascular disease (CVD) and CVD-related mortality.¹ Therefore, it is important to clarify the biomarkers for CVD in patients with NAFLD.

High apolipoprotein B/A1 ratio (apo B/A1), high lipoprotein(a), and NAFLD have been suggested as a risk factors for CVD.¹⁻³ The apo B/A1 is also associated with NAFLD, whereas the relationship between lipoprotein(a) and NAFLD remains controversial.⁴⁻⁷ Recent studies have reported that lipoprotein(a) in patients with NAFLD was lower than that in non-NAFLD patients, and the predictive value of lipoprotein(a) for CVD risk is impaired in patients with NAFLD.⁴⁻⁶

Recently, “metabolic-associated fatty liver disease (MAFLD)” has been proposed to replace “nonalcoholic fatty liver disease.”^{8,9} Metabolic-associated fatty liver disease is diagnosed based on hepatic steatosis detected by imaging, blood biomarkers, or histology in addition to the presence of overweight/obesity, type 2 diabetes, or evidence of metabolic dysregulation. It has been reported that the MAFLD criteria can better identify patients with metabolic dysfunction and high risk of disease progression, including CVD, than NAFLD criteria.¹⁰

Currently, few studies regarding the association between apolipoprotein and lipoprotein(a) and MAFLD have been performed. This study aimed to investigate the association between apolipoprotein B/A1 (apo B/A1) ratio, lipoprotein(a), and MAFLD based on new diagnostic criteria in a Korean population.

Materials and Methods

The study subjects were enrolled from the general Korean population that visited the author’s institution for a routine health checkup. This cross-sectional study consisted of 14,419 adults who underwent abdominal ultrasonography among 51,496 subjects in the Korean population visiting a comprehensive health promotion center from January 2021 to December 2021. Clinical and biochemical data include age, gender, medical history, systolic blood pressure, diastolic blood pressure, body mass index (BMI), waist circumference, total protein, albumin, aspartate aminotransferase (AST), alanine aminotransferase (ALT), gamma-glutamyltransferase

TABLE 1. Clinical and laboratory data of Korean population with and without MAFLD^a

	Non-MAFLD			MAFLD			P value
	Male (n = 5447)	Female (n = 3994)	Total (n = 9441)	Male (n = 4216)	Female (n = 762)	Total (n = 4978)	
Age (y)	47 (46–47)	44 (44–44)	45 (45–46)	46 (45–46)	47 (46–48)	46 (46–46)	.0002
Sex (M/F)	5447/3994 (1.36)			4216/762 (5.53)			<.0001
Waist circumference (cm)	84.4 (84.2–84.6)	78.3 (78.1–78.6)	81.9 (81.7–82.1)	92.9 (92.7–93.3)	90.6 (89.6–91.7)	92.7 (92.4–93.0)	<.0001
Body mass index (/kg/m ²)	23.5 (23.4–23.6)	21.5 (21.4–21.6)	22.7 (22.7–22.8)	26.5 (26.3–26.6)	26.6 (26.3–27.0)	26.5 (26.4–26.6)	<.0001
Waist-hip ratio	0.88 (0.88–0.88)	0.87 (0.86–0.87)	0.87 (0.87–0.88)	0.92 (0.92–0.92)	0.92 (0.92–0.93)	0.92 (0.92–0.92)	<.0001
Total protein (g/dL)	7.3 (7.3–7.3)	7.3 (7.3–7.3)	7.3 (7.3–7.3)	7.4 (7.4–7.4)	7.4 (7.3–7.4)	7.4 (7.4–7.4)	<.0001
Albumin (g/dL)	4.9 (4.9–4.9)	4.8 (4.8–4.8)	4.9 (4.9–4.9)	5.0 (4.9–5.0)	4.8 (4.8–4.8)	4.9 (4.9–4.9)	<.0001
AST (IU/L)	21 (21–21)	18 (17–18)	20 (19–20)	15 (24–25)	21 (20–22)	24 (24–24)	<.0001
ALT (IU/L)	21 (21–21)	14 (13–14)	18 (17–18)	32 (32–33)	23 (22–24)	31 (30–31)	<.0001
GGT (IU/L)	26 (25–26)	14 (14–14)	20 (19–20)	41 (40–41)	23 (22–25)	37 (36–38)	<.0001
Total cholesterol (mg/dL)	199 (198–200)	195 (194–197)	197 (196–198)	205 (204–207)	202 (198–205)	205 (203–206)	<.0001
HDL (mg/dL)	57 (56–57)	68 (67–68)	61 (61–61)	49 (48–49)	53 (52–54)	50 (49–50)	<.0001
LDL (mg/dL)	130 (128–131)	120 (119–121)	126 (125–126)	135 (134–136)	130 (128–132)	134 (133–135)	<.0001
Triglyceride (mg/dL)	102 (100–103)	76 (75–77)	90 (89–91)	156 (153–159)	124 (118–130)	151 (148–153)	<.0001
Apolipoprotein B/A1 ratio	0.72 (0.71–0.73)	0.58 (0.58–0.59)	0.66 (0.65–0.66)	0.84 (0.83–0.85)	0.75 (0.74–0.77)	0.83 (0.82–0.83)	<.0001
Apolipoprotein A (mg/dL)	157 (156–157)	170 (170–172)	162 (162–163)	147 (146–148)	155 (152–157)	148 (147–149)	<.0001
Apolipoprotein B (mg/dL)	113 (112–114)	100 (99–101)	107 (107–108)	124 (123–125)	116 (114–118)	123 (122–124)	<.0001
Lipoprotein(a) (mg/dL)	9.72 (9.23–10.21)	10.27 (9.72–10.94)	9.93 (9.62–10.28)	7.32 (6.87–7.65)	10.54 (9.05–11.56)	7.68 (7.39–8.05)	<.0001
Fasting glucose (mg/dL)	95 (95–96)	92 (92–92)	94 (94–94)	100 (100–101)	99 (98–100)	100 (99–100)	<.0001
HbA1C (%)	5.6 (5.6–5.6)	5.5 (5.5–5.5)	5.5 (5.5–5.6)	5.8 (5.8–5.8)	5.8 (5.8–5.9)	5.8 (5.8–5.8)	<.0001
Insulin (mU/L)	5.04 (4.96–5.14)	5.39 (5.28–5.49)	5.19 (5.12–5.26)	8.89 (8.70–9.08)	11.09 (10.56–11.53)	9.18 (9.01–9.34)	<.0001
HOMA-IR	1.198 (1.178–1.222)	1.231 (1.202–1.261)	1.211 (1.194–1.231)	2.261 (2.213–2.303)	2.727 (2.624–2.916)	2.332 (2.277–2.377)	<.0001
hs-CRP (mg/L)	0.47 (0.46–0.48)	0.37 (0.36–0.39)	0.43 (0.42–0.44)	0.82 (0.79–0.84)	1.03 (0.95–1.15)	0.845 (0.82–0.88)	<.0001
FIB-4	0.860 (0.849–0.869)	0.806 (0.794–0.816)	0.834 (0.826–0.844)	0.770 (0.759–0.781)	0.713 (0.692–0.747)	0.763 (0.753–0.772)	<.0001
NFS	-2.826 (-2.866 to -2.792)	-2.925 (-2.979 to -2.884)	-2.87 (-2.898 to -2.84)	-2.600 (-2.640 to -2.560)	-2.585 (-2.693 to -2.446)	-2.599 (-2.637 to -2.564)	<.0001
APRI	0.285 (0.282–0.288)	0.227 (0.224–0.230)	0.261 (0.258–0.263)	0.319 (0.314–0.324)	0.247 (0.241–0.257)	0.309 (0.306–0.313)	<.0001

ALT, alanine aminotransferase; APRI, AST/platelet ratio index; AST, aspartate aminotransferase; FIB-4, fibrosis-4; GGT, gamma-glutamyltransferase; HbA1C, hemoglobin A1c; HDL, high-density lipoprotein; HOMA-IR, homeostasis model assessment-insulin resistance; hs-CRP, high-sensitivity C-reactive protein; LDL, low-density lipoprotein; MAFLD, metabolic-associated fatty liver disease; NFS, NAFLD fibrosis score.

^aContinuous data are expressed as median (95% CI).

(GGT), total cholesterol, high density lipoprotein (HDL)-cholesterol, low density lipoprotein (LDL)-cholesterol, lipoprotein(a), apolipoprotein A1, apolipoprotein B, triglyceride, fasting glucose, insulin, HbA1c, insulin, and high-sensitivity C-reactive protein (hs-CRP).

The BMI was calculated as body weight (kilograms) divided by height in meters squared (m²). Scores were calculated by formulas presented in previous studies as follows^{11–14}: homeostasis model assessment-insulin resistance (HOMA-IR) = (insulin × glucose)/405; fibrosis-4 (FIB-4) = age × AST/platelet × ALT^{1/2}; NAFLD fibrosis score (NFS) = -1.675 + 0.037 × age + 0.094 × BMI + 1.13 × fasting glucose intolerance/diabetes (Yes = 1, No = 0) + 0.99 × AST/ALT ratio - 0.013 × platelet - 0.66 × albumin; AST/platelet ratio index (APRI) = [(AST/upper limit of normal AST) × 100]/platelets.

Hepatic steatosis was assessed using abdominal ultrasonography by experienced physicians and MAFLD was diagnosed according to the Asian Pacific Association for the Study of the Liver (APASL) guidelines.^{8,9} The presence of hepatic fibrosis in patients with MAFLD

was assessed by using serum panels such as NFS >0.676, FIB-4 >2.67, and APRI >0.562.^{12–14} Hepatic fibrosis was defined as a score above the cutoff in more than 2 panels. This study was approved by the Institutional Review Board of Samsung Changwon Hospital.

Clinical data between MAFLD and non-MAFLD were compared using the χ^2 and Mann-Whitney tests, as appropriate. Multivariate logistic regression was conducted to analyze the independent association between apo B/A1 ratio, lipoprotein(a), and MAFLD. All statistical analyses were done by SPSS statistical software (version 18).

Results

The prevalence of MAFLD in the general Korean population was 34.5% (4978/14,419) and was higher in males (43.6%, 4216/9663) than in females (16.0% 762/4,756). There were significant differences in clinical and laboratory findings between MAFLD and non-MAFLD in both males and females (TABLE 1). Patients with MAFLD had higher BMI, waist

circumference, waist-hip ratio, total cholesterol, LDL-cholesterol, triglyceride, apo B, apo B/A1 ratio, fasting glucose, HbA1c, insulin, HOMA-IR, and hs-CRP ($P < .0001$ for all, **TABLE 1**). Compared to MAFLD patients without hepatic fibrosis, lipoprotein(a), apo B, and apo B/A1 ratio were significantly lower in MAFLD patients with hepatic fibrosis ($P < .0001$) (**FIGURE 1**). Lipoprotein(a) levels are inversely associated with the MAFLD ($P < .0001$) (**TABLE 1, FIGURE 1**).

Multivariate logistic regression analysis revealed that apo B/A1 ratio (odds ratio: 3.913, $P = .019$), HOMA-IR (odds ratio: 1.536, $P = .000$), and HbA1c (odds ratio: 1.619, $P = .000$) were independently associated with the MAFLD, whereas total cholesterol ($P = .103$), LDL-cholesterol ($P = .225$), and triglyceride ($P = .104$) were not associated with MAFLD (**TABLE 2**).

Discussion

This study demonstrates that apo B/A1 ratio and lipoprotein(a) levels had opposite associations with MAFLD. The apo B as the carrier of chylomicrons and LDL is a key atherogenic lipoprotein, whereas apo A1 is the major component of HDL particles. The apo B/A1 ratio has

been reported to be directly related to the risk for CVD and can be useful for cardiovascular risk stratification.^{2,3} Also, lipoprotein(a) as an LDL-like particle has been reported to be another independent biomarker for CVD.³ Therefore, high apo B/A1 and high lipoprotein(a) have been considered conventional cardiovascular risk factors. However, this study showed that lipoprotein(a) level was paradoxically reduced in subjects with MAFLD, especially with hepatic fibrosis. Considering that lipoprotein(a) is synthesized in the liver, serum lipoprotein(a) levels might decrease in hepatic fibrosis. Furthermore, the apo B/A1 ratio level in patients with hepatic fibrosis was lower than that in patients without fibrosis. This suggests that hepatic fibrosis might attenuate the clinical utility of apo B/A1 ratio in patients with MAFLD.

There are some studies regarding inverse associations between lipoprotein(a) and diabetes and metabolic syndrome.^{15,16} It could be inferred that lipoprotein(a) level decreases in patients with MAFLD because diabetes and metabolic syndrome are also risk factors for NAFLD and MAFLD. Few studies regarding the association between apolipoprotein and lipoprotein(a) and MAFLD have been performed.¹⁷ To the best of my knowledge, this is the first study regarding the association between apo B/A1 ratio, lipoprotein(a), and MAFLD in a Korean

FIGURE 1. Comparison of lipoprotein(a) (A), apolipoprotein B (B), apolipoprotein B/A1 ratio (C) among subgroups with or without metabolic-associated fatty liver disease (MAFLD) and hepatic fibrosis. * $P < .0001$.

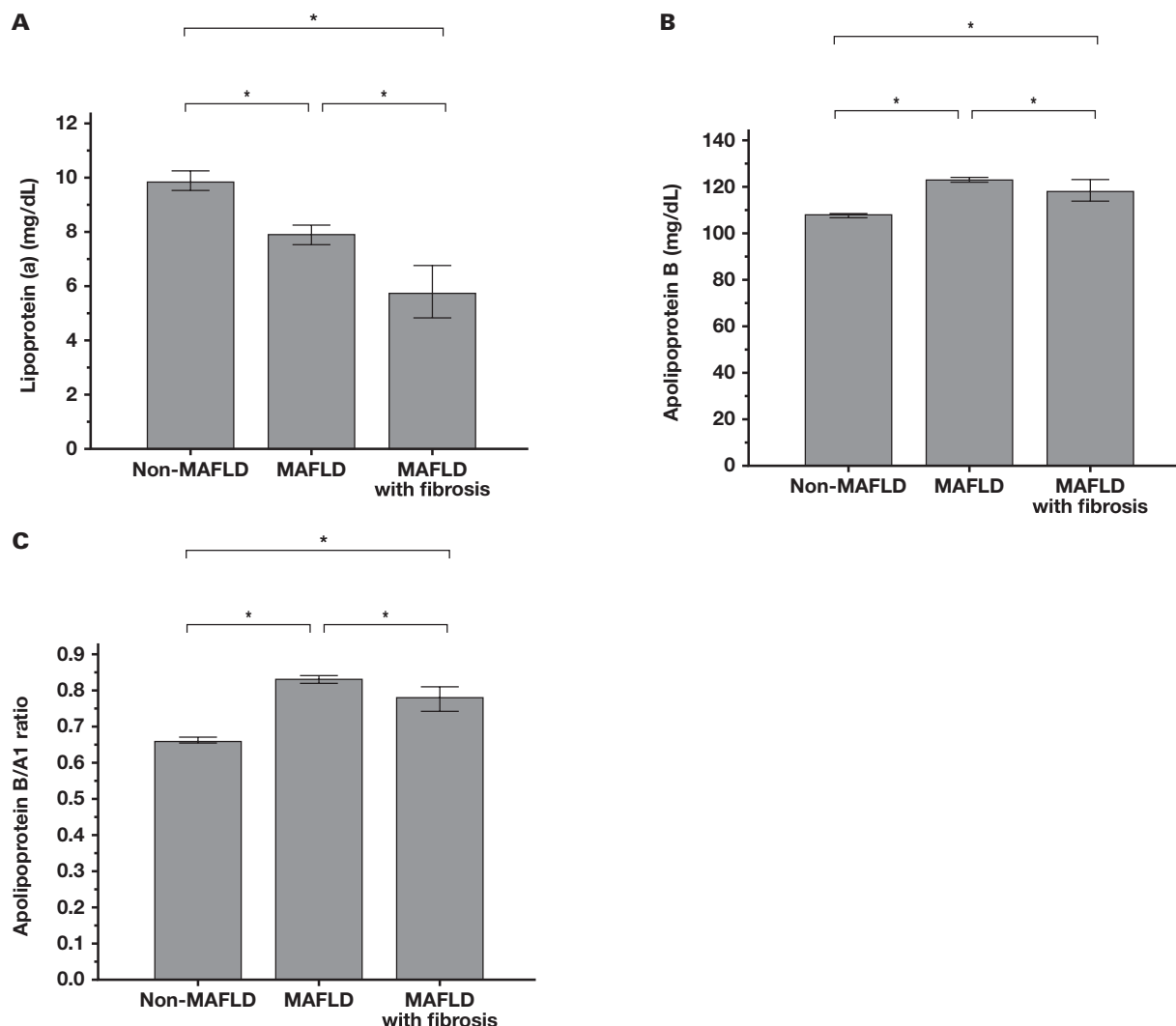


TABLE 2. Association with MAFLD by multiple logistic regression analysis

	Coefficients	Standard error	Walds	P value	Odds ratio	95% CI for odds ratio	
						Lower	Upper
Age	0.023	0.003	54.191	.000	1.023	1.017	1.03
Sex	-0.659	0.065	102.298	.000	0.517	0.455	0.588
Body mass index	0.269	0.018	227.096	.000	1.308	1.263	1.355
Waist circumference	0.047	0.006	54.762	.000	1.048	1.035	1.061
Cholesterol	-0.006	0.004	2.664	.103	0.994	0.987	1.001
LDL-cholesterol	-0.005	0.004	1.471	.225	0.995	0.987	1.003
HDL-cholesterol	-0.042	0.007	35.38	.000	0.959	0.945	0.972
Triglyceride	0.001	0.001	2.647	.104	1.001	1.000	1.002
Apolipoprotein A1	0.021	0.004	25.121	.000	1.021	1.013	1.029
Apolipoprotein B	0.015	0.005	7.271	.007	1.015	1.004	1.026
Apolipoprotein B/A1 ratio	1.364	0.583	5.486	.019	3.913	1.249	12.258
HOMA-IR	0.429	0.026	269.395	.000	1.536	1.459	1.617
HbA1C	0.482	0.043	125.802	.000	1.619	1.488	1.761
HS-CRP	0.027	0.011	6.052	.014	1.027	1.005	1.05

HbA1C, hemoglobin A1c; HDL, high-density lipoprotein; HOMA-IR, homeostasis model assessment-insulin resistance; hs-CRP, high-sensitivity C-reactive protein; LDL, low-density lipoprotein; MAFLD, metabolic-associated fatty liver disease.

population. This study could contribute to a better understanding of biomarker-driven therapeutics and clinical translation of the various therapeutics for fatty liver diseases.^{18,19}

Some limitations should be noted. First, fatty liver in this study was diagnosed by abdominal ultrasonography, which may be insensitive in case of mild steatosis and obesity. However, ultrasonography is the most common approach for fatty liver and the APASL guidelines also recommend use of imaging techniques as well as liver biopsy. Second, hepatic fibrosis was assessed by using noninvasive serum panels. Third, this was a cross-sectional study regarding the association between apo B/A1 ratio, lipoprotein(a), and MAFLD and does not prove the causality of them. Future prospective studies would be recommended to investigate a causal relationship between apo B/A1 ratio, lipoprotein(a), and MAFLD.

In conclusion, apo B/A1 ratio could be a useful biomarker for MAFLD, whereas lipoprotein(a) should be used with caution as a predictive biomarker for MAFLD in a Korean population. The apo B/A1 ratio was also less valuable as a predictive biomarker in MAFLD patients with hepatic fibrosis. Further clinical study would be warranted to investigate the relationship between lipoprotein(a) and CVD risk in MAFLD patients with hepatic fibrosis.

Acknowledgments

This work was supported by the Sungkyunkwan University School of Medicine, Samsung Changwon Hospital.

Conflict of Interest Disclosure

The author has nothing to disclose.

REFERENCES

- Powell EE, Wong VW, Rinella M. Non-alcoholic fatty liver disease. *Lancet*. 2021;397(10290):2212–2224. doi:10.1016/S0140-6736(20)32511-3.

- Andrikoula M, McDowell IF. The contribution of ApoB and ApoA1 measurements to cardiovascular risk assessment. *Diabetes Obes Metab*. 2008;10(4):271–278. doi:10.1111/j.1463-1326.2007.00714.x.
- Dahlen GH. Lp(a) lipoprotein in cardiovascular disease. *Atherosclerosis*. 1994;108(2):111–126. doi:10.1016/0021-9150(94)90106-6.
- Jung I, Kwon H, Park SE, et al. Serum lipoprotein(a) levels and insulin resistance have opposite effects on fatty liver disease. *Atherosclerosis*. 2020;308:1–5. doi:10.1016/j.atherosclerosis.2020.07.020.
- Nam JS, Jo S, Kang S, Ahn CW, Kim KR, Park JS. Association between lipoprotein(a) and nonalcoholic fatty liver disease among Korean adults. *Clin Chim Acta*. 2016;461:14–18. doi:10.1016/j.cca.2016.07.003.
- Wu T, Ye J, Shao C, et al. The ability of lipoprotein (a) level to predict early carotid atherosclerosis is impaired in patients with advanced liver fibrosis related to metabolic-associated fatty liver disease. *Clin Transl Gastroenterol*. 2022;13(7):e00504. doi:10.14309/ctg.000000000000504.
- Brown WV, Moriarty PM, Remaley AT, Tsimikas S. JCL Roundtable: should we treat elevations in Lp(a)? *J Clin Lipidol*. 2016;10(2):215–224. doi:10.1016/j.jacl.2016.02.012.
- Eslam M, Sarin SK, Wong VW, et al. The Asian Pacific Association for the Study of the Liver clinical practice guidelines for the diagnosis and management of metabolic associated fatty liver disease. *Hepatol Int*. 2020;14(6):889–919. doi:10.1007/s12072-020-10094-2.
- Eslam M, Newsome PN, Sarin SK, et al. A new definition for metabolic dysfunction-associated fatty liver disease: an international expert consensus statement. *J Hepatol*. 2020;73(1):202–209. doi:10.1016/j.jhep.2020.03.039.
- Farahat TM, Ungan M, Vilaseca J, et al. The paradigm shift from NAFLD to MAFLD: a global primary care viewpoint. *Liver Int*. 2022;42(6):1259–1267. doi:10.1111/liv.15188.
- Matthews DR, Hosker JP, Rudenski AS, Naylor BA, Treacher DF, Turner RC. Homeostasis model assessment: insulin resistance and beta-cell function from fasting plasma glucose and insulin concentrations in man. *Diabetologia*. 1985;28(7):412–419. doi:10.1007/BF00280883.
- Sterling RK, Lissen E, Clumeck N, et al; APRICOT Clinical Investigators. Development of a simple noninvasive index to predict significant fibrosis in patients with HIV/HCV coinfection. *Hepatology*. 2006;43(6):1317–1325. doi:10.1002/hep.21178.
- Angulo P, Hui JM, Marchesini G, et al. The NAFLD fibrosis score: a noninvasive system that identifies liver fibrosis in patients with NAFLD. *Hepatology*. 2007;45(4):846–854. doi:10.1002/hep.21496.

14. Shaheen AA, Myers RP. Diagnostic accuracy of the aspartate aminotransferase-to-platelet ratio index for the prediction of hepatitis C-related fibrosis: a systematic review. *Hepatology*. 2007;46(3):912–921. doi:10.1002/hep.21835.
15. Sung KC, Wild SH, Byrne CD. Lipoprotein (a), metabolic syndrome and coronary calcium score in a large occupational cohort. *Nutr Metab Cardiovasc Dis*. 2013;23(12):1239–1246. doi:10.1016/j.numecd.2013.02.009.
16. Koschinsky ML, Marcovina SM. The relationship between lipoprotein(a) and the complications of diabetes mellitus. *Acta Diabetol*. 2003;40(2):65–76. doi:10.1007/s005920300007.
17. Zhao Y. Association between apolipoprotein B/A1 and the risk of metabolic dysfunction associated fatty liver disease according to different lipid profiles in a Chinese population: a cross-sectional study. *Clin Chim Acta*. 2022;534:138–145. doi:10.1016/j.cca.2022.07.014.
18. Negi CK, Babica P, Bajard L, Bienertova-Vasku J, Tarantino G. Insights into the molecular targets and emerging pharmacotherapeutic interventions for nonalcoholic fatty liver disease. *Metabolism*. 2022;126:154925. doi:10.1016/j.metabol.2021.154925.
19. Tarantino G, Balsano C, Santini SJ, et al. It is high time physicians thought of natural products for alleviating NAFLD: is there sufficient evidence to use them? *Int J Mol Sci*. 2021;22(24):13424. doi:10.3390/ijms222413424.

Clinical role of serum tumor markers SCC, NSE, CA 125, CA 19-9, and CYFRA 21-1 in patients with lung cancer

Aiwen Sun, BS¹

¹Beijing Chao-Yang Hospital, Capital Medical University, Beijing, China.
Corresponding author: Aiwen Sun; saw7000238704@163.com.

Key words: lung cancer; tumor markers; CYFRA 21-1; diagnosis

Abbreviations: BCDs, benign chest diseases; NSE, neuron-specific enolase; CA 125, cancer antigen 125; SCC, squamous cell carcinoma-related antigen; NSE, neuron-specific enolase; CA 19-9, cancer antigen 19-9; CYFRA 21-1, cytokeratin fragment 19; CT, computed tomography; ORs, odds ratios; ROC, receiver operating characteristic; AUC, area under the curve; SCLC, small cell lung cancer; NSCLC, non-small cell lung carcinoma

Laboratory Medicine 2023;54:638-645; <https://doi.org/10.1093/labmed/lmad020>

ABSTRACT

Objective: The aim of the study was to assess the diagnostic value of tumor markers in discriminating between lung cancer and benign chest diseases (BCDs).

Methods: There were 322 patients enrolled in this investigation including 180 cases of lung cancer and 142 cases of BCD. Serum neuron-specific enolase (NSE), cancer antigen 125, cancer antigen 19-9, squamous cell carcinoma-related antigen, and cytokeratin fragment 19 (CYFRA 21-1) were compared between different populations, cancer stages, and before and after treatment. Logistic regression and receiver operating characteristic curves were used to evaluate the diagnostic markers.

Results: Both NSE and CYFRA 21-1 were significantly associated with lung cancer. The CYFRA 21-1 showed the best performance, as well as its combinations, for lung cancer diagnosis. It also showed significant change 6 months after radical surgery in lung cancer patients.

Conclusion: The marker CYFRA 21-1 could be developed as an adjuvant marker for the early diagnosis of lung cancer and as a prognostic marker for lung cancer treatment.

Introduction

Lung cancer is the most common cancer and the leading cause of cancer death in China,¹ with a mortality of 610.2 per 100,000.² Early diagnosis

is critical for lung cancer patients to receive adequate and appropriate treatments in a timely manner to improve mortality.^{3,4} For lung cancer, the 5-year survival rate can reach 70% to 80% when the patients are diagnosed at early stages, but the rate is less than 15% when they are diagnosed at advanced stages.⁵ Based on the SEER Cancer Statistics Review 2016, with current approaches, only 16% of diagnosed lung cancer patients did not have metastases.⁶ This was partly due to poor detection because of the lack of history or symptoms of lung cancer. The primary screening methods for lung cancer include chest X-ray, computed tomography (CT), magnetic resonance imaging, and positron emission tomography. Although the low-dose CT widely used in lung cancer screening effectively reduces mortality, it has a considerable cost to the health system and the patient's body. Low-dose CT also has the problem of false positives.^{7,8} These issues would make noninvasive, convenient, and low-cost circulating screening markers highly valuable for the diagnosis of lung cancer and its progression assessment.

Currently, tumor markers such as neuron-specific enolase (NSE), cancer antigen 125 (CA 125), cancer antigen 19-9 (CA 19-9), squamous cell carcinoma-related antigen (SCC), and cytokeratin fragment 19 (CYFRA 21-1) are widely used for noninvasive cancer screening and monitoring of its progression.⁹⁻¹⁴ They have become increasingly accessible to patients, but their effectiveness is still unsatisfactory due to the heterogeneity of tumors and individuals. The clinical role of the serum tumor markers NSE, CA 125, CA 19-9, SCC, and CYFRA 21-1 in lung cancer remains unclear. In this study, changes in serum levels of tumor marker NSE, CA 125, CA 19-9, SCC, and CYFRA 21-1 were evaluated in patients with lung cancer to identify the most suitable markers for the diagnosis of lung cancer.

Materials and Methods

Ethical Approval

The study was carried out in accordance with the Declaration of Helsinki (as revised in 2013). This was a retrospective observational study covering a total of 322 patients successively admitted to Beijing Chao-Yang Hospital, and it was approved by the Ethics Committee of Beijing Chao-Yang Hospital.

Patients

The inclusion criteria were as follows: (1) patients diagnosed with lung cancer by pathological examination with a confirmed TNM staging; (2)

patients with complete data regarding serum levels of NSE, CA 125, CA 19-9, SCC, and CYFRA21-1 before treatment; and (3) patients with complete clinical data. Accordingly, 180 patients with lung cancer who met the criteria were enrolled. Also enrolled were 142 patients with benign chest diseases (BCD) as controls, for whom clinical data for tumor markers were available for this study. Data on clinicopathological characteristics, including sex, age, and TNM tumor staging information, were recorded for analysis.

Blood Sample Collection and Tumor Marker Measurement

Blood samples were obtained before patients received any therapy. The samples were centrifuged at 1000g for 15 min, followed by collection of serum. Electrochemiluminescence technology was used for immunoassay analysis per the manufacturer's instruction (Roche cobas e601 module) to measure the concentration of NSE, CA 125, CA 19-9, SCC, and CYFRA 21-1 in each sample. Levels above the following values was considered abnormal: NSE, 16.3 ng/mL; CA 125, 35 U/mL; CA 19-9, 39 U/mL; SCC, 1.5 ng/mL; and CYFRA 21-1, 3.3 ng/mL.

Statistical Analysis

Information is presented here as number (percentage) or median (interquartile range) for categorical characteristics. Univariate and multiple logistic regression models were used to identify correlation, in which odds ratios (ORs) with 95% CIs were calculated using SPSS (version 22.0 IBM). Diagnostic efficacy was evaluated using the receiver operating characteristic (ROC) curve. A two-tailed Wilcoxon paired test was used to compare biomarker levels before and after treatment.

Results

Clinicopathological Characteristics of the Study

Population

The clinicopathological characteristics of all study participants, specifically age, tumor stage, and other chest diseases, are summarized in **TABLE 1**. There was no significant difference in age or sex between the lung cancer group and the benign chest disease (BCD) control group. The lung cancer patients were distributed relatively evenly across tumor stages, with 67 in stage I (37.2%), 53 in stage III (29.4%), 40 in stage IV (22.3%), and 20 in stage II (11.1%). The BCDs of patients in the control group included tuberculosis (2, 1.4%), chronic obstructive pulmonary disease (40, 28.2%), lung infection (22, 15.5%), pulmonary embolism (31, 21.8%), pulmonary fibrosis (13, 9.2%), and asthma (34, 23.9%).

Levels of NSE, CA 125, CA 19-9, SCC, and CYFRA 21-1 in Different Populations

Information on serum levels of NSE, CA 125, CA 19-9, SCC, and CYFRA 21-1 of the two study groups is listed in **TABLE 2**. Median levels of NSE and CYFRA 21-1 in the control group (12.47 ng/mL and 2.44 ng/mL) were significantly lower than those in the lung cancer group (14.94 ng/mL and 3.31 ng/mL) with $P < .001$. The rate of above-normal levels in the lung cancer group was much higher than in the control group for all 5 markers. In the lung cancer group, 51.7% of the participants showed a higher level of CYFRA 21-1, whereas 14.1% of participants with BCDs had a higher level of CYFRA 21-1.

We further evaluated the correlation between each marker and the lung cancer stages. The NSE, CA 125, and CYFRA 21-1 markers showed

TABLE 1. Clinicopathological characteristics

	Lung cancer group (n = 180)	Control group (n = 142)
Age, y		
Mean	61.79	62.66
Range	28–85	32–88
Sex		
Male	114	97
Female	66	45
Tumor stage, n (%)		
I	67 (37.2)	NA
II	20 (11.1)	NA
III	53 (29.4)	NA
IV	40 (22.3)	NA
Benign chest diseases, n (%)		
Tuberculosis	NA	2 (1.4)
Chronic obstructive pulmonary disease	NA	40 (28.2)
Lung infection	NA	22 (15.5)
Pulmonary embolism	NA	31 (21.8)
Pulmonary fibrosis	NA	13 (9.2)
Asthma	NA	34 (23.9)

NA, not applicable.

stepwise increases along with cancer progression (**TABLE 2**, median and range). Their levels during late stages (stages III and IV) were significantly higher than at early stages (stages I and II), as shown in **FIGURE 1**. Particularly for CYFRA 21-1, patients as early as stage II had significantly higher levels than those in the control group, which implies the possibility of an early marker.

These results indicate that NSE level and CYFRA 21-1 level are closely associated with lung cancer, and CYFRA 21-1 showed the divergence well in different stages of lung cancer.

Identification of Diagnostic Markers for Lung Cancer

To assess their value for diagnosis, univariate regression analyses were performed to identify biomarkers associated with the result (lung cancer or not). The markers NSE (OR = 1.119, $P < .001$), CA 19-9 (OR = 1.018, $P = .043$), and CYFRA 21-1 (OR = 2.007, $P < .001$) were found to be positive independent diagnostic risk factors, but SCC (OR = 1.040, $P = .405$) and CA 125 (OR = 1.004, $P = .104$) were not, as shown in **TABLE 3**. Additional multiple logistic regression analyses were performed, and the results showed NSE (OR = 1.070, $P = .022$) and CYFRA 21-1 (OR = 1.914, $P < .001$) to be true independent positive markers that were significantly correlated with lung cancer when the combination of the 3 factors was considered (**TABLE 3**).

Diagnostic Characteristics of Tumor Markers in Lung Cancer

The ROC curve was used for the assessment of the diagnostic performance of NSE, CA 19-9, CYFRA 21-1 and their combinations to discriminate patients with lung cancer patients from CBD patients (**FIGURE 2**). Results showed that the combination of CYFRA 21-1 and NSE had the best performance (area under the curve [AUC] = 0.748), followed by the single markers CYFRA 21-1 (AUC = 0.736), NSE

TABLE 2. Comparison of positive rates of SCC, NSE, CA 125, CA 19-9, and CYFRA 21-1 in the two groups

	Lung cancer group (n = 180)	Control group (n = 142)	P value
SCC (ng/mL) baseline			.345
Median (range)	0.51 (0.2–70)	0.59 (0.2–9.23)	
Normal (<1.5), n (%)	162 (90.0)	123 (86.6)	
Elevated (≥1.5), n (%)	18 (10.0)	19 (13.4)	
NSE (ng/mL) baseline			<.001
Median (range)	14.94 (8.15–311.6)	12.47 (7–35.69)	
Normal (<16.3), n (%)	113 (62.8)	122 (85.9)	
Elevated (≥16.3), n (%)	67 (37.2)	20 (14.1)	
CA 125 (U/mL) baseline			.353
Median (range)	12.49 (3.68–3064)	14.88 (2.84–327.4)	
Normal (<35), n (%)	134 (74.4)	112 (78.9)	
Elevated (≥35), n (%)	46 (25.6)	30 (21.1)	
CA 19-9 (U/mL) baseline			.076
Median (range)	12.29 (0.6–455.3)	9.7(0.6–93.4)	
Normal (<39), n (%)	165 (91.7)	137 (96.5)	
Elevated (≥39), n (%)	15 (8.3)	5 (3.5)	
CYFRA 21-1 (ng/mL) baseline			<.001
Median (range)	3.31 (0.89–55.52)	2.44 (0.54–5.17)	
Normal (<3.3), n (%)	87 (48.3)	122 (85.9)	
Elevated (≥3.3), n (%)	93 (51.7)	20 (14.1)	

CA 19-9, cancer antigen 19-9; CA 125, cancer antigen 125; CYFRA 21-1, cytokeratin fragment 19; NSE, neuron-specific enolase; SCC, squamous cell carcinoma-related antigen.

(AUC = 0.659), and CA 19-9 (AUC = 0.599) (FIGURE 2A–D). The combination of CYFRA 21-1 and NSE has better AUC but has compromised specificity from 0.852 to 0.789 compared to the individual CYFRA 21-1 level. On the other hand, analysis of early diagnosis for lung cancer showed CYFRA 21-1 has the best performance (AUC = 0.612), followed by CA 19-9 (AUC = 0.585) and NSE (AUC = 0.562), as shown in FIGURE 2E–G. Although the performance of CYFRA 21-1 is not good enough to become an ideal early diagnostic marker, the specificity is as high as that of current lung cancer diagnosis, demonstrating that it could be a complement to the existing lung cancer early detection procedures to increase specificity. It is noteworthy that the combination of CYFRA 21-1 with NSE did not improve the performances at all for early diagnosis (AUC = 0.616) (FIGURE 2H).

Potential of CYFRA 21-1 as a Prognostic Marker for Lung Cancer

Because serum levels of some of the markers were significantly different across the tumor stages of lung cancer (FIGURE 1), although not qualified as early markers (FIGURE 2B), the question remained whether they could be prognostic markers for lung cancer. An in-house database of follow-up visits to the hospital was searched and it was found that 37 of the enrolled participants had been retested for the tumor markers in the 6-month follow-up visit after an operation following the first test. Paired comparisons of all 5 marker levels before and after surgery were performed (FIGURE 3). Results indicated that only CYFRA 21-1 had a significant decrease after tumor resection, whereas both CA 125 and CA 19-9 showed even higher levels after resection. This suggests the potential of CYFRA 21-1 as a prognostic marker for lung cancer treatment.

Discussion

The tumor marker CYFRA 21-1, a fragment of the protein cytokeratin 19 implicated in the transformation of epithelial cells to cancer cells, is released into circulation from inside cells when they undergo necrosis. Several studies have attempted to assess CYFRA 21-1 as a diagnostic biomarker of lung cancers.^{15,16} This is consistent with previous reports stating that CYFRA 21-1 is more specific than sensitive for the diagnosis¹⁷; even so, it is more sensitive than some other tumor antigen markers. The marker NSE, also known as enolase-2, is a multifunctional cytoplasmic enzyme, changes in which are related to several diseases, such as inflammation and cancers. Generally, NSE is expressed in some specific tissues but is elevated in serum when malignancy develops, especially lung cancers.¹⁸ Neuron-specific enolase usually works better individually than other tumor antigen markers,¹⁹ but its levels are also significantly higher in patients with benign lung diseases than in healthy controls.^{18,20} Similar to CYFRA 21-1, NSE has shown low sensitivity. However, Chen et al²⁰ reported that NSE is a biomarker with a high positive rate, but CYFRA 21-1 has a better sensitivity for stage I small cell lung cancer (SCLC). In this study, ROC revealed that both CYFRA 21-1 and NSE have relatively high specificity but poor sensitivity. All these could partly explain much, if not all, of why NSE can hardly be complementary to CYFRA 21-1 to improve the performance although both of them are independent factors. This situation is slightly different from some other reports in which NSE, CA 125, CA 19-9, or SCC could help improve the lung cancer diagnostic performance of CYFRA 21-1 when combined with it.^{21–23} Although many previous studies have presented significant correlations between cancers and CA 125, CA 19-9 or SCC levels, their role as diagnostic or prognostic biomarkers is still controversial. In this study, CA 19-9

FIGURE 1. Variations of tumor markers across lung cancer stages and the benign chest disease patients: SCC (A), NSE (B), CA 125 (C), CA 19-9 (D) and CYFRA 21-1 (E). Rank sum (Kruskal-Wallis) test was used for analysis. * $P < .05$, ** $P < .01$, vs control group.

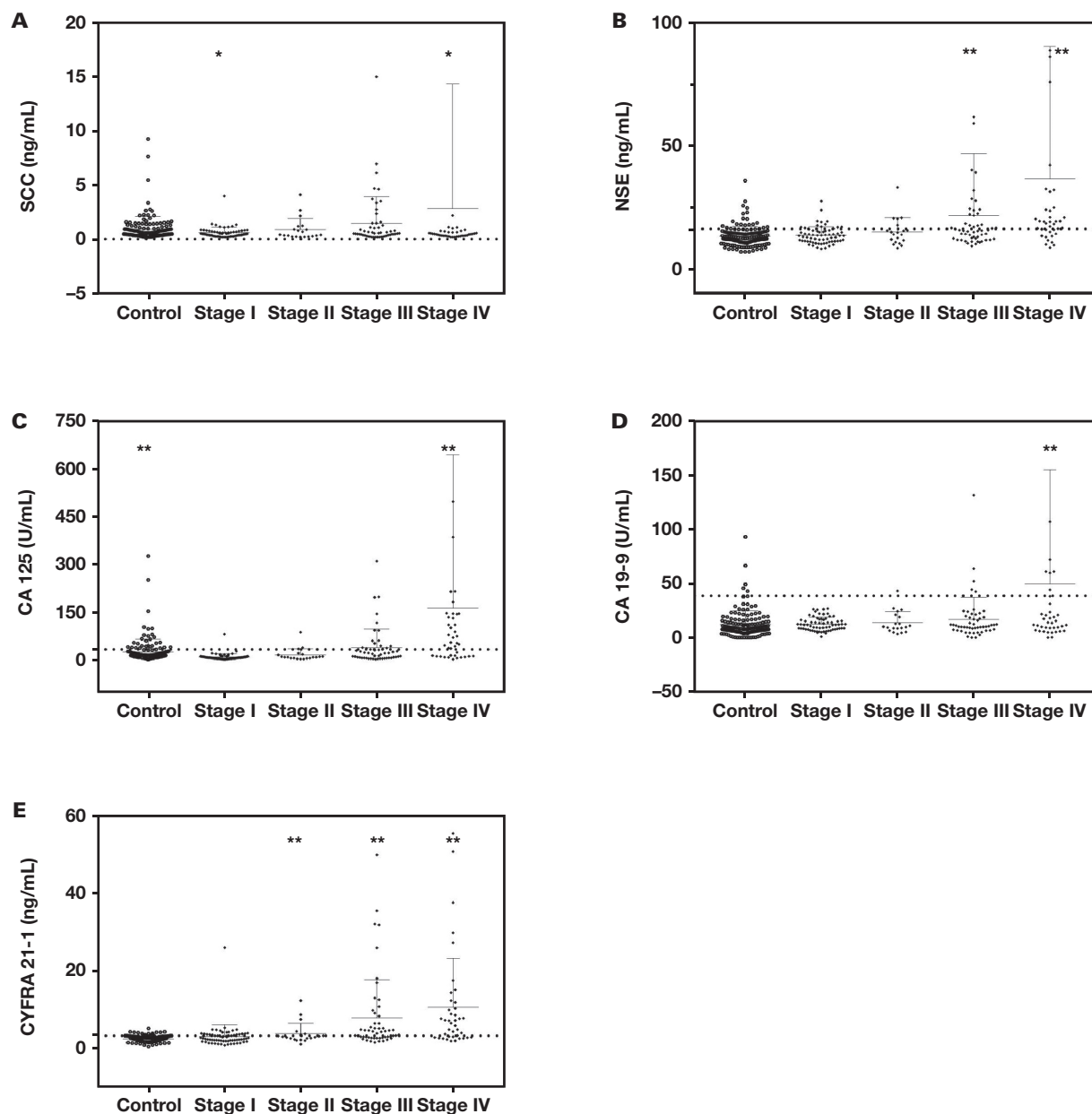


TABLE 3. Univariate and multiple logistic regression analyses to identify the individual risk factors for lung cancer

Various	Univariate logistic regression			Multiple logistic regression		
	OR	95% CI	P value	OR	95% CI	P value
SCC	1.040	0.948–1.141	.405	NA	NA	NA
NSE	1.119	1.060–1.182	<.001	1.070	1.010–1.134	.022
CA 125	1.004	0.999–1.009	.104	NA	NA	NA
CA 19-9	1.018	1.001–1.036	.043	1.004	0.987–1.022	.640
CYFRA 21-1	2.007	1.566–2.571	<.001	1.914	1.479–2.476	<.001

CA 19-9, cancer antigen 19-9; CA 125, cancer antigen 125; CYFRA 21-1, cytokeratin fragment 19; NA, not applicable; NSE, neuron-specific enolase; OR, odds ratio; SCC, squamous cell carcinoma-related antigen.

FIGURE 2. Receiver operating characteristic (ROC) analysis of identified lung cancer risk factors for diagnosis and early diagnosis. ROC of NSE (A, E), CA 19-9 (B, F), CYFRA 21-1 (C, G), and the combination of CA 19-9 and CYFRA 21-1 (D, H) for whole lung cancer patients (A-D) and early-stage lung cancer patients (E-H).

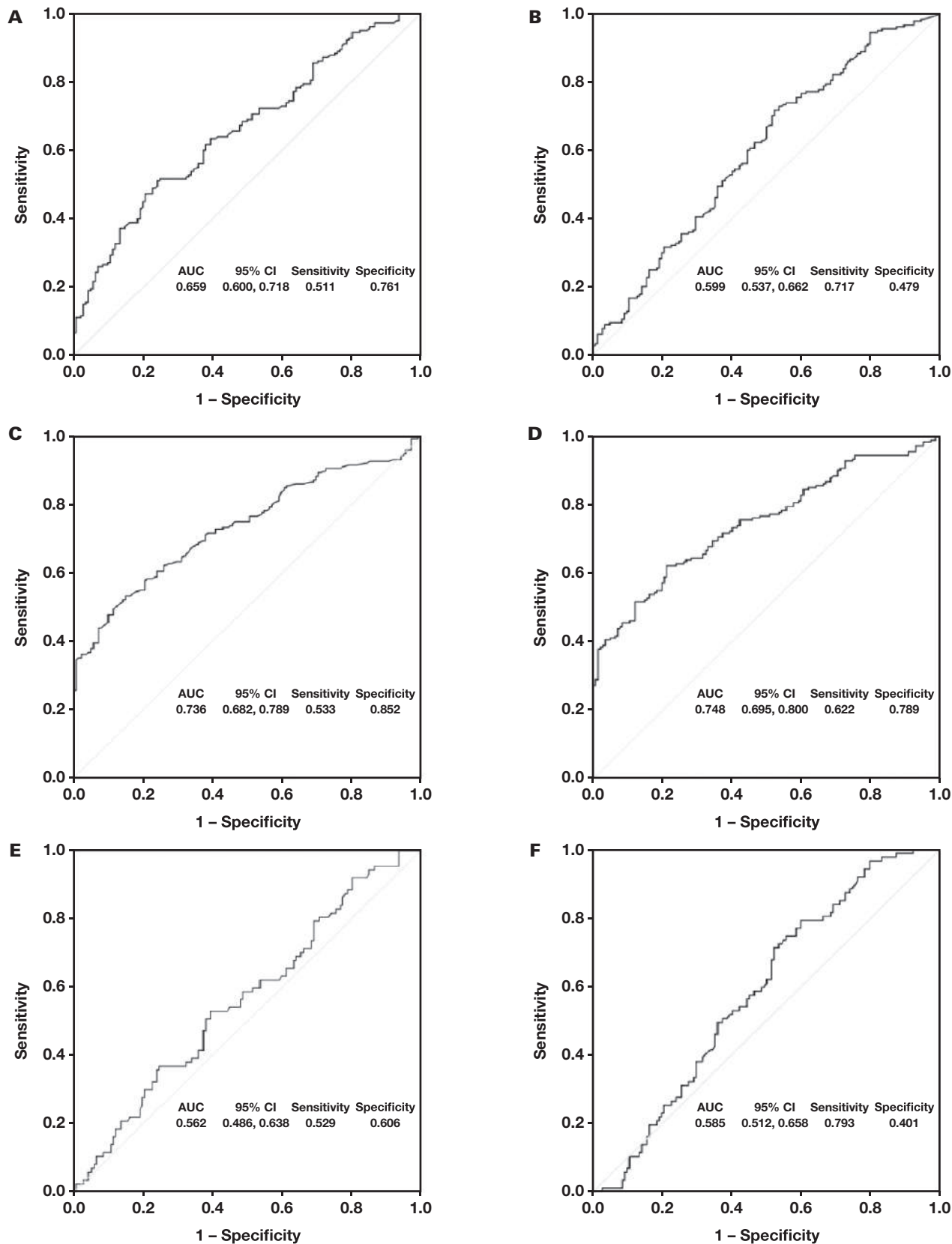
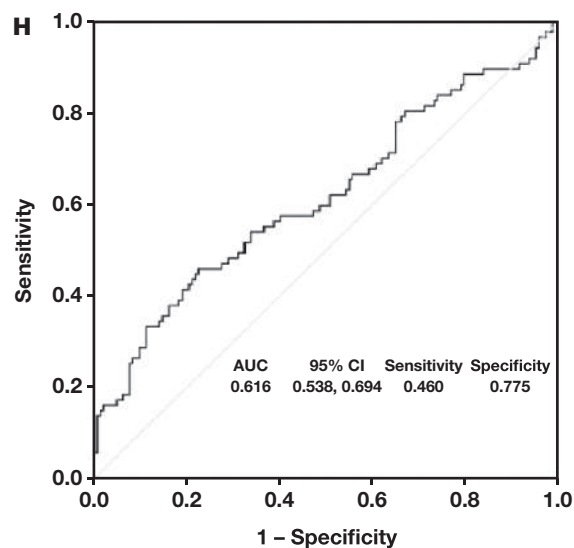
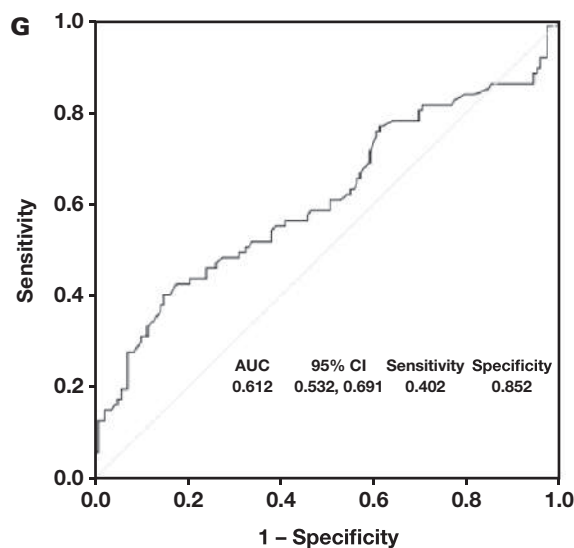


FIGURE 2. (cont)



presented limited significance as an independent risk factor in univariate regression. Heterogeneities in diseases, population, gender, geography, and other situations may explain the discrepancies. For instance, CA 19-9 might be more related to liver cancers and performed better when it was combined with radiological and imaging features of the cancer patients.²⁴ The marker CA 125 was found to be more specific for women with advanced-stage ovarian cancer, but it is also a marker for women with endometriosis.²⁵ Early studies support the diagnostic role of SCC in squamous types of cancers, but recent evidence has shown contrasting roles in non-SCLC (NSCLC), which implies a possible dual pathogenic role of SCC in different histologic types of NSCLC.²⁶ Therefore, a more detailed and rational grouping may explain the correlations of these biomarkers for specific patients.

Early diagnosis significantly improves the survival rates of lung cancer patients. In general, survival rates are 5 to 10 times higher for those diagnosed early than for those diagnosed late.²⁷ These results indicate that none of the markers except CYFRA 21-1 have much potential for the early diagnosis of lung cancer. This is not surprising and is consistent with the findings of previous reports, because solid tumors at such an early stage are so small that they are difficult to detect with noninvasive methods such as circulating biochemical alterations alone. Despite the poor performance in early diagnosis, we found CYFRA 21-1 to have relatively high specificity in the ROC analyses. This indicates that CYFRA 21-1 could be developed as an adjuvant diagnostic marker with existing detection methods such as CT to increase specificity and improve the situation of overdiagnosis.

The result of this study also showed CYFRA 21-1 was significantly associated with different stages of lung cancer, especially the late stages with a relatively high tumor burden, providing new information on the potential of CYFRA 21-1 to become a prognostic marker. Although many studies have been conducted on the role of biomarkers in diagnosis, few have assessed their role in cancer progression, so this result could shed light on such uses. Yu et al²⁸ found that CYFRA 21-1 was significantly higher in the patients with advanced lung cancers and associated with the overall survival in NSCLC, whereas Cabrera et al²⁹ reported that high levels of CYFRA 21-1 are related to distant metastasis. Recently, Chen et al³⁰ showed CYFRA 21-1 was significantly different

across lung cancer stages in particular NSCLC, and Yoshimura et al³¹ reported that the CYFRA 21-1 level measured 4 months after treatment is a valuable prognostic marker for NSCLC patients. In this work, a database was searched to collect clinical information on follow-ups of recruited patients, and it was found that the biomarker levels of 37 participants were measured 6 months after radical surgery. Similar to the above studies, the levels of CYFRA 21-1, but not the other markers of these patients, exhibited a decreased pattern. These observations agree with studies by others that CYFRA 21-1 is relevant to high tumor burden and poor survival of cancer patients.^{32,33} Also, CYFRA 21-1 was reported to predict therapeutic efficacy of chemotherapy³⁴ and immunotherapy.³⁵ Another study showed that a higher level of CYFRA 21-1 was correlated with more advanced stages and shorter overall survival in lung cancer²⁸ and was considered a prognostic marker in advanced NSCLC.³¹ Here, the results on CYFRA 21-1 further support this conclusion for early and advanced stages of Chinese lung cancer patients. However, the sample size in this study is very small. More clinical data on the long-term outcome using CYFRA 21-1 are required in future studies to establish a prognostic model.

Interestingly, rather than declining, CA 125 and CA 19-9 levels increased during the 6 months after tumor resection in 26 patients, although their CYFRA 21-1 level decreased. It is presumed that the levels were affected by inflammation caused by the surgery, because upregulation of CA 125 has also been reported to be associated with inflammation and congestion,^{36,37} and upregulated levels of CA 19-9 are common in pancreatitis and cholecystitis and co-occurred with upregulation of the inflammatory protein CRE.^{38,39}

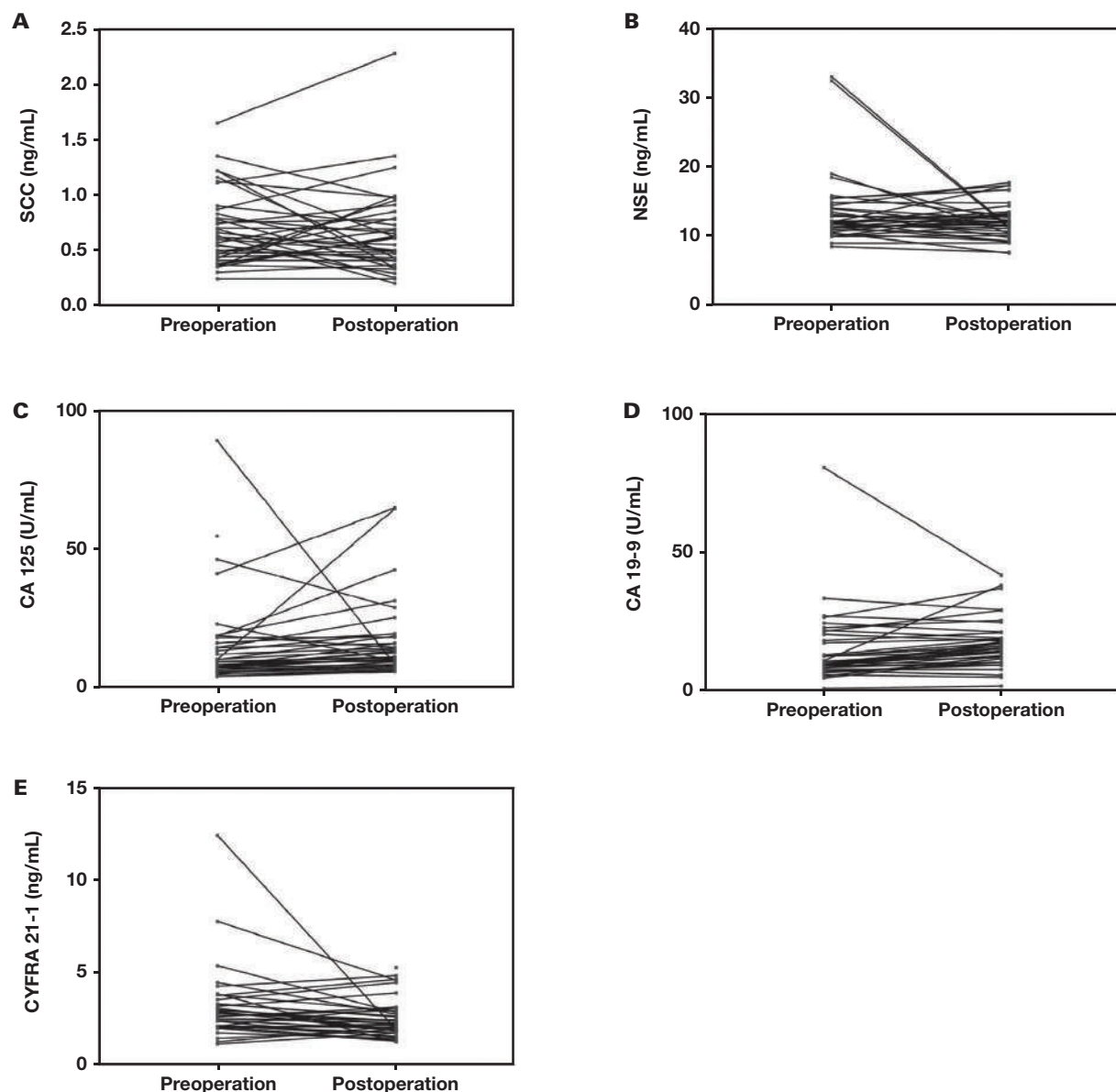
Conclusion

Based on the results of this study, it was concluded that CYFRA 21-1 could be developed as an adjuvant marker for the early diagnosis of lung cancer and as a prognostic marker for lung cancer treatment.

Limitations

This study had several limitations that should be recognized. First, the sample size was relatively small. This could have led to selection

FIGURE 3. Changes in serum levels of the five markers from preoperation to postoperation: SCC ($P > .05$) (A), NSE ($P > .05$) (B), CA 125 ($P = .003$) (C), CA 19-9 ($P = .001$) (D), and CYFRA 21-1 ($P = .015$) (E). CA 125 and CA 19-9 levels increased significantly when CYFRA 21-1 level decreased significantly.



bias, so a multiple-center study with a larger sample size is required to validate and assess the performance of CYFRA 21-1. Second, due to the retrospective nature of the study, there was a lack of follow-up visits of the enrolled patients to analyze long-term outcomes of cancer stages that would indicate progression, overall survival, and progression-free survival. Third, there was no analysis of the subtypes of lung cancer.

Acknowledgments

The author is thankful for the helpful contributions of all staff of the clinical laboratory.

Conflicts of Interest Disclosure

The author has nothing to disclose.

REFERENCES

1. Chen W, Zheng R, Zhang S, et al. Cancer incidence and mortality in China, 2013. *Cancer Lett.* 2017;401:63–71. doi:10.1016/j.canlet.2017.04.024.
2. Chen W, Zheng R, Baade PD, et al. Cancer statistics in China, 2015. *CA Cancer J Clin.* 2016;66(2):115–132. doi:10.3322/caac.21338.
3. Rodriguez M, Ajona D, Seijo LM, et al. Molecular biomarkers in early stage lung cancer. *Transl Lung Cancer Res.* 2021;10(2):1165–1185. doi:10.21037/tlcr-20-750.
4. Jones GS, Baldwin DR. Recent advances in the management of lung cancer. *Clin Med.* 2018;18(suppl 2):s41–s46. doi:10.7861/clinmedicine.18-2-s41.
5. Siegel R, Naishadham D, Jemal A. Cancer statistics, 2013. *CA Cancer J Clin.* 2013;63(1):11–30. doi:10.3322/caac.21166.
6. Doll KM, Rademaker A, Sosa JA. Practical guide to surgical data sets: surveillance, epidemiology, and end results (SEER)

- database. *JAMA Surg.* 2018;153(6):588–589. doi:10.1001/jamasurg.2018.0501.
7. National Lung Screening Trial Research T, Aberle DR, Adams AM, Berg CD, et al. Reduced lung-cancer mortality with low-dose computed tomographic screening. *N Engl J Med.* 2011;365(5):395–409. doi:10.1056/NEJMoa1102873
 8. Mulshine JL, D'Amico TA. Issues with implementing a high-quality lung cancer screening program. *CA Cancer J Clin.* 2014;64(5):352–363. doi:10.3322/caac.21239.
 9. Liu L, Xie W, Xue P, Wei Z, Liang X, Chen N. Diagnostic accuracy and prognostic applications of CYFRA 21-1 in head and neck cancer: a systematic review and meta-analysis. *PLoS One.* 2019;14(5):e0216561. doi:10.1371/journal.pone.0216561.
 10. Yang G, Xiao Z, Tang C, Deng Y, Huang H, He Z. Recent advances in biosensor for detection of lung cancer biomarkers. *Biosens Bioelectron.* 2019;141:111416. doi:10.1016/j.bios.2019.111416.
 11. Coppola A, La Vaccara V, Farolfi T, et al. Role of CA 19.9 in the management of resectable pancreatic cancer: state of the art and future perspectives. *Biomedicines.* 2022;10(9):2091. doi:10.3390/biomedicines10092091.
 12. Cedres S, Nunez I, Longo M, et al. Serum tumor markers CEA, CYFRA21-1, and CA-125 are associated with worse prognosis in advanced non-small-cell lung cancer (NSCLC). *Clin Lung Cancer.* 2011;12(3):172–179. doi:10.1016/j.clcc.2011.03.019.
 13. Li M, Jiang F, Xue L, et al. Recent progress in biosensors for detection of tumor biomarkers. *Molecules.* 2022;27(21):7327. doi:10.3390/molecules27217327.
 14. Zhang R, Siu MKY, Ngan HYS, Chan KKL. Molecular biomarkers for the early detection of ovarian cancer. *Int J Mol Sci.* 2022;23(19):12041. doi:10.3390/ijms231912041.
 15. He X, Wang M. Application value of serum TK1 and PCDGF, CYFRA21-1, NSE, and CEA plus enhanced CT scan in the diagnosis of non-small cell lung cancer and chemotherapy monitoring. *J Oncol.* 2022;2022:8800787. doi:10.1155/2022/8800787.
 16. Okamura K, Takayama K, Izumi M, Harada T, Furuyama K, Nakanishi Y. Diagnostic value of CEA and CYFRA 21-1 tumor markers in primary lung cancer. *Lung Cancer.* 2013;80(1):45–49. doi:10.1016/j.lungcan.2013.01.002.
 17. Ciarloni L, Ehrensberger SH, Imaizumi N, et al. Development and clinical validation of a blood test based on 29-gene expression for early detection of colorectal cancer. *Clin Cancer Res.* 2016;22(18):4604–4611. doi:10.1158/1078-0432.CCR-15-2057.
 18. Xu CM, Luo YL, Li S, et al. Multifunctional neuron-specific enolase: its role in lung diseases. *Biosci Rep.* 2019;39(11):BSR20192732. doi:10.1042/BSR20192732.
 19. Molina R, Auge JM, Filella X, et al. Pro-gastrin-releasing peptide (proGRP) in patients with benign and malignant diseases: comparison with CEA, SCC, CYFRA 21-1 and NSE in patients with lung cancer. *Anticancer Res.* 2005;25(3A):1773–1778.
 20. Chen Z, Liu X, Shang X, Qi K, Zhang S. The diagnostic value of the combination of carcinoembryonic antigen, squamous cell carcinoma-related antigen, CYFRA 21-1, neuron-specific enolase, tissue polypeptide antigen, and progastrin-releasing peptide in small cell lung cancer discrimination. *Int J Biol Markers.* 2021;36(4):36–44. doi:10.1177/17246008211049446.
 21. Chen ZQ, Huang LS, Zhu B. Assessment of seven clinical tumor markers in diagnosis of non-small-cell lung cancer. *Dis Markers.* 2018;2018:9845123. doi:10.1155/2018/9845123.
 22. Wang W, Xu X, Tian B, et al. The diagnostic value of serum tumor markers CEA, CA19-9, CA125, CA15-3, and TPS in metastatic breast cancer. *Clin Chim Acta.* 2017;470:51–55. doi:10.1016/j.cca.2017.04.023.
 23. Wang W, Liu M, Wang J, et al. Analysis of the discriminative methods for diagnosis of benign and malignant solitary pulmonary nodules based on serum markers. *Oncol Res Treat.* 2014;37(12):740–746. doi:10.1159/000369488.
 24. Eschrich J, Kobus Z, Geisel D, et al. The diagnostic approach towards combined hepatocellular-cholangiocarcinoma-state of the art and future perspectives. *Cancers.* 2023;15(1):301. doi:10.3390/cancers15010301.
 25. Brons PE, Nieuwenhuyzen-de Boer GM, Ramakers C, Willemsen S, Kengsakul M, van Beekhuizen HJ. Preoperative cancer antigen 125 level as predictor for complete cytoreduction in ovarian cancer: a prospective cohort study and systematic review. *Cancers.* 2022;14(23):5734. doi:10.3390/cancers14235734.
 26. Zhu H. Squamous cell carcinoma antigen: clinical application and research status. *Diagnostics.* 2022;12(5):1065. doi:10.3390/diagnostics12051065.
 27. Cho H, Mariotto AB, Schwartz LM, Luo J, Woloshin S. When do changes in cancer survival mean progress? The insight from population incidence and mortality. *J Natl Cancer Inst Monogr.* 2014;2014(49):187–197. doi:10.1093/jncimonographs/igu014.
 28. Yu Z, Zhang G, Yang M, et al. Systematic review of CYFRA 21-1 as a prognostic indicator and its predictive correlation with clinicopathological features in non-small cell lung cancer: a meta-analysis. *Oncotarget.* 2017;8(3):4043–4050. doi:10.18632/oncotarget.14022.
 29. Cabrera-Alarcon JL, Carrillo-Vico A, Santotoribio JD, et al. CYFRA 21-1 as a tool for distant metastasis detection in lung cancer. *Clin Lab.* 2011;57(11–12):1011–1014.
 30. Li J, Chen Y, Wang X, Wang C, Xiao M. The value of combined detection of CEA, CYFRA21-1, SCC-Ag, and pro-GRP in the differential diagnosis of lung cancer. *Transl Cancer Res.* 2021;10(4):1900–1906. doi:10.21037/tcr-21-527.
 31. Yoshimura A, Uchino J, Hasegawa K, et al. Carcinoembryonic antigen and CYFRA 21-1 responses as prognostic factors in advanced non-small cell lung cancer. *Transl Lung Cancer Res.* 2019;8(3):227–234. doi:10.21037/tlcr.2019.06.08.
 32. Kanaji N, Kadota K, Tadokoro A, et al. Serum CYFRA 21-1 but not vimentin is associated with poor prognosis in advanced lung cancer patients. *Open Respir Med J.* 2019;13:31–37. doi:10.2174/1874306401913010031.
 33. Kanaji N, Bandoh S, Ishii T, et al. Cytokeratins negatively regulate the invasive potential of lung cancer cell lines. *Oncol Rep.* 2011;26(4):763–768. doi:10.3892/or.2011.1357.
 34. Sone K, Oguri T, Nakao M, et al. CYFRA 21-1 as a predictive marker for non-small cell lung cancer treated with pemetrexed-based chemotherapy. *Anticancer Res.* 2017;37(2):935–939. doi:10.21873/anticancer.11402.
 35. Shirasu H, Ono A, Omae K, et al. CYFRA 21-1 predicts the efficacy of nivolumab in patients with advanced lung adenocarcinoma. *Tumour Biol.* 2018;40(2):1010428318760420. doi:10.1177/1010428318760420.
 36. Kumric M, Kurir TT, Bozic J, et al. Carbohydrate antigen 125: a biomarker at the crossroads of congestion and inflammation in heart failure. *Card Fail Rev.* 2021;7:e19. doi:10.15420/cfr.2021.22.
 37. Oliveira Junior WV, Turani SD, Marinho MAS, et al. CA-125 and CCL2 may indicate inflammation in peritoneal dialysis patients. *J Bras Nefrol.* 2021;43(4):502–509. doi:10.1590/2175-8239-JBN-2020-0255.
 38. Zhang W, Wang Y, Dong X, et al. Elevated serum CA19-9 indicates severe liver inflammation and worse survival after curative resection in hepatitis B-related hepatocellular carcinoma. *Biosci Trends.* 2022;15(6):397–405.
 39. Nurmi AM, Mustonen HK, Stenman UH, Seppanen HE, Haglund CH. Combining CRP and CA19-9 in a novel prognostic score in pancreatic ductal adenocarcinoma. *Sci Rep.* 2021;11(1):781. doi:10.1038/s41598-020-80778-0.

Semaphorin 3A levels in vascular and nonvascular phenotypes in systemic sclerosis

Mehmet Kayaalp, MD,¹ Abdulsamet Erden, MD,² Hakan Apaydin, MD,³ Serdar Can Güven, MD,³ Berkan Armağan, MD,³ Merve Çağlayan Kayaalp, MD,¹ Esmâ Andac Uzdoğan, MD,⁴ Şeymanur Ala Enli, MD,¹ Ahmet Omma, MD,⁵ Orhan Kucuksahin, MD²

¹Department of Internal Medicine, Yıldırım Beyazıt University, Ankara, Turkey,

²Department of Internal Medicine, Division of Rheumatology, Ankara City Hospital, Yıldırım Beyazıt University, Ankara, Turkey, Departments of

³Rheumatology and ⁴Biochemistry, Ankara City Hospital, Ankara, Turkey,

⁵University of Health Sciences, Rheumatology, Ankara, Turkey.

Corresponding author: Hakan Apaydin; drhakanapaydin@gmail.com.

Key words: digital ulcer; pulmonary hypertension; semaphorin 3A; systemic sclerosis; vasculopathy

Abbreviations: Sema3A, semaphorin 3A; SSc, systemic sclerosis; DU, digital ulcer; SRC, scleroderma renal crisis; PAH, pulmonary arterial hypertension; ET-1, endothelin-1; NO, nitric oxide; VEGF, vascular endothelial growth factor; CRP, C-reactive protein; ESR, erythrocyte sedimentation rate; NP-1, neutrophilin 1; RA, rheumatoid arthritis; OA, osteoarthritis; VDAI, Valentini disease activity index; mRSS, modified Rodnan skin score

Laboratory Medicine 2023;54:646-651; <https://doi.org/10.1093/labmed/lmad019>

ABSTRACT

Objective: Semaphorin 3A (Sema3A) plays a regulatory role in immune responses. The aim of this study was to evaluate Sema3A levels in patients with systemic sclerosis (SSc), especially in major vascular involvements such as digital ulcer (DU), scleroderma renal crisis (SRC), pulmonary arterial hypertension (PAH), and to compare Sema3A level with SSc disease activity.

Methods: In SSc patients, patients with DU, SRC, or PAH were grouped as major vascular involvements and those without as nonvascular, and Sema3A levels were compared between the groups and with a healthy control group. The Sema3A levels and acute phase reactants in SSc patients, as well as their association with the Valentini disease activity index and modified Rodnan skin score, were evaluated.

Results: The Sema3A values (mean \pm SD) were 57.60 ± 19.81 ng/mL in the control group ($n = 31$), 44.32 ± 5.87 ng/mL in patients with major vascular involvement SSc ($n = 21$), and 49.96 ± 14.00 ng/mL in the nonvascular SSc group ($n = 35$). When all SSc patients were examined

as a single group, the mean Sema3A value was significantly lower than controls ($P = .016$). The SSc with major vascular involvement group had significantly lower Sema3A levels than SSc with nonmajor vascular involvement group ($P = .04$). No correlation was found between Sema3A, acute phase reactants, and disease activity scores. Also, no relationship was observed between Sema3A levels and diffuse (48.36 ± 11.47 ng/mL) or limited (47.43 ± 12.38 ng/mL) SSc types ($P = .775$).

Conclusion: Our study suggests that Sema3A may play a significant role in the pathogenesis of vasculopathy and can be used as a biomarker in SSc patients with vascular complications such as DU and PAH.

Introduction

Systemic sclerosis (SSc) is a connective tissue disorder with an unclear etiology characterized by vasculopathy, autoimmunity, and fibrosis of skin and internal organs.¹ Major vascular involvements comprise digital ulcers (DU) and pulmonary arterial hypertension (PAH), which may lead to significant morbidity and even mortality.¹⁻⁵ Frequent periods of vasospasm and subsequent fibrointimal proliferation result in tissue hypoxemia/ischemia and damage. Endothelial dysfunction, a major underlying pathologic factor of vasculopathy, arises from increased levels of endothelin-1 (ET-1), a potent vasoconstrictor, in skin, lungs, and the sera, and decreased levels of nitric oxide (NO), which is a potent vasodilator. Vascular endothelial growth factor (VEGF) further contributes to the pathologic process via defective angiogenesis and profibrotic effects.⁶

Acute-phase reactants such as C-reactive protein (CRP) and erythrocyte sedimentation rate (ESR) levels can be within normal range in patients with SSc, and the search for biomarkers predicting prominent vasculopathy (DU, renal crisis, PAH) is in progress.⁷ Accordingly, predictive values for ET-1 and VEGF have been investigated.⁸ Likewise, the role of another biomarker of DU and PAH, semaphorin 3A (Sema3A), is also a matter of interest.

Semaphorins are molecules that are thought to mediate various biological processes such as axonal growth, inflammation, apoptosis, angiogenesis and bone remodeling.⁹ Sema3A is a member of the semaphorin family affecting the nervous system, tumor growth, autoimmunity, and

rheumatic diseases via its receptor neutrophilin 1 (NP1).¹⁰ Sema3A is assumed to be involved in competitive inhibition against VEGF via NP1.¹¹ Reduced levels of Sema3A in the sera and the synovial fluid of rheumatoid arthritis (RA) patients in comparison with osteoarthritis (OA) patients has been demonstrated.¹² Furthermore, injection of Sema3A reduced disease activity and joint damage in mice with RA.¹³ Similarly, it has been observed that serum Sema3A levels are lower in lupus patients when compared to healthy controls.¹⁴ Injection of Sema3A reduced the level of proteinuria in mice with lupus nephritis.¹⁵ In familial Mediterranean fever patients, Sema3A levels during an attack were observed to be lower than healthy subjects.¹⁶ In SSc patients, Rimar et al¹⁷ reported levels of Sema3A were reduced in comparison with healthy controls but were similar to those of lupus patients. In contrast, Romano et al¹⁸ observed similar Sema3A levels in SSc patients and healthy subjects, yet in SSc patients with a history of DU, levels of Sema3A receptor NP1 were lower than in patients without DU. Because reduced levels of Sema3A have been demonstrated in various vasculopathic conditions such as diabetic retinopathy, lupus, and SSc (particularly in patients with DUs), it is intriguing to consider whether Sema3A can distinguish major vascular involvements in SSc.

In this study, we aimed to evaluate Sema3A levels in SSc patients with and without major vascular involvement and to better elucidate the contribution of Sema3A to the etiopathogenesis.

Materials and Methods

Study Design

This study was conducted with Yıldırım Beyazıt University Faculty of Medicine Clinical Research Ethics Committee approval (IRB No. E21-21) and was therefore carried out in accordance with ethical standards set forth in the 1964 Declaration of Helsinki and its latter amendments.

Study Subjects

Between March 1 and June 1, 2021, consecutive SSc patients at Yıldırım Beyazıt University Faculty of Medicine and Ankara City Hospital Rheumatology Clinic meeting 2013 American College of Rheumatology/European League Against Rheumatism SSc classification criteria¹⁹ between ages 18 and 70 were enrolled. Patients under the age of 18, or those with peripheral arterial disease, pregnancy, or malignancy were excluded from the study. A control group was formed from healthy subjects with similar age and gender characteristics, without any disease or drug use. Written consent was obtained from all participants. Data regarding demographics, clinical characteristics, laboratory and imaging findings, and pulmonary function test results were obtained from hospital records and are recorded. Valentini disease activity index (VDAI) score and modified Rodnan skin score (mRSS) were calculated.

The patient cases were defined as diffuse and limited scleroderma according to skin involvement. Diffuse cutaneous systemic sclerosis is the form of the disease that extends from the distal of the extremities to the proximal and the trunk and shows the hardening of the skin in a relatively short time, such as months or years. Limited systemic sclerosis is slower progression to the proximal parts of the upper extremities.

The mRSS is a semiquantitative method for evaluation of skin thickness through palpation. Seventeen skin areas (on the face, anterior chest, abdomen and upper arm, forearm, hand, fingers, thigh, leg, foot bilaterally) are scored using a semiquantitative scale of 0 to 3 (0,

normal skin; 1, mild thickness; 2, moderate thickness; 3, severe thickness with inability to pinch the skin into a fold) up to a maximum score of 51.²⁰ The VDAI was used to measure disease activity. It comprises 10 variables: presence of sclerodema, digital necrosis, arthritis, mRSS greater than 14, lung carbon monoxide diffusing capacity lower than 80%, ESR greater than 30 mm/h, hypocomplementemia (low C3 and/or C4), and patient-reported worsening of cardiopulmonary, and skin and vascular symptoms in the past month. The total score ranges from 0 to 10.²¹ The North American working group defines DU as a lesion with a visually noticeable depth and loss of continuity of the epithelial lining, which may be peeling or covered with a crust or necrotic tissue.²² Pulmonary arterial hypertension is defined as mean pulmonary artery pressure >20 mmHg, pulmonary wedge pressure <15 mmHg, and pulmonary vascular resistance \geq 3 Wood's units.²³ Among SSc patients, patients with PAH, DU, and SSc renal crisis were grouped as patients with major vascular involvement.

Laboratory Investigations

Venous participant samples were centrifuged at 1000g at 4°C for 10 minutes. Separated serum samples were stored at -80°C until biochemical workup. Before analyses, frozen serum samples were thawed at room temperature and vortexed to homogenization. The Sema3A levels were measured by a commercial enzyme-linked immunosorbent assay kit (Human Semaphorin 3A ELISA, Elabscience) in accordance with the manufacturer's manual (with intra-assay and interassay coefficients of variation, 3.77% and 4.2%, respectively).

Statistical Analysis

Statistical analysis of the data was conducted with SPSS 24.0 (IBM) package program. Normality of variables was evaluated with Shapiro-Wilk test and visually by plots and histograms. Continuous variables were presented as mean \pm SD and compared between groups by Student *t*-test or one-way analysis of variance test, according to number of groups compared. Categorical variables are presented as number and percentage and compared between groups by χ^2 test or by Fisher exact test in case the 1 or more cell count is less than 5. All *P* values <.05 were considered statistically significant.

Results

A total of 56 SSc patients (21 with major vascular involvement) and 31 healthy controls were enrolled. Demographics, comorbidities, and SSc manifestations are presented in **TABLE 1**. No differences regarding age and sex were observed between SSc patients and healthy controls. The age in SSc group was 51.78 \pm 11.33 (mean \pm SD) years, with Raynaud's phenomenon being the most common symptom (100%) followed by sclerodactyly (82.1%), gastroesophageal reflux (62.5%), dyspnea (46%), and arthritis (33.9%). When the antibody profiles of patients with diffuse and limited scleroderma were evaluated, anti-SCL-70 positivity was higher in diffuse SSc (18 [64.2]) than in limited SSc (7 [21.8]) (*P* < .001) (**TABLE 2**).

Mean Sema3A levels were significantly lower in SSc patients than healthy subjects (47.85 \pm 11.88 vs 57.60 \pm 19.8 ng/mL, *P* = .016). In SSc patients with major vascular involvements, Sema3A levels were lower than in both healthy subjects and SSc patients without major vascular involvements (**TABLE 3**). In SSc patients without major vascular involvements, Sema3A levels were not significantly different from

TABLE 1. Demographics and Clinical Characteristics of Patients With Systemic Sclerosis and Control Group

	All SSc patients (n = 56)	Control group (n = 31)		P value
Age (y), mean (SD)	51.78 (11.33)	47.45 (12.24)		.101 ^a
Sex, female, n (%)	53 (94.6)	29 (93.5)		.834 ^a
		SSc patients		
	All SSc patients (n = 56)	Major vascular involvement (n = 21)	Nonmajor vascular (n = 35)	P value
Sex, female, n (%)	53 (94.6)	19 (90.5)	34 (97.1)	.549 ^a
Age (y), mean (SD)	51.78 (11.33)	48.40 (13.4)	53.7 (9.5)	
Smoking, n (%)				
Nonsmoker	37 (66.1)	14 (66.7)	23 (65.7)	.916 ^a
Smoker	7 (12.5)	3 (14.3)	4 (11.4)	
Ex-smoker	12 (21.4)	4 (19)	8 (22.9)	
Age at diagnosis (y), mean (SD)	41.96 (12.71)	37.71 (11.83)	44.51 (12.7)	.052 ^b
Clinical findings, n (%)				
Raynaud's phenomenon	56 (100)	21 (100)	35 (100)	
Calcinosis	3 (5.4)	2 (9.5)	1 (2.9)	.549 ^b
Sclerodactyly	46 (82.1)	19 (90.5)	27 (77.1)	.29 ^a
Telangiectasia	17 (30.4)	9 (42.4)	8 (22.9)	.202 ^a
Arthritis	19 (33.9)	6 (28.6)	13 (37.1)	.716 ^a
GERD	35 (62.5)	14 (66.7)	21 (60)	.831 ^a
Dysphagia	19 (33.9)	9 (42.9)	10 (28.6)	.423 ^a
Dyspnea	26 (46.4)	9 (42.9)	17 (48.6)	.890 ^a
Cough	19 (33.9)	9 (42.9)	10 (28.6)	.423 ^a
Digital ulcer	21 (37.5)	21 (100)	0 (0)	<.001 ^b
Lung involvement	20 (35.7)	10 (47.6)	10 (28.6)	.249 ^a
PAH	1 (1.8)	1 (4.8)	0 (0)	.375 ^b
Current medications, n (%)				
Acetylsalicylic acid	41 (73.2)	16 (76.2)	25 (71.4)	
Calcium channel blockers	27 (48.2)	11 (52.4)	16 (45.7)	
Corticosteroid	21 (37.5)	10 (47.6)	11 (31.4)	
Hydroxychloroquine	32 (57.1)	12 (57.1)	20 (57.1)	
Methotrexate	7 (12.5)	4 (19)	3 (8.6)	
Bosentan	0	0	0	
Phosphodiesterase V inhibitors	6 (10.7)	4 (19)	2 (5.7)	
Pentoxifylline	11 (19.6)	4 (19)	7 (20)	
Proton pump inhibitors	11 (19.6)	5 (23.8)	6 (17.1)	
Mycophenolate mofetil	5 (8.9)	4 (19)	1 (2.9)	
Azathioprine	11 (19.6)	5 (23.8)	6 (17.1)	
Colchicine	10 (17.9)	5 (23.8)	5 (14.3)	
ACE inhibitors or ARB	16 (28.6)	6 (28.6)	10 (28.6)	
Nonsteroidal anti-inflammatory drugs	4 (7.1)	1 (4.8)	3 (8.6)	
Rituximab	1 (1.8)	1 (4.8)	0 (0)	
Cyclophosphamide	2 (3.6)	0	2 (5.7)	

ACE, angiotensin-converting enzyme inhibitors; ARB, angiotensin II receptor blockers; GERD, gastroesophageal reflux disease; PAH, pulmonary arterial hypertension; SSc, systemic sclerosis.

^aPearson χ^2 test.

^bFisher exact test.

Downloaded from https://academic.oup.com/labmed/article/54/6/646/7143707 by guest on 28 February 2025

healthy subjects (49.96 ± 14 vs 57.6 ± 19 , 81 ng/mL, $P = .07$). The Sema3A levels were also similar when SSc patients were grouped as limited and diffuse (TABLE 3).

When SSc patients were subgrouped according to VDAI (3 as cutoff) and mRSS scores (14 as cutoff), no significant differences were observed in CRP, ESR, fibrinogen, and Sema3A levels (TABLE 4).

Discussion

Our results demonstrated significantly reduced levels of Sema3A in SSc patients compared with healthy subjects. Furthermore, Sema3A levels were significantly lower in SSc patients with major vasculopathic manifestations (DU, SRC, and PAH) than SSc patients without. Sema3A levels were not significantly different between patients without major vascular involvement and healthy subjects. When SSc patients were grouped according to mRSS and VDAI, Sema3A levels were similar.

The semaphorin family comprises nearly 20 extracellular signal proteins, playing roles in various biological processes, including in-

flammation, apoptosis, fibrosis, angiogenesis, and bone remodeling. In class 8, 1 and 2 semaphorins exist in nonvertebrates, whereas 3 to 7 exist in vertebrates and 8 in viruses. In class 1, 4 to 6 act as transmembrane proteins, 2, 3, and 5 are secreted, and 7 bound to glycosylphosphatidylinositol. Semaphorins are found in immune pathways and tumor pathogenesis in addition to neurons, where they were first discovered. Semaphorin 3A and VEGF competitively bind to NP-1 receptor. Additionally, Sema3A downregulates CD100 and upregulates CD72 in B lymphocytes. In CD19, CD25 B regulatory lymphocytes, expression of interleukin 10, transforming growth factor β , and Sema3A were increased. Semaphorin 3A also inhibits the Ras/mitogen-activated protein kinase (MAPK) pathway in T cells.²⁴ Semaphorin 3A is effective in the collapse of the actin cytoskeleton in endothelial cells.²⁵ It was determined that Sema3A increased hepatocellular carcinoma progression in cells by increasing the expression of the gelsolin-like actin-capping protein, galectin-3, enolase 2, and epithelial cell adhesion molecule. Semaphorin 6D exerts distinct biological activities on endothelial cells in different regions of the cardiac tube.²⁶ Satue et al²⁷ found the Sema E gene was overexpressed in metastatic lung cancer cells.

Semaphorin 3A has been demonstrated to be involved in the pathogenesis of various rheumatic conditions. In RA, Sema3A levels were reduced both in the sera and the synovial fluid in comparison to OA and healthy controls and had a negative correlation with disease activity parameters.¹² In patients with lupus and antiphospholipid syndrome, Sema3A levels were lower than in controls and further reduced in existence of a thrombotic event or obstetric comorbidity.²⁸ In another study on lupus patients, Sema3A levels were lower in lupus patients with nephritis than in patients without.²⁹ Semaphorin 3A injections altered

TABLE 2. Antibody Positivity Percentages in Patients With Limited and Diffuse Cutaneous Scleroderma

	lcSSc, n (%)	dcSSc, n (%)	P^a
Anti-centromere	13 (40.6)	6 (21.4)	.083
Anti-Scl-70	7 (21.8)	18 (64.2)	<.001

dcSSc, diffuse cutaneous scleroderma; lcSSc, limited cutaneous scleroderma.

^aPearson χ^2 test.

TABLE 3. Comparisons of Semaphorin 3A Levels Between Different Involvement of SSc Patients and Control Group^a

	SSc patients		Control group	P value			
	Major vascular involvement SSc	Nonmajor vascular SSc	Control group	P value	P ₁	P ₂	P ₃
Semaphorin 3A (ng/mL), mean (SD)	47.85 (11.88)		57.60 (19.81)	.016 ^b			
Semaphorin 3A (ng/mL), mean (SD)	44.32 (5.87)	49.96 (14.00)	57.6 (19.81)	.008 ^c	.04	.001	.07
	Diffuse cutaneous SSc	Limited cutaneous SSc	P value				
Semaphorin 3A (ng/mL), mean (SD)	48.36 (11.47)	47.43 (12.38)	.775 ^c				

SSc, systemic sclerosis.

^aP₁: major vascular involvement SSc vs nonmajor vascular SSc; P₂: major vascular involvement SSc vs control group; P₃: nonmajor vascular SSc vs control group.

^bStudent t-test.

^cAnalysis of variance.

TABLE 4. Evaluation of Disease Activity With Semaphorin 3A and Acute-Phase Reactants According to Valentini Disease Activity Score and Modified Rodnan Skin Score

	Valentini disease activity score <3	Valentini disease activity score >3	P value ^a
Semaphorin 3A (ng/mL), mean (SD)	47.92 (12.57)	47.85 (12.57)	.916
CRP, mean (SD)	2.24 (3.79)	8.22 (12.55)	.169
ESR (mm/h), mean (SD)	13.62 (8.12)	23.6 (20.30)	.159
Fibrinogen (g/l), mean (SD)	3.11 (0.96)	2.86 (0.81)	.627
	Modified Rodnan skin score <14	Modified Rodnan skin score >14	
Semaphorin 3A (ng/mL), mean (SD)	47.57 (13.55)	47.73 (10.01)	.96
CRP (mg/l), mean (SD)	2.93 (5.91)	3.31 (7.10)	.829
ESR (g/l), mean (SD)	15.10 (9.21)	16.00 (14.45)	.784
Fibrinogen, mean (SD)	3.06 (1.09)	2.93 (5.91)	.915

CRP, C-reactive protein; ESR, erythrocyte sedimentation rate.

^aStudent t-test.

neovascularization in mice with diabetic retinopathy VEGF.³⁰ In our study, we observed further reduced levels of Sema3A in SSc patients with major vascular involvement, regardless of VDAI and mRSS scores, in accordance with the potential protective role of Sema3A in vasculopathic processes.

Pulmonary arterial hypertension is one of the most devastating vasculopathic complications of SSc, with significant functional deterioration and increased mortality. Decreased NO and prostacyclin expression and increased ET-1 production lead to endothelial damage and dysfunction.³¹ In the pathogenesis of DU, VEGF, endostatin, ET 1, asymmetric dimethyl-L-arginine, platelet activating factor acetyl hydrolase, galectin-1, and angiopoietin-like protein 3 are assumed to play a role.^{32,33} It has been reported that Sema3E levels were higher in SSc patients than in patients with Raynaud's phenomenon, with early capillaroscopic changes and with DUs.³⁴ In another study, increased VEGF and decreased NP-1 levels were observed in SSc patients.³⁴ Rimar et al¹⁷ reported decreased levels of Sema3A in SSc and demonstrated a negative correlation with anti-Scl-70 positivity. On the other hand, Romano et al¹⁸ observed similar Sema3A levels in SSc patients and healthy subjects, yet in SSc patients with history of DU, levels of Sema3A receptor NP-1 were lower than in patients without DU. In our study, DU was present in all SSc patients in the vasculopathic group and the Sema3A levels were significantly lower than in the nonvasculopathic group, which imply that decreased Sema3A levels can be attributed to its increased consumption in a prominent vasculopathic process.

There were several limitations to our study in addition to its single-center and cross-sectional nature. The number of patients with PAH and renal crisis was limited. The participant composition of this study was female (94.65% and 93.5% in the SSc and control groups, respectively). Systemic sclerosis is a rare disease and the female-to-male ratio ranges from 3: 1 to 8: 1,¹ similar to our study. The female-dominated sample did not cause bias due to the nature of the disease. Furthermore, most of the patients were under appropriate treatment. Although patients under treatment were included in the study due to the cross-sectional nature of the study, no statistically significant difference was found between drug use in the vascular and nonvascular groups. Further studies of a prospective nature involving treatment-naive patients will better demonstrate the true role of Sema3A in SSc and related vasculopathy.

Conclusion

Our results suggest a relation between vasculopathy and Sema3A levels in SSc and imply that Sema3A may be a biomarker for distinguishing patients with potential to manifest major vascular involvement. Larger and prospective studies would further elucidate the potential use of Sema3A in SSc patients as a biomarker.

Conflict of Interest Disclosure

The authors have nothing to disclose.

REFERENCES

1. Varga J. *Clinical Manifestations and Diagnosis of Systemic Sclerosis (Scleroderma) In Adults*. Waltham, MA: UpToDate. 2020. <https://www.medilibrary.org/uptodate/show/7539>.
2. Ingegnoli F, Ughi N, Mihai C. Update on the epidemiology, risk factors, and disease outcomes of systemic sclerosis. *Best Pract Res Clin Rheumatol*. 2018;32(2):223–240. doi:10.1016/j.berh.2018.08.005.
3. Varga J. *Risk Factors for and Possible Causes of Systemic Sclerosis (Scleroderma)*. Waltham, MA: UpToDate; 2005. <https://www.medilibrary.org/uptodate/show/7557>.
4. Hughes M, Herrick AL. Digital ulcers in systemic sclerosis. *Rheumatology*. 2017;56(1):14–25.
5. Hopkins W, Rubin LJ. Treatment of pulmonary arterial hypertension (group 1) in adults: pulmonary hypertension-specific therapy. *UpToDate*. Retrieved October 20, 2021. <https://www.medilibrary.org/uptodate/show/8250>.
6. Kayser C, Fritzler MJ. Autoantibodies in systemic sclerosis: unanswered questions. *Front Immunol*. 2015;6:167. doi:10.3389/fimmu.2015.00167.
7. Muangchan C, Harding S, Khimdas S, Bonner A, Baron M, Pope J. Association of C-reactive protein with high disease activity in systemic sclerosis: results from the Canadian Scleroderma Research Group. *Arthritis Care Res*. 2012;64(9):1405–1414. doi:10.1002/acr.21716.
8. Silva I, Teixeira A, Oliveira J, Almeida I, Almeida R, Vasconcelos C. Predictive value of vascular disease biomarkers for digital ulcers in systemic sclerosis patients. *Clin Exp Rheumatol*. 2015;33(4 suppl 91):S127–S130.
9. Garcia S. Role of semaphorins in immunopathologies and rheumatic diseases. *Int J Mol Sci*. 2019;20(2):374. doi:10.3390/ijms20020374.
10. Staton CA. Class 3 semaphorins and their receptors in physiological and pathological angiogenesis. *Biochem Soc Trans*. 2011;39(6):1565–1570. doi:10.1042/BST20110654.
11. Gu C, Giraudo E. The role of semaphorins and their receptors in vascular development and cancer. *Exp Cell Res*. 2013;319(9):1306–1316.
12. Takagawa S, Nakamura F, Kumagai K, et al. Decreased semaphorin3A expression correlates with disease activity and histological features of rheumatoid arthritis. *BMC Musculoskelet Disord*. 2013;14(1):1–11.
13. Catalano A. The neuroimmune semaphorin-3A reduces inflammation and progression of experimental autoimmune arthritis. *J Immunol*. 2010;185(10):6373–6383. doi:10.4049/jimmunol.0903527.
14. Vadasz Z, Toubi E. Semaphorin 3A—a marker for disease activity and a potential putative disease-modifying treatment in systemic lupus erythematosus. *Lupus*. 2012;21(12):1266–1270. doi:10.1177/0961203312456753.
15. Bejar J, Kessler O, Sabag AD, et al. Semaphorin3A: a potential therapeutic tool for lupus nephritis. *Front Immunol*. 2018;9:634. doi:10.3389/fimmu.2018.00634.
16. Rimar D, Rosner I, Slobodin G, et al. Semaphorin3A, a potential immune regulator in familial Mediterranean fever. *Clin Exp Rheumatol*. 2016;34(suppl 102):52–55.
17. Rimar D, Nov Y, Rosner I, et al. Semaphorin 3A: an immunoregulator in systemic sclerosis. *Rheumatol Int*. 2015;35(10):1625–1630. doi:10.1007/s00296-015-3269-2.
18. Romano E, Chora I, Manetti M, et al. Decreased expression of neuropilin-1 as a novel key factor contributing to peripheral microvasculopathy and defective angiogenesis in systemic sclerosis. *Ann Rheum Dis*. 2016;75(8):1541–1549. doi:10.1136/annrheumdis-2015-207483.
19. Van Den Hoogen F, Khanna D, Fransen J, et al. 2013 classification criteria for systemic sclerosis: an American College of Rheumatology/ European League against Rheumatism collaborative initiative. *Arthritis Rheum*. 2013;65(11):2737–2747. doi:10.1002/art.38098.
20. Medsger T, Silman A, Steen V, et al. A disease severity scale for systemic sclerosis: development and testing. *J Rheumatol*. 1999;26(10):2159–2167.
21. Della Rossa A, Valentini G, Bombardieri S, et al. European multicentre study to define disease activity criteria for systemic sclerosis: I. Clinical and epidemiological features of 290 patients from 19 centres. *Ann Rheum Dis*. 2001;60(6):585–591. doi:10.1136/ard.60.6.585.

22. Baron M, Chung L, Gyger G, et al. Consensus opinion of a North American Working Group regarding the classification of digital ulcers in systemic sclerosis. *Clin Rheumatol*. 2014;33(2):207–214. doi:10.1007/s10067-013-2460-7.
23. Simonneau G, Montani D, Celermajer DS, et al. Haemodynamic definitions and updated clinical classification of pulmonary hypertension. *Eur Respir J*. 2019;53(1):1801913. doi:10.1183/13993003.01913-2018.
24. Catalano A, Caprari P, Moretti S, Faronato M, Tamagnone L, Procopio A. Semaphorin-3A is expressed by tumor cells and alters T-cell signal transduction and function. *Blood*. 2006;107(8):3321–3329. doi:10.1182/blood-2005-06-2445.
25. Guttman-Raviv N, Shraga-Heled N, Varshavsky A, Guimaraes-Sternberg C, Kessler O, Neufeld G. Semaphorin-3A and semaphorin-3F work together to repel endothelial cells and to inhibit their survival by induction of apoptosis. *J Biol Chem*. 2007;282(36):26294–26305. doi:10.1074/jbc.M609711200.
26. Toyofuku T, Kikutani H. Semaphorin signaling during cardiac development. *Adv Exp Med Biol*. 2007;600:109–117. doi:10.1007/978-0-387-70956-7_9.
27. Martín-Satué M, Blanco J. Identification of semaphorin E gene expression in metastatic human lung adenocarcinoma cells by mRNA differential display. *J Surg Oncol*. 1999;72:18–23. doi:10.1002/(sici)1096-9098(199909)72:1<18::aid-jso5>3.0.co;2-p.
28. Kart Bayram GS, Erden A, Bayram D, et al. Semaphorin 3A levels in lupus with and without secondary antiphospholipid antibody syndrome and renal involvement. *Lab Med*. 2022;53(3):285–289. doi:10.1093/labmed/lmab096.
29. Doron R, Merav L, Nasrin E, et al. Low urine secretion of semaphorin3a in lupus patients with proteinuria. *Inflammation*. 2022;45(2):603–609. doi:10.1007/s10753-021-01570-4.
30. Binet F, Beaulieu N, Beauchemin K, et al. Semaphorin3A-trap accelerates vascular regeneration in ischemic retinopathy and reduces retinal edema. *Investig Ophthalmol Vis Sci*. 2019;60(9):1648.
31. Matucci-Cerinic M, Kahaleh B, Wigley FM. Evidence that systemic sclerosis is a vascular disease. *Arthritis Rheum*. 2013;65(8):1953–1962.
32. Yanaba K, Asano Y, Tada Y, Sugaya M, Kadono T, Sato S. Clinical significance of circulating platelet-activating factor acetylhydrolase levels in systemic sclerosis. *Arch Dermatol Res*. 2012;304(3):203–208. doi:10.1007/s00403-011-1196-y.
33. Ichimura Y, Asano Y, Akamata K, et al. Serum angiopoietin-like protein 3 levels: possible correlation with progressive skin sclerosis, digital ulcers and pulmonary vascular involvement in patients with systemic sclerosis. *Acta Derm Venereol*. 2014;94(2):157–162.
34. Chora I, Romano E, Manetti M, et al. Evidence for a derangement of the microvascular system in patients with a very early diagnosis of systemic sclerosis. *J Rheumatol*. 2017;44(8):1190–1197. doi:10.3899/jrheum.160791.

Comparison of the optimized direct spectrophotometric serum prolidase enzyme activity assay method with the currently used spectrophotometric assay methods and liver fibrosis indexes to distinguish the early stages of liver fibrosis in patients with chronic hepatitis B infection

Huseyin Kayadibi, MD,^{1,2}  İbrahim Hakkı Köker, MD,³ Zuhul Guçin, MD,⁴ Hakan Şentürk, MD,³ Sakine Candan Merzifonlu, MD,⁵ Ali Tüzün İnce, MD³

¹Department of Medical Biochemistry, Eskisehir Osmangazi University School of Medicine, Eskisehir, Turkey, ²Department of Medical Biochemistry, Hitit University School of Medicine, Corum, Turkey, Departments of ³Gastroenterology and ⁴Pathology, Bezmialem University School of Medicine, Istanbul, Turkey, ⁵Biochemistry Laboratory, Corum Chest Diseases Hospital, Corum, Turkey. Corresponding author: Huseyin Kayadibi; mdkayadibi@yahoo.com

Key words: APRI; early stage; FIB-4; HBV; liver fibrosis; optimized prolidase assay

Abbreviations: SPEA, serum prolidase enzyme activity; CHB, chronic hepatitis B; ALT, alanine aminotransferase; AST, aspartate aminotransferase; AAR, AST-to-ALT ratio; API, age platelet index; APRI, AST-to-platelet ratio index; CDS, cirrhosis discriminate score; FIB-4, fibrosis index based on four factors; GUCI, Goteborg University Cirrhosis Index; HCl, hydrochloric acid; TCA, trichloroacetic acid; GAA, glacial acetic acid; OPA, orthophosphoric acid; CV, coefficients of variation; CLSI, Clinical and Laboratory Standards Institute; INR, international normalization ratio; ROC, receiver operating characteristic; AUROC, areas under the curve; GSH, reduced glutathione

Laboratory Medicine 2023;54:652-658; <https://doi.org/10.1093/labmed/lmad025>

ABSTRACT

Objective: The aim of this study was to optimize the currently used direct spectrophotometric serum prolidase enzyme activity (SPEA) assay method and compare its diagnostic accuracy with current precipitation and direct spectrophotometric assay methods, AST-to-ALT ratio, age platelet index, AST-to-platelet ratio index, cirrhosis discriminate score, Doha score, FIB-4, FibroQ, fibrosis index, Goteborg University Cirrhosis Index, King's score, and Pohl score for distinguishing Ishak F0 from F1–F3 in patients with chronic hepatitis B (CHB) infection.

Methods: Liver biopsy results from 112 patients were included in this study.

Results: The SPEA values were 529 (292–794) U/L, 671 (486–927) U/L, and 1077 (867–1399) U/L with the precipitation, current, and optimized direct spectrophotometric assay methods, respectively. According to multivariate logistic regression analysis optimized direct spectrophotometric SPEA was the only statistically significant parameter to predict the early stages of liver fibrosis.

Conclusions: Optimized direct spectrophotometric SPEA assay method could be used to distinguish early stages of liver fibrosis in patients with CHB infection instead of the currently used spectrophotometric SPEA assay methods and other evaluated liver fibrosis indexes.

Distinguishing the early stages of liver fibrosis is critical for the management of patients with chronic hepatitis B (CHB) infection.^{1,2} To determine the stage of liver fibrosis, liver biopsy is the gold standard diagnostic tool used today. However, it is invasive, prone to many complications, and inconsistent results may be encountered due to sampling error or within-between observer variabilities.^{3–5} For these reasons, there is a great need for a simple, noninvasive, cost-effective, and easily accessible biochemical test such as serum prolidase enzyme activity (SPEA).

Prolidase enzyme (EC 3.4.13.9) is a manganese-dependent cytosolic exopeptidase that is involved in the degradation of iminodipeptides with proline and/or hydroxyproline at the C-terminus in the final step of collagen breakdown.^{6,7} Spectrophotometric SPEA assay methods used today are the precipitation and direct assays. The direct spectrophotometric SPEA assay method is more practical and less time-consuming than the precipitation assay.^{8,9} However, higher accuracy in a direct spectrophotometric SPEA assay method is needed, as different results are obtained with the currently used spectrophotometric SPEA assay methods carried out for determination of fibrosis stages in different kinds of diseases, as the prolidase enzyme has been shown to be important in the pathophysiology of different kinds of disorders.^{10–14}

In this study, we aimed to optimize the currently used spectrophotometric SPEA assay method and compare its diagnostic accuracy with the precipitation and currently used direct spectrophotometric SPEA assay methods and other noninvasive liver fibrosis indexes such as aspartate aminotransferase (AST)-to-alanine aminotransferase (ALT) ratio (AAR), age platelet index (API), AST-to-platelet ratio index (APRI), cirrhosis discriminant score (CDS), Doha score, fibrosis index based on four factors (FIB-4), FibroQ, fibrosis index, Goteborg University Cirrhosis Index (GUCI), King's score, and Pohl score for the differentiation of early stages of liver fibrosis (F0 vs F1–F3) in liver biopsy performed patients with CHB infection.

Materials and Methods

Patient Selection

After gaining the approval of the local ethics committee of Hitit University (2016-18) and informed consent from all participants, patients with CHB infection who had a liver biopsy 1 to 3 day after having blood drawn were included in this study; 14 stage 0 and 10 stage 1 liver fibrosis patients' SPEA were analyzed from blood samples drawn within 6 months after liver biopsy. Patients <18 years of age, taking antiviral treatment, with co-infection with hepatitis C, D, or HIV, autoimmune hepatitis, or cholangitis were excluded from the study.

Materials

Human recombinant prolidase, trizma base, $\text{MnCl}_2 \cdot 4\text{H}_2\text{O}$, reduced glutathione (GSH), Triton X-100, gly-pro, proline, hydrochloric acid (HCl), trichloroacetic acid (TCA), glacial acetic acid (GAA), orthophosphoric acid (OPA) and ninhydrin were used for spectrophotometric SPEA assay methods. All chemicals were of analytical grade. Absorbances were measured at 515 nm using a UV/Vis spectrophotometer (Biochrom Libra S60).

Procedures of the Precipitation and Direct Spectrophotometric SPEA Assay Methods

In the precipitation spectrophotometric SPEA assay method, the serum sample was diluted and activated with 50 mM pH 7.8 Tris-HCl buffer containing 1 mM MnCl_2 and then incubated at 37°C for 180 minutes (original method is 24 hours). Activated serum was mixed with 50 mM of pH 7.8 Tris-HCl buffer containing 94 mM glycine-L-proline and 1 mM MnCl_2 for the enzyme-substrate incubation at 37°C for 30 minutes. At the end of this incubation, 0.45 M TCA was added immediately and samples were centrifuged. For the ninhydrin reaction, supernatant, GAA, and ninhydrin reagent (25 g/L ninhydrin was prepared with 600 mL GAA and 400 mL of 6 M orthophosphoric acid mixture) were pipetted, vortexed, and incubated at 90°C for 10 minutes. At the end of the incubation, absorbances were read against the reagent blank in spectrophotometer at the 515 nm wavelength.

In the currently used direct spectrophotometric SPEA assay method, the serum sample was diluted and activated with 50 mM pH 7.0 Tris-HCl buffer containing 50 mM MnCl_2 and 1 mM GSH, and incubated at 37°C for 30 minutes. Enzyme-substrate incubation was performed for 5 minutes at 37°C with 50 mM pH 7.8 Tris-HCl buffer containing 144 mM glycine-L-proline, 50 mM MnCl_2 , and 1 mM GSH. To inhibit the SPEA by pH change, GAA was added immediately. For the ninhydrin reaction, 50 mM pH 7.8 Tris-HCl buffer and ninhydrin reagent (30 g/L ninhydrin was prepared with 0.5 M orthophosphoric acid) were pipetted, vortexed, and incubated at 90°C for 20 minutes. At the end of the incubation,

samples were immediately kept in ice water, and absorbances were read against the sample blank in which the substrate was not added in the spectrophotometer at the 515 nm wavelength.

Optimization of the Direct Spectrophotometric SPEA Assay Method

Enzyme-substrate incubation, activation, and proline assay steps of the currently used direct spectrophotometric SPEA assay method have been optimized as follows, and method validation was performed.

Enzyme-Substrate Incubation Step

Optimum enzyme-substrate incubation time and temperature were determined by incubation of the gly-pro substrate with the presence or absence of human recombinant prolidase at 37°C, 45°C, 50°C, and 55°C for 5, 10, 15, 20, 25, 30, 40, 50, and 60 minutes after activation with 1 mM GSH and 50 mM $\text{MnCl}_2 \cdot 4\text{H}_2\text{O}$ at 37°C for 30 minutes.

Activation Step

This step was optimized using different concentrations of $\text{MnCl}_2 \cdot 4\text{H}_2\text{O}$, GSH and Triton X-100 as activators at 45°C for 0, 5, 10, 15, 20, 25, 30, 40, 50, 60, 90, 120, 150, and 180 minutes of incubation. For incubation temperature, 45°C was selected based on the maximum SPEA that was determined at this temperature in the enzyme-substrate incubation step.

Proline Assay Step

For the optimization of proline-ninhydrin condensation step, the following experiments were done. First, it was decided whether the samples should be cooled at room temperature or in ice water after the incubation of 12.5 mg/dL of proline standard with ninhydrin reagent (25 g/L ninhydrin, 0.6 L GAA, and 0.4 L 6 M OPA) at 80°C by considering whether pH 7.8 Tris-HCl buffer was necessary or not. Second, optimum ninhydrin reagent was determined by comparing the coefficients of variation (CV) percentage and maximum delta absorbance values obtained with the following 4 different ninhydrin reagents for 12.5 mg/dL of proline standard repeated 20 times in 60 minutes of incubation at 80°C: reagent A: 12.5 g ninhydrin was dissolved in 1 L GAA; reagent B: 25 g ninhydrin was dissolved in 1 L 0.5 M OPA; reagent C: 25 g ninhydrin was dissolved in 0.6 L GAA and 0.4 L 6 M OPA; reagent D: 20 g ninhydrin was dissolved in 0.6 L GAA and 0.4 L distilled water. Third, optimum ninhydrin concentration was determined by taking into account the lowest CV percentage and maximum delta absorbance results obtained with the use of following ninhydrin reagents in 40, 45, 50, 60, 70, and 80 minutes of incubation for 12.5 mg/dL and 24 mg/dL of proline standards at 80°C: reagent E: 10 g ninhydrin was dissolved in 0.6 L GAA and 0.4 L distilled water; reagent F: 15 g ninhydrin was dissolved in 0.6 L GAA and 0.4 L distilled water; reagent G: 20 g ninhydrin was dissolved in 0.6 L GAA and 0.4 L distilled water; reagent H: 25 g ninhydrin was dissolved in 0.6 L GAA and 0.4 L distilled water. Fourth, optimum reading interval was determined according to the stability time of proline-ninhydrin condensation in ice water. For this purpose, a series of 12.5 mg/dL of proline standards were incubated at 80°C for 45 minutes and cooled for 5, 10, 20, 30, 40, 50, 60, 70, 80, and 90 minutes in ice water.

Method Validation

Intra- and inter-day precisions and linearity were performed according to the protocols of the Clinical and Laboratory Standards Institute (CLSI).

Intra- and Inter-Assay Precision.—The intra- and inter- assay precision studies were done based on CLSI EP05-A3 and CLSI EP15-A3 protocols, respectively.^{15,16} Both of these precision studies were performed using low and high SPEA levels of pooled human sera separately. Intra-assay precision was determined by analyzing a total of 40 samples, 20 in the morning and 20 in the afternoon, at low and high SPEA levels, respectively, of pooled human sera within a day. The inter-assay precision was determined based on a total of 20 measurement results by analyzing 4 replicates per day over a total of 5 consecutive days for low and high SPEA levels of pooled human sera separately.

Linearity.—Linearity was determined according to the CLSI EP06-A protocol.¹⁷ In this experiment, human serum pool with a high SPEA level (4492 U/L) was diluted with human serum pool with a low SPEA level (150 U/L) according to the procedure that was determined in CLSI EP06-A protocol using 8 different sample combinations. Each dilution was measured 3 times in a single run, and linearity was evaluated by linear regression analysis. The observed values were plotted against the expected values wherein $R^2 > 0.99$ was considered as linear and acceptable.

Other Biochemistry Tests

The AST, ALT, albumin, total bilirubin, direct bilirubin, international normalization ratio (INR), and complete blood count analysis were done with commercially available kits. The AAR, API, APRI, CDS, Doha Score, FIB-4, FibroQ, fibrosis index, GUCI, King's Score and Pohl Score were calculated as follows:

AAR = AST/ALT; API = [Age in years: <30 = 0; 30–39 = 1; 40–49 = 2; 50–59 = 3; 60–69 = 4; ≥70 = 5. Platelet ($\times 10^9/L$): ≥225 = 0; 200–224 = 1; 175–199 = 2; 150–174 = 3; 125–149 = 4; <125 = 5]; APRI = $100 \times (\text{AST}/\text{AST upper limit of normal})/\text{Platelet} (\times 10^9/L)$; CDS = [Platelet ($\times 10^9/L$) + (ALT/AST) + INR. Platelet ($\times 10^9/L$): ≥340 = 0; 280–339 = 1; 220–279 = 2; 160–219 = 3; 100–159 = 4; 40–99 = 5; <40 = 6]. ALT/AST: ≥1.7 = 0; 1.2–1.7 = 1; 0.6–1.19 = 2; <0.6 = 3. INR: ≤1.1 = 0; 1.1–1.4 = 1; >1.4 = 2]; Doha score = $8.5 - [0.2 \times \text{albumin} (\text{g/dL})] + (0.01 \times \text{AST}) - [0.02 \times \text{Platelet} (\times 10^9/L)]$; FIB-4 = $\text{Age} \times \text{AST}/\text{Platelet} (\times 10^9/L) \times \text{ALT}^{1/2}$; FibroQ = $10 \times \text{Age} \times \text{AST} \times \text{INR}/\text{Platelet} (\times 10^9/L) \times \text{ALT}$; Fibrosis index = $8 - (0.01 \times \text{Platelet} (\times 10^9/L)) - \text{albumin} (\text{g/dL})$; GUCI = $100 \times \text{AST} \times \text{INR}/\text{Platelet} (\times 10^9/L)$; King's score = $\text{Age} \times \text{AST} \times \text{INR}/\text{Platelet} (\times 10^9/L)$; Pohl score = Positive if AAR ≥1 and Platelet ($\times 10^9/L$) <150.

Liver Biopsy

Liver biopsy was used as the gold standard diagnostic tool to compare the diagnostic accuracy of the spectrophotometric SPEA assay methods. Liver fibrosis stages were determined according to the Ishak staging system.¹⁸ A single senior pathologist (Z.G.) interpreted all liver biopsy specimens independent of the SPEA results.

Statistical Analysis

Hitit University licensed IBM SPSS 23 package program was used for statistical analysis of the results. According to the Kolmogorov–Smirnov analysis, continuous variables were presented as mean ± SD or median (25th–75th quartile), as appropriate. Kruskal–Wallis analysis of variance (ANOVA) or one-way ANOVA with Bonferroni correction and nonparametric related samples Friedman two-way ANOVA by ranks test were done for the comparison of groups. Spearman correlation analysis was used to determine the associations between fibrosis stages and biochemistry tests. The diagnostic powers of spectrophotometric SPEA assay methods and commonly used fibrosis indexes were determined by

performing receiver operating characteristic (ROC) analysis for the differentiation of F0 and F1 to F3 fibrosis stages. For the prediction of early stage liver fibrosis, logistic regression analyses were used. A $P < .05$ was considered statistically significant.

Results

Patients Characteristics

According to the Ishak fibrosis score, the numbers of patients with F0, F1, F2, and F3 fibrosis were 42, 43, 21, and 6, respectively. The SPEA values were 529 (292–794) U/L, 671 (486–927) U/L, and 1077 (867–1399) U/L with the precipitation, currently used direct and optimized direct assay methods, respectively. Demographics, laboratory test values, and SPEA results of the spectrophotometric assay methods based on fibrosis stages are presented in **TABLE 1**.

Associations between the early stages (F0–F3) of liver fibrosis and optimized direct SPEA, currently used direct SPEA, precipitation SPEA, age, albumin, ALT, AST, direct bilirubin, total bilirubin, INR, platelets, AAR, API, CDS, Doha score, FIB-4, FibroQ, fibrosis index, GUCI, King's score, and Pohl score are shown in **TABLE 2**.

Optimized Direct Spectrophotometric SPEA Assay Method

Enzyme-Substrate Incubation Step

The highest enzyme activity was determined at 5 minutes of incubation at 37°C, 45°C, 50°C, and 55°C incubation temperatures; the highest enzyme activity was obtained at 45°C.

Activation Step

In 0, 5, 10, 15, 20, 25, 30, 40, 50, 60, 90, 120, 150, and 180 minutes of activation incubations at 45°C, the highest enzyme activity was achieved at 150, 120, 30, and 25 minutes, consecutively, without a statistically significant difference ($P = .440$). To not increase the total analysis time for the SPEA assay method, 30 minutes incubation time was preferred. After deciding the optimum activation time, optimum concentrations of $\text{MnCl}_2 \cdot 4\text{H}_2\text{O}$, GSH, and Triton X-100 as an activator were determined by 25 mM, 38 mM, 51 mM, 63 mM, 76 mM, and 101 mM of $\text{MnCl}_2 \cdot 4\text{H}_2\text{O}$; 1 mM and 2 mM of GSH; and 0.1% Triton X-100 combinations. The highest enzyme activity was obtained with the combination of 63 mM $\text{MnCl}_2 \cdot 4\text{H}_2\text{O}$ and 1 mM GSH as activators.

Proline Assay Step

The maximum delta absorbance value was obtained with the addition of pH 7.8 Tris-HCl buffer by cooling the samples in ice water. In the comparison of the delta absorbance values obtained with ninhydrin reagents A, B, C, and D, the lowest CV percentage and maximum delta absorbance value were obtained with reagent D. In comparison of the delta absorbance values obtained with ninhydrin reagents E, F, G, and H, maximum delta absorbance value with the lowest CV% was obtained with reagent F. As a result, for the proline assay, it was decided to incubate the samples for 45 minutes at 80°C with ninhydrin reagent containing 15 g/L ninhydrin, 0.6 L GAA, and 0.4 L distilled water. Optimum reading interval was up to 90 minutes for samples kept in ice water because there were no statistically significant differences among the absorbance values, according to the nonparametric related samples Friedman two-way analysis of variance by ranks test ($P = .943$).

TABLE 1. Demographics and laboratory test results according to the liver fibrosis stages

Variables	Stage 0 (n = 42)	Stage 1 (n = 43)	Stage 2 (n = 21)	Stage 3 (n = 6)	P
Age, y	41 ± 12	43 ± 11	45 ± 11	50 ± 16	.320
Sex, F/M	19/23	18/25	10/11	0/6	.182
Optimized direct SPEA, U/L	922 (795–1126) ^a	1034 (919–1332) ^b	1384 (1100–1766)	1790 (1403–2548)	<.001
Currently used direct SPEA, U/L	634 (480–880)	685 (529–807)	909 (516–986)	733 (469–932)	.502
Precipitation SPEA, U/L	389 (255–678)	557 (294–802)	658 (407–1294)	767 (594–965)	.049
Albumin, g/L	44 ± 3.2 ^c	43 ± 2.4	42 ± 4.5	40 ± 2.0	.008
ALT, U/L	32 (19–56)	39 (18–69)	58 (33–89)	83 (64–541) ^d	.004
AST, U/L	24 (18–29) ^e	25 (18–48)	41 (26–72)	46 (36–224)	.002
Direct bilirubin, mg/dL	0.22 (0.17–0.30)	0.22 (0.19–0.33)	0.27 (0.22–0.37)	0.43 (0.20–0.65)	.054
Total bilirubin, mg/dL	0.58 (0.39–0.80)	0.59 (0.44–0.83)	0.69 (0.62–0.89)	1.14 (0.75–1.49) ^f	.020
INR	1.04 ± 0.07 ^g	1.07 ± 0.09	1.11 ± 0.11	1.16 ± 0.09	.001
Platelets, ×10 ⁹ /L	232 ± 62 ^h	214 ± 44	207 ± 53	154 ± 42	.009
AAR	0.80 (0.58–1.00)	0.76 (0.53–1.01)	0.75 (0.55–0.93)	0.49 (0.42–0.65)	.102
API	2 (2–4) ⁱ	3 (2–4)	4 (2.5–5)	6 (3–8)	.024
APRI	0.29 (0.24–0.41) ^j	0.32 (0.25–0.72) ^k	0.52 (0.38–0.93)	0.92 (0.56–5.65)	<.001
CDS	4.54 (4.03–5.38)	4.99 (4.07–5.99)	5.11 (4.40–6.36)	6.67 (5.75–7.53) ^l	.009
Doha score	3.17 (2.60–4.00) ^m	3.84 (2.92–4.77)	3.97 (3.14–5.03)	5.21 (4.28–7.71)	.005
FIB-4	0.79 (0.63–1.02) ⁿ	0.94 (0.63–1.29)	0.97 (0.82–1.84)	2.24 (1.10–3.38)	.006
FibroQ	1.48 (1.12–1.91)	1.59 (1.17–2.38)	1.57 (1.13–2.81)	2.09 (1.15–3.17)	.561
Fibrosis index	1.27 (0.86–1.70)	1.59 (1.14–1.95)	1.69 (1.09–2.28)	2.45 (1.86–2.99) ^o	.002
GUCI	10 (8.5–15) ^p	12 (8.9–26)	19 (14–39)	35 (22–226) ^r	<.001
King's score	4.24 (3.56–6.22) ^s	5.77 (3.10–8.93)	8.59 (5.91–16.9)	18.7 (12.6–106) ^t	<.001
Pohl score (+/–)	1/41	0/43	0/21	0/6	

ALT, alanine aminotransferase; AST, aspartate aminotransferase; INR, international normalization ratio; AAR, AST-to-ALT ratio; API, age platelet index; APRI, AST-to-platelet ratio index; CDS, cirrhosis discriminate score; GUCI, Goteborg University Cirrhosis Index; SPEA, serum prolidase enzyme activity.

^aP = .001 vs stage 2, P = .001 vs stage 3.

^bP = .026 vs stage 3.

^cP = .034 vs stage 2.

^dP = .014 vs stage 0, P = .05 vs stage 1.

^eP = .016 vs stage 2, P = .019 vs stage 3.

^fP = .045 vs stage 0, P = .044 vs stage 1.

^gP = .015 vs stage 2, P = .009 vs stage 3.

^hP = .007 vs stage 3.

ⁱP = .05 vs stage 3.

^jP = .008 vs stage 2, P = .005 vs stage 3.

^kP = .038 vs stage 3.

^lP = .006 vs stage 0, P = .044 vs stage 1.

^mP = .007 vs stage 3.

ⁿP = .020 vs stage 3.

^oP = .004 vs stage 0, P = .05 vs stage 1.

^pP = .004 vs stage 2, P = .003 vs stage 3.

^qP = .031 vs stage 1.

^rP = .002 vs stage 2, P = .002 vs stage 3.

^sP = .034 vs stage 1.

Method Validation

Intra- and Inter-Assay Precision.—The intra-assay CV levels were 7.4% and 6.2%, whereas inter-assay CV levels were 9.2% and 7.7% for low and high SPEA levels of pooled human sera, respectively.

Linearity.—The correlation coefficient of the SPEA calibration curve was found to be 0.992 ($P < .001$). The SPEA was linear between 150 and 4492 U/L.

Diagnostic Accuracy of the Spectrophotometric SPEA Assay Methods and Biochemical Tests

According to the ROC analysis to distinguish the F0 from F1 to F3 fibrosis stages, areas under the curve (AUROC) with 95% CI for the precipitation, currently used, and optimized direct spectrophotometric SPEA assay methods were 0.638 (0.519–0.757), 0.585 (0.461–0.708),

and 0.775 (0.669–0.880) ($P = .014$, $P = .187$, and $P < .001$), respectively. AUROC values for other parameters are presented in **FIGURE 1**. The AUROC of optimized direct spectrophotometric SPEA was higher than the other evaluated 11 liver fibrosis indexes in our study cohort. In addition, optimized direct spectrophotometric SPEA was the only statistically significant parameter according to the multivariate logistic regression analysis among the statistically significant parameters in univariate logistic regression analysis for the prediction of early stage liver fibrosis (**TABLE 3**).

Discussion

To the best of our knowledge, this is the first study in which direct spectrophotometric SPEA assay method was optimized. The diagnostic accuracy of currently used spectrophotometric SPEA assay methods and

TABLE 2. Associations between the early stages (F0–F3) of liver fibrosis and evaluated parameters

Variables	Early stages of liver fibrosis
Optimized direct SPEA, U/L	$r = 0.462, P < .001$
Currently used direct SPEA, U/L	$r = 0.131, P = .167$
Precipitation SPEA, U/L	$r = 0.263, P = .005$
Age, y	$r = 0.114, P = .231$
Albumin, g/L	$r = -0.290, P = .002$
ALT, U/L	$r = 0.307, P = .001$
AST, U/L	$r = 0.329, P < .001$
Direct bilirubin, mg/dL	$r = 0.228, P = .017$
Total bilirubin, mg/dL	$r = 0.219, P = .021$
INR	$r = 0.363, P < .001$
Platelets, $\times 10^9/L$	$r = -0.268, P = .005$
AAR	$r = -0.155, P = .105$
API	$r = 0.270, P = .004$
APRI	$r = 0.377, P < .001$
CDS	$r = 0.260, P = .006$
Doha score	$r = 0.310, P = .001$
FIB-4	$r = 0.321, P = .001$
FibroQ	$r = 0.130, P = .176$
Fibrosis index	$r = 0.328, P = .001$
GUCI	$r = 0.400, P < .001$
King's score	$r = 0.414, P < .001$
Pohl score (+/-)	$r = -0.111, P = .250$

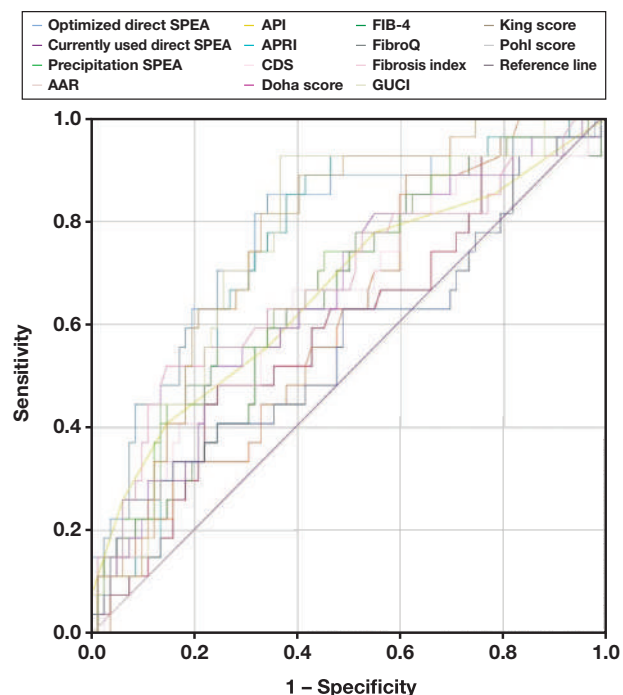
ALT, alanine aminotransferase; AST, aspartate aminotransferase; INR, international normalization ratio; AAR, AST-to-ALT ratio; API, age platelet index; APRI, AST-to-platelet ratio index; CDS, cirrhosis discriminate score; GUCI, Göteborg University Cirrhosis Index; SPEA, serum prolidase enzyme activity.

some liver fibrosis indexes, AAR, API, APRI, CDS, Doha score, FIB-4, FibroQ, fibrosis index, GUCI, King's score and Pohl score, were also evaluated to distinguish the F0 and F1 to F3 liver fibrosis stages in patients with CHB infection. According to this study, an optimized direct spectrophotometric SPEA assay method could be preferred over the currently used methods, as well as some fibrosis indexes for the evaluation of early liver fibrosis stages in patients with CHB infection.

Hepatitis B is a worldwide viral infection, causing acute and chronic liver diseases. According to WHO, 296 million people were living with CHB infection in 2019, and approximately 820,000 of these patients died, generally from cirrhosis and hepatocellular carcinoma-related complications.¹⁹ Starting medical therapy for CHB infection as soon as possible prevents or delays cirrhosis, complications, hepatocellular carcinoma, and transition to the decompensated phase and increases survival.^{1,2} Liver biopsy is currently the gold standard diagnostic tool for staging the liver fibrosis, but it is invasive and carries many risks and complications.^{3–5} Therefore, the search for noninvasive methods like SPEA to diagnose the early stages of liver fibrosis is critical.

There are 2 spectrophotometric SPEA assay methods used today. One of them requires TCA precipitation whereas the other does not.^{8,9} Of these, the direct assay method is cost-effective, more practical, and less time-consuming than the precipitation method. However, the analytical steps of the direct method should be optimized in terms of activators such as $MnCl_2 \cdot 4H_2O$ and GSH concentrations, incubation times and in-

FIGURE 1. Areas under the curve (AUROC) of serum prolidase enzyme activities and liver fibrosis indexes to distinguish the F0 from F1–F3 liver fibrosis stages. ALT, alanine aminotransferase; AST, aspartate aminotransferase; INR, international normalized ratio. AAR, AST-to-ALT ratio; API, age platelet index; APRI, AST-to-platelet ratio index; CDS, cirrhosis discriminate score; GUCI, Göteborg University Cirrhosis Index; SPEA, serum prolidase enzyme activity.



	AUROC (95 CI%)	P
Optimized direct SPEA	0.775 (0.670-0.880)	<.001
Currently used direct SPEA	0.592 (0.469-0.716)	.152
Precipitation SPEA	0.641 (0.521-0.761)	.028
AAR	0.614 (0.499-0.728)	.077
API	0.663 (0.537-0.789)	.011
APRI	0.745 (0.644-0.846)	<.001
CDS	0.642 (0.521-0.763)	.028
Doha score	0.659 (0.540-0.777)	.014
FIB-4	0.685 (0.570-0.801)	.004
FibroQ	0.565 (0.432-0.698)	.312
Fibrosis index	0.682 (0.557-0.807)	.005
GUCI	0.755 (0.653-0.856)	<.001
King score	0.762 (0.669-0.856)	<.001
Pohl score (+/-)	0.506 (0.381-0.631)	.925

cubation temperatures for activation, enzyme-substrate incubation, and proline-ninhydrin condensation steps, as these factors are not evaluated in the currently used direct SPEA assay method. Therefore, in this study, optimum activation, enzyme-substrate, and proline-ninhydrin condensation incubation conditions were determined for the direct spectrophotometric SPEA assay method based on the higher enzyme activity to improve the diagnostic power of SPEA in a collagen metabolism-related disorder like fibrosis in patients with CHB infection. On the other hand, Triton X-100 is used in the precipitation spectrophotometric SPEA assay method,⁸ but it should be noted that the use of Triton X-100 is forbidden in the European Union since January 2021 due to its effect as a hormone disrupter. Therefore, the precipitation spectrophotometric SPEA assay method has become less practical and will not be appropriate for future studies. Because Triton X-100 is not used in direct spectrophotometric SPEA assay methods, optimized direct spectrophotometric SPEA assay method would be the method of choice in the future for spectrophotometric SPEA analysis.

TABLE 3. Variables associated with the prediction of early stage liver fibrosis by univariate and multivariate logistic regression analyses

Variables	Univariate analysis			Multivariate analysis		
	OR (95% CI)	Wald	P	OR (95% CI)	Wald	P
Optimized direct SPEA, U/L	1.002 (1.001–1.004)	15.5	<.001	1.002 (1.001–1.004)	9.23	.002
Precipitation SPEA, U/L	1.001 (1.000–1.002)	5.70	.017	1.001 (1.000–1.002)	1.71	.191
Albumin, g/L	0.113 (0.026–0.492)	8.45	.004	0.231 (0.022–2.446)	1.48	.223
ALT, U/L	1.004 (1.000–1.007)	3.95	.047	0.991 (0.965–1.017)	0.48	.489
Direct Bilirubin, mg/dL	9.106 (0.974–85.15)	3.75	.053	2.760 (0.147–51.70)	0.46	.497
Total bilirubin, mg/dL	3.782 (1.191–12.01)	5.09	.024	1.708 (0.183–15.98)	0.22	.639
INR	3359 (22.38–504.235)	10.1	.001	133.2 (0.007–2,689.836)	0.94	.333
Platelets, $\times 10^9/L$	0.990 (0.982–0.999)	4.77	.029	1.017 (0.920–1.124)	0.11	.744
AAR	0.215 (0.041–1.119)	3.34	.068	0.006 (0.000–5.306)	2.19	.139
API	1.421 (1.116–1.810)	8.12	.004	1.344 (0.546–3.307)	0.42	.520
APRI	1.323 (1.001–1.747)	3.88	.049	0.029 (0.000–116.1)	0.70	.402
CDS	1.487 (1.033–2.141)	4.56	.033	0.268 (0.040–1.822)	1.81	.178
Doha score	1.444 (1.075–1.939)	5.97	.015	5.829 (0.046–736.4)	0.51	.475
FIB-4	1.682 (1.075–2.633)	5.18	.023	0.262 (0.001–87.52)	0.21	.651
FibroQ	1.420 (0.939–2.148)	2.76	.097	1.553 (0.076–31.86)	0.08	.775
Fibrosis index	2.786 (1.411–5.501)	8.72	.003	0.189 (0.000–4.251)	0.11	.744
GUCI	1.007 (1.000–1.014)	4.02	.045	1.087 (0.891–1.326)	0.67	.412
King's score	1.019 (1.001–1.037)	4.51	.034	1.039 (0.800–1.350)	0.08	.774

ALT, alanine aminotransferase; AST, aspartate aminotransferase; INR, international normalization ratio; AAR, AST-to-ALT ratio; API, age platelet index; APRI, AST-to-platelet ratio index; CDS, cirrhosis discriminate score; GUCI, Goteborg University Cirrhosis Index; SPEA, serum prolidase enzyme activity.

Apart from activator, incubation time, and temperature, spontaneous hydrolysis of gly-pro is a problem that should be addressed in spectrophotometric SPEA assay methods. To increase accuracy, spontaneous hydrolysis of gly-pro should be minimized. In this study, whether the spontaneous formation of glycine and proline from gly-pro substrate could be stopped with 5, 10, 15, and 20 minutes of incubation in ice water or not was also investigated. In this experiment, mean SPEA of the samples that were not kept in ice water and kept in ice water for 5 minutes were the same ($P = 1.000$), but mean SPEA of the samples that were kept in ice water for 10, 15, and 20 minutes were statistically significantly lower ($P = .008$). Therefore, it was shown, in ice water, that enzyme-substrate incubation time should be as short as possible to achieve minimum spontaneous hydrolysis of gly-pro substrate as well as the maximum SPEA.

Sample blank was added for each sample to eliminate the interference that may derive from ornithine, citrulline, cysteine, lysine, and hydroxylysine at the ninhydrine condensation step.²⁰

In the study by Myara et al,⁸ as in our study, it was concluded that SPEA increased in patients with liver fibrosis. They did not find a statistically significant association between fibrosis stages and SPEA, but there were statistically significant correlations between the fibrosis stages and both precipitation and optimized direct spectrophotometric SPEA assay method results in our study. This may be explained by the optimization of the currently used direct spectrophotometric SPEA assay method as well as the inclusion of patients with early stage liver fibrosis (F0–F3) in our study. Myara and colleagues considered that SPEA may increase only in the early stage of liver fibrosis and may decrease in advanced liver fibrosis due to slower collagen turnover in the advanced liver fibrosis stages as a result of the high level of collagen deposition. In our study, both the precipitation and optimized direct spectrophotometric SPEA assay method results increased at least until stage 3, but the

currently used direct spectrophotometric SPEA assay method results increased until stage 2 liver fibrosis. It is not known whether the precipitation and optimized direct spectrophotometric SPEA assay method results increase or decrease in patients with cirrhosis, but according to this study, it can be predicted that results of the currently used direct spectrophotometric SPEA assay method will decrease.

Myara et al⁸ found that SPEA was not statistically significantly correlated with ALT, AST, alkaline phosphatase, γ -glutamyltransferase, total bilirubin, or albumin, but in our study, optimized direct spectrophotometric SPEA assay method results statistically significantly correlated with AST, ALT, albumin, and platelets, whereas precipitation spectrophotometric SPEA assay method results statistically significantly correlated only with AST. According to the ROC and logistic regression analyses, SPEA measured by the optimized direct spectrophotometric assay had the highest diagnostic accuracy among the evaluated parameters. We therefore considered that especially the optimized direct spectrophotometric SPEA assay method could be used to distinguish the early stages of liver fibrosis.

Duygu et al²¹ concluded that SPEA measured with the currently used direct spectrophotometric assay method increased in patients with CHB infection and inactive hepatitis B infection compared with the control group, and SPEA may be used as a biomarker in CHB infection, as in our study. They did not find an association between SPEA and Knodell fibrosis score. In our study, there was no statistically significant association between fibrosis stages and currently used direct spectrophotometric SPEA assay method results, as in their study. Both of these results show that currently used direct spectrophotometric SPEA assay method may not have enough diagnostic accuracy especially to distinguish the liver fibrosis stages, and it should be optimized as was done in our study.

Nazligul et al²² observed a statistically significant correlation between precipitation spectrophotometric SPEA results and fibrosis score in patients with CHB and chronic viral hepatitis C (n=29 and n=25, respectively). They found that SPEA was statistically significantly higher in patients with chronic viral hepatitis than controls. According to their analysis, there was no statistically significant difference for SPEA, ALT, and fibrosis scores in terms of the chronic viral hepatitis etiology. They concluded that SPEA may be used for predicting stage of liver fibrosis in patients with viral hepatitis.

One study limitation is that the blood samples were not drawn within 3 days of the liver biopsy in 14 stage 0 and 10 stage 1 liver fibrosis patients for the SPEA assays. However, no interference was expected due to the time interval between liver biopsy and blood draw for SPEA results, because patients were not taking antiviral treatment, did not have co-infection with hepatitis C, D, or HIV, autoimmune hepatitis, or cholangitis and had F0 and F1 stage liver fibrosis, and <6 histological activity index. In addition, most of these blood samples were drawn within 2 months after liver biopsy.

In conclusion, optimized direct spectrophotometric SPEA assay method could be preferred instead of the currently used spectrophotometric SPEA assay methods to distinguish the early stages of liver fibrosis (F0 vs F1–F3) in patients with CHB infection. In this optimized direct spectrophotometric SPEA assay method, after 30 minutes of activation with pH 7.0 Tris-HCl buffer containing 63 mM MnCl₂·4H₂O and 1 mM GSH at 45°C, enzyme-substrate incubation was performed for 5 minutes at 45°C with pH 7.8 Tris-HCl buffer containing 94 mM of glycine-L-proline substrate. At the end of this incubation, GAA was added immediately to inhibit the SPEA by pH change. For the ninhydrin reaction, ninhydrin reagent (600 mL of GAA, 400 mL of distilled water, and 15 g/L ninhydrin) and pH 7.8 Tris-HCl buffer are pipetted, vortexed, and then incubated at 80°C for 45 minutes. At the end of the incubation, samples were immediately kept in ice water for 5 minutes and absorbances were read against the reagent blank in spectrophotometer at 515 nm wavelength within 90 minutes.

Funding

This study was supported by Hitit University. Project numbers are TIP19002-16.002 and TIP19002-19.001.

Conflict of Interest Disclosure

The authors have nothing to disclose.

REFERENCES

1. Terrault NA, Lok ASF, McMahon BJ, et al. Update on prevention, diagnosis, and treatment of chronic hepatitis B: AASLD 2018 hepatitis B guidance. *Hepatology*. 2018;67(4):1560–1599.
2. European Association for Study of Liver and Asociacion Latinoamericana para el Estudio del Hígado. EASL-ALEH clinical practice guidelines: non-invasive tests for evaluation of liver disease severity and prognosis. *J Hepatol*. 2015;63(1):237–264.
3. Seeff LB, Everson GT, Morgan TR, et al; HALT-C Trial Group. Complication rate of percutaneous liver biopsies among persons with advanced chronic liver disease in the HALT-C trial. *Clin Gastroenterol Hepatol*. 2010;8(10):877–883. doi:10.1016/j.cgh.2010.03.025.
4. Regev A, Berho M, Jeffers LJ, et al. Sampling error and intraobserver variation in liver biopsy in patients with chronic HCV infection. *Am J Gastroenterol*. 2002;97(10):2614–2618. doi:10.1111/j.1572-0241.2002.06038.x.
5. Castera L, Pinzani M. Biopsy and non-invasive methods for the diagnosis of liver fibrosis: does it take two to tango? *Gut*. 2010;59(7):861–866. doi:10.1136/gut.2010.214650.
6. Wilk P, Wątor E, Weiss MS. Prolidase- a protein with many faces. *Biochimie*. 2021;183:3–12. doi:10.1016/j.biochi.2020.09.017.
7. Aganga IE, Lanaghan ZM, Balasubramaniam M, et al. Prolidase: a review from discovery to its role in health and disease. *Front Mol Biosci*. 2021;8:723003.
8. Myara I, Myara A, Mangeot M, et al. Plasma prolidase activity: a possible index of collagen catabolism in chronic liver disease. *Clin Chem*. 1984;30(2):211–215.
9. Ozcan O, Gultepe M, Ipcioğlu OM, et al. Optimization of the photometric enzyme activity assay for evaluating real activity of prolidase. *Turk J Biochem*. 2007;32(1):12–16.
10. Kurien D'Souza A, Miller D, Matsumoto H, et al. Prolidase deficiency and the biochemical assays used in its diagnosis. *Anal Biochem*. 2006;349(2):165–175. doi:10.1016/j.ab.2005.10.018.
11. Krishna G, Sivakumar PT, Dahale AB, et al. Increased prolidase activity in Alzheimer's dementia: a case-control study. *Asian J Psychiatr*. 2020;53:102242. doi:10.1016/j.ajp.2020.102242
12. Sawicka MM, Sawicki K, Łysoń T, et al. Proline metabolism in malignant gliomas: a systematic literature review. *Cancers*. 2022;14(8):2030. doi:10.3390/cancers14082030
13. Pellegrinelli V, Cuenca SR, Rouault C, et al. Dysregulation of macrophage PEPD in obesity determines adipose tissue fibro-inflammation and insulin resistance. *Nat Metab*. 2022;4(4):476–494.
14. Say M, Tella E, Boccara O, et al; on behalf of the Angio-Dermatology Group of the French Society of Dermatology, the Research Group of the French Society of Pediatric Dermatology. Leg ulcers in childhood: a multicenter study in France. *Ann Dermatol Venereol*. 2022;149(1):51–55. doi:10.1016/j.annder.2021.05.004.
15. Clinical Laboratory Standards Institute (CLSI). *Evaluation of Precision of Quantitative Measurement Procedures; Approved Guideline*. 3rd ed. Clinical and Laboratory Standards Institute; 2018 document EP05-A3E.
16. Clinical Laboratory Standards Institute (CLSI). *User Verification of Precision and Estimation of Bias; Approved Guideline*. 3rd ed. Clinical and Laboratory Standards Institute; 2014 document EP15-A3.
17. Clinical Laboratory Standards Institute (CLSI). *Evaluation of the Linearity of Quantitative Measurement Procedures: A Statistical Approach; Approved Guideline*. Clinical and Laboratory Standards Institute; 2003 document EP06-A.
18. Ishak K, Baptista A, Bianchi L, et al. Histological grading and staging of chronic hepatitis. *J Hepatol*. 1995;22(6):696–699. doi:10.1016/0168-8278(95)80226-6.
19. <https://www.who.int/news-room/fact-sheets/detail/hepatitis-b>
20. Chinard FP. Photometric estimation of proline and ornithine. *J Biol Chem*. 1952;199(1):91–95.
21. Duygu F, Aksoy N, Cicek AC, Butun I, Unlu S. Does prolidase indicate worsening of hepatitis B infection? *J Clin Lab Anal*. 2013;27(5):398–401. doi:10.1002/jcla.21617.
22. Nazligul Y, Aslan M, Taskin A, et al. Serum prolidase activity may be an index of liver fibrosis in chronic viral hepatitis. *East J Med*. 2015;20(3):125–130.